Cranfield University

SCHOOL OF ENGINEERING

PhD Thesis

Academic Year 2002-2003

Stephen Ogajiye Tamuno-ojuemi Ogaji

Advanced Gas-path Fault Diagnostics for Stationary Gas Turbines

Supervisor: Prof. Riti Singh

This thesis is submitted in partial fulfilment of the requirements for the degree of Doctor of Philosophy

ABSTRACT

The reliabilities of the gas-path components (compressor, burners and turbines) of a gas turbine (GT) are usually high when compared with those of other GT systems such as fuel supply and control. However, in the event of forced outage, downtimes are normally high, giving a relatively low availability.

The purpose of condition monitoring and fault diagnostics is to detect, isolate and assess (i.e. estimate quantitatively the magnitude of) the faults within a system, which in this case is the gas turbine. An effective technique would provide a significant improvement in economic performance, reduce operational and maintenance costs, increase availability and improve the level of safety achieved. However, conventional analytical techniques such as gas-path analysis and its variants are limited in their applications to engine diagnostics due to several reasons that include their inability to:- operate effectively in the presence of noisy measurements; distinguish effectively sensor bias from component faults; preserve the nonlinearity in the gas-turbine parameter relationships; and the requirement for more sensors for achieving accurate diagnostics. The novelty of this research stems from its objective of overcoming most of these limitations and much more.

In this thesis, we present the approach adopted in developing a diagnostic framework for the detection of faults in the gas-path of a gas turbine. The framework involves a large-scale integration of artificial neural networks (ANNs) designed and trained to detect, isolate and assess the faults in the gas-path components of the engine. Input to the diagnostic framework are engine measurements such as spool speeds, pressures, temperatures and fuel flow while outputs are either levels of changes in sensor(s) for the case of sensor fault(s) or the level of changes in efficiencies and flow capacities for the case of faulty components. The diagnostic framework has the capacity to assess both multiple component and multiple sensor faults over a range of operating points. In the case of component faults, the diagnostic system provides changes in efficiencies and flow capacities from which interpretations can be sought for the nature of the physical problem. The implication of this is that the diagnostic system covers a wide range of problems - both likely and unlikely-.

The technique has been applied to several developed test cases, which are not only thermodynamically similar to operational engines, but also covers a range of engine configurations and operating conditions. The results obtained from the developed approach has been compared against those obtained from linear and nonlinear (recursive linear) gas-path analysis, as well as from the use of fuzzy logic. Analysis of the results demonstrates the promise of ANN applied to engine gas-path fault diagnostic activities.

Finally, the limitations of this research and direction for future work are presented.

ACKNOWLEDGEMENT

First, I would like to express my gratitude to Professor Riti Singh, my supervisor and mentor. But for his initial recommendation for a place of study, his guidance and encouragement through the tortuous paths of this study, I may not have arrived where I am presently. He helped to expand my horizon and ensured that I actively participated in a number of international conferences.

My explicit regards go to staff at the department of power, propulsion and aerospace engineering that includes Professor Pericles Pilidis, Mrs Susanne Gow, Mrs Rachel Roper who gave me their attention when I needed it. Professor Douglas Probert deserves mention for the time spent in helping to develop my technical writing skills and for his extensive useful advice. Efforts of those involved in proofreading this thesis are appreciated.

The Association of Commonwealth University (ACU) deserves appreciation for selecting me from the eligible thousands and for sponsoring my family and me through the period of this programme.

My wife, Barrister (Mrs) Joy O. Ogaji and our baby daughter, Miss Daniela I.S. Ogaji were, without any ado, instrumental in my completion of this programme. Their understanding and encouragements were vital especially during periods of emotional crisis. My regards also go to my larger family, for their support and prayers.

Lastly but above all, I would like to thank GOD, who heard my prayers and made a way for me to achieve my ambition of becoming better prepared to improve the lot of others. He preserved my health and gave me understanding.

TABLE OF CONTENT

GLOSSARY OF TERMS (INCLUDING JARGON)

Advanced diagnostic technique (ADT)	A diagnostic approach that applies state-of-the-art tools.
APPROX	A network that is designed to provide quantitative estimates.
Architecture	A graph describing the layout of a neural network.
Artificial neural network (ANN)	A collection of mathematical models that emulates some of the observed properties of biological nervous systems and draws on the analogies of adaptive biological learning.
Bias	A fixed component of measurement error, which remains constant no matter how many times the measurement is taken.
CLASS	A network that is designed to provide qualitative results.
Dimensionality	The number of independent units contained in a given layer of a network.
Epoch	The presentation of a set of training (input and/or target) vectors to a network and the calculation of the new weights.
Evolving Approaches	Techniques based on artificial intelligence that are being explored for engine diagnostics.
Expert system (ES)	A computer program that contains a knowledge base and a set of algorithms or rules that infer new facts from that knowledge and from incoming data.
Feedforward network	A form of network connectivity in which outputs go to following but not preceding neurons.
Fuzzy logic (FL)	A form of algebra applied in decision making with imprecise data. It employs a range of values between extremes of perfection i.e. “true” or “false”.
Gas-path fault diagnostics (GPFD)	The process of isolating and assessing faults in an engine’s gas-path.
Gas-path faults (GPF)	Faults that affect the working-fluid’s flow path in a gas

	turbine. They include fouling and erosion.
Gas-Path Analysis (GPA)	A commonly-used term for performance analysis
Generalisation	The ability of a network to produce a required output from an input vector, similar to its training set.
Kalman Filter (KF)	An algorithm for producing best estimates of the component changes and sensor biases that produced an observed set of gas-path measurement differences from expectation.
Noise	A random component of measurement error caused by numerous small effects, which cause disagreements between repeated measurements of the same parameter.
Pattern	A vector of inputs.
Testing	The process of ascertaining the generalisation ability of a trained network.
Training	A procedure whereby a network is adjusted to do a particular job.

LIST OF APPENDIXES

LIST OF FIGURES

LIST OF TABLES

ABBREVIATIONS

a	δ correction exponent
AI	Artificial intelligence
ANN	Artificial neural network
APPROX	Approximation network
ATT	Average training time
AUTOASSOC	Autoassociative network
b	θ correction exponent
c	γ correction exponent
CC	Combustor chamber
CCP	Correctly classified patterns
CF	Component fault
CLASS	Classification network
CPR	Compressor pressure ratio
DACS	Data and analysis centre for software
DCF	Dual component fault
DFD	Data flow diagram
DOD	Domestic object damage
DSA	Dual step analysis approach
ES	Expert system
F	Fault
FOD	Foreign object damage
FL	Fuzzy logic
GLR	Generalised likelihood ratio
GLT	General likelihood test
GPA	Gas-path analysis
GPF	Gas-path fault
GPFD	Gas-path fault diagnosis
GT	Gas turbine
GUI	Graphic user interface
HCF	High cycle fatigue

HPT	High pressure turbine
ICP	Incorrectly classified patterns
IPC	Intermediate pressure compressor
KF	Kalman filter
LALG	Learning algorithm
LCF	Low cycle fatigue
LPT	Low pressure turbine
LS	Least-square
MCF	Multiple component fault
MLD	Multiple likelihood detector
MMKF	Multi-modal Kalman filter
MSE	Mean square error
N/N1	Low pressure relative shaft speed (2-spool engine)
	Gas generator relative speed (1-spool engine)
N2	High pressure relative shaft speed
NF	No fault
OEM	Original equipment manufacturer
O & G	Oil and gas
PT	Power turbine
SCF	Single component fault
SF	Sensor fault
SFDI	Sensor fault detection and isolation
SFDIA	Sensor fault detection, isolation and accommodation
SOP	Shaft ouput power
SPLRT	Sequential probability likelihood ratio test
SSE	Sum square of error
TCF	Triple component fault
TET	Turbine entry temperature
TIT	Turbine inlet temperature
TSA	Triple step analysis approach
TTP	Total test patterns
TTRP	Total training patterns
WFE	Main combustor fuel flow

WLS	Weighted least-square
X, Z, z	Input parameters

Notations

η	Component efficiency
Γ	Component flow capacity/function
σ	Standard deviation
γ	Shaftpower ratio, which is measured shaftpower divided by shaftpower at reference point.
δ	Pressure ratio, which is prevailing intake pressure divided by reference point intake pressure
θ	Temperature ratio, which is prevailing ambient temperature divided by reference point ambient temperature.
Δ	Difference

Subscripts

a	Ambient
bki	Corrected baseline for sensor i in pattern k
C	Compressor
cki	Network prediction for sensor i in pattern k
CT	Compressor turbine
i	Sensor i
ki	Sensor i in pattern k
PT	Power turbine
T	Turbine

Sensor Nomenclature

N1	GG speed
N2	GG (HP) speed
P2	IP compressor delivery pressure
P2 (Avon), P3 (RB211)	GG compressor delivery pressure
P4 (Avon), P6 (RB211)	GG exhaust pressure
T2	IP compressor delivery temperature
T2 (Avon) , T3 (RB211)	GG compressor delivery temperature

T6	GG exhaust temperature
WFE	GG fuel flow

CHAPTER 1

INTRODUCTION

1.1 Gas Turbines

Gas turbines (GTs) are mechanical devices operating on a thermodynamic cycle, usually with, air as the working fluid. The air is compressed, mixed with fuel and burnt in a combustor, with the generated hot pressurised gas expanded through a turbine to generate power. This is used for driving the compressor and for providing the means to overcome external loads (i.e. for thrust or shaft power).

In a general sense, an engine may be viewed as being composed of the following equipment and their respective constituents (Urban, 1972):

- Gas-path components – compressors, burners and turbines.
- Rotating components – engine bearings, rotors, gear trains.
- Accessory components – fuel control, fuel pump, control system, lubrication system, ignition system, and engine air-bleed system.

However, it is common in the simplest of forms to describe the GT as consisting primarily of the gas-path components.

GTs are playing an increasingly important role in peoples' lives as well as in their endeavours, in such applications as mechanical drives in the oil and gas sector, electricity generation in the power sector, and propulsion systems in the aerospace/marine sector amongst others. Enhancements in design, aerothermodynamics and materials/cooling technology are not only increasing the rate and zone of GT applications, but are also enhancing their economic operations via improvements in

thermal/component efficiencies, longer times between overhauls (TBOs), and higher overall performance levels.

The emergence of GTs for stationary applications date back to the early 1950s (Spector, 1989) when the steam-turbine design was coupled with aero-thermodynamic technology that existed in military aircraft GTs. When considering performance, these GTs had pressure ratios of the order of 12 to 1, firing temperatures of 649 – 816 ^{o}C and thermal efficiencies in the range of 23 – 27%. Today, improvements in design, aerothermodynamics and materials/cooling technology have seen efficiency rise to over 45% at higher operating temperatures and pressures.

GTs are now becoming increasingly employed in both combined production of heat-and-power (cogeneration), combined cycles (use of gas turbines upstream and steam turbines downstream) and in some cases, combined cycles with heat generation. These applications have considerably increased the use of the system. Also GTs are able to use a wide range of fuels, from low heating value gases to coal, producing the low levels of pollutant emissions.

In the sphere of pipeline applications, aeroderivative GTs are more popular than their heavy-frame counterparts. Aeroderivatives are, in extreme cases now known to run for periods of over 100,000 hours between overhauls: this is obviously a major improvement over available past figures where Agrawal et al (1978) reported TBOs of the order of 35,000 hours.

For stationary purposes, aeroderivative GTs and their heavy-frame counterparts have power ranges in which the use of one would be preferred over the other. This is presented as:

Condition	**Choice**
Required shaft power < 15 MW	Aeroderivatives or heavy frame

40 MW< Required shaft power > 15MW	Aeroderivatives
60 MW> Required shaft power	Heavy frame

For base-load applications, especially in the utility industry, a survey by Waldman (1986) indicated an upsurge in the demand for large GT units with the number of those in the range of 60MW and above, tripled in 1986 when compared with figures for 1985.

GT reliabilities, whilst high, remain lower than those of steam turbines, which are designed to much lower cycle temperatures. Grenstad et al. (1982) report that GTs operating in peaking service fail about three times more often than steam turbines: this factor increases to ten when auxiliary equipment is included in the comparison.

The relative value of a GT in cost per kilowatt output (£/kW) is of importance in considering ownership. The overall cost of ownership of a GT includes the initial cost of equipment installation, cost of fuel consumed, applied labour and maintenance cost, that is, all costs involved in keeping the GT operational. This consideration is based on the fact that variation of efficiencies have to be taken into account in life-cycle computations.

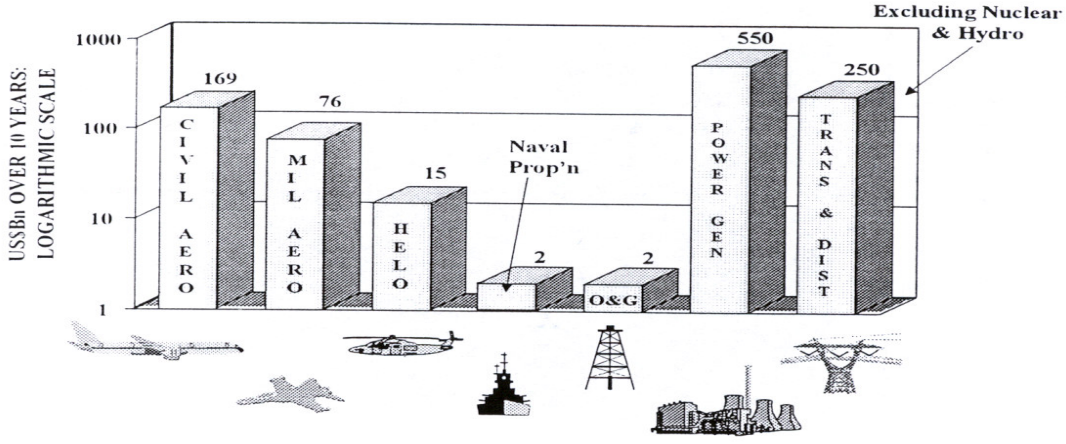

Figure 1.1 The market for power systems (Singh, 1996)

The future is bright for the GT industry and especially for stationary applications where its market is exceeding that of combined military and civil aero GTs, as shown in Figure1.1

1.2 Problem Definition

As stated in the previous section, GTs are increasingly being used for electrical power generation, mechanical drives in the oil, gas sector and for propulsion in aero and marine sectors amongst others. Also three main systems of GT – accessory, rotating equipment and gas-path components, have their own particular associated problems.

The reliabilities of the gas-path components (compressor, burners and turbines) within a GT are usually high when compared with those of other GT systems, such as fuel supply and control (Figure 1.2). However, their availabilities could be relatively low as high downtimes are normally associated with these components when subjected to forced outages. One way of improving availability is by improved maintenance practices that involve applying such approaches as condition-based monitoring (CBM).

However, before maintenance is undertaken, faults have to be detected and the faulty component(s) isolated. Faults may affect the performance, availability and life of the GT. For the particular case of the gas-path, faults can range from those that require washing to restore performance like fouling, to those that require that the plant be shut down for maintenance arising from such problems as foreign and domestic object damage (FOD and DOD). Degradation in the GT can lead to creep and fatigue damage - two important mechanisms that limit the life of GT engines. Operating degraded GTs is often uneconomic.

Various fault diagnostic techniques either are currently in use or are being developed. These techniques can be classified either as qualitative or quantitative or as conventional or evolving. If the latter classification method is adopted, then we have

such techniques as fault trees (FT), fault matrixes (FM) and gas-path analysis (GPA) approaches that are based on the least-squares (LS) algorithm as belonging to the conventional approach, while the techniques based on "artificial intelligence" such as expert systems (ES), fuzzy logic (FL), genetic algorithms (GA) and artificial neural networks (ANN) belong to what can be described as the "evolving approaches". While the conventional approaches have been researched for many years, the evolving approaches are still generating research interest. The reason for this is the potential they present as well as the simplicity of their implementation. From available information in the public domain, it is not an overstatement to conclude that the evolving approaches could be at the dawn of their general acceptance by GT manufacturers and users.

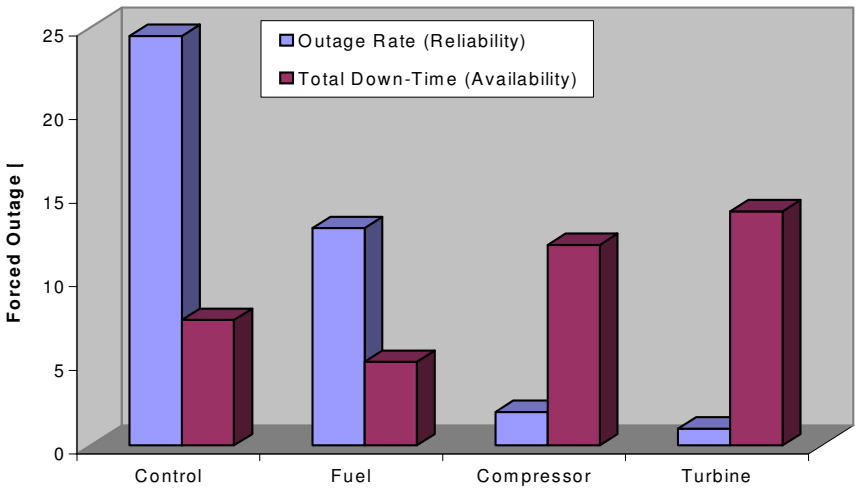

Figure 1.2 Forced Outage and Downtime Rate (Singh, 1999)

Before the advent of GPA tools, gas-path faults have been diagnosed predominantly by qualitative means such as fault trees and fault matrixes. Symptoms were noted and matched to predetermined patterns. Experienced engineers need often identify trend shifts in engine measurements and isolate the faulty module or component from the patterns/fingerprints, but the fact remains that the apparent fault could have:-

- been due to measurement noise
- resulted from one or more sensor biases
- resulted from more than one component
- been minimal and so allow for continued engine operation until such a time that the necessary labour and materials have been assembled in order to rectify the fault.

Answers to these concerns cannot be provided by qualitative approaches whether they be conventional or evolving. GPA and its variants as well as some artificial intelligence techniques can provide quantitative results of gas-path faults. A recent update of these techniques is contained in the Von Karman Institute lecture series 2003-01 on gas turbine condition monitoring and fault diagnosis edited by Mathioudakis and Sieverding (2003).

GPA tool based on least square (LS) was introduced to the diagnostic scene by Urban, (1972). The initial formulation was limited to quantifying the faults in just one component and did not address the fact that GT parameter interrelationships are non-linear. Kamboukos and Mathioudakis (2003) have shown that a substantial amount of error is observed in fault diagnosis when linear techniques are used, expecially, as fault levels go beyond the small deviations range. Escher (1995), introduced an recursive form of Urban's GPA tool to account for some degree of non-linearity in the system. However, both Urban's initial formaulation and Escher's iterative update of the Jacobian matrix failed to address the sensor bias and noise problem.Other GPA tools based on the LS have been introduced over the years and include weighted least-squares algorithm, WLS (Urban, 1980; Volponi, 1982, Doel, 1994a, 1994b) and the Kalman filters, KF (Luppold et al, 1989, Volponi et al. 2000). These approaches are currently being applied by OEMs and GT users as they provide partial solutions to some of the concerns raised above.

Artificial intelligence (AI) tools like expert system (ES) and and fuzzy logic (FL) provide more or less qualitative answers, though FL is now being explored for providing clear and definite results in gas-path fault diagnostics (Marinai et al, 2003). However, they are well adapted for the description of results obtained by quantitative approaches. Possible considerations that provide quantitative results in the AI domain narrow down to GA and ANN. It is being suggested in the field of research (Doel, 1994a, 1994b, Volponi et al, 2000, Mathioudakis, 2003) that ANN could provide better answers to gas-path fault diagnostic (GPFD) problems in GTs. Amongst other things, this research will seek to identify ways in which ANN can be applied to improve gas-path diagnostics.

1.3 Data Sources

A GT is a complex system with many components, whose individual characteristics determine the overall performance characteristics of the engine. Subjecting this engine to test in such a way that components are stripped and recoupled to allow for fault implantation is not only costly and laborious, but sometimes may introduce new faults and ultimately produce erroneous data. Further, original equipment manufacturers (OEMs) are often reluctant to part with performance information concerning their GTs as they consider such proprietary and may have implications with respect to their competitive positioning. Research has shown that it is not necessary to physically strip engines and obtain fault patterns (MacLeod, 1991).

A most enticing way out of this dilemma is via a computer simulation of the behaviour of the engine. With respect to the gas-path, this may be via the use of non-linear aero-thermodynamic models or trained neural networks (Torella et al, 2000; Melissa et al, 1998) to study the performance of the GT. In addition, when considering the number of sensors and time required for effective data trending in fault identification, system complexity favours the adoption of computer simulation techniques in engine-diagnostic studies (MacIsaac, 1992).

Simulation codes have long been in existence (Seller et al, 1975) and various simulation models are available in the public domain, which may be grouped simply on the basis of the platform they run on (Ismail et al, 1991, Perz, 1991):

- Analog simulation
- Hybrid simulation
- Digital simulation

Robust simulation programs are principally based on the matching of the various components of the GT to ensure flow, work and speed compatibility, while allowing for all forms of losses and bypasses. Such programs should permit the user to assemble the components in any desired configuration. In addition, modular features that permit individual component studies are necessary.

The process of simulation should consider the off-design behaviour of the engine, over a wide range of operating conditions, varied by power settings, ambient conditions or elevational considerations. Thus, additional requirements of a good simulation program should include flexibility (ability to both handle obvious requirements and keep abreast of latest developments), credibility (readily understandable to various classes of users and ability to employ commonly available data), availability (not associated with lengthy set-up times) and reliability (assure repeatability/easy verifiability of results).

A number of computer simulation models have been developed at Cranfield University with most having the ability to perform engine-deterioration studies. Amongst such programs are TURBOMATCH (Macmillan, 1974), PYTHIA (Escher, 1995) and DETEM (Grewal, 1988). The later programs have built upon Turbomatch, using it as the kernel and adding some other functionality such as transient simulation, GPA and graphic user interface (GUI) capabilities. A significant feature of Turbomatch is its genericity - which has been enhanced over the years - that is its ability to simulate different GT engines and their peculiarities as incorporated component maps are scaled

to suit the desired engine specification via the use of scaling factors (SF) for efficiency, non-dimensional mass flows, and pressure ratios amongst others, with the relationship:

$$SF=\frac{X_{act}}{X_{ref}} = \frac{\text{Value of parameter in actual engine map}}{\text{Value of parameter in reference map}} \quad 1.1$$

A number of authors (Stamatis et al, 1990; MacLeod, 1991; Torella et al, 2000) have used scaling factors for fault simulation. Adjustments to scaling factors are transmitted to the parameters they represent - though not in the same proportion since, in addition to adjusting the component maps via rescaling, rematching of the engine also takes place: thus, arbitrary engine configurations can be simulated with the thermodynamic properties/parameters of the working fluid at every station (inlet and outlet of components) quantitatively obtained.

The foregoing suggests that most of the data that are used in this research were obtained by simulation as it is actually possible to tune computer models to reflect reality and so with minimal adjustments, developed models can be adapted to actual engines.

1.4 Thesis Structure

This thesis presents the methodology and results obtained from the application of ANN in developing diagnostic frameworks for the gas-path of the GT. In this section, the thesis structure, outlined in Figure 1.3, is briefly discussed.

Chapter 2 provides a survey of the literature concerning some of the faults, which occur in the gas-path of a GT and their implications. Various approaches that have and are still being used and researched for their diagnosis are examined. AI techniques were also considered, highlighting their strengths and weaknesses. Finally, research opportunities were identified.

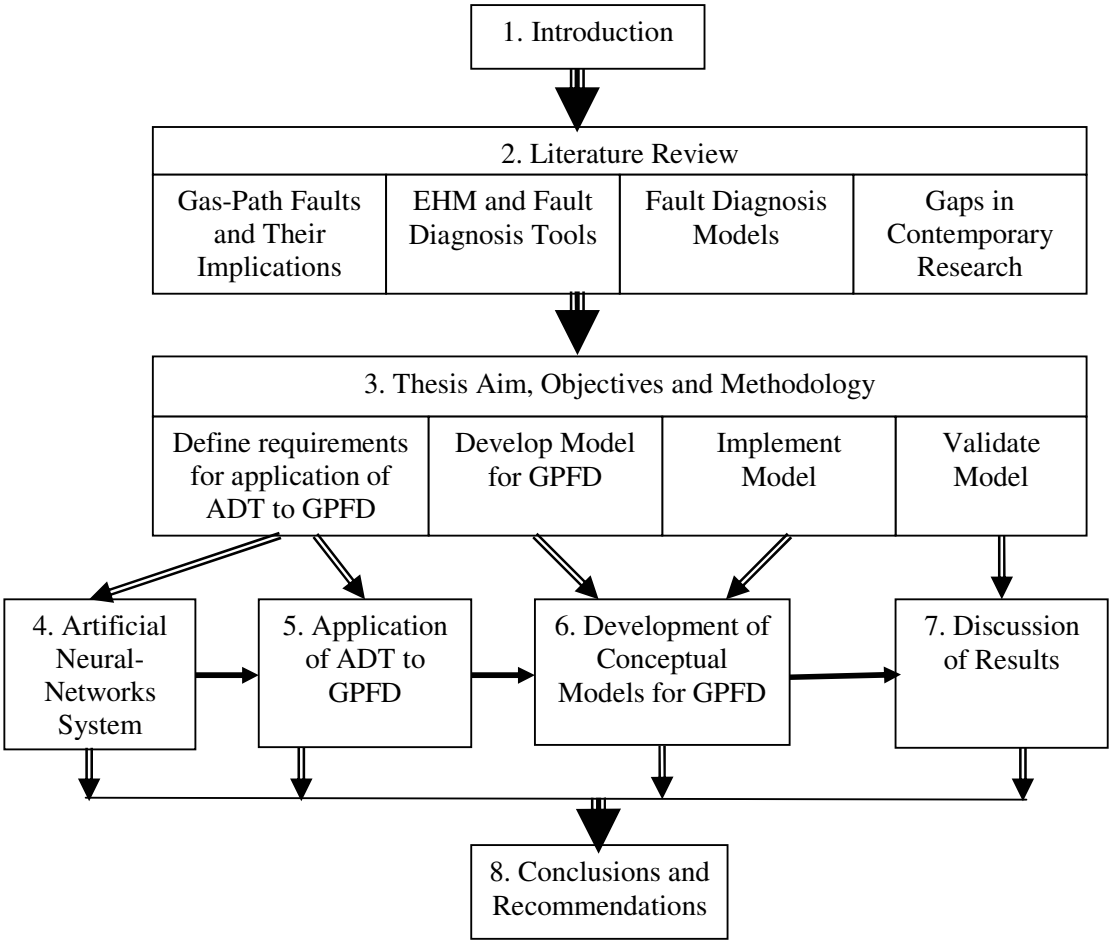

Figure 1.3 Thesis Structure

Chapter 3 presents a brief description of the thesis aim and objectives. The chapter discusses the methodology adopted in conducting this research to ensure that the aim and objectives of the research are met.

Chapter 4 introduces the advanced diagnostic tool – artificial neural networks (ANNs), which would be used in the research. The features and peculiarities of ANNs are discussed.

Chapter 5 considers the requirements for the application of ANN to gas-path fault diagnostics. Background works such as the selection of a sensor set as well as parameter correction relations are developed in this chapter.

Chapter 6 develops and implements conceptual models for gas-path fault diagnosis (GPFD). The philosophies behind the application of the developed framework to sensor and component fault detection are discussed. Four case studies are used to validate the developed GPFD framework. The case studies are used to validate the effectiveness and workability of the diagnostic framework.

Chapter 7 presents the results obtained from the case studies and offers critical analysis of the results.

Chapter 8 presents the conclusions based on this research in addition to outlining the limitations, contributions and directions for future considerations.

1.5 Summary

GTs are widely used for power generation, as mechanical drives for oil, gas industries and as propulsion systems in aero and marine applications. A GT is normally affected by faults that could be present in any one of the three major components of the GT. The gas-path of the GT presents an interesting case to be examined because some faults associated with it usually take considerable time and resources to fix which go to reduce the availability and profitability of such a machine and its operation. Diagnosing the faults in the gas-path of a GT has been the subject of much research interest and this is so because:

- The GT parameter relationships are inherently non-linear and this calls for approaches that would take this into consideration.
- Measurements from the installed sensors have interferences from operational and environmental noises that need to be considered in any analysis.

- One or more sensors could be biased and this has to be differentiated from a component fault.
- Faults could exist simultaneously in more than one component in the gas-path of the GT.
- There is the need to know the quantity of faults present in any faulty component as this information would assist in planning the necessary maintenance actions.
- Development of tools that could be applied even to on-line diagnosis, that is, tools that present fast isolation and quantification of faults, are being sought.

Various diagnostic paradigms have been applied in the past: some are currently applied while others are being investigated for the future. Each technique has its own merits and limitations that will be examined in chapter 2.

Because of the difficulty of obtaining real life data for the analysis in this research, a sufficiently accurate non-linear simulation programme called TURBOMATCH is used for generating all the data including validation data.

Finally, we would like to state that the references cited in this thesis have been arranged alphabetically in the reference section to enable easy location by readers.

CHAPTER 2

LITERATURE REVIEW

2.1 Introduction

GT plays an increasingly important role in power generating and propulsion systems. In chapter 1, it was stressed that various systems of the GT and particularly the gas-path components are subjected to degradations and faults during operation. There are several ways of diagnosing these degradations and faults, some are either in use or are being proposed. The purpose of this chapter is to find solutions to the problems of how to diagnose gas-path fault (GPF) from the literature. To achieve this, the literature is used to provide initial answers to the following questions:

1. What are the issues/problems of GPF?
2. How do they affect the GT operation?
3. What are the diagnostic techniques available and how are they applied to fault diagnosis?
4. Are there any limitations to these techniques?

What follows presents the structure of this chapter. In section 2.2, some of the GPFs and their implications on the operation of the GT are presented. The available diagnostic techniques and their limitations are addressed in section 2.3. Typical diagnostic models are presented in section 2.4. The chapter concludes with an overall assessment of the quantitative approaches setting the scene for the development of an alternative approach. It should be noted that whilst this chapter provides a comprehensive review of diagnostic techniques, the focus of this thesis is on the application of ANN to GPFD.

2.2 GPFs and Their Implications

2.2.1 GPFs

COMPRESSOR
- Fouling
- Blade fatigue
- Blade corrosion/pitting
- Surge promoted by fouling, IGV control and steam injection
- Erosion, Corrosion
- LCF/HCF
- FOD

COMBUSTOR
- Corrosion
- Fretting corrosion
- Cracking
- Fuel Quality
- Nozzle imbalance/clogging
- Leakages
- Vibration and pulsations

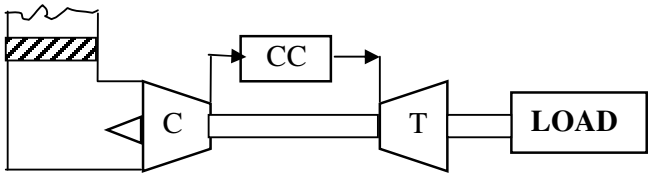

FILTER
- Fouling, Clogging
- Airflow distortion
- Icing problems
- Loss of airtightness
- Humidity effects

MECHANICAL PROBLEMS
- Bearing problems
- Critical speeds
- Unbalance, Looseness and Misalignment
- Foundations
- Rotor bows

TURBINE
- Fouling
- Corrosion
- Blade coating problems
- FOD/DOD
- Bearing distress
- Excessive back pressure
- Erosion, HCF, LCF
- Hot corrosion/sulphidation
- Nozzle bowing, Creep

Figure 2.1 Complexities involved in GT problems

GTs incurs a variety of faults as shown in Figure 2.1 (Meher-Homji et al, 1993). These faults, which can originate from the gas-path components, rotating components or other GT systems affect the component's or overall performance of the engine. The gas-path components can be considered as the compressor, combustor and turbine, but for the purpose of this research, it is limited to the compressor(s) and turbines. The combustor is omitted because its efficiency normally remains constant with time (Diakunchak,

1992; Escher, 1995) and thus its alteration with time does not cause a significant change in the engine's performance parameters, a feature required for GPFD.

A GPF that can be described by directional changes in measurement variables or by its effect on the independent (performance) variables can be diagnosed. Because it is not possible to describe all the possible faults that affect the gas-path of the GT, below is presented the most frequent that account for substantial performance loss during operation of a GT.

Fouling: Fouling is one of the most common causes of engine performance deterioration facing users of GTs (Upton, 1974; Lakshminarasimha et al, 1994) and can account for more than 70% of all engine performance loss accumulated during operation (Diakunchak, 1992). Fouling is the accumulation of foreign and domestic deposits on the blade surfaces causing an increase in their surface roughness, changes in shape of airfoil/airfoil inlet angle and reduction in airfoil throat opening (Zaita et al, 1998; Diakunchak, 1992). Fouling primarily results in mass flow and compressor delivery pressure (CDP) reduction, and ultimately in power reduction and increased heat rate (Aker and Saravanamuttoo, 1989; Lakshminarasimha et al, 1994; Diakunchak, 1992) with a slight change in compressor efficiency (Agrawal et al, 1978). Fouling has been indicated to ensue in 40 - 50% of the compressor stages (Aker and Saravanamuttoo, 1989). Fouled or worn turbine seals result in a loss of efficiency on all turbines available in the gas generator and an increase in engine's exhaust temperature (Urban, 1972, Diakunchak, 1992). There is, however, a limit to fouling, and this is determined by the aerodynamic forces that prevent further deposition on blades (Zaita et al, 1998). Performance deterioration due to fouling is, for the most part, recoverable by cleaning (washing) and a recommendation for cleaning time is when the estimated mass flow decrease reaches the 2 - 3 % level relative to normal operation (Diakunchak, 1992).

Tip Clearance: Increase in tip clearance has the effect of reducing both efficiency and flow capacity. MacIsaac, (1992) reports that for a 0.8% tip clearance increase, an axial

compressor, using fault severity assignment, gave a 3% reduction in flow and a 2% reduction in efficiency; a view corroborated by MacLeod, (1991). This shows a much greater response of efficiency to tip clearance than fouling.

Erosion: Materials exposed to particle impacts are eroded and subjected to deterioration of their surface quality, changes in airfoil profile and throat openings, with increases in blade and seal clearances. With the GT, the result of this on the gas-path component is a decrease in performance. In the compressor, the eroded blade leads to a loss of compressor delivery pressure and mass flow rate (Batcho et al, 1987; Lakshminarasimha et al, 1994). A further influence of erosion is to make the front stages of an high pressure compressor (HPC) and low pressure compressor (LPC) for a multiple-component GT prone to surge. Erosion has been shown to affect the rear stages of a compressor (due to higher pressure in this region) more significantly than the early stages (Zaita et al 1998). Erosion on turbine nozzles/blades has the effect of increasing the turbine flow function and reducing efficiency, and hence output power.

Corrosion: When loss of materials from flow path components is caused by the chemical reaction between the components and contaminants that enter the GT with the inlet air, fuel or injected water/steam, the process is called corrosion (Diakunchak, 1992). Corrosion is experienced more at the hot end with the presence of elements such as vanadium, sodium and lead, enhancing the high-temperature corrosion of turbine airfoils. The effect is a reduction of engine performance.

Object Damage: This is the result of an object striking the gas-path components of the GT. The origin of such particles could be via the inlet section with the working fluid (foreign object damage (FOD)) or particles from the engine itself breaking off and being carried downstream (domestic object damage (DOD)). Here again, the effect is a deterioration of the engine's performance. The fault signature with respect to its effect on performance is sometimes indistinguishable from that of fouling.

From the foregoing, GPFs have their distinct features/signatures on their effects on the independent variables. Some faults may have identical signatures and would require a combination of diagnostic techniques to isolate them.

2.2.2 Implications of GPFs

Besides low - life failures due to poor design or manufacture, creep and fatigue stand out as two important mechanisms for limiting the life of GTs.

The strength of many materials, and particularly metals, is reduced with an increase in temperature. This has been attributed to the fact that prolonged exposure to high temperatures causes a progressive deformation of grain boundaries and other metallurgical instabilities. This phenomenon, called creep or thermal fatigue, passes through three stages before fracture (failure) occurs. Primary creep is usually interpreted as an adaptation stage; secondary creep as the useful life period; while tertiary creep corresponds to decreased resistance due to advanced age. Microscopically, creep failures at higher temperatures result more from inter-granular cracking mode, whilst at lower temperatures it is from trans-granular cracking. The relationship between the power output and deterioration on turbine creep life is shown in Figure 2.2[1]. The time taken for failure to occur in creep is also dependent on the stress and other environmental conditions (corrosion). Information available in the public domain indicates that OEMs normally quote engine life on 100% power at ISO conditions. For an aeroderivative GT, this could typically correspond to 20,000 hours, and even longer for an industrial GT. Most engines rarely operate at full power, and so at 90% power, such an aeroderivative GT with no deterioration will have a creep life of about 5 times that at 100 percent power, that is 100,000 fired hours as shown in Figure 2.2. These figures are lower for a "deteriorated" engine with compressor faults such as fouling, which is shown to be more detrimental to engine life than turbine faults such as erosion.

[1]Gas-path Analysis Limited: http://www.gpal.co.uk/xcreep.htm

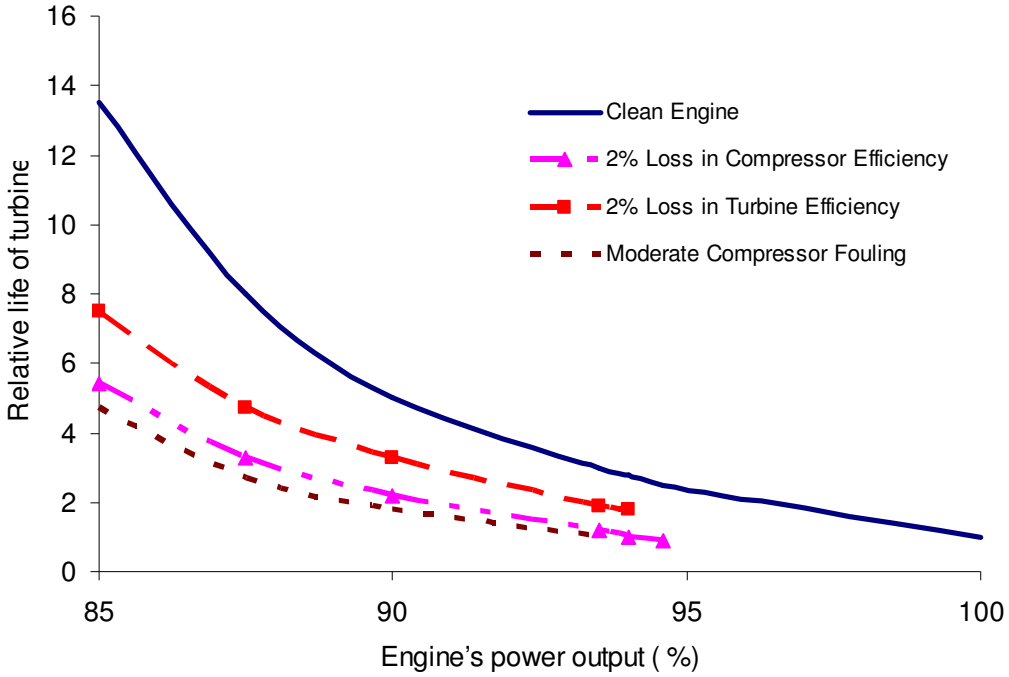

Figure 2.2 Effect of power output and performance deterioration on an engine's creep life

Performance deterioration generally results in reduced power output and higher specific fuel consumption for the same spool speeds and turbine entry temperatures. For an engine suffering from a deterioration of performance, to attain the normal power output, the engine has to be run at higher spool speeds and/or higher turbine entry temperatures. This results in greater rates of fuel consumption and a shorter life-cycle (due to increased creep damage). Berenblut et al, (1982) notes that an increase in hot section temperature of 10-20 ^{o}C would cause a two-fold reduction of blade life. There is obviously a critical temperature beyond which creep failure can result from plastic deformation. It is necessary to note that the creep life, in addition to oxidation, determines the time between overhauls (TBOs) and turbine life usage manifests itself by creep damage.

The availability of an engine is directly proportional to the time taken to get it back from an undesirable to a desirable state of functionality. Singh, (1999) presented the availability levels for the case of a GT (Figure 1.2). With competitive pressures, a number of design advances are applied to various components of a machine. The high cost of the gas-path components coupled with the low likelihood that they will be required means that they are often not held as spares. In the case of damage/fault, manufacture of such spare components can take several weeks. This is an undesirable situation especially when viewed from the perspective of costs induced by downtime. The frequency of this occurring can be reduced by the use of an effective diagnostic tool to monitor the performance of the GTs. Other implications of GPFs include:

- Possible spread of damage to engine parts hitherto not faulty.
- Danger posed by such a faulty machine to operators and other personnel.

2.3 Engine-Health Monitoring and Fault-Diagnosis Tools

The previous section considered some of the faults that affect the gas-path of a GT. These faults ranged from those that leave permanent damage on the affected engine component i.e. foreign object damage, to those that are recoverable by washing i.e. fouling. When faults exist, there is every need for them to be diagnosed so that the necessary maintenance actions can be carried out and hence unnecessary damage to the plant avoided.

This section describes the available engine-health monitoring (EHM) techniques and highlights their advantages and disadvantages. EHM, also called engine-condition monitoring (ECM), can be viewed as a process or group of techniques that are geared towards ensuring the continuous functioning of an engine. Saravanamuttoo, (1992) described EHM as an ambitious system with the prime goal of diagnosing deterioration and identifying the faults. This view is corroborated by other contributors to the field (Stamatis et al, 1990).

The type or choice of EHM to adopt from the perspective of the user would depend on several factors, which include:

- Initial cost of acquisition
- Potential savings in cost with use
- Importance of operation
- Proven reliability of the monitoring system
- Nature of component or equipment

Despite these considerations, the need for an EHM process cannot be overemphasised, especially when viewed from the accruable benefits amongst which are:

- Prevention of catastrophic failure
- Improved safety
- Reduced maintenance and downtime cost due to early detection of possible failure
- Increased availability
- Prevention of trial-and-error in fault diagnosis, that is, an uncertain kind of fault fixing especially when such involves the change of components with the view to seeing if it works or not and so on. This invariably implies that work scope is defined.

Given that the components of a GT can simply be grouped under three categories that is gas-path, accessory equipment and rotating machinery, then, the monitoring required by each of these would be different with the effect that an overall EHM would comprise the sub-component EHMs.

EHM has given rise to one of the maintenance paradigms known as condition based maintenance (CBM) which supports that machines should be maintained only when they are found to be distressed, not when they are completely damaged, like breakdown maintenance nor on a periodic basis, like planned preventive maintenance.

Various fault diagnostic techniques are either currently in use or are being proposed. These approaches can be classified either as qualitative or quantitative or as conventional or evolving. If we adopt the latter classification method, then we have such techniques as visual inspection, fault trees, fault matrix, vibration analysis and GPA approaches that are based on the least-squares algorithm as belonging to the conventional approach. Then the techniques based on artificial intelligence such as expert systems (ES), fuzzy logic (FL), genetic algorithms (GA) and artificial neural networks (ANNs) belong to what we have called the "evolving" approaches. The conventional approaches have been well researched but the evolving approaches are still generating more research interest and could be at the dawn of its general acceptance by users.

2.3.1 Conventional Approaches

The classification of conventional approaches includes all such diagnostic techniques that have been and are still in use at the moment. Amongst the identified EHM techniques that fall under this category are:

- Visual inspection
- Fault tree
- Fault matrix
- Trend analysis
- Vibration monitoring
- GPA

The principles behind each of these approaches are described as well as their limitations in implementing their intended task.

2.3.1.1 Visual Inspection

This is an EHM technique that relies on visible changes on an engine to detect faults. Visual inspection can be carried out externally or internally where the former helps to

detect leaks of gas, oil, fuel, and defects on accessory and control linkages, the latter is used to detect cracks, tears, burns, deposits, corrosion, deformations amongst others. The methods applied in visual monitoring include the use of light probes, boroscopes and endoscopes, stroboscopes, dye penetrants, infrared thermography, X-ray and γ- ray examinations, and thermographic paints.

Advances in visual monitoring have resulted in repairs being made on otherwise inaccessible sections of the engine without disassembly and installation of video systems that provide real-time images of the section being inspected. The more sophisticated EHM techniques normally require a visual inspection to be done before a decision is taken on their diagnosis. However, visual monitoring results require experience to interpret them and in some cases results may be subjective.

2.3.1.2 Fault Tree

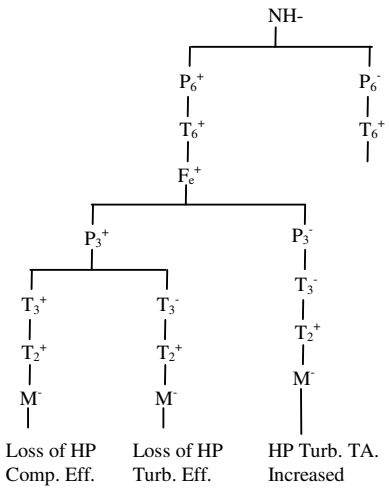

Figure 2.3 Example of a Fault Tree (Singh and Escher, 1995)

Fault tree is one of the oldest EHM techniques. Its logic is based on fault identification through tracking its features on an established map of fault patterns (Figure 2.3). It is synonymous with moving from a root directory (changed parameter) through various

subdirectories (associated changed parameters) until the probable physical fault is identified. The shortcomings of this method are:

- It is mechanical
- It can only be used effectively by experienced hands
- It is applicable only to single-fault identification/situations
- It provides qualitative rather than quantitative values
- It does not consider the existence of a sensor fault

2.3.1.3 Fault Matrix

This EHM technique sometimes called the fault-coefficient matrix (Figure 2.4) relies on comparing changes in dependent (measurable) variables with pre-calculated directional deviations of such variables to ascertain the best match from a library of tabulated faults. This technique can be applied primarily to single faults. With limited measurements, attempts to use this method on a fault situation involving more health indices (independent variables) than measured variables may end up with a wrong diagnosis as similar fault-signatures may be presented by a combination of faults. Dupuis et al (1985) suggests that for a stationary GT, a possible solution to this dilemma is the use of two fault matrices, one based on constant gas generator speed and the other on constant power.

Type	**Fault**	**TIT**	**SOP**	**m_f**	**CPR**	**Vibration**	**Indication**
Turbine(Generator)	Rotor Damage	↑	↑	↑	↑	Yes	η_t Low
	Nozzle Erosion	↑	↑	↑	↓	No	Γ_t High
Turbine (Power)	Rotor Damage	0	↓	0	0	Yes	η_{tp} Low, EGT High
	Nozzle Erosion	↓	↓	↓	↓	No	Γ_{tp} High
Compressor	F.O.D.	↑	↓	↑	↓	Yes	η_c Low, m_1 Low,
	Dirty	↓	↓	↓	↓	No	η_c Low

Figure 2.4 Example of an Engine Fault Matrix (Singh and Escher, 1995)

2.3.1.4 Trend Analysis

Observations on trended parameters/measurements are recorded against time. This would entail keeping stacks of history cards manually or otherwise for each machine component. In addition to this fact, results from this technique are qualitative and appropriate scheduling of maintenance is not easily achieved.

2.3.1.5 Vibration Monitoring

Vibration monitoring is one of the techniques applied to rotating machinery diagnosis with which some gas-path components can be associated.

Vibration is a periodic motion about an equilibrium position and it is a significant cause of failure or malfunctions in machines especially those with high speed rotating components like the GT. A survey of 13 plants as presented by Lifson et al, (1989) shows that vibration related outages are responsible for approximately 3.3% of all unavailable operating hours and 4.2% of all outages.

A vibration monitoring system (VMS) is made up of vibration measuring elements, interconnecting cable assemblies, processing electronics and display system. To detect and diagnose vibration related problems, it is necessary that selected transducers should be able to measure the vibration (machine housing or shaft) most likely to reveal the expected failure characteristics (Lifson et al, 1989). In vibration measurement, transducers such as eddy current probes, velocity pick-ups, accelerometers, dual probes and a combination of several other transducer types may be employed. The eddy current probes are used to ascertain rotor related malfunctions such as imbalance, misalignment, shaft bow and fluid film bearing instability problems. Velocity pick ups and accelerometers are applied to bearing housing related problems such as bearing failure, support looseness, casing or foundation resonance's, loose parts and gear or blade problems amongst other possible uses. Lifson et al, (1989) has provided a summary of

the advantages, disadvantages, and applications of the various transducer types used for GT vibration monitoring.

The subject of vibration measurements is a complex issue. Forces causing vibration in a GT change in amplitude and direction according to the rotational speed of the concerned parts. The problem then lies in the fact that different component faults generate different frequencies or spectra of vibration, which are themselves a constituent of different frequencies. A form of solution thus lies in transforming this time domain complex waveform (plot of amplitude against time) into a series of discrete sine waves in the frequency domain (plots of amplitude against frequency) using fast Fourier transforms (FFT) or other amenable techniques. Figure 2.5 displays these different domains.

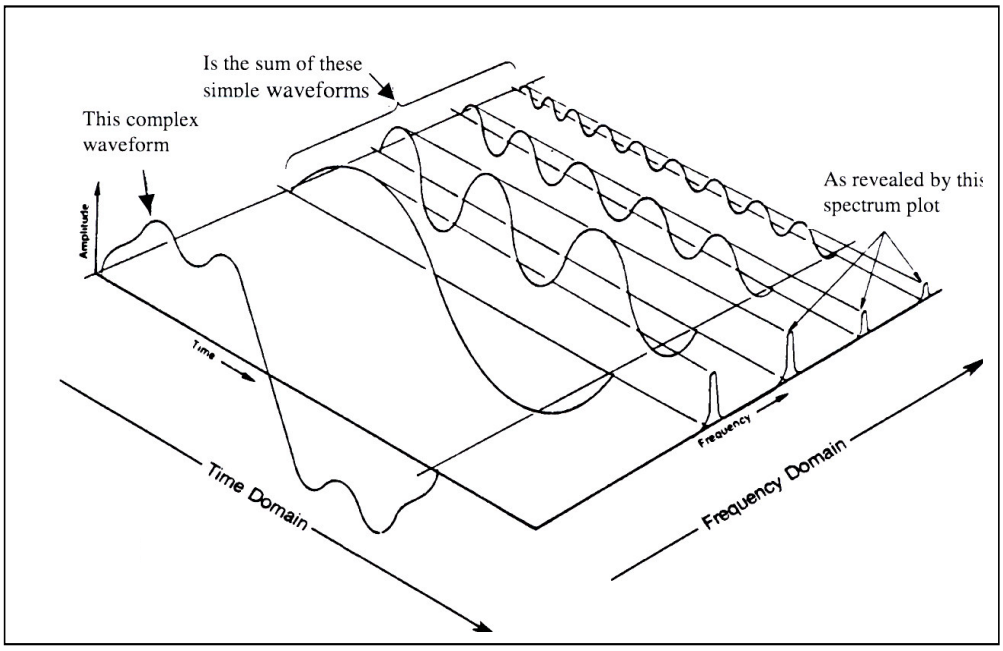

Figure 2.5 Time and Frequency Domains

The effectiveness/suitability of a transducer as a vibration monitoring devise is hinged on its frequency bandwidth, environmental factors (operational temperature and noise

limit), and positioning/mounting required. The shaft vibration levels for fault diagnosis can be obtained either from absolute shaft vibration levels or from relative shaft displacements. While the former combines vibration readings from eddy current probes to those of the seismic probes the displacement of the latter detects a vibration problem and the readings from seismic transducers are then used to diagnose the cause of the problem (Lifson et al, 1989). It is obvious that relative data are more accurate than absolute values as they tend to eliminate environmental effects like vibrations emanating from the mounting that are error sources. In general, when vibration levels or rms. vibration velocity are extracted, the relationship with the vibration energy and hence the vibration damage potential is determined (Tsalavoutas et al, 2000, Meher-Homji et al, 1992).

Amongst the techniques of vibration analysis, is spectral analysis. Spectral signatures, which show the difference between a spectrum with fault and a healthy spectrum, are compared to the signature of specific faults – implying the existence of a fault signature database - using such techniques as Neural networks in pattern recognition to diagnose the specific fault. Other vibration analysis techniques are proximity analysis (for basic shape defects), orbital analysis (for identifying unbalance and misalignment defects from X and Y motion of rotor), time waveform (provides information on the physical behaviour of the entire machine), and phase analysis.

Due to large variations of possible vibration related malfunctions in a GT and since there is the possibility for allowable vibration levels to vary for the different OEMs product, setting an ‘across the board’ limit beyond which a machine should be taken out for repairs due to excessive vibration may not be the right thing to do, as the level of vibration considered by one OEM to be detrimental may be absolutely normal for another OEM. The suggestion thus is that the OEM is in the best position to offer information on acceptable and unacceptable levels not excluding inputs from users’ experience. There are also available guidelines/recommendations from international standards organization on this issue. Lifson et al, (1989) presented a possible working

range of vibration levels including alarm and shutdown limits obtained from statistical data. Even with the foregoing, another perceived difficulty in limit setting is the large amplitude changes that occur near resonance and the associated difficulty in predicting the precise frequency at which a resonance will occur. “Speed bands” are frequently used to address this problem (Doel, 1990).

Industrial GT vibration levels are directly proportional to the shaft bearing clearances and vibrations of aeroderivative GTs are reported to be highest in the gas generators and lowest in the free turbine. In addition, there is the tendency for vibration levels to increase with usage and deterioration.

For a vibration monitoring system to be justifiable, its overall cost must be less than the accruable benefit. It can be argued that the cost of a vibration monitoring system would be more than written off if just one catastrophic failure is detected and prevented over the lifetime of a GT unit. A vibration monitoring system that is properly designed to anticipate and, manage vibration related problems is obviously an indispensable aspect of an overall predictive EHM program.

2.3.1.6 Gas-path Analysis (GPA)

This technique of EHM has received a lot of focus as it lends itself to diagnosing faults in the gas-path components. It is possible with this method to obtain quantitative values for multiple faults from which a scheduled maintenance - pre-assembly of man and materials - can be arranged. Its logic depends on using the measurable data from the engine gas-path (dependent variables) to determine changes in the component characteristics and mass flows (independent/primary performance variables) from which the presence or otherwise absence of a fault(s) can be established.

The consistency of the entire system is hinged on the credibility of the data used (Agrawal et al, 1978). One of the potential sources of data inconsistency is data non-

repeatability and notable causes of this could be bias and noise that set in from calibration and operating environment. The limitations of such technique thus lies on the robustness of its design and data used. Available techniques for assessing gas-path problems include linear GPA, non-linear GPA, weighted least-square algorithm, Kalman filters and artificial intelligence techniques such as, Expert Systems, Fuzzy logic, Genetic Algorithms and Neural Networks.

GPA provides the basis for the machinery-monitoring scheme at the component level rather than at plant level. In what follows, we present a brief review of the principles behind GPA and then go on to consider some forms of its applications to GPFD. The use of artificial intelligence is considered in section *2.3.2: Evolving Approaches*, and is thus tagged because they are still in the process of being widely applied in the diagnostic industry.

a. GPA Basics

In the course of its useful life the gas containment path of a GT is susceptible to encountering a wide variety of physical problems which were presented earlier. GPA has as its aim, the detection, isolation and quantification of some of the GPFs that have observable impacts on the measurable (dependent) variables. This implies that those faults, such as blade cracks that cannot be implicitly detected via these measurable variables, as well as those failures that occur suddenly, such as fracture, cannot be analytically identified by GPA.

The primary use of dependent parameters to isolate GPFs is premised on the fact that primary performance parameters or independent variables such as component flow capacities and efficiencies are not directly measurable. They are thermodynamically correlated to the dependent variables, such that changes in the latter are induced by changes in the former, with the possibility of accurately identifying the faulty component(s) hinging on the choice of measurements taken. The basis of GPA is

represented diagrammatically by Figure 2.6. It should be stressed that any parameter in itself is not necessarily indicative of fault in any particular element. For example, at any given rotor speed, a change in compressor discharge pressure does not mean there is a compressor fault. The change may also have been due to a turbine fault.

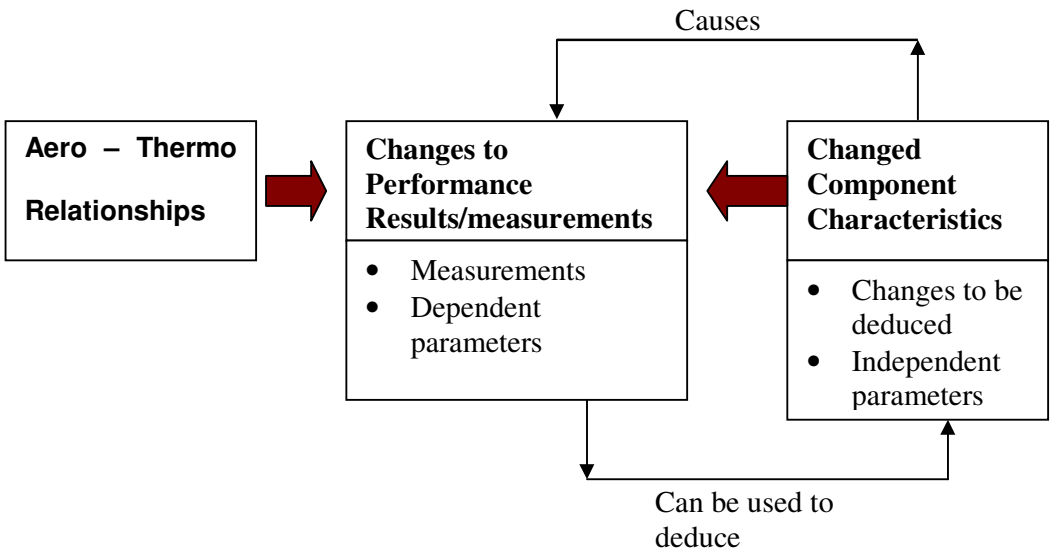

Figure 2.6 Principle of GPA

The implementation of GPA as an EHM system has been limited to some extent by the sensor component (Hall et al, 1997). Sensors lack robustness, their placement positions in the turbine in most cases are sub-optimal, their suite selection is ineffective with respect to the required array of faults to be identified and the results of these are high fault alarm rates. In response to some of these sensor problems, GPA programmes are designed to provide relative rather than absolute answers, in fact, the ability to cope with large deviations of performance values from baselines has been viewed as the single most important feature of GPA programmes (Doel, 1994). However, it will not be out of place to note that most GPA programmes do not meet up with this requirement.

The classical GPA technique presented by Urban (1972) popularly tagged the 'linear GPA approach' fell short of effective diagnosis because of the linearization built into it and the non consideration of measurement errors and biases. Thus improvements to this model were sought. One of such is the weighted-least-squares, which has been reported to be the predominant technique adopted by major OEMs (Doel, 1997, Stamatis et al, 1992). With the basic weighted-least-squares algorithm as the kernel, OEMs attach additional packages to achieve their desired goals. For instance, Rolls Royce is said to offer a "concentrator" module to emphasise module problems, General Electric provide "fault logic" to improve diagnostics of large component or measurement faults while Hamilton Standards provides a "large measurement and error recovery algorithm" (Doel, 1994b referencing Volponi, 1982).

Finally it needs be stated that in addition to fault detection and quantification, GPA can also be used for:

1. Identification and use of appropriate measurement selections that are sensitive to the desired faults.
2. Selection of health factors or state variables or independent variables that portray the fault with least root mean square (RMS) error of estimation.

b. Approaches to GPA

The approaches to GPA studies can be viewed from a number of perspectives, linear and non-linear GPA techniques, weighted-least-squares approach and Kalman filtering. In what follows we briefly discuss each of these approaches to GPA. As stated earlier, other approaches involving the use of artificial intelligence would be presented subsequently.

(i). Linear GPA Method

The emergence of the linear analysis approach to deterioration studies has been attributed to the works of Urban (1974) while working for Hamilton Standards

(MacIsaac, 1992). In principle, linear GPA (LGPA) depends on the first approximation/derivative of the Taylor series expansion of the governing equations describing the performance of a GT over a specific point/range to produce the fault coefficients. A vector of deltas of some measurable performance parameters are used with the fault coefficient to obtain deviations of some parameters called independent variables via some system of matrix inversions. This relationship is expressed simply as:

$$\delta y = [J]\, \delta x \qquad \text{hence,} \tag{2.1}$$

$$\delta x = [J^{-1}]\, \delta y \tag{2.2}$$

Where δx are the changes in the independent parameters

δy are the changes in the dependent parameters

J is called the influence coefficient matrix (ICM), and

J^{-1} is the fault coefficient matrix (FCM).

Limitations of this methodology are –

- Rates of deterioration are not possibly linear. The assumption of linearity presents us with unrealistic levels of deterioration outside a defined range.
- It is unable to handle or cope with large changes arising from a specific fault (MacIsaac, 1992). Since the algorithm is linear in the measured variables, the solution error is proportional to the measurement deviations thus better results can only be obtained with small deviations (Doel, 1994a, Kamboukos, and Mathioudakis, 2003).
- It requires a large number of measurement suite for analysis since below a certain number of instrumentation level, convergence to a solution is not obtained.
- LGPA does not consider sensor faults and measurement noises.

(ii). Non-linear GPA (NLGPA) Method

This is an improvement on the LGPA method and basically involves further recursive use of LGPA. This process reduces the residual errors between estimations and actual

fault. NLGPA approach was developed in Cranfield University (Singh and Escher, 1995; Escher, 1995). Baselines of measurable performance parameters are established via matching type calculations and effects of variation of some critical parameters on these baselines used to generate a fault matrix. This process is illustrated diagrammatically in Figure 2.7 while the mathematical formulation of this method is given in APPENDIX A.1.

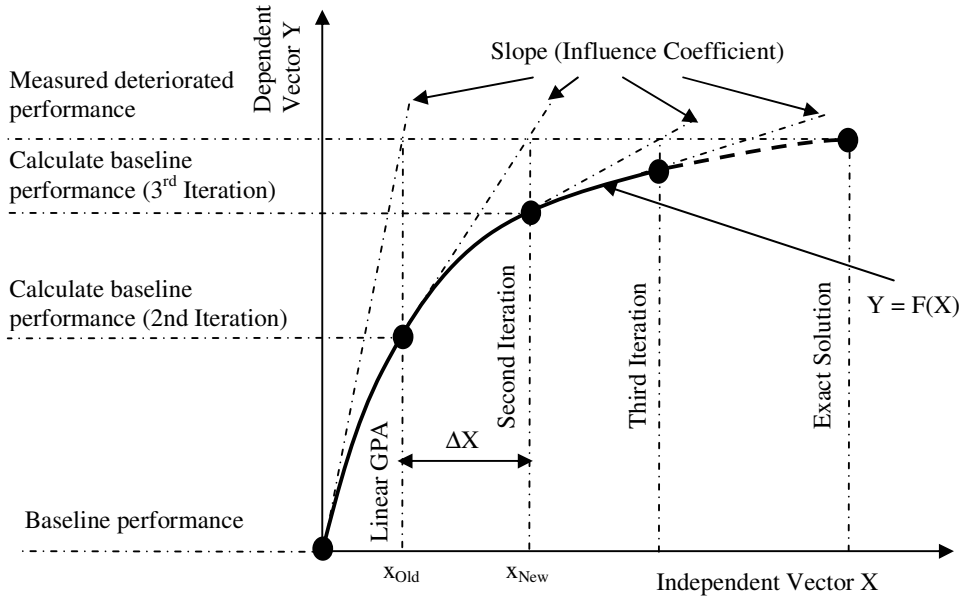

Figure 2.7 Simplified illustration of Linear and Non-Linear GPA methods

A reported advantage of this method (Escher, 1995) is its ability to handle abrupt changes in measurements caused by operational damage. However, amongst its perceived disadvantages are:

- The fault matrix generated if not interpreted is difficult to apply except by highly trained personnel
- Measurement faults and sensor bias are not considered in this technique.

- Experience from use shows that the programme does not converge to a reasonable set of results for large variation in component faults.

(iii). Weighted Least-squares (WLS) Method

The method of least-squares was invented by a "young revolutionary" in his day, Karl Friedrich Gauss (Sorenson, 1970). Gauss was 18 years old at the time of his first use of the least-squares method in 1795. Gauss (1963) defined the least-squares method in the following manner: "…*the most probable value* of the unknown quantities will be that in which the sum of squares of the differences between the actually observed and the computed values multiplied by numbers that measure the degree of precision is a minimum". The difference between the observed and computed measurement values is generally called the *residual*.

A GPA solution from a weighted-least-square perspective is obtained from a linear function of the differences between the measurements and their predicted values. The gain matrix used in computing the solution of the problem may be obtained from the influence coefficient matrix (ICM) and assumed variances from state variables and measurement errors. There is also the possibility to obtain the gain matrix without knowledge of the measurements (Doel, 1994b) using the weighted-least-squares algorithm on specific faults, since there is the basic assumption that sensors respond appropriately to component deterioration, that is, temperature and pressure probes mounted on a compressor should be able to give an indication of the state of health of the compressor. The mathematical formulation of WLS algorithm as presented by Doel (1994a and 1994b) is outlined in APPENDIX A.2.

WLS analysis is a quantification tool that estimates efficiencies and flow capacities of a GT component including the measurement error leaving the burden of deciding the significance or otherwise of a deviation – such as to warrant taking out equipment for maintenance – to the user. It has been shown that weighted-least-squares techniques can

be used to reduce the sensitivity to errors (Urban, 1980; Volponi, 1982). The strengths and weaknesses of the WLS approach would be presented when a specific model of its application, called TEMPER is described in section 2.4.2.

(iv). Kalman Filtering

Kalman (1960) in his first paper on discrete-time, recursive mean square filtering presented a system of equations that were not only extremely convenient for digital computer implementation but also posed the estimation problem in a general framework that has had a unifying influence on known results. The Kalman filter, as his equations came to be known, provides an estimate of the state of the system at the current time based on all measurements of the system obtained up to and including the present time. It represents essentially a recursive solution of Gauss' original least-squares problem. The basic difference between the least-square method and the Kalman filter is that while the latter allows for state changes from one time to the next, the former requires that the equation of motions must be exact descriptions, and therefore the problem of dynamic modelling is raised. Sorenson (1970) argues that this difference is nontrivial requiring a modification to the least-squares framework such that noise is considered as the error in the plant model at each stage.

Basic assumptions of the Kalman filter include:

- The systems are linear
- Noise is independent from one sampling time to the next
- The noise and initial state of the system are assumed to be Gaussian

The summary of the Kalman filtering problem and its solution as given by Sorenson (1970) are hereby presented. Two essential ingredients of the system are the state assumed to be described by:

$$\mathbf{x}_{k+1} = \mathbf{\Phi}_{k+1,k}\mathbf{x}_k + \mathbf{w}_k \tag{2.3}$$

and the measurement data related to the state by:

$$\mathbf{z}_k = \boldsymbol{H}_k\mathbf{x}_k + \mathbf{v}_k \tag{2.4}$$

where $\{\mathbf{w}_k\}$ and $\{\mathbf{v}_k\}$represent independent white noise sequences (that is they are both mutually independent and independent of $\mathbf{x}$) with zero means.

Φ is the identity matrix which defines how $\mathbf{x}$ varies over time.

$\mathbf{x}$ is the state vector.

$\boldsymbol{H}$ is the system matrix

The estimate of the signal:

$$\mathbf{s}_k = \boldsymbol{H}_k \mathbf{x}_k \tag{2.5}$$

is given by

$$\hat{\mathbf{s}}_{k/k} = \boldsymbol{H}_k \hat{\mathbf{x}}_{k/k} \tag{2.6}$$

One way of obtaining the solution of this recursive, linear, mean-square estimation problem is given below. The estimate is given as the linear combination of the estimate predicted in the absence of new data, or

$$\hat{\mathbf{x}}_{k,k-1} = \Phi_{k,k-1} \hat{\mathbf{x}}_{k-1/k-1} \tag{2.7}$$

and the residual $\mathbf{r}_k$. Thus the mean square estimate is

$$\hat{\mathbf{x}}_{k/k} = \boldsymbol{\Phi}_{k,k-1} \hat{\mathbf{x}}_{k-1/k-1} + \boldsymbol{K}_k \left[\mathbf{z}_k - \boldsymbol{H}_k \boldsymbol{\Phi}_{k,k-1} \hat{\mathbf{x}}_{k-1/k-1} \right] \tag{2.8}$$

The gain matrix $\boldsymbol{K}_k$ (weighting matrix used to update state estimates from observations) can be considered as being chosen to minimise

$$E\left[\left(\hat{\mathbf{x}}_k - \hat{\mathbf{x}}_{k/k} \right)^T \left(\hat{\mathbf{x}}_k - \hat{\mathbf{x}}_{k/k} \right) \right]$$

and is given by

$$\boldsymbol{K}_k = \boldsymbol{P}_{k/k-1} \boldsymbol{H}_k^T \left(\boldsymbol{H}_k \boldsymbol{P}_{k/k-1} \boldsymbol{H}_k^T + \boldsymbol{R}_k \right)^{-1} \tag{2.9}$$

where $\boldsymbol{R}$ is the measurement repeatability covariance matrix.

The matrix $\boldsymbol{P}_{k/k-1}$ is the covariance of the error in the predicted estimate and is given by

$$\boldsymbol{P}_{k/k-1} = E\left[\left(\mathbf{x}_k - \hat{\mathbf{x}}_{k/k-1} \right) \left(\mathbf{x}_k - \hat{\mathbf{x}}_{k/k-1} \right)^T \right]$$

$$= \boldsymbol{\Phi}_{k/k-1} \boldsymbol{P}_{k-1/k-1} \boldsymbol{\Phi}_{k,k-1}{}^{T} + \boldsymbol{Q}_{k-1} \tag{2.10}$$

The $\boldsymbol{P}_{k/k}$ is the covariance of the error in the estimate $\hat{\mathbf{x}}_{k/k}$.

$$\boldsymbol{P}_{k/k} = E\left[\left(\mathbf{x}_k - \hat{\mathbf{x}}_{k/k}\right)\left(\mathbf{x}_k - \hat{\mathbf{x}}_{k/k}\right)^{T}\right]$$

$$= \boldsymbol{P}_{k/k-1} - \boldsymbol{K}_k \boldsymbol{H}_k \boldsymbol{P}_{k/k-1} \tag{2.11}$$

Equations (2.8), (2.9), (2.10) and (2.11) form the system of equations that make up the Kalman filter in its full recursive form (Sorenson, 1970; Provost, 1994).

To reduce approximation errors associated with the KF, the so-called "extended Kalman filter, EKF" is generally used in practice (Sorenson, 1970). In this case the nonlinear system is linearized by employing the best estimates of the state vector as the reference values used at each stage for linearization.

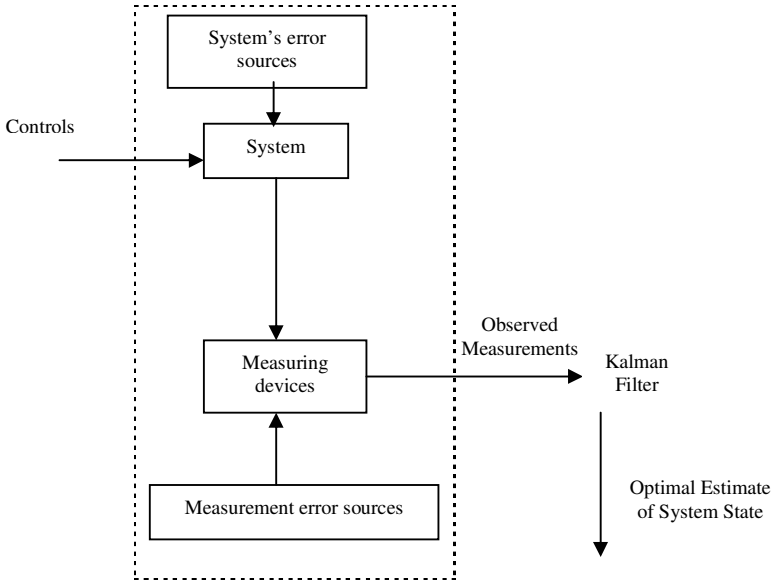

Figure 2.8 A typical Kalman filter application

Kalman filter concepts have been applied to aspects of engine performance and diagnostics with a typical application principle shown in Figure 2.8.

2.3.2 Evolving Approaches

With great strides being taken to make science function with some degrees of independence, incursions have been made into the biological sciences to abstract from some of its features and develop high level systems. Artificial intelligence (AI), branching out into such areas as Expert Systems, Fuzzy Logic, Genetic Algorithm, and Neural Networks amongst others has been the result. The sequel will seek to present a basic overview of these AI tools that are being applied in GT fault diagnostics. It is necessary to note here that some school of thought do not consider Genetic Algorithm as an AI based technique but classify it as an optimisation based approach.

2.3.2.1 Expert Systems

The various techniques of EHM in one way or the other either has similar patterns of approach or are complimentary. It is possible to use one technique to obtain outputs in engineering terms such as efficiency, flow function, vibration levels, and another technique for the interpretation of such data. This aspect of assisting in data interpretation via rules or otherwise is one of the possible areas of application of expert systems (ES).

The development of ES has been one of the leading goals of artificial intelligence (AI). ES attempt to emulate the type of reasoning about real world problems, a task normally performed by human specialist or experts. ES technique of approximate reasoning have been implemented in a wide variety of fields such as medical diagnosis, chemical analysis, computer architecture design, planning systems, tactical threat assessment, and situation assessment for military applications. Recent works have shown that they can be applied (equally) to EHM and fault diagnostics (Doel, 1990; Ali et al, 1990; Torella et al, 1993, 2000; DePold and Gass, 1999; Spina et al, 2002). As a typical application of ES to the fault diagnostic domain, Torella et al (1999) discussed the application of ES for the diagnosis and troubleshooting of GTs apparatuses from a probabilistic

relationship between failures (causes) and symptoms (behaviour) since an observed symptom could be the result of a number of causes having different degrees of probabilities and vice versa. The developed model was coded as belief networks (graphs formed by nodes representing faults and symptoms with arcs used to link and represent the probabilistic dependencies among them). In any case, the results from ES are generally qualitative.

An ES brings to bear a knowledge base (which represents faults, algorithms, and heuristic relationships) about the domain of application on the control structure or inference engine. What is implied is that, facts are matched to patterns in a process called pattern matching with the underlying mechanism leading to an interpretation via an inference engine.

A sample rule is conceptually indicated as:

IF (fact)	**THEN** (action)	**ELSE** (alternative action)
Condition	consequence	alternative consequence

which interpretation could be: the verification or not of a fact (**IF**) leads to the firing of an action (**THEN**) or other action (**ELSE**) respectively.

Most ES are developed on shells which could be broad based such as CLIPS (C language integrated production systems) or tailored to meet specific objectives such as General Electric's GEN-X (GENeric eXpert system), which is their platform for developing diagnostic packages.

Initial attempts to integrate ES – incorporating procedural maintenance for diagnosed faults – with GPA failed predominantly from insufficient instrumentation set to permit a meaningful modular diagnosis and also from insufficient PC power at that time (Doel and Lapierre 1989, Doel 1990). Thus, considerations necessary for the use of ES include:

- A determination of the scope of problem the system will be expected to address
- The expected symptoms of such problems

- Model of the knowledge to be codified
- Language in which to express the model
- Ways of representing the knowledge in that language
- Verification and validation of rules used in constructing the system else inferences from such a system would be erroneous.

Addressing some of these will require a history of observed or conceivable problem scenarios with enough instrumentation to detect associated patterns for such scenarios.

In synopsis, ES can be well applied as an inference engine in a diagnostic setup using rules and possibly incorporating probabilistic features (range of possible causes) for observed symptoms. This inherent advantage especially with respect to GPFD would be better enhanced when integrated with such tools as GPA and/or ANNs which will generate the required symptoms for the expert system to use in diagnosing the cause(s) and if required the possible maintenance steps to be carried out.

2.3.2.2 Fuzzy Logic

Fuzzy logic is currently growing in the number and variety of applications, with applications areas ranging from finance to earthquake. From a narrow sense, FL is a logical system, which is an extension of multivalued logic and is expected to serve as logic of approximate reasoning but in a wider sense, FL is more or less synonymous with the theory of fuzzy sets, that is, a theory of classes with unsharp boundaries. In more specific terms therefore unlike classical logical systems, FL aims at modelling the imprecise modes of reasoning that play an essential role in the human ability to make rational decisions in an environment of uncertainty and imprecision (Zadeh, 1988). This ability in turn depends on our ability to infer an approximate answer to a question based in a store of knowledge that is inexact, incomplete, or not totally reliable. In FL, everything, including truth, is a matter of degree and thus exists between and including the two extremes available in classic logic.

Practical application of FL has been more popular in knowledge based control systems with almost all industrial applications of this technique attributed to Japanese companies (Zadeh, 1988; Isik, 1991). In GT diagnostic, very few materials are available in the public domain on the application of FL. Ganguli (2001a and 2001b) applied FL to isolate single GT module faults. Inputs to the FL system are measured deltas and outputs are engine model faults. The results showed FL to have good success rates except for the IPC and HPC where fault isolation accuracies were given as 97% and 94% respectively. Marinai et al (2003) applied FL technology to GPFD of a three-spool turbofan engine. The system is designed to isolate and quantify single component faults. Results from tests carried out on the IPC showed good fault estimation capabilities.

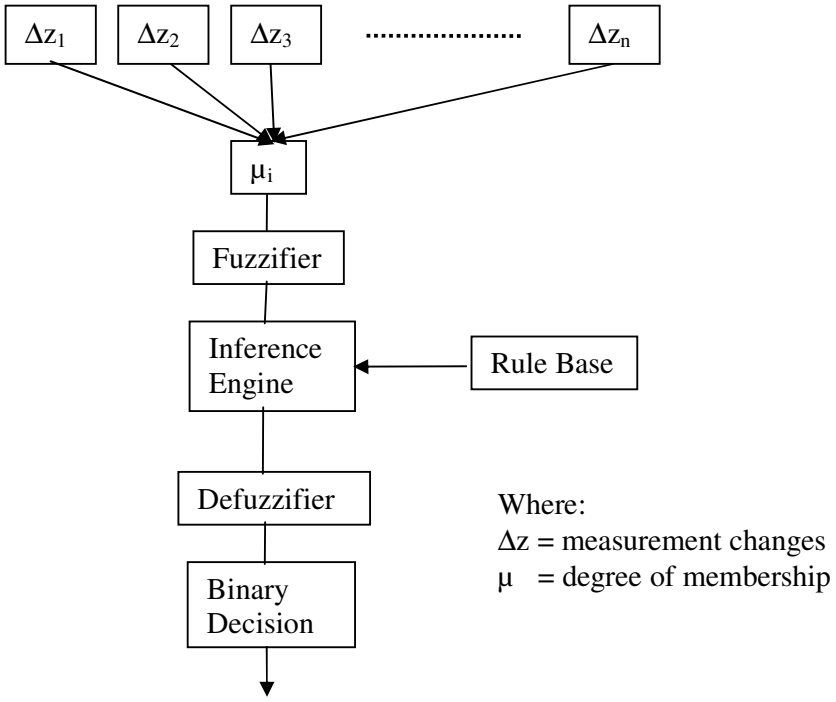

Figure 2.9 Representation of fuzzy system for trend shift detection

A typical FL system for diagnostics, maps definite input to definite outputs using four basic components: rules, fuzzifier, inference engine and defuzzifier as shown in Figure

2.9 (Ganguli, 2001a, 2001b). Once rules driving the FL system have been fixed, the FL system can be expressed as a mapping of inputs to outputs. The fuzzifier maps definite input numbers into fuzzy sets while the inference engine maps the fuzzy sets to fuzzy sets and determines the way in which the fuzzy sets are combined. If clear and definite numbers are required as output, a defuzzifier is used to calculate crisp values from the fuzzy values.

From the foregoing we would agree with Isik (1991) that FL offers solutions to problems where concepts are subjective, quantities are known only imprecisely and system models are descriptive rather that analytic. Limitations of a FL system then lie in:

- The degree of subjectiveness from which terminal data sets (TDS) or answers are derived from initial data sets (IDS).
- The number of rules that need to be executed for decision/answers to be reached.
- The length of time required to arrive at a decision especially for activities with critical reaction times.
- The relative ease with which codes can be maintained especially for complex applications.
- The degree of stability of the designed system since it would be close to impossible to apply well-known system analysis techniques to ascertain this (Isik, 1991).

2.3.2.3 Genetic Algorithms

Genetic algorithms (GA) have been described as search algorithms based on the mechanics of natural selection and natural genetics (Goldberg, 1989). They combine survival of the fittest among string structures with a structured yet randomised information exchanges to form a search algorithm with some of the innovative flair of human search. They are said to be robust in that when compared with other traditional optimisation and search methods as calculus based methods, enumerative schemes and

random search algorithms, they create a balance between efficiency and efficacy necessary for survival in many different environments. This is said to be enhanced by the fact that:

- GAs work with a coding of the parameter set not the parameters themselves.
- GAs search for a population of possible solutions (strings) rather than a single solution to be upgraded iteration by iteration. The feature of global searching makes it less likely than calculus based methods to get stuck in a local minimum rather than the global minimum.
- GAs use payoff (objective function) information, not derivatives or other auxiliary knowledge.
- GAs use probabilistic transition rules, not deterministic rules.

A typical GA is based on three operators: selection/reproduction, crossover and mutation. The selection operator chooses the strings to be used in the next generation according to a "survival of the fittest criterion": the objective function to be minimised is mapped onto a fitness function to be maximised and the larger the fitness the higher the probability of survival. The crossover operator allows information exchange between strings, in the form of swapping of parts of the parameter vector in an attempt to generate fitter strings. Mutation as an insurance policy against premature loss of important notion occasional (with small probability) randomly alters the value of a string position without exceeding the predecided upper and lower thresholds (Goldberg, 1989).

GA has been applied to a number of fault diagnosis activities. This includes diagnosis of faulty signals in nuclear power plants (Yangping et al, 2000). GA is applied to GT fault diagnosis when it is viewed as an optimisation problem since an engine problem could result from one of a vast possible combination of performance and measurement parameters that will be able to reproduce that engine problem. Typically, a search space

developed by varying the flow capacity from -3.5% to +3.5% and a deterioration in efficiency from 0 to 3.5% for the LPC of a test model compared with data generated by introducing 2% deterioration in the LPC is shown in Figure 2.10. Each point in the surface plot is a potential solution and the best solution is the point having the lowest objective solution.

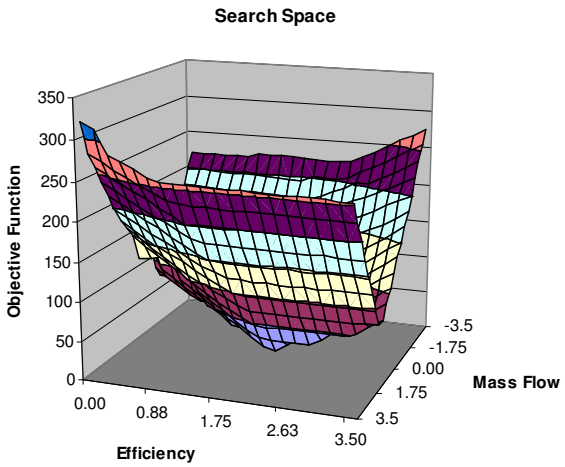

Figure 2.10 A Typical Search-Space (Sampath et al, 2002a)

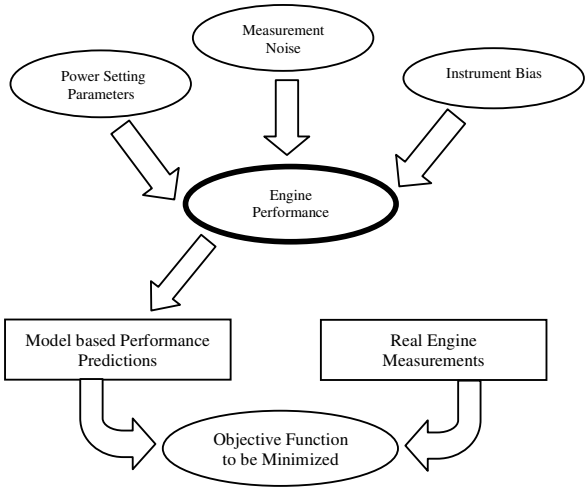

Figure 2.11 Schematic diagram of diagnostics strategy (Sampath et al, 2002a)

Broadly, the strategy adopted here, as shown in Figure 2.11, is to obtain a set of measurements from an engine performance model by planting known sets of faults and comparing it with the measurements from an actual engine. The simulated measurement set closest to the actual measurement set is indicative of the faults.

Recent works (Zedda and Singh, 1999; Gulati et al, 2000, Sampath et al, 2002a, 2002b, 2002c) have indicated the potentials of applying this optimisation technique to GT and sensor fault diagnosis under single (SOPA) and multiple (MOPA) operating points analysis respectively.

2.3.2.4 Artificial Neural Networks

The possibility of incorporating artificial neural networks (ANNs) in engine health monitoring has recently been the subject of much research after its successful application to other endeavours of life such as medicine (diagnosis of diseases), finance (prediction of stocks) amongst others.

Eustace et al (1995) described a neural network as a diagrammatic representation of a mathematical equation that receives values (inputs) and gives out results (outputs). Typical architecture for feedforward neural networks that would be applied in this research are presented in chapter 4.

The inherent non-linearity in GT performance and diagnostic relationships and the obvious limitations of the analytical model based technique otherwise known as GPA, makes the need for consideration of alternative technique such as ANNs inevitable.

The basic steps involved in obtaining a typical supervised feedforward ANN includes:

1. Assessing the problem to be solved in a bid to seek the possibility of discretising it.
2. Generating training and test data.

3. Defining and training various network architectures in order to seek the optimal architecture(s). The training process joggles the weights and biases to obtain the set that optimises performance via reduced errors and good generalisation. The weight adjustment for the case of a back propagation network that operates on the gradient descent technique is done via the relation:

$$\Delta w_{ij} = \eta\left(-\frac{\partial E(n)}{\partial w_{ij}}\right) + \alpha \Delta w_{ij}(n-1)$$

where E is the difference between the outputs and the targets for the nth input otherwise called the "error" to be minimised, η and α are the learning rate and momentum constants respectively.

4. Testing the ANNs with enough data to ascertain generalisation abilities.

ANN has been applied by a number of authors to fault diagnostic activities. Such areas include:

- **Sensor(s) faults**. Single sensor fault diagnosis for industrial power plants (Simani and Fantuzzi, 2000). Single sensor fault diagnosis for a space shuttle main engine (Guo and Nurre, 1991). Prediction of a failed sensor and actuators in automobile engines (Dong et al, 1997).
- **GT faults**. Aeroengine fault and sensor bias detection (Kobayashi and Simon, (2001), Zedda and Singh (1998)). Fault diagnosis of fleet engines (Eustace and Merrington, 1995). Faulty sensor and component isolation for a single spool GT (Kanelopoulos et al, 1997). Jet engine parameter trending and engine malfunction prediction (Denney, 1993). Diagnosis and prognosis for the fuel system faults of a AGT-1500 military tank's GT (Illi et al, (1994)).
- **Jet and Rocket Engines**: Detection of bearing failure and fuel interruptions in real time as well as stipulating the severity and duration of the fault (Dietz, et al, 1989).
- **Nuclear power plant.** Nuclear power plant diagnostics (Guo and Uhrig, 1992; Parlos et al. 1994; Tsai and Chou, 1996), signal validation (Upadhyaya and

Eryurek, 1992; Fantoni and Mazzola, 1996), control (Jous and Williams, 1990; Bakal et al., 1995), plant state identification (Barlett and Uhrig, 1992; Tsoukalas, 1994), prediction of plant parameters (Sofa et al, 1990) and optimisation (Fukuzaki et al, 1992).

- **Mechanical damage.** Detection of rotating machinery gearbox and bearing housing faults (Paya et al, 1997). Prediction of propulsion system rotor unbalance (Huang et al, 2001), GT blade fault diagnosis (Angelakis et al, 2001).

Generally, ANN has been shown to significantly improve symptom interpretation in case of malfunctions of mathematically difficult to describe systems and processes (Barschdorff, 1991).

In section 2.4.5, we shall describe in more detail, diagnostic applications of ANN that are centred on the gas-path of the GT.

2.4 Fault Diagnosis Models

In the previous sections of this chapter, we have considered the faults that affect the gas-path of a GT and the various monitoring approaches applied to detect and diagnose them. Because condition based maintenance can only be enhanced with a better knowledge of the engine status, it is necessary to dwell more on the quantitative approaches to GPFD namely, GPA and its variants, GA and ANN.

In order to give more insight into the application procedures of the various quantitative approaches described in the previous sections, we shall in this section present typical examples from researchers on their adopted methodology for GPFD of GTs. The idea being pursued here is to seek the level of work done and to ascertain the degree to which the GPFD problem has been tackled and thus determine if there is need for further work. It should be noted that the examples considered in this section have been

subjectively chosen as the best possible illustration, to represent typical application of such a technique to GPFD.

2.4.1 GPA Applications to GPFD

Tsalavoutas et al (2000) developed a Window based integrated engine health monitoring system comprising GPA and vibration monitoring. Data acquisition and validation was done online and the data subsequently organised into a database at user defined time intervals. Performance analysis had the option of being done online or offline. The diagnostics features extracted and assessed from the vibration sensors included overall vibration levels, power spectra and spectra signatures. Criteria used for data validation included:

- Checking whether the value is within the expected range for the corresponding variable
- Checking if this value is compatible with the rest of the measurements
- Employing thermodynamic analysis for verification

Component faults were evaluated based on health indices exceeding some pre-set limits and then a comparison with established fault patterns via a technique akin to expert system rules was done. The developed program had graphic features built into it.

A similar approach to this subject of EHM based on integration technology was initially presented by Meher–homji et al (1993).

2.4.2 WLS Algorithm Applications to GPFD

Doel (1994a and 1994b) described an algorithm developed by General Electric based on weighted least-squares fault diagnostic algorithm called Turbine Engine Module Performance Estimation Routine (TEMPER). A special feature known as “fault logic” was added to TEMPER to enhance its applicability to deviations that are far from the

nominal range. The fault-logic is used to search for large deviations in component performance, or for large measurement errors, when the solution residual is large. The solution residual J_o provides the mechanism for recognizing that a specific case is far from nominal conditions. TEMPER assumes that J_o follows the Chi-squared distribution and the fault logic is invoked whenever the residual exceeds the 95 percent limit.

Some of the observed strengths of this approach include:

- Applies statistical techniques to estimate sensor error which shows a marked improvement over earlier versions of GPA techniques that did not consider sensor error.
- TEMPER through its fault logic has the ability to cope with large deviations

Observed weaknesses of the TEMPER algorithm based on the least-squares approach (Doel, 1994a, 1994b) are:

- The assumption of linearity in the algorithm implies that the solution error is proportional to the measurement deviation, thus a doubled turbine efficiency deviation would give rise to a doubled solution error, that is, a fixed percentage error applies. It needs be noted that GT parameter relationships are highly nonlinear as opposed to the linearity assumption used in this technique.
- Because of the relationship between measurement deviation and solution error, the weighted least-squares algorithm is best suited for small measurement deviations. A fault logic routine has been included in TEMPER to reduce this problem.
- Pure faults (measurement errors and module performance deviations) are generally underestimated with the remaining deviation attributed to other measurement errors and performance deviations. This effect is known as smearing.
- The size of error is proportional to the size of actual performance fault.
- Changes to systems not included in the least-squares analysis are interpreted as changes to other performance parameters included in the analysis. For instance,

a change in turbine cooling flow is indistinguishable from a turbine performance fault (affecting both efficiency and flow function) and because the former is not included in the analysis, changes to it are interpreted as changes in the latter.

- TEMPER does not provide any aid in interpreting the results and there have been a number of cases where it has identified the same component again and again even though it has been overhauled.
- Multiple algorithms are required for different levels of performance deviation. For small deviations, TEMPER normal routine is followed and when the solution residual exceeds a given percentage confidence limit, which signals a large shift in measurement error or component deviation, an alternate strategy known as the TEMPER fault logic is employed. This approach would require some considerable time to converge.

Suggested improvements to TEMPER and other comparable GPA algorithms (Doel, 1994a, and 1994b) are:

- Increasing the number of redundant sensors to improve the fidelity of the solutions.
- Including redundant power setting parameters that can be used to include power setting parameter errors in the analysis.
- Analysis of engine data should be done on two simultaneous readings. The idea here is that for two close operating points, the module performance deviations would be identical and fault present at one of the operating points would be re-echoed at the other. Also several authors have suggested that the simultaneous analysis of multiple readings increases the information available to the analysis (Stamatis et al, 1989, Gulati et al 2000).
- The use of a deterioration model to improve the a priori estimates. Possible drifts resulting from age are included while specifying the input.

Some of these remedial actions, such as those advocating the increase in sensor suite are likely to attract penalties. These penalties include cost, weight, reliability and even performance. Thus while some increase in the number of sensors may be desirable, it is likely that the number required to eliminate all problems with the weighted least-square algorithm would not be cost effective.

2.4.3 KF Applications to GPFD

Luppold et al (1989) described an algorithm for estimating both the cause and level of anomalous GT engine performance using Kalman filter technique. The filter utilizes a piecewise linear state variable engine model to estimate five component deviations which as reported by authors, fully characterise engine off-nominal engine performance.

Volponi et al (2000) comparatively applied both KF and ANN to single fault isolation in GTs. The single faults according to the authors comprised of engine module, engine system and instrumentation faults. It is showed that for this level of fault, both methodologies compare favourably. However limitation of the KF approach to diagnostics stems from:

- The assumption of linear systems while GT parameter relationships are inherently nonlinear. Applications to nonlinear scenarios require assuming knowledge of an approximate solution and describing the deviations from the reference by linear equations (Sorenson, 1970).
- The problem of divergence which produces unsatisfactory results. Divergence is said to occur when the error covariance matrix computed by the filter becomes unjustifiably small compared with the actual error in the estimate (Sorenson, 1970).
- Its use of every measurement to perform all calculations whether relevant to the fault source or not. This leads to "smearing" and can produce potentially misleading results as non-faulty components are implicated in an attempt to isolate the faulty components.

- The fact that faults could be underestimated by a margin of 50% or more reduces the probability of isolating the faulty components in scenarios where multiple faults are present in the engine.

2.4.4 GA Applications to GPFD

Zedda and Singh (1999a, 1999b) proposed a genetic algorithm diagnostic system to diagnose faults in the gas-path of a GT. The authors applied the objective function given in equation (2.11) which would be minimized for a single operating point case for well-instrumented engines.

$$\mathbf{J}(\mathbf{x},\mathbf{w}) = \sum_{j=1}^{NM} \frac{\left|\mathbf{z}_j - \mathbf{h}_j(\mathbf{x},\mathbf{w})\right|}{\mathbf{z}_{odj}(\mathbf{w})\sigma_j} \tag{2.12}$$

where:

$\mathbf{z}_{odj}$ is the value of the j-th measurement in the off design undeteriorated condition.

$\mathbf{z} \in R^M$ is the measurement vector having M number of measurements

$\mathbf{h} \in R^{NM}$ is a nonlinear vector valued function from the engine performance model.

$\mathbf{x} \in R^N$ is the performance parameter vector with N number of parameters.

$\mathbf{w} \in R^P$ is the vector of the environment and power setting parameters (e.g. inlet condition parameters and fuel flow) with P as the number of parameters.

σ is the standard deviation used to account for measurement noise.

The estimation of the performance parameters is structured as shown in Figure 2.12.

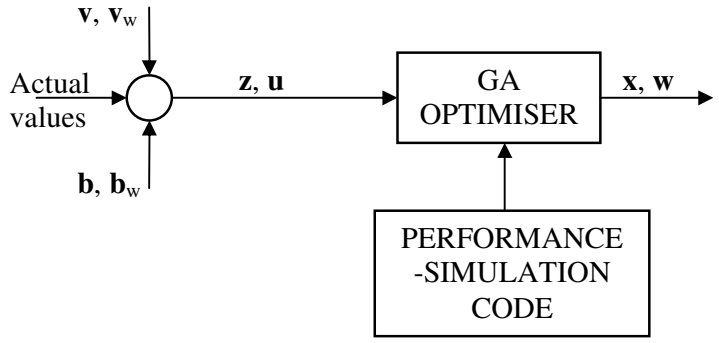

Figure 2.12 Layout of the diagnostic process

Where:

b is the vector of biases associated with the measured parameters

$\mathbf{b}_w$ is the vector of baises associated with the operating point setting parameters

v is the vector of noise associated with the measured parameters

$\mathbf{v}_w$ is the vector of noise associated with the operating point setting parameters

u is the vector of measured values associated with the operating point setting parameters and is mathematically defined as:

$$\mathbf{u} = \mathbf{w} + \mathbf{b}_w + \mathbf{v}_w \tag{2.13}$$

The authors tested their diagnostic model with simulated data from a low bypass ratio turbofan, the EJ200 powerplant of the European Fighter Aircraft (EFA2000). A Rolls Royce nonlinear steady state performance simulation model (RRAP) was used to generate the engine data. Ten performance parameters were used to monitor the health of the engine components while the applied instrumentation suite intended to be available on a test bed is made of sixteen measurements with three of these, ambient temperature, ambient pressure and main combustor fuel flow used as the power setting parameters.

The average results from about 150 test cases run showed that for one faulty component and two biased sensors the percentage of successful component classification (S.C.C.) is

93.3 and for Successful Sensor Classification (S.S.C.) is 98.3 with an average root mean square (RMS) of 0.037. When the number of faulty components was increased to two with the number of biased sensors remaining the same, the percentage of S.C.C. increased to 98.1 with s.s.c. being 91.8 and an average RMS of 0.181. The increased S.C.C. is based on the isolation of at least one of the faulty components.

The methodology described by the authors though interesting requires an initial assumption to be made of the number of biased sensors for proper function of the GA optimiser, but this does not seem feasible in reality, as one does not know what to expect in a typical fault diagnosis scenario.

Gulati et al (2000) extended the work of Zedda and Singh (1999a, 1999b) to cater for the diagnosis of engines with poor instrumentation. In order to accommodate more than one operating point, equation 2.14 was developed from equation 2.12. This approach is known as the multiple operating point analysis (MOPA).

$$\mathbf{J}(\mathbf{x},\mathbf{w}) = \sum_{m=1}^{OP} \sum_{j=1}^{NM} \frac{\left|\mathbf{z}_{jm} - \mathbf{h}_j(\mathbf{x},\mathbf{w}_m)\right|}{\mathbf{z}_{odj}(\mathbf{w}_m)\sigma_j} \tag{2.14}$$

Here, OP is the number of operating points.

The diagnostic structure adopted here is similar to that proposed by Zedda and Singh (1999a, 1999b). The difference lies in the number of times the GA optimizer is summed. The idea of MOPA stipulates that the more operating points that are evaluated, the more sensory information that would be available because measurements for different operating points are different for the same sensor though fault features are expected to be retained.

The authors tested their approach on the RB199, which is a three-spool engine with eight components. The engine health was monitored with nine measurements and another three- fuel flow and ambient pressure and temperature, used to set the operating point. The results showed the single operating point analysis (SOPA) approach developed by Zedda and Singh (1999a, 1999b) to be insensitive to faults under limited instrumentation while in some cases of its application otherwise non-faulty performance parameters were identified as faulty. Using three groups having three operating points each with the three operating points in each group separated by fuel flow differences of the range 1-2%, 5-6% and 15-17% respectively, it was found that operating points situated with 5-6% distance from one another gave optimal results. This optimality was both in the identification of the faulty sensor and in the degree of accuracy obtained. One possible reason for the result of this middle range distance being better than those of points spaced at about 1-2% away could be that the measurements from these latter points were more or less similar and that additional sensory information required was not provided for. Also extending points beyond some given limit would introduce error from component map distortions. Further results from the authors work showed that limiting the number of operating points to two could eliminate the risk of inaccuracies introduced by the difficulty of locating operating points.

Generally, limitations of the GA approach to GPFD are:

- It is computationally expensive. This implies that it requires large computing resources.
- It requires a long time to converge to a solution and this grows with the possible number of combinations of fault scenarios.
- Because optimal population size and number of generations cannot be predetermined, results from this technique fluctuate with the various choices of these parameters.
- Multiple runs of the GA optimiser may be required to shoreup the confidence in results.

- Its result is heavily affected by the choice of measurement set.

In addition, Kobayashi and Simon (2001) state that limitations of the MOPA approach to fault diagnostics includes:

- Assumption that degradation does not progress as operating points are traversed.
- It requires more time to reach a diagnosis.
- Additional restrictions may be imposed on the selection of diagnostic sensors by the control mode as this can limit the number of sensors that can be used across multiple operating points.

2.4.5 ANN Applications to GPFD

Zedda and Singh (1998) proposed the use of a modular based diagnostic framework for a twin spool turbofan GT with low bypass, thermodynamically similar to the Garret TFE 1042. In their work, the authors considered the possibility of using multiple nets in the detection and quantification of faults within three of the four (FAN, HPC, HPT and LPT) components of this GT unit. Seven sensors were considered for the isolation of fault in eight performance parameters. The analysis considered a single operating point and component faults were split into two categories – soft and hard, which required that different diagnostic path be traversed for the detected category. Single component faults were also considered. The diagnostic procedure modules consisted of pre-classification, classification, data validation, training set selection and net training. The results were reportedly encouraging by the authors.

Kobayashi and Simon (2001), proposed a hybrid neural network-genetic algorithm technique for engine performance diagnostics. A General Electric simulation programme for the XTE46 – a scaled unclassified representation of an advanced military twin spool turbofan engine, was used to generate data for constructing the diagnostic process. Faults were modelled by adjustments to efficiencies and/or flow coefficient scalars of the Fan (FAN), Booster (BST), High Pressure Compressor (HPC),

High Pressure Turbine (HPT) and Low Pressure Turbine (LPT). This gave nine health parameters to be estimated. The authors chose twelve sensed parameters to monitor the engine and compute the health parameters. In their approach, a neural network estimator was designed to estimate the engine health parameters from sensor measurements while genetic algorithm was applied to the sensor bias detection task. The authors claimed that the approach of incorporating genetic algorithms would reduce the size of the network training set significantly while inferring that ANN will not perform well if sensor bias is present in the measurements used to train it. In general, the results showed good estimation capabilities of the designed system with estimation errors below the 30% level considered by the authors are their satisfactory mark. The authors suggested that, an area of further work would require a systematic way of selecting and/or locating sensors for health estimation as simply increasing the number of sensors does not guarantee improved estimation performance. However, it is observed that:

- The approach of using a GA to coordinate the bias data set, the neural networks and the engine model could have a multiplying effect on any misdiagnosis. This is premised on the fact that an improperly estimated fault by the neural network estimator would result in a defective estimation error that may then be interpreted by the GA during optimisation, as a sensor bias.
- Contrary to the authors' argument, it has been shown that combining sensor biased patterns and component fault patterns in a training set, but not a superimposition of these, can be well handled by an ANN (Ogaji and Singh, 2002c, 2003; Ogaji et al, 2003)
- The number of health parameters predicted simultaneously during each diagnostic run was not clear. Were the nine health parameters meant to be predicted simultaneously or was is one at any time?
- The maximum considered faulty sensor was limited to one.
- As indicated by the authors, choice and location of sensors play an important role in correct diagnosis due to improved observability of the health parameters linked to the considered faults.

Kanelopoulos et al (1997) applied multiple neural networks in the simulation of performance and qualitative diagnosis of faults in a single shaft GT. The authors suggested that two networks with the first used to isolate sensor faults and the subsequent one to isolate component faults would provide better results than applying a single network for the combined task. This work amongst others gave impetus to the idea of using a specialised network for a specialised task.

Eustace and Merrington (1995) applied probabilistic neural network to diagnose faults in any engine within a fleet of 130 engines. This idea is interesting especially when one considers the fact that even for healthy engines, measured parameters vary naturally from engine-to-engine within a fleet. The General Electric F404 low by-pass ratio afterburning turbofan engine was chosen for consideration. This engine has six modules – fan, compressor, HPT, LPT and afterburner/final nozzle section. The authors used a statistical correlation technique to select five from eight available engine-monitoring parameters as inputs to the network. Residuals obtained from the difference of a measured parameter and its baseline – which was computed from correlative relationship with another parameter, were used to train the network. Faulty data were generated by fault implantation on a single engine and superimposed linearly on the fault free data of the fleet of which 60 were to generate the network and 70 to test the network. This superimposition was done to reduce the time and cost involved in fault implant tests. Implanted faults were in the form of off-nominal adjustments to both the compressor variable geometry (CVG) and exhaust nozzle final area. Results from the network test showed that an average accuracy of 87.6% was achieved with test patterns of about 4900. Considering the variability in the baseline used, the obtained result can be deemed acceptable. However, it is necessary to note that:

- The assumption of a linear relationship between the effect of an implanted fault on one engine and the other engines in the fleet introduces its own errors to the analysis process.

- It is definitely not going to be possible to carry out a quantitative analysis of the detected fault using this approach because of the variation from engine-to-engine data used in building the baseline.

Cifaldi and Chokani (1998) discussed the use of ANN with the backpropagation and delta learning rule in predicting the performance of six components (diffuser, compressor, burner, turbine, nozzle and mechanical shaft) of a turbojet engine while simultaneously giving an overview of its possible application to vibration related faults. Ten thousand training patterns were generated with the simulation programme and another twenty-five patterns were used to test the trained network. Each of these patterns represented an operating point. The result of their study showed that the mechanical, burner, compressor and turbine efficiency trends were well predicted while the efficiency trends of the diffuser and nozzle were poorly predicted. The authors attributed this poor performance to the choice of the instrumentation. Some observations made from this work include:

- The use of twenty-five patterns only to assess the performance of a net trained with ten thousand patterns is insufficient. This is because the generalisation abilities of networks can be best validated by testing with sufficient data.
- The need for an appropriate instrumentation set is vital to proper fault diagnosis.

Green and Allen (1997) discussed the need to incorporate ANNs with other AI tools to obtain a cognitive (awareness), ontogenetic (learning organism) engine health monitoring (EHM) system or COEHM with estimation of lifing, diagnostic and prognostic capabilities.

Guo et al (1996) applied an Autoassociative neural network (AANN) for sensor validation. The authors in their analysis assumed a redundancy in the instrumentation set. This may imply that a non-redundant instrumentation set cannot be successfully applied with AANN for sensor validation since according to the authors, the number of

neurons in the bottleneck must not be less than the minimum number of sensors required to generate all sensor estimates in case of a detected failure.

Napolitano et al (1996) while comparing the approaches of Kalman filters (KF) and ANN for sensor failure detection, isolation and accommodation (SFDIA), used units without physical redundancy in the sensory capabilities. Basing their analysis on soft failures/faults, the authors in the ANN aspect, applied multiple ANNs in the form of main and decentralised networks (MNN, DNNs) to perform SFDIA. The application of multiple nets makes it possible to infer that if errors are to be minimised for this and other complex applications, then more than one net need be employed with each, applied to a specific aspect of the problem.

Weidong et al (1996); **Lu et al**, (2000), used the relativity of inputs and outputs of an ANN to detect the presence or otherwise of faults in sensors, with the output, said to represent a better approximation of the sensors correct measurements. This network output can then be fed to other networks, probably, for component fault diagnosis.

The foregoing shows that much work has been and is still being done in the area of ANN application to GT fault diagnostics, the recency of its emergence notwithstanding. In section 4.5, some of the strengths and weaknesses of the ANN approach to fault diagnosis shall be presented.

2.5 Gaps in Contemporary Research

The fact that much work has been done in the area of fault diagnosis is not in doubt. Most of the work carried out in GPFD, the tool used notwithstanding have been qualitative – isolating the faulty component without consideration given to the level of fault. The few researchers that have tried to consider the quantitative aspect of this problem were restricted to looking at one component or the other or just limited to a single sensor in case of sensor faults. Only one group of authors (Zedda and Singh,

1998) attempted the consideration of more than one-component faults in the light just discussed.

In view of the importance placed on engine availability by both OEM and users, an effective performance diagnosis approach cannot be overlooked. The goal in this research would be to consider, based on the contributions of predecessors, and evolve a unique approach to GPFD. The diagnostic framework should be:

- Fast in undertaking a diagnosis
- Reliable with a high percentage of success rates
- Suitable to the nonlinear relationships of GT parameters
- Modular to allow for easy update to each segment of the overall structure
- Tolerant to measurement noise
- Applicable to multiple sensor fault diagnosis
- Applicable to multiple component fault diagnosis
- Operate within a given range of operating conditions

In view of the desirable features of ANN, we have considered its application to this work.

2.6 Conclusions

While GPFs are varied, their effect on the performance of the GT could be devastating-economically and otherwise, if not checked. Not only will the cost of continued operation under an undiagnosed fault increase, the level of competition in the various industries to which GTs are applied would result in negligent service providers being run out from the market, especially when their services are classed unreliable and unsafe.

Various techniques are available to diagnose faults in the GT, some of which have been termed conventional and others evolving. Each technique has its own strengths and

weaknesses and a welcome development would be to harness the strengths of various techniques into a combined engine health monitoring (COEHM) scheme. There is however a threshold to the number of monitoring techniques that can be economically considered together, since beyond this threshold, the return on investment (ROI), that is the difference between the cost of monitoring and benefits derived from monitoring, takes a negative trend (Figure 2.13). However, when cost of monitoring is juxtaposed with cost of failure, Myrick (1982), Simmons and Lifson (1985) agree that total plant losses associated with equipment failure far outweighs the cost of an extensive multi-parameter monitoring system, albeit, that is only when the system works.

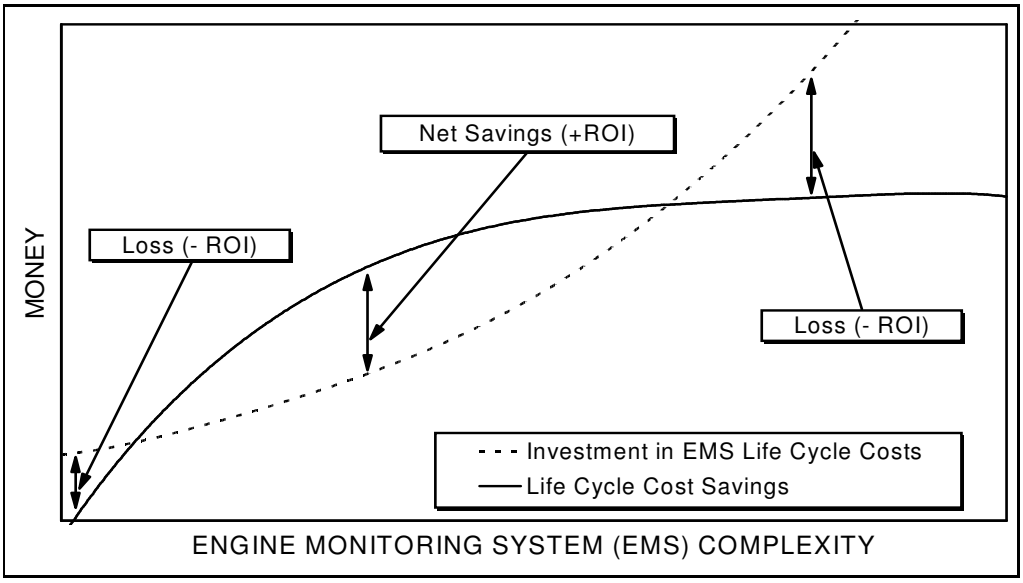

Figure 2.13 Return on investment (ROI) of engine monitoring system (Singh and Escher, 1995)

Quantitative approaches to monitoring provide the GT user with necessary information that should help plan an effective condition based maintenance (CBM) programme. Because faults can be present in multiple gas-path components and/or multiple sensors, and given the peculiarities of the GT parameter relationships, better ways of tackling the issue of GPFD are required. Current diagnostic models have fallen short of these requirements, creating a research opportunity.

This thesis does not intend to create a COEHM scheme, but would use a bank of ANNs in conjunction with a light use of expert system – that describes the results of the ANN-, to qualitatively and quantitatively describe faults affecting the engine's gas-path.

CHAPTER 3

RESEARCH AIM, OBJECTIVES AND METHODOLOGY

3.1 Introduction

In chapter 2, an exploration of the literature revealed some of the faults that affect the gas-path of the GT as well as the diagnostic approaches that have and are being considered for their diagnosis. Our literature search threw up some important conclusions that are outlined in section 2.5.

In this chapter, the research aim will be stated and the objectives with which we intend to achieve the aim will be outlined.

3.2 Research Aim

The aim of this research is to develop a framework for the application of advanced GPFD to GTs.

3.3 Research Objectives

To achieve the research aim, there are a number of issues to be addressed. The following summarises the research objectives.

- To conduct a review of literature for critical analysis in order to identify research opportunities in terms of available approaches for application of ADT to GPFD
- To define the requirements for the application of ADT to GPFD
- To develop a conceptual model for GPFD
- To develop a mock system using ADT to implement the conceptual model
- To evaluate the effectiveness of the developed diagnostic framework with case studies

3.4 Scope of Research

This research focuses on a GT for stationary applications under steady-state conditions. This does not imply that the developed framework is not applicable to other domains such as a GT for propulsion or under transient conditions. In fact, this thesis presents a developed case study that shows with very little modification, the diagnostic paradigm can be applied to fault diagnosis of a turbofan engine under transient conditions.

3.5 Research Methodology

This section describes the research methodology as shown in Figure 3.1. The methodology guided the main activities of this research and thus formed the basis of the thesis.

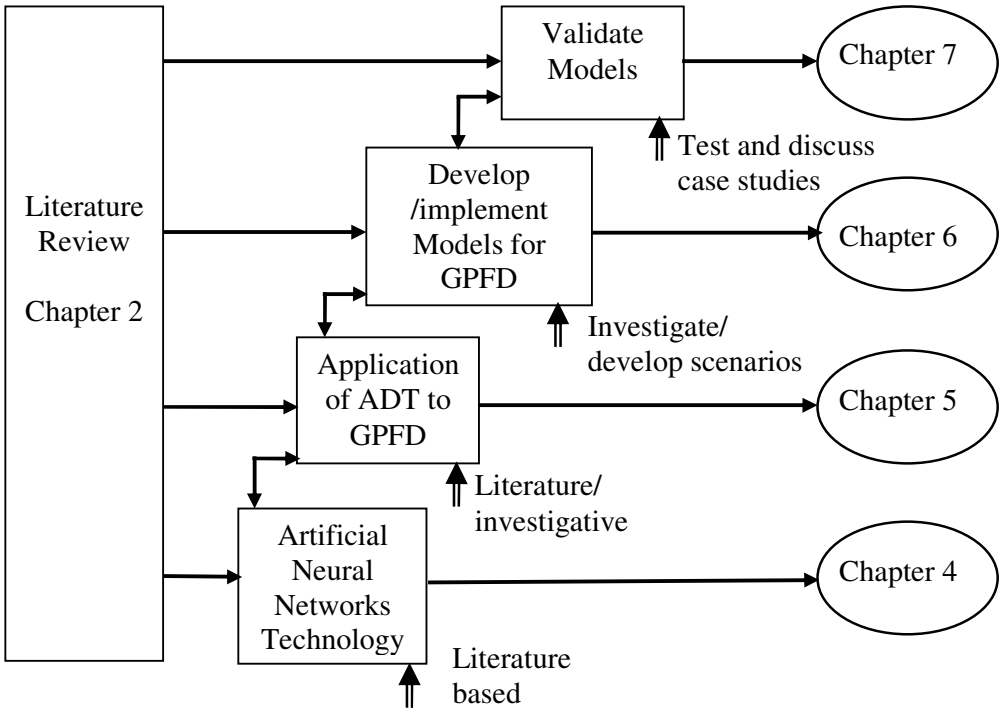

Figure 3.1 Research methodology

3.5.1 Literature Review

This was carried out to identify the theory and practices in GPFD of GTs. It involved a consideration of both the faults that affect the gas-path of the GT and the available diagnostic approaches. The review provided a broad understanding of the existing researches, analysed strengths and weaknesses of different diagnostic approaches and identified research opportunities in existing knowledge.

3.5.2 Artificial Neural Networks (ANNs) System

Some of the research opportunities identified during the literature review are premised on the qualitativeness of diagnostic approaches, limitations of diagnosis to those occurring for a single component or single sensor as well as the high level of inaccuracies given from tests for those authors that provided relative quantitative test results.

Most of the papers reviewed, in their recommendations pointed to ANNs as a technique that could enhance the diagnostic potentials of GPFs. In the light of this suggestion and considering the peculiarities of GT parameter relationships in addition to the required diagnostic features stated in section 2.5 of this thesis, it was decided to investigate the use of ANN for this task.

The what's and how's of ANNs as well as the qualities that need to be considered in drawing appropriate conclusions on the features of ANNs to use for a particular task are discussed.

3.5.3 Application of an ADT to GPFD

Before commencing engine-fault diagnosis, some vital decisions/activities need to be undertaken such as:

- The engine model to be used has to be chosen and thermodynamically designed, as real life data are not usually available.
- The number of sensors and their locations have to be determined.
- The measured parameters have to be corrected to appropriate baseline values in order to accommodate measurements over a given range of operating points.

An engine, thermodynamically similar in behaviour to the Rolls Royce industrial RB211, was chosen for the initial development of the diagnostic framework. A nonlinear GPA technique was applied to optimise the measurement set selection and a parameter correction process was developed to make corrections for all measured parameters. The implication of this is that for a given engine configuration, an optimised set of measurements would guarantee improved observability of the performance changes. In addition, for a wide range of the power-setting parameter and ambient conditions, the diagnostic model can still be applied without recourse to regenerating data from the thermodynamic engine model.

3.5.4 Developing and implementing models for GPFD

Engine diagnostics will require a diagnostic philosophy. Because the research is focused on the gas-path of the GT, then such hardware that comes into contact with the working fluid needs to be considered in designing an appropriate diagnostic framework. In this case, the hardware includes the gas-path components (compressors and turbines) and the sensors. In addition to determining a flow diagram for the diagnostic process, appropriate algorithms for detecting sensor faults as well as component faults will be defined. Four case studies will be implemented. The engine configurations basically fall into three categories – single-spool stationary, two-spool stationary and two-spool turbofan engines. Training and testing of all the networks in each engine set are done using simulated data. The various networks for a given engine are coded in a computer program to enable it to operate in a batch mode, so that when measurements from a test case are entered into the graphic user interface (GUI) console and RUN, the user is

immediately presented with the status of the engine. This status could indicate either a fault or a no fault scenario. If a fault is detected, the nature and extent of the fault is presented.

3.5.5 Validating the developed structure

The purpose of validation was to test the usability and effectiveness of the developed gas-path diagnostic system. To achieve this, the individual case studies designed earlier were presented with various GPF scenarios involving single and multiple sensor and component faults. Massive tests of diagnostic programs are necessary to assess their performance and generalisation abilities to faults hitherto unseen. Results from various tests were collated and analysed using both quantitative and qualitative techniques. The significance of these results and other aspects of the diagnostic program development are critically discussed.

3.6 Summary

This chapter has discussed the aim, objectives and scope of the research. The methodology that has guided this research is discussed: it includes a review of the pertinent literature, a description of ANNs, application of ADT to GPFD, development of a conceptual model for the GPFD, implementing the conceptual model and validating the developed structure. Overall, the aim of this research is to develop a framework for the application of an advanced GPFD to GTs. Though the scope is limited to stationary applications, the developed approach will be shown to be suitable for other applications. Achieving the aim would provide GT operators with an alternative and probably more appropriate approach to the problem of GPFD.

The next chapter introduces ANN as an advanced diagnostic tool for GPFD. Its features and necessary functions that need to be defined prior to engine diagnostic applications are presented.

CHAPTER 4

ARTIFICIAL NEURAL-NETWORK SYSTEM

4.1 Introduction

In chapter 2, the review of literature has highlighted the need for an effective gas-path diagnostic technique, which can undertake fault detection, isolation and assessment (quantification), in GTs. To achieve this, chapter 3 has highlighted the research methodology. This chapter discusses artificial neural networks (ANNs), the tool that is being explored to develop the advanced diagnostic framework for GPFD.

The chapter is structured as follows. Section 4.2 introduces the subject of ANN. The necessary factors to consider in applying ANN to engine fault diagnostics are presented in section 4.3. The approaches to network training are considered in section 4.4. Section 4.5 distinguishes between the feedforward and recurrent networks while section 4.6 outlines the case for an ANN diagnostic tool. Finally, a summary of the chapter is presented in section 4.7. It should be noted that most standard textbooks on ANN provide information on its theory, but the current exercise is undertaken to draw up salient points that would be of specific interest when carrying out engine diagnostics with ANN.

4.2 What are ANNs?

Neurobiology estimates the human brain to consist of one hundred billion nerve cells or neurons (Kevin, 1997). These communicate via electrical signals that are short-lived impulses or ‘spike’ in the voltage of the cell wall membrane. Biological neurons (Figure 4.1) have three principal components: the dendrites, the cell body (Soma) and the axon. A neuron's dendritic tree is connected to about a thousand neighbouring neurons. When one of those neurons fire, a positive or negative charge is received by one of the

dendrites. The strengths of all the received charges are added together through the processes of spatial and temporal summation. Spatial summation occurs when several weak signals are converted into a single large one, while temporal summation converts a rapid series of weak pulses from one source into one large signal. The aggregate input is then passed to the cell body or Soma. If the aggregate input is greater than the axon hillock's threshold value, then the neuron *fires*, and an output signal is transmitted down the axon. The strength of the output is constant, regardless of whether the input was just above the threshold, or a hundred times as great. The output strength is unaffected by the many divisions in the axon; it reaches each terminal button with the same intensity it had at the axon hillock.

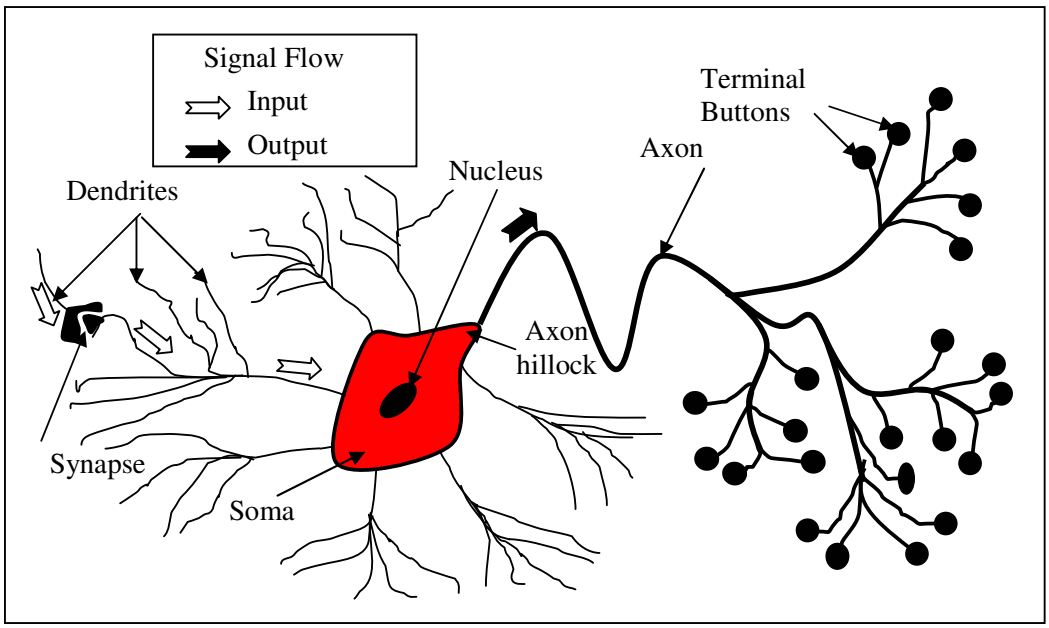

Figure 4.1 A typical biological neuron

Although ANNs have been around since the late 1950's, it was not until mid-1980 that algorithms became sophisticated enough for general applications. Also referred to as connectionist architectures, parallel-distributed processing systems, an ANN is an information-processing paradigm inspired by the way the densely interconnected,

parallel structure of the mammalian brain processes information. ANNs are collections of mathematical models that emulate some of the observed properties of biological nervous systems and draw on the analogies of adaptive biological learning. The key element of the ANN paradigm is the novel structure of the information processing system. It is composed of a large number of highly interconnected processing elements that are analogous to neurons and are tied together with weighted connections that are analogous to synapses. A typical neuronal model is thus comprised of weighted connectors, an adder and a transfer function (Figure 4.2).

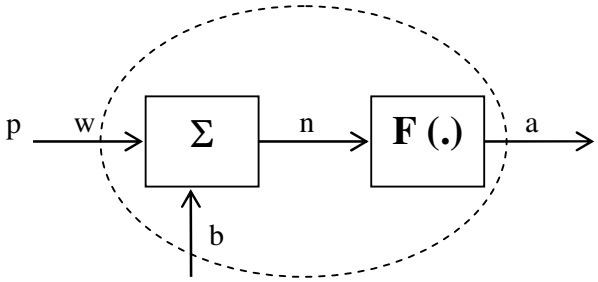

Figure 4.2 A single mathematical neuronal model

The basic relationship here is:

$$n = wp + b \tag{4.1}$$

$$a = F(wp + b) \tag{4.2}$$

where a = network output signal

w = weight of input signal

p = input signal

b = neuron specific bias

F = transfer/activation function

n = induced local field or activation potential

Learning in biological systems involves adjustments to the synaptic connections that exist between the neurons. This is true of ANNs as well. Learning typically occurs by example through training, or exposure to a truthed set of input/output data where the training algorithm iteratively adjusts the connection weights (synapses). These

connection weights store the knowledge necessary to solve specific problems. From equations (4.1) and (4.2), it can be seen that a simple neuron performs the linear sum of the product of the synaptic weight and input with the bias, which value is then passed through an activation or transfer function that limits the amplitude of the output of a neuron. Activation functions can take various forms ranging from hard limit, through pure linear to sigmoid and the choice of which to use depends on the desired output from the network and the characteristics of the system being modelled.

Typical and practical networks are normally multi-input and probably multi-layered and in such cases, the variables in equations (4.1) and (4.2) now take a different format with **w** being the matrix of weights and **a**, **p** and **b** representing vectors of their respective definitions.

Two key similarities between biological and artificial networks (Haykin, 1999) are:

1. Their building blocks are highly interconnected computational devices though the artificial neurons are much inferior to their biological counterparts.
2. The function of the network is determined by the nature of connection between the neurons.

ANNs are excellent at developing systems that can perform information processing similar to what our brain does. Some characteristics of biological networks include the following:

- They are non-linear devices
- They are highly parallel in processing, robust and fault tolerant
- They can easily handle imprecise, fuzzy, noisy and probabilistic information
- They can generalise from known tasks or examples.

ANNs attempts to mimic some or all of these characteristics by using principles from the nervous system to solve complex problems in an efficient manner.

4.3 ANNs – Types, Characteristics and Operation

ANNs are being applied to an increasing number of practical problems of considerable complexity. They are good pattern recognition engines and robust classifiers, with the ability to generalize in making decisions about imprecise input data. They offer ideal solutions to a variety of classification problems such as speech, character and signal recognition, as well as functional prediction and system modelling where the physical processes are not understood or are highly complex. ANNs, as a branch of artificial intelligence, also applies computational intelligence techniques to diagnostics.

ANNs can be applied under supervised mode in conditions where there is an established relationship from a model or in unsupervised modes where this condition does not exist and it is desired to interpret available data. This makes it different from traditional diagnostic techniques, which are wholly model based, that is, they require mathematical representations of the engine for analysis.

ANNs are by far the most popular AI technique applied to fault diagnostics. This position is strengthened by the capabilities derivable from the application of the technique as would be highlighted in section 4.6.

In this section, we shall discuss the types of ANNs and their architecture in addition to some factors that need to be understood before ANN can be successfully applied to productive tasks such as GPFD of GTs.

4.3.1 ANN Application Domains in GTs

ANN can be used to perform four basic functions in a plant such as the gas turbine. These functions are:-

- Generate performance parameters
- Estimate plant/process condition

- Estimate sensor data
- Validate sensor data and sieve faulty/noisy measurements from good measurements.

These functions would require networks that classify patterns, associate patterns and approximate functions/relationships. Typical fault diagnosis areas to which ANNs have been applied were presented in sections 2.3.2.4 and 2.4.5.

4.3.2 Types of ANN and Architectures

Various types of ANNs are currently available. Some of the more popular include the perceptron, multilayer perceptron, radial basis function, learning vector quantization, Hopfield, and Kohonen, to name a few. In addition to networks being differentiated into the supervised and unsupervised classes, they can also be classified as feedforward or recurrent (that is, implement feedback). This latter form of classification depends on how data is processed through the network. The sequel discusses some popular network types.

4.3.2.1 Perceptron

Rosenblatt (1958) first introduced the Perceptron (Figure 4.3). These networks are composed of just a single layer of computational nodes into which binary input patterns are fed and binary outputs are obtained. The number of neurons in this computational layer (output layer) could vary from one to some finite value.

A typical member of this category is the Adaline network having an output layer of only one neuron node. Generally, the application of this type of networks to real problem domain such as engine diagnostics is limited because of their limited computational and non-linearity capabilities.

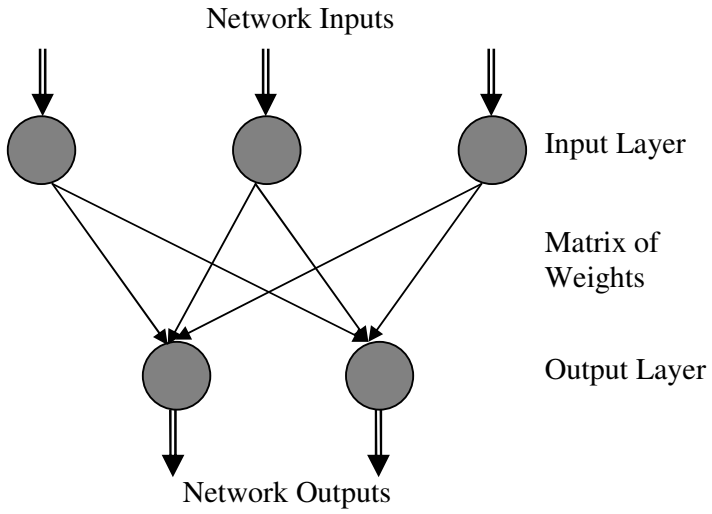

Figure 4.3 The Perceptron

4.3.2.2 Multilayer Perceptrons

Minsky and Papert (1969) introduced the Multi-Layer-Perceptron (MLP). It is an extended form of the Perceptron and has one or more hidden neuron layers between its input and output layers. MLPs are appropriate to non-linear functions and for solving classification problems. Typical architectures of this network which were used extensively in this research are shown in Figures 4.4 and 4.5.

MLPs are not capable of performing outside the range of data for which it has been trained. In addition, as the neural network grows in size, training can become a complicated issue. Some important decisions have to be made such as the appropriate number of hidden layers to be included, the number of processing elements (neurons) to be used for each of the layers, and the features to be retained.

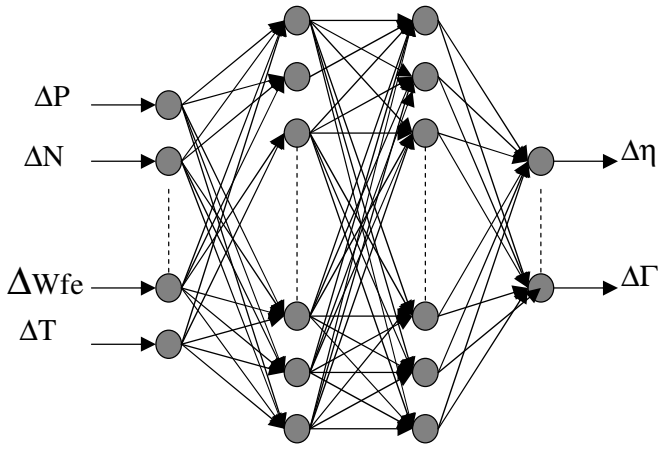

Figure 4.4 A 2-hidden layered feedforward network

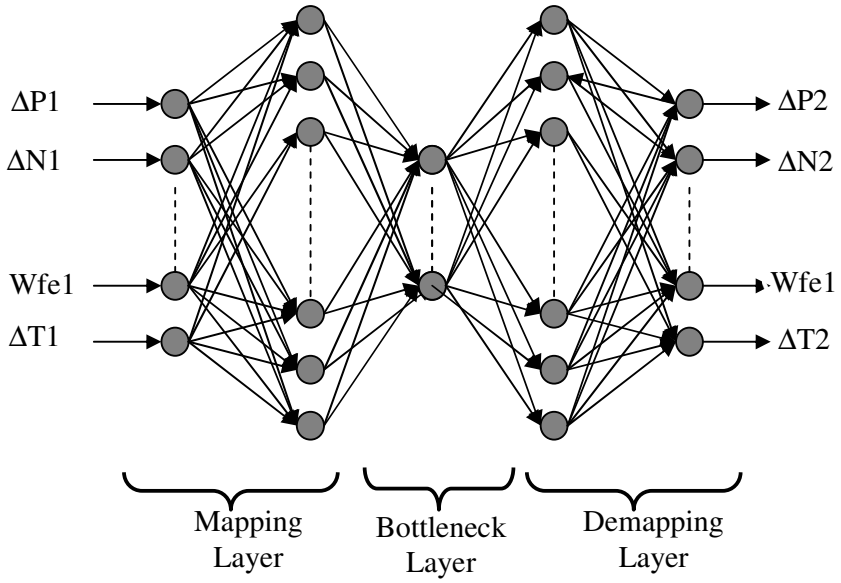

Figure 4.5 Autoassociative feedforward network

A unique type of the MLP is the autoassociative neural networks (AANN) (Kramer, 1991) which has proved useful in sensor fault diagnosis and noise filtering (Zedda and Singh 1998; Ogaji et al, 2002a).

4.3.2.3 Radial Basis Function

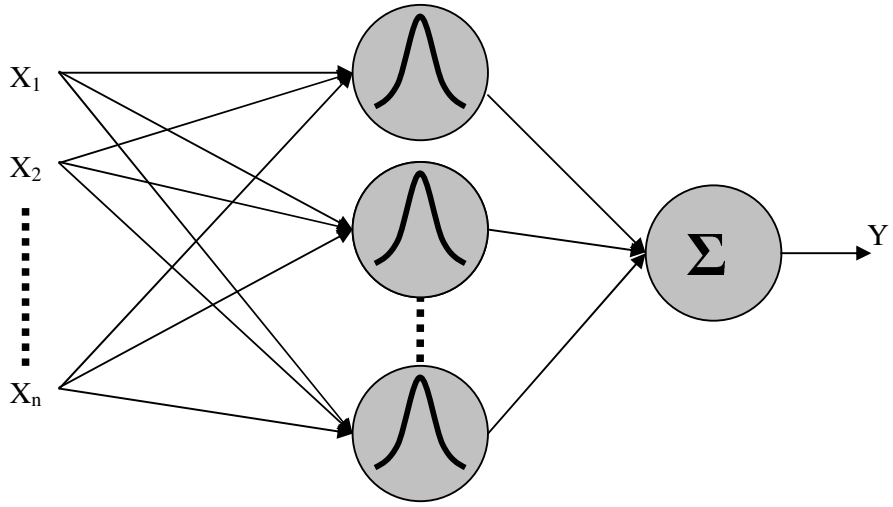

Figure 4.6 An RBF network with one output

The radial basis function (RBF) is a variant of the multilayer feedforward network with BP algorithm. Learning with the RBF is viewed as a curve-fitting (approximation) problem in a high-dimensional space. The RBF neural network has been demonstrated to be useful as a classifier and function approximator. The RBF can be thought of as a nearest neighbour classifier; with the capability of identifying inputs that do not match anything seen before (Brotherton et al, 2000). A typical RBF network (Figure 4.6) consists of two computational layers. Outputs of the first layer, made of radbas functions - which could be Gaussian, multiquadric, inverse-multiquadric or Cauchy - are a function of the distance between the network input and the "centre" of the basis function. For Gaussian radial (transfer) function (equation 4.3), the farther the input from the centre, the smaller the neuron output, in other words, response is localised to inputs close to their centres. This is in contrast to the typical MLP that use weighted sum of inputs and the sigmoid transfer function. The RBF network is often complemented by a linear second layer and this produces a weighted sum of the outputs of the first layer. RBFs generally train faster than MLPs but require more neurons.

$$\text{radbas}(n) = \exp(-n^2) = \exp\left(-\frac{\|x-c\|^2}{r^2}\right) \qquad 4.3$$

where: $\|.\|$ is the Euclidean norm

x is an m-dimensional input vector

c the centre of the function

r is the width/radius of the Gaussian function

RBF networks are useful in tasks such as function approximation, pattern classification, modelling of dynamic systems and time series. However, application of RBFs for GPFD was discontinued due to poorer generalisation observed when compared to results from other network types.

4.3.2.4 Learning Vector Quantization

Learning vector quantization (LVQ) algorithm is a supervised learning technique with the basic idea being to find a natural grouping in a set of patterns.

An LVQ network typically consists of two layers- an input layer and an output layer. It represents a set of reference vectors, the coordinates of which are the weights of the connections leading from the input neurons to an output neuron. Hence, it is possible to say that each output neuron corresponds to one reference vector.

The learning method of LVQ is often called competition learning, because it works as follows (Anderson and McNeill, 1992): For each training pattern, the reference vector that is closest to it is determined with the corresponding output neuron called the winner neuron. The weights of the connections to this neuron - and this neuron only: the winner takes all - are then adapted. The direction of the adaption depends on whether the class of the training pattern and the class assigned to the reference vector coincide or not. If they coincide, the reference vector is moved closer to the training pattern; otherwise it is moved farther away. The *learning rate* controls the movement of the reference vector. It

states, as a fraction of the distance to the training pattern, how far the reference vector is moved. Usually the learning rate is decreased in the course of time, so that initial changes are larger than changes made in latter epochs of the training process. Learning may be terminated when the positions of the reference vectors hardly change anymore.

LVQ is a useful tool for data compression and its difference from other self organising maps (SOMs) such as Kohonen feature maps is that the numbers of classes or clusters are pre-chosen.

4.3.2.5 Hopfield Networks

The Hopfield Net (Figure 4.7) was first introduced by the physicist, Hopfield (1982), and belongs to neural net types, which are called "thermodynamical models"- because as feedback networks the term *energy* is used instead of *error*. It consists of a set of neurons, where each neuron is connected to each other neuron.

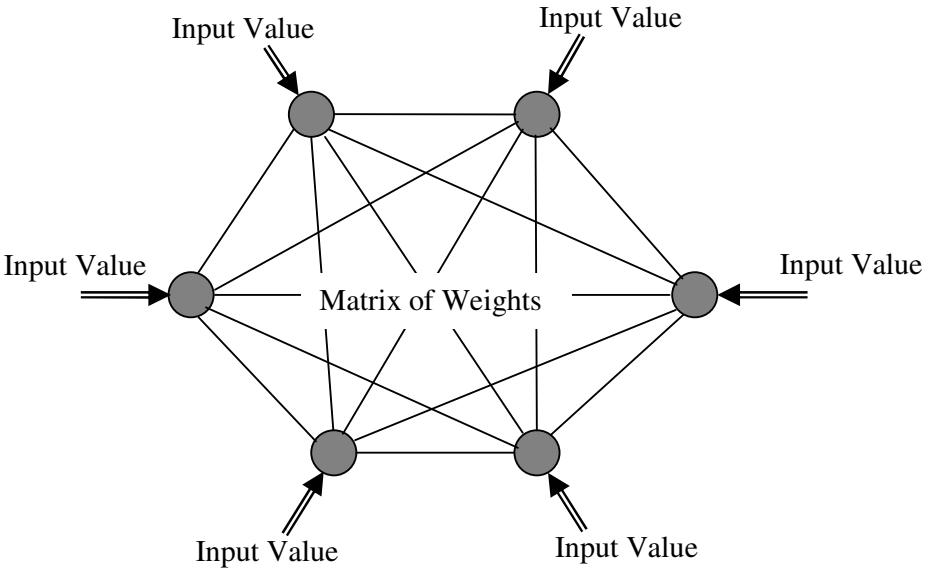

Figure 4.7 Structure of the Hopfield network

There is no differentiation between input and output neurons. Input values are applied simultaneously to all neurons. A neuron, chosen at random, sums the weightings on the

connections to it from other active units. If this sum is greater than a given threshold, the neuron fires, alternatively, the neuron becomes inactive should the sum be less that the threshold. This process is repeated with other neurons until a stable state is attained. The Hopfield model is used as an autoassociative memory to store and recall a set of bitmap images. Images are stored by calculating a corresponding weight matrix. Thereafter, starting from an arbitrary configuration, the memory will settle on exactly that stored image, which is nearest to the starting configuration in terms of Hamming distance (the number of bits that differ between two binary strings). Thus given an incomplete or corrupted version of a stored image, the network is able to recall the corresponding original image.

The importance of the different Hopfield networks in practical application is limited due to theoretical limitations of the network structure but, in certain situations, they may form interesting models. Generally, these networks are useful in pattern association and optimization problems.

4.3.2.6 Probabilistic Neural Network.

Specht (1988, 1990) developed the probabilistic neural network (PNN). PNN is used to provide solution to pattern classification problems through an approach developed in statistics, called Bayesian classifiers. In Bayes theory, the relative likelihood of events as well as priori information to improve prediction is considered.

PNN uses a supervised training set to develop distribution functions within a pattern (middle) layer. In the recall mode, the developed functions are used to determine the likelihood of a given pattern being a member of a class or category with the criteria solely based on the closeness of the input feature vector to the distribution function of a class.

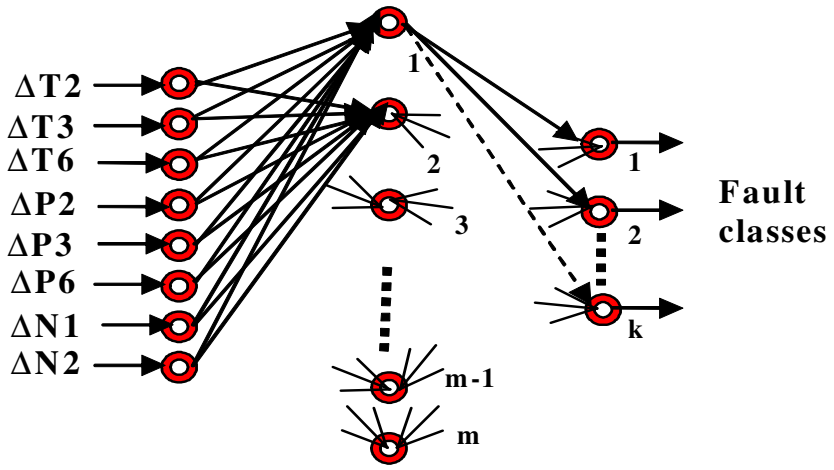

Figure 4.8 Structure of a PNN

PNN has three layers. The input layer has as many elements as there are separable parameters needed to describe the objects to be classified. The middle layer organizes the training set such that each input vector is represented by an individual processing element. And finally, the output layer, also called the summation layer, has as many processing elements as there are classes to be recognized. Figure 4.8 shows a typical PNN with **m** hidden layer neurons and **k** output classes.

PNNs are simple on design and with sufficient data are guaranteed to generalize well in classification tasks. Training of the PNN is much simpler than with backpropagation. However, the pattern layer can be quite huge if the distinction between categories is varied and at the same time quite similar in special areas. In addition, PNNs are slower to operate in the recall mode as more computations are done each time they are called.

4.3.2.7 Kohonen Feature Map

Kohonen (1982) first introduced the Kohonen Feature Map that can be represented as shown in Figure 4.9. It is very useful neural net type, for simulating the learning process of the human brain. The "heart" of this type is the *feature map*, a neuron layer where neurons organize themselves according to certain input values. The type of this neural

net is both feedforward (input layer to feature map) and feedback (feature map). A major difference between this network and a number of other networks is that learning is unsupervised.

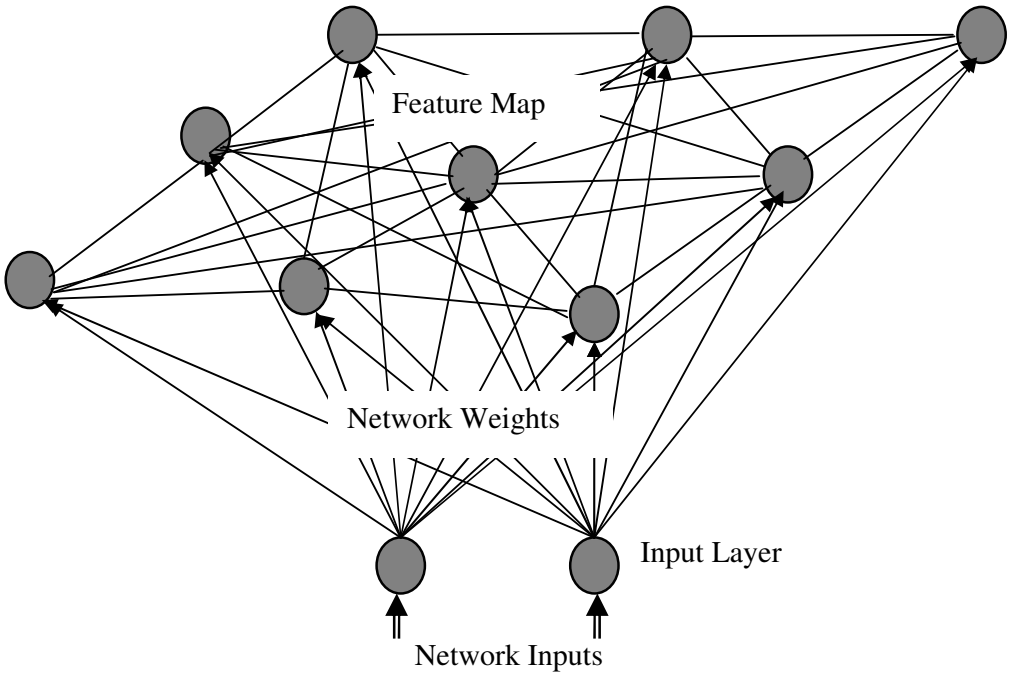

Figure 4.9 Kohonen feature map

These network types can be applied to pattern classification, optimization problems and simulation tasks.

4.3.3 Learning Rules and Algorithms

Learning rules are the procedure used by a network to modify/adjust its weights and biases with the ultimate goal being to tune the network to the intended task. While learning different inputs, the weight values are changed dynamically until their values are *balanced*, so each input will lead to the desired output. The training of neural net results in a matrix that holds the weight values between the neurons. Once a neural net had been trained correctly, it is expected to be able to find the desired output to a given input that had been learned, by using these matrix values.

ANN learning algorithms fall basically into two categories – supervised (learning with a teacher) and unsupervised (learning without a teacher). Other seemingly new categories such as self-supervised and reinforced learning can properly be subsumed into the unsupervised learning category. These two learning paradigms are discussed further in section 4.4.

Because mans understanding of how neural processing actually works is limited, may laws have been put forward with new ideas still being developed. In what follows, a few of the major laws as well as some learning procedures will be presented as examples.

4.3.3.1 Hebb Rule

Hebb (1949) introduced the first learning rule. His basic rule is: *When an axon of cell A is near enough to excite a cell B and repeatedly or persistently takes part in firing it, some growth process or metabolic change takes place in one or both cells such that A's efficiency, as one of the cells firing B, is increased.* This implies that if a neuron receives an input from another neuron and if both are highly active (mathematically have the same sign), the weight between the neurons should be strengthened.

4.3.3.2 Hopfield Law

The Hopfield law is similar to Hebb's rule with the difference being the specification of the magnitude of the strengthening or weakening. It states that, "If the desired output and the input are either active or both inactive, increment the connection weight by the learning rate, otherwise decrement the weight by the learning rate."

4.3.3.3 Delta Rule (DR)

This rule is a further variation of Hebb's Rule and is commonly used. The rule is based on the continuous modification of the strengths of the input connections to reduce the difference (the delta) between the desired output value and the actual output of a processing element. This rule, also referred to as the Widrow-Hoff Learning Rule and

the Least Mean Square (LMS) Learning Rule predominantly uses linear activation functions and the output $a_j(p)$ of input/output pattern **p** is the same as the induced local field $v_j(p)$; that is,

$$a_j(p) = v_j(p) = \sum_{i=1}^{M} w_{ji}(p)a_i(p) \tag{4.4}$$

where

w_{ji} (p) = weight from the ith to the jth unit following presentation of pattern **p**.

$a_i(p)$ = value of the ith element of the input pattern

M = Number of elements in input vector

The operation of the DR is such that the delta error in the output layer is transformed by the derivative of the transfer function and is then used in the previous neural layer to adjust input connection weights. Typically, the rule for changing weights following presentation of input/output pair **p** is given by:

$$\Delta w_{ji}(p) = \eta\left(t_j(p) - a_j(p)\right)a_i(p) \tag{4.5}$$

$$\Delta w_{ji}(p) = \eta e_j(p)a_i(p) \tag{4.6}$$

where

$t_j(p)$ = target value for jth member of the output pattern for pattern **p**

$a_j(p)$ = actual output value of the jth member of the output pattern obtained when input pattern **p** was presented.

$e_j(p)$ = difference (error) between target and actual output of the jth member of pattern **p**.

Δw_{ji} (p) = change required on the weight from the ith to the jth unit following presentation of pattern **p**.

η = learning rate

We note that from equations (4.5) and (4.6), the error e_j (p) for jth output element is given by:

$$e_j(p) = t_j(p) - a_j(p) \tag{4.7}$$

If there are K units in the output, then the sequential cost function or mean square error for the pth iteration is defined as:

$$E(p) = \frac{1}{2}\sum_{j \in C} e_j^2(p) \tag{4.8}$$

where the set C includes all units in the output layer of the network.

The DR however, is not of much practicable benefit in engine diagnostics, as the complexity of such a task requires networks with more than one modifiable connection layer.

4.3.3.4 Backpropagation (Gradient Descent) Learning

Backpropagation (BP) is an extension of the least mean square (LMS) algorithm employed to train MLPs. LMS and BP are approximate steepest descent algorithms that minimise squared error. Rumelhart et al (1985) reported the development of the BP algorithm, which has emerged as the most popular algorithms for training of MLPs. BP is so called because computations of derivatives begin at the last layer and are propagated backwards through the network, layer-by-layer. BP is a recursive form of the DR with the additional effect that nonlinear activation functions are required. The input data is repeatedly presented to the neural network. With each presentation, the output of the neural network is compared to the desired output and an error is computed. This error is then fed back (backpropagated) to the neural network and used to adjust the weights such that the error decreases with each iteration and the neural model gets closer and closer to producing the desired output. A typical learning process is shown in Figure 4.10.

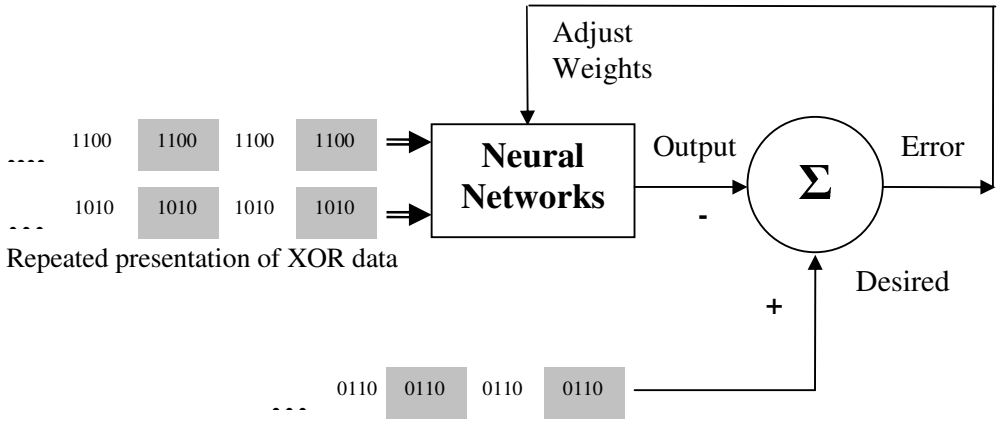

Figure 4.10 ANN training to model the exclusive-or (XOR) data

Generally, the learning structure from a high-level perspective is:

Initialise weights

Repeat

For the set of training patterns

Train on those pattern(s)

End for loop

Until error is acceptably, low

From a mathematical perspective, BP uses the chain rule to compute the derivatives in the hidden layers. The derivation of the BP algorithm is contained in many standard textbooks on neural networks (Hagan et al, 1996; Kevin, 1997; Haykin, 1999), in the sequel; we will present a brief outline of the working principle, since BP forms the initial basis for learning algorithms that would be applied in this research. Two possible scenarios are looked into: (1) when the neuron is output and (2) when it is hidden. For both scenarios, the weight update routine is similar with the difference being in the local gradient expression to apply.

(A) Output Neurons

Step 1: Propagation of Input Through Network

The function (input) or layer signal a_i, propagates through the network as defined by the relation:

$$a_j(p) = \Phi_j \sum_{i=1}^{M} \left(w_{ji}(p) a_i(p) \right) \tag{4.9}$$

$$= \Phi_j(v_j(p)) \tag{4.10}$$

where Φ_j is a non-linear activation function applied to neuron j.

M is the number of input elements including the bias

$v_j(p)$ is the induced local field, i.e. the product of connection weights and signals. It is defined as:

$$v_j(p) = \sum_{i=1}^{M} w_{ji}(p) a_i(p) \tag{4.11}$$

Step 2: Sensitivity Computation

The instantaneous error, that is, error resulting from the presentation of each pattern set was given in equation (4.8). The average error however, over all patterns p in the set P is obtained from:

$$\bar{E} = \frac{1}{2P} \sum_{p=1}^{P} \sum_{j \in C} e_j^2(p)$$

$$= \frac{1}{P} \sum_{p=1}^{P} E(p) \tag{4.12}$$

where equation (4.12) defines the batch cost function as a measure of the performance parameter E(p). This averaged form of the equation is most representative of the process performance and it is the objective of the learning process to minimise this cost function through the mechanism of free parameters (weights and biases) adjustments.

According to the chain rule of differentiation:

$$\frac{\partial E(p)}{\partial w_{ji}(p)} = \frac{\partial E(p)}{\partial e_j(p)} \frac{\partial e_j(p)}{\partial a_j(p)} \frac{\partial a_j(p)}{\partial v_j(p)} \frac{\partial v_j(p)}{\partial w_{ji}(p)} \tag{4.13}$$

Using equations (4.7)-(4.11) in (4.13) gives:

$$\frac{\partial E(p)}{\partial w_{ji}(p)} = -e_j(p)\Phi_j'(v_j(p))a_i(p) \tag{4.14}$$

Step 3: Determine Weight Update

The correction to be applied to synaptic weights, $\Delta w_{ji}(p)$, is proportional to the sensitivity factor, $\partial E(p)/\partial w_{ji}(p)$ with the constant of proportionality being the BP learning-rate parameter, η. Thus:

$$\Delta w_{ji}(p) = -\eta\frac{\partial E(p)}{\partial w_{ji}(p)} \tag{4.15}$$

where the negative sign indicates the gradient descent phenomenon of the BP approach. Substituting equation (4.14) in (4.15), we obtain:

$$\Delta w_{ji}(p) = \eta\delta_j(p)a_i(p) \tag{4.16}$$

where $\delta_j(p)$ is the local gradient from neuron j defined as:

$$\delta_j(p) = -\frac{\partial E(p)}{\partial v_j(p)}$$

$$= \frac{\partial E(p)}{\partial e_j(p)}\frac{\partial e_j(p)}{\partial a_j(p)}\frac{\partial a_j(p)}{\partial v_j(p)} \tag{4.17}$$

$$= e_j(p)\Phi_j'(v_j(p)) \tag{4.18}$$

(B) Hidden Neurons

The presence of hidden neurons requires a recursive treatment of the typical DR to cater for such hidden neurons. If the subscript j is taken to represent a hidden neuron and k an output neuron, then such a networks output can typically be computed from:

$$a_k(p) = \Phi_k\sum_{j=1}^{L} w_{kj}(p)a_j(p) \tag{4.19}$$

where L is the number of neurons in the hidden layer j. Also we note that:

$$a_j(p) = \Phi_j(v_j(p)) \tag{4.20}$$

The instantaneous error from neuron k in the output layer is given by:

$$E(p) = \frac{1}{2}\sum_{k\in C} e_k^2(p) \tag{4.21}$$

where

$$e_k(p) = t_k(p) - a_k(p) \tag{4.22}$$

$$= t_k(p) - \Phi_k(v_k(p)) \tag{4.23}$$

From equation (4.23), we have:

$$\frac{\partial e_k(p)}{\partial v_k(p)} = -\Phi_k'(v_k(p)) \tag{4.24}$$

Noting that from equation (4.19), the induced local field is:

$$v_k(p) = \sum_{j=1}^{L} w_{kj}(p)a_j(p) \tag{4.25}$$

then

$$\frac{\partial v_k(p)}{\partial a_j(p)} = w_{kj}(p) \tag{4.26}$$

The chain rule expression in equation (4.13) can be modified slightly to give:

$$\frac{\partial E(p)}{\partial w_{ji}(p)} = \frac{\partial E(p)}{\partial a_j(p)}\frac{\partial a_j(p)}{\partial v_j(p)}\frac{\partial v_j(p)}{\partial w_{ji}(p)} \tag{4.27}$$

where j now denotes a hidden layer.

It can be shown that:

$$\frac{\partial E(p)}{\partial a_j(p)} = \sum_{k=1}^{D} e_k(p)\frac{\partial e_k(p)}{\partial v_k(p)}\frac{\partial v_k(p)}{\partial a_j(p)} \tag{4.28}$$

where D is the number of neurons in the output layer.

Substituting equations (4.24) and (4.25) into (4.28) gives:

$$\frac{\partial E(p)}{\partial a_j(p)} = -\sum_{k=1}^{D} e_k(p)\Phi_k'(v_k(p))w_{kj}(p)$$

$$= -\sum_{k=1}^{D} \delta_k(p)w_{kj}(p) \tag{4.29}$$

From equation (4.17) we can re-define $\delta_j(p)$ in the form:

$$\delta_j(p) = \frac{\partial E(p)}{\partial a_j(p)}\frac{\partial a_j(p)}{\partial v_j(p)} \tag{4.30}$$

Differentiating equation (4.20) with respect to $v_j(p)$ and combining the result with equation (4.29) in (4.30) gives:

$$\delta_j(p) = \Phi_j'(v_j(p))\sum_{k=1}^{D}\delta_k(p)w_{kj}(p) \tag{4.31}$$

which is the BP formula for the local gradient in a hidden neuron.

Equations (4.16), (4.18) and (4.31) effectively summarise the BP learning algorithm for a MLP. Equation (4.16) implies that the weight on each connection should be changed by an amount corresponding to the product of an error signal and the function signal sending activation along the connection. Equations (4.18) and (4.31) on the other hand specifies the type of error signal to be used in computing the weight change and this depends on the computational layer involved. For an output neuron, equation (4.18) is applied while for a hidden neuron, equation (4.31) is applied.

It should be noted that in the computation of the induced local field, the bias has been subsumed in the weight and function signal terms by considering the bias as having a weight of w_{j0} or w_{k0} and an input nomenclature of a_0. This approach enhances the ease of following through the derivation.

The learning rate η, when increased has the ability to hasten learning but there is a limit to this increment as instability resulting from net oscillations may occur. This has thus led to the introduction of an adaptive technique to regulate the learning rate and therefore a momentum term is added to the learning rule. If $\Delta w_{ji}(n)$ is the n^{th} change in weight w, then:

$$\Delta w_{ji}(n) = \eta\delta_j(n)a_i(n) + \alpha\,\Delta w_{ji}(n-1) \tag{4.32}$$

$$0 <= \alpha < 1$$

The momentum term $\alpha\Delta w_{ji}(n-1)$ is the momentum constant α, multiplied by the previous weight change.

The momentum constant determines the effect of past weight changes on the current direction of movement in the weight space. The operation of this technique is such that if the current and previous weight estimates are of the same sign, weight change would be cumulative and the net gathers momentum, thus the path is a descent. If they are of opposite signs, their combined values produce a lower change in weight and we are undulating up and down and a reduction in weight update would rapidly bring stability. The application of momentum thus accelerates convergence in addition to enhancing stability of the network.

Unlike the DR, BP learning is useful for networks with internal representations, that is, networks with hidden layers. Rumelhart et al (1985) states that without hidden units, the error surface is shaped like a bowl with only one minimum making it possible for the DR operating on gradient descent to find the best set of weights. However, with hidden units, the error surface is not concave upwards and the possibility of being stuck in a local minima exist, thus the need for alternative learning rules.

4.3.3.5 Delta-bar-Delta Learning

The delta bar delta learning was developed by Jacobs (1988) to improve the learning rate of standard feedforward, backpropagation networks. It is algorithmically different from BP learning.

In the backpropagation procedure, the standard learning rates are applied on a layer by layer basis and the momentum term is usually assigned globally. The delta-bar-delta paradigm uses a learning method where each weight has its own self-adapting coefficient and it also does not use the momentum factor of the backpropagation architecture. In other words, every connection weight of a network has its own learning rate. This approach is motivated by the assumption that the step size appropriate for one connection weight may not be appropriate for all weights in that layer. Further, these learning rates should be allowed to vary over time. Different learning rates for each

connection and adaptivity in the learning rate values is believed to reduce convergence time. However, this process is complicated in that empirical evidence suggests that each weight may have quite different effects on the overall error.

4.3.3.6 Extended Delta-Bar-Delta Learning

Minai and Williams (1990) developed the extended delta bar delta algorithm as a natural outgrowth from Delta-bar-Delta algorithm. The difference with the Delta-bar-Delta is the addition of an exponential decay to the learning rate increase, and a re-inclusion of the momentum term as was in the BP algorithm. In addition, the learning rate and momentum coefficient were kept below certain levels to prevent wild jumps and oscillations in the weights.

4.3.3.7 Levenberg Marquardt Algorithm

Levenberg Marquardt (LM) algorithm is one of the fastest tested algorithms for training MLPs of moderate size. LM does not require the computation of the Hessian matrix (Demuth and Beale, 2001) as does other approaches such as the quasi-Newton methods but approximates it as shown by the relation in equation (4.33)

$$H = J^T J \tag{4.33}$$

With the gradient computed from

$$g = J^T e \tag{4.34}$$

where J is the Jacobian matrix containing the first derivatives of the network errors with respect to the weights and biases and **e** is the vector of network errors. A major drawback of this algorithm is the storage space required for large problem sets because matrices with dimensions equal to the number of patterns by the number of network free parameters has to be inverted during each iteration.

4.3.3.8 Bayesian Regularisation (BR)

One of the problems that impede the effective use of ANN in real application is inability to determine the optimal architecture for a particular problem which would otherwise

improve generalisation of the networks to scenarios it has not seen before. Various ways to tackle this problem have been suggested and include early stopping and regularisation. A regularisation technique has to be applied during training to ensure that only relevant features will, indeed survive after convergence. The use of regularisation involves modifying the performance function that is usually chosen to be the sum of square of network errors on the training set. If the performance function is modified to include a term that weights the network free parameters and network error (equation (4.35)), then the network would be caused to have smaller weights and biases and thus forcing the network response to be smoother and less likely to overfit.

$$MSEreg = \gamma mse + (1 - \gamma)\, msw \tag{4.35}$$

Where MSEreg is the regularised performance function

mse is the network performance function

msw is the mean square of network free parameters

γ is the performance ratio

The Bayesian regularisation algorithm was found to provide excellent results during classification and relatively poorer results during function approximation when compared to other training functions such as scaled conjugate gradient. Another limitation of BR algorithm is that it is computational expensive as large matrix dimensions are involved during training.

4.3.3.9 Conjugate Gradient.

In order to speed up network training, higher-order information about the error surface at any given point is required. One approach that belongs to the class of techniques called *second-order optimisation* is the conjugate gradient method. Network architectures operating on this technique use a standard feedforward recall structure, which is not based on BP, though they all begin by searching in the steepest descent direction (negative gradient) on the first iteration. Instead, the directed random search adjusts the weights randomly. In most conjugate gradient algorithms, this weight

adjustment will require the use of a line search in conjugate directions to approximate a step size. This can be time consuming because of its trial and error nature.

Moller (1993) introduced one of the variations of this algorithm called *scaled conjugate gradient* (SCG), which operates without line searching. In order to avoid the computationally expensive and time-consuming line search of other conjugate gradient algorithms, the SCG combines a model-thrust region approach, known from Levenberg-Marquardt algorithm, with the conjugate gradient technique. What is implied is that a scaling mechanism is used to approximate the step size rather than a line search. In addition to circumventing a line search, no user-defined parameters are required, thus avoiding activities that would be crucial to the success of the algorithm's convergence. The SCG has been shown to be more effective and faster than other conjugate gradient algorithms and BP (Moller, 1993). Our empirical analysis of the algorithms, showed the robustness of the SCG especially in driving the performance error to lower levels, and thus it was used for training the networks reported in this thesis. A brief description of the mathematical processes behind the SCG is given in APPENDIX A.3.

4.3.3.10 Kohonen's Learning Law

Kohonen (1982) developed a learning procedure that was inspired by learning in biological systems. This procedure, premised on competition amongst processing elements assigns as winner, the processing element with the largest output thus empowering it with the capability of inhibiting its competitors as well as exciting its neighbours. The winning element alone is permitted to provide an output with its neighbours allowed a weight update. The size of the neighbourhood is not static during training, thus, it is usually to commence with a larger definition of the neighbourhood and then narrow it as training progresses. Because the winning element is defined as the one that has the closest match to the input pattern, Kohonen networks model the distribution of the inputs (Anderson and McNeill, 1992). This is considered good for

statistical or topological modelling of the data and is sometimes referred to as self-organizing maps or self-organizing topologies.

4.3.4 Transfer Functions

A transfer function or activation function is required for limiting the amplitude of the output of a neuron. Some of these can also be referred to as squashing functions in that they squash (limit) the permissible amplitude range of the output signal to some finite value.

Transfer function could be placed in three categories – hard limit or step functions, linear transfer functions and sigmoidal transfer functions.

The hard limit transfer function (Figure 4.11a) limits the output of the neuron to either 0, if the net input, n, argument is less than 0, or 1, if the net input argument is greater than or equal to 0. This type of transfer function can be applied in classification problem which is an all or non affair.

Linear transfer functions (Figure 4.11b), more commonly applied as linear approximators in *Linear Filters,* provide linear outputs from net inputs and both have a direct variation. Application of this type of transfer function in diagnostic is limited to output layers in a multilayer network. Since the gas turbine parameter relationships are predominantly non-linear, use of a linear activation function in the hidden layer units achieves no advantage; in addition linear activation functions are discontinuous and hence will not suffice for backpropagation networks where a derivative of the transfer function is required in computing the weight change.

The sigmoid transfer function, takes net input, n, in a range of plus and minus infinity and squashes it into the range [0, 1], for Log-Sigmoid (logistic) transfer function (Figure 4.11c), and an output range of [-1, 1], for Tangent-Sigmoid (hyperbolic tangent) transfer

function (Figure 4.11d). These transfer functions otherwise referred to as non-symmetric and anti-symmetric respectively, are commonly applied in backpropagation networks and more particularly in engine diagnostics because they are differentiable and well adapted for nonlinear environments. In cases where zero input means as possible, tangent sigmoid transfer functions are reported to provide faster convergence as well as avoiding the problem of systematic bias on neurons located beyond the first hidden layers of a MLP (Haykin, 1999). The mathematical definitions of these transfer functions are given in equations (4.36) and (4.37). This research predominantly, uses the Tangent Sigmoid transfer function for all network nodes requiring weight adjustments.

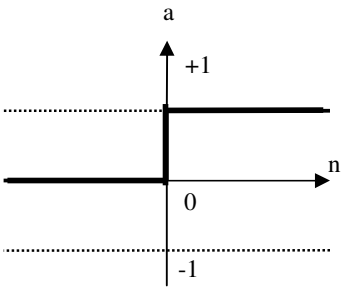

(a) Step transfer function

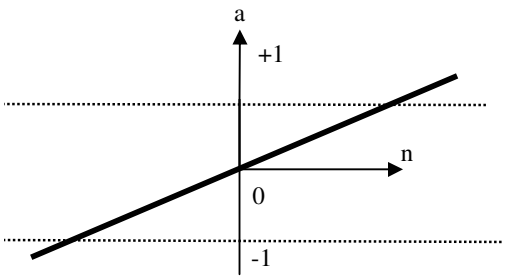

(b) Linear transfer function.

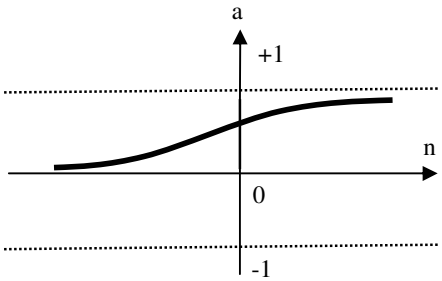

(c) Logistic transfer function.

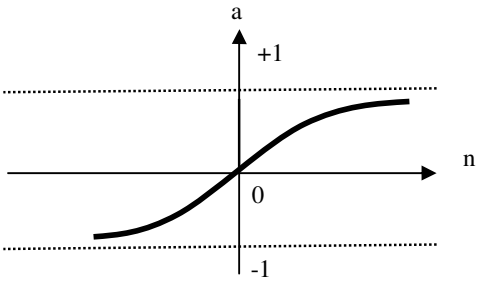

(d) Hyperbolic tangent transfer function.

Figure 4.11 Typical transfer functions

$$a_j = \text{logsig}(n_j) = \frac{1}{1+\exp^{-n_j}} \tag{4.36}$$

$$a_j = \text{tansig}(n_j) = \frac{e^{n_j} - e^{-n_j}}{e^{n_j} + e^{-n_j}} \tag{4.37}$$

where n is this case is the induced local field(i.e. the weighted sum of all synaptic inputs plus the bias) of neuron j, and a_j is the output of the neuron.

4.4 Teaching an ANN

4.4.1 Supervised Learning.

A number of currently available ANNs are trained with supervision. This mode of training requires comparison of the network actual output with a desired target. Weights, which are usually randomly set to begin with, are adjusted either on presentation of each pattern (sequential training) or after a presentation of all patterns in the training set (batch training). The overall objective is to minimise the error from processing elements by modifying connection weights until an acceptable network accuracy level is attained.

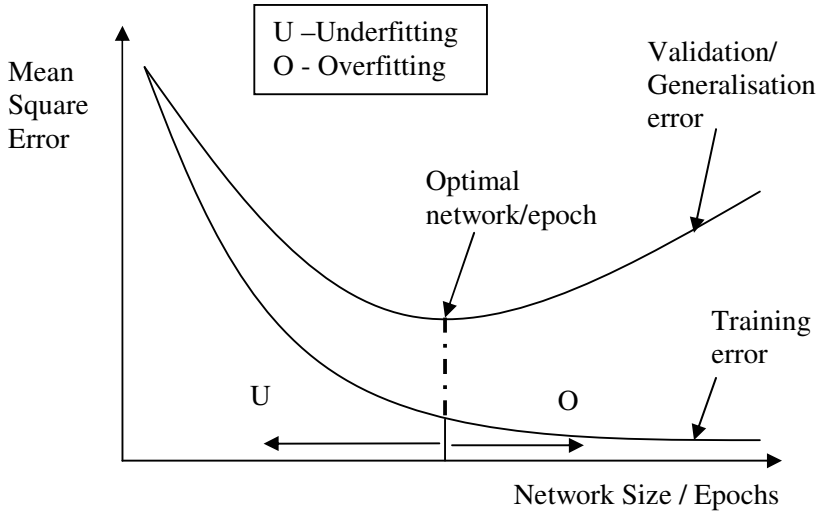

Figure 4.12 Network underfitting and overfitting during training.

Networks based on the supervised concept require training before they can be useful. The training process requires presentation of a set of inputs and desired outputs (target) to the network. In most applications, actual data are used but in the absence of such, representative simulated data are applicable. Depending on the complexity of the problem, training can consume a lot of time; in fact, this can run into weeks in cases with inadequate processing power. Training is considered complete when the neural network reaches a user defined performance level. This level signifies that the network has achieved the desired statistical accuracy as it produces the required outputs for a given sequence of test inputs i.e. the network generalises well. Before the optimal point, the network will underfit the problem space and beyond it, overtraining or overfitting occurs (Figure 4.12). Underfitting implies that the network free parameters are not sufficient or have not been trained enough to learn the representations of the problem features while in overfitting, the network free parameters are either excessive or overtrained such that undesired contributions in the input space due to noise are stored in synaptic weights of the network.

When good generalisation to test data has been achieved, the network weights are then frozen for the application. It is possible to allow some continual training of a trained network in order to adapt to changing conditions.

It is important that the training set covers the range of conditions expected otherwise the network may not generalise well. Because networks learn from examples, large sets are normally required to set up ANN applications. Because of the differences in sets of training patterns, it is best to allow networks find the best weights from the total set of fact, thus, batch-training approach would give better results that sequential approach.

4.4.2 Unsupervised Learning.

Unsupervised learning holds great promise for the future: computers could someday learn on their own in a true robotic sense (Anderson and McNeill, 1992). However, the

use of unsupervised leaning is currently limited to networks known as self-organizing maps (SOMs). Though SOMs are not in widespread use, they can provide a solution in a few instances, proving that their promise is not groundless. They have been proven more effective than many algorithmic techniques for numerical aerodynamic flow calculations (Anderson and McNeill, 1992).

Networks trained on unsupervised learning use no external influences to adjust their weights; rather, they internally monitor their performance. The learning process involves a search for regularities or trends in the input signals, with adaptations made according to the function of the network.

The basis for learning in unsupervised training could be by cooperation among clusters of processing elements or by competition between processing elements. In the former case, an external input activating any node in a cluster leads to an increased activity in that cluster while reduction of the external input to nodes in a cluster inhibits the entire cluster's activity. In the case of competition amongst clusters, training could amplify the responses of specific groups to specific stimuli with the result that these groups become associated with each other.

Increased understanding of unsupervised learning is still the subject of research. Governments are reportedly interested in this research because military situations often do not have a data set available to train a network until a conflict arises (Anderson and McNeill, 1992). However, unsupervised learning finds application in vector quantisation, Kohonen feature maps and Hopfield networks amongst others.

4.4.3 Learning Rates.

Learning rate is a crucial factor in the design of a network. A slow learning rate would mean lengthy time for setting up a network while a faster learning rate may lead to instability and inability of the network to make fine discriminations as would a slower

learning rate. One way to increase the learning rate without leading to oscillation is to include a momentum term in the computation of the weight increment as shown in equation (4.32)

Besides learning rate affecting the length of time for training, other factors that require consideration in this regard include size of the network, complexity of the network, network architecture, learning rule and desired level of accuracy. All these are critical to the networks overall performance.

4.5 Feedforward and Recurrent Networks

The difference between the recurrent networks and the feedforward networks lies in the former having at least one feedback loop. The feedback could be described as *self* or *no self* depending on whether or not a neuron's output is fedback to itself. The Elman and Hopfield networks are typical members of the recurrent architecture. Application of recurrent networks has been tested and found unsuitable for gas-path diagnostic tasks because of problems of convergence and local minima (Zedda and Singh, 1998)

4.6 Why Use An ANN?

ANN has been considered for the proposed diagnostic not only because of the limitations of current diagnostics techniques but also because of the potentials derivable from its full utilisation. In the sequel, we present some of the strengths of an ANN diagnostic system. Because there is no perfect system in existence, ANN limitations are also highlighted.

4.6.1 ANN Strengths

Amongst the identifiable advantages of ANN in diagnostics are:

1. The computational time required is shorter when compared to the aero-thermodynamic model after a net structure/architecture has been selected, trained and verified. Aero-thermodynamic models perform various degrees of

iterations of non-linear equations, which take a considerable longer time that those performed by the ANN.

2. Because ANNs can be trained with data obtained from a particular engine, they can be fully adapted to the conditions of that engine. This implies a better representation of that engine.
3. They possess the robustness to handle noisy data and measurement biases. In fact, ANN can be used in scenarios with low signal-to-noise ratios (S/N).
4. They posses an inherent ability to handle the highly non-linear relationships that exist between GT parameters.
5. Fewer sensors can be accommodated for fault diagnosis as long as the sensor measurements have some correlation with the faults.
6. The can be applied online due to fast speeds in recall mode.
7. They can work with large numbers of variables or parameters.
8. For cases with insufficient measurements, it is not usually possible to determine analytically, the number of components and hence the number of performance parameters that could be simultaneously varied by gas-path faults. This is a necessary condition for the application of such diagnostic techniques as GPA and its variants. ANN, as a computational intelligence technique, provides solutions from knowledge acquired from the environment through training.
9. They provide general solutions with good predictive accuracy.
10. In poorly modelled dynamics, neural networks possess a greater potential that other diagnostic techniques because it relies on the learning accumulated either online or from offline simulations (Napolitano et al, 1996).
11. They create their own relationship amongst information - no equations are required! That extends their problem solving capability to problems that we do not understand and know how to solve.
12. Most gas-path diagnostics techniques such as those using the weighted least-squares method and its variants, are model based, that is they are suitable for problems in engine performance diagnostics where influence coefficients are available as the model. ANN on the other hand can be used as model free

estimators because inputs and outputs cannot only be generated from models, but also from real data, or a combination of both. This feature is very useful if modelling information such as influence coefficients are not available.

4.6.2 ANN Weaknesses

Drawbacks of the ANN approach to diagnostic include:

1. Like other AI tools, ANNs are unable to perform creditably outside the range of data they have been exposed to, which implies that a massive use of data from encountered and foreseeable faults/conditions of operation would be required in their development.
2. Training times are long though this depends on the network type, size and the amount of training data. Trained networks with frozen weights would require retraining when machine stale operating conditions changes. This could mean retraining after machine overhaul as an instance.
3. Its deficiency in providing descriptive results though it is extremely predictive. We cannot access the neural network's "reasoning", but we can inspect and display the predictions it makes. The users are left to apply the knowledge of their business and some additional tools such as expert systems to reconstitute the explanations for the decision.
4. It is sometimes difficult to place a confidence value on the result of a network.
5. Limited operating points capability. As the number of operating points increases, the diagnostic error is bound to increase except a more effective means of data correction to standard day conditions is devised.

4.7 Summary

The development of an ANN was inspired by the way that the densely interconnected, parallel structure of the mammalian brain processes information. In the biological network, the receptive network of the dendrites carry electrical signals to the cell body (Soma) that effectively sums and thresholds these signals and via the axon, these

processed signals are transmitted to other neurons dendrites by a synapse interface. The ANN comprising weights, adders and transfer functions tend to mimic some of the characteristics of the biological network.

ANNs are being applied to a number of real-world problems of considerable complexity and importance. Application in such areas as pattern classification and system prediction are already well founded. As a branch of computational intelligence, ANN applies computational intelligence techniques to diagnostics.

Because of the diversity of problems seeking solutions, various structures of ANNs have evolved with continuous improvements being made to existing techniques. Available networks types include the perceptron, multilayer perceptron, radial basis function, learning-vector quantization, Hopfield, probabilistic networks and Kohonen, to name but a few. When training is considered, these networks fall into two categories, supervised and unsupervised. In the former, an established relationship from a model is available but in the latter, this condition does not exist: thus the network has to learn the data without a teacher or a prescribed target.

Learning algorithms are the procedures used by a network for weights and bias adjustments/modifications with the ultimate goal being to tune the network to achieve the intended task. Many learning laws are in common use. Most of these laws are some sort of variation of the best-known and oldest learning law, Hebb's Rule stated as "*When an axon of cell A is near enough to excite a cell B and repeatedly or persistently takes part in firing it, some growth process or metabolic change takes place in one or both cells such that A's efficiency, as one of the cells firing B, is increased*". A few of the learning laws have been presented. Procedures based on error backpropagation are more prominent at the moment.

Though the application of ANN to such task as engine diagnostics has some drawbacks, the strengths of such a diagnostic procedure would no doubt, eclipse its weaknesses.

In this research, various network types are used to find solutions for different tasks based on the relative advantages for such tasks. A scaled conjugate gradient algorithm is used, as the learning algorithm because of its ability to train a network to an acceptable level of generalisation error. The transfer/activation function for all training nodes is hyperbolic tangent sigmoid since it is differentiable and demonstrates an increasing nonlinearity capability.

CHAPTER 5

APPLICATION OF ADT TO GPFD

5.1 Introduction

In chapter 4, ANN, which is the central mechanism behind the advanced diagnostic technique was examined. Various types of ANN were considered, some of the available learning algorithms were discussed, and most frequently used transfer functions were examined. In addition, the teaching techniques of ANN were presented, finally, the advantages of an ANN diagnostic application were outlined.

Previous chapters have undertaken the ground preparation tasks and in this chapter we intend to lay the foundational blocks for a GPFD tool. The chapter is organised as follows. Section 5.2 seeks to provide answers to some key diagnostic questions. These questions border around defining the engine model and selecting appropriate sensor suite. Section 5.3 concentrates on data generation and correction amongst others. Section 5.4 discusses the network rules relevant to this work while issues regarding the network size are addressed in section 5.5. Finally, the chapter concludes with a summary of key findings in sections 5.6.

5.2 Requirement for Application of ADT to GPFD

5.2.1 What Engine Models?

For the purpose of this research, four engine models are considered. Two of these engines are thermodynamically similar to the Rolls Royce Avon and the Rolls Royce RB 211-24GT, the third is thermodynamically similar to the General Electric LM2500+ while the fourth is a 2-spool turbofan engine. These engines have been chosen as case studies to represent the classes of two and three shaft engines for stationary applications under steady state conditions while the turbofan engine considers the application of the

developed diagnostic structure to aeroengines under transient conditions. In what follows, we present a more detailed description of each engine.

5.2.1.1 Roll Royce Avon

The Rolls-Royce Avon was first made available in 1964. The industrial Avon is a single spool GT with shaftpower rating of about 14.5 MW. The RR Avon is used principally in the oil and gas industry to drive oil pumps or gas compressors with a small number used for electrical power generation. It is a mature engine with most units achieving over 150,000 running hours and cumulative operating hours of about 50 million. A typical view of such an engine is shown in Figure 5.1 and the schematic with station numbering is shown in Figure 5.2.

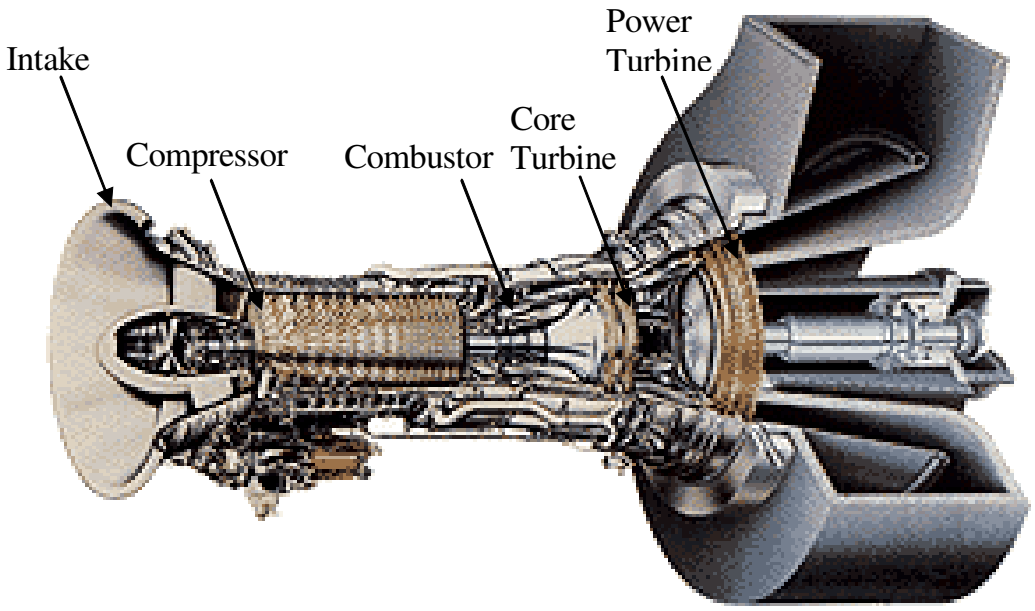

Figure 5.1 Typical 2-shaft aeroderivative GT with power turbine.

Information available from GT world handbook was used to thermodynamically model this engine. The results of this modelling with the corresponding error are shown in Table 5.1.

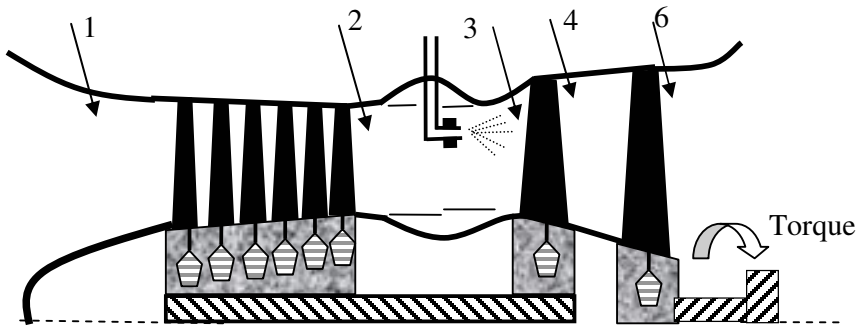

Figure 5.2 Schematic of a 2-shaft GT engine configuration

Table 5.1 Comparison between predictions using the thermo-mathematical model and published values for the RR Avon GT

Parameter	Units	Published[2]	Prediction	Difference
Mass Flow	kg/s	77.1	76	1.1
Pressure ratio		8.8	8.8	0
Shaftpower	kW	14580	14500	80
Thermal Efficiency	%	28.2	29.6	-1.4
EGT	^{o}C	442	434	8

5.2.1.2 General Electric LM2500+ (PK)

Table 5.2 Comparison between predictions using the thermo-mathematical model and published values for the LM2500+ GT

Parameter	Units	Published[3]	Prediction	Difference
Mass flow	kg/s	83.2	83.2	0
Pressure ratio		23.1	23.1	0
Shaftpower	kW	29080	29080	0
Thermal efficiency	%	38	39.08	-1.08
EGT	^{O}C	509.9	509.9	0

[2] Gas-Turbine World Handbook, 1998-99
[3] Ibid (1)

GE's LM2500+ GT is a simple cycle 2-shaft machine consisting of a gas generator and a power turbine which was first made available in 1998. The LM2500+ is a direct descendant of the GE LM2500, which is a direct derivative of the CF6-6 aeroengine. Some of its distinct features when compared to the LM2500 include an additional stage of compressor bladed disk (blisk) forward of the LM2500 first stage blading thus forming the zero stage in this engine. In addition, there is a redesign of the compressor first stage using wide chord without mid-span dampers, higher simple cycle efficiency, dual fuel capability (distillate and gas), dry low emissions (NOx and CO) combustion technology, variable speed operation and excellent part load efficiency. Its introductory rating is 27.6MW (37,000 hp) with a thermal efficiency in excess of 37%. The compressor has 17 stages, the high-pressure turbine 2 stages and the power turbine, 6 stages. Comparison of a thermodynamic model of this engine with published values is shown in Table 5.2.

5.2.1.3 Roll Royce RB211-24GT

The RB211-24GT is an aero-derivative GT system comprising a Rolls-Royce RB211 gas generator and a Cooper-Bessemer industrial power turbine. This engine was first introduced in 1974 and latter upgraded in 1999. The gas generator features two spools, designed for high-pressure ratio operation. The first (IP) spool consists of a seven-stage axial compressor coupled to a single-stage turbine. Concentric with this is the HP spool, consisting of a six-stage compressor and single-stage turbine. The two spools are mechanically independent, allowing each to run at its optimum speed. The engine is rated to provide shaftpower of 31.8 MW (42,600hp). Information obtained from a GT user, reveals that nine gas-path measurements (Table 5.7) are available for this engine. The schematic of such an engine is shown in Figure 5.3 while the thermodynamic comparison with the published design values are shown in Table 5.3.

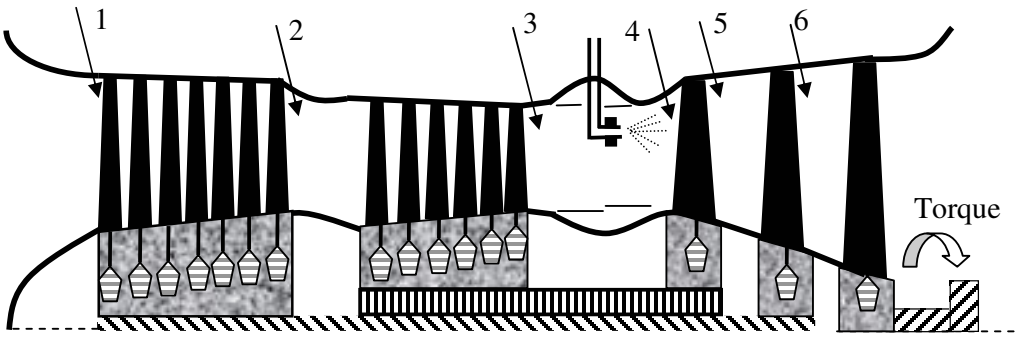

Figure 5.3 Twin spool stationary GT engine configuration

Table 5.3 Comparison between predictions using the thermo-mathematical model and published values for the RB211-24GT GT

Parameter	Units	Published[4]	Prediction	Difference
Mass flow	Kg/s	92.08	92.08	-
Pressure ratio		21.1	21.1	-
Shaftpower	KW	31780	31780	-
Thermal efficiency	%	40.1	38.8	-1.3
EGT	^{o}C	510.0	510.3	0.3

In all three-engine models presented, a non-linear robust engine simulation package was used to assemble the engine models. Engine performance deterioration is modelled by adjustments to efficiency and flow capacity scaling factors of the component(s) under consideration. This has the effect of rescaling the component maps. The intention here is to use the engine models to generate training and test data for the networks. An actual application of the developed approach would no longer need the engine model after the networks have been trained since the network parameters would be frozen at this time. Constantly generating training data and retraining networks would prove counter productive. This is because; some networks require reasonably long periods for training, hence a major advantage of ANN, which is its speed of convergence in the recall phase,

[4] Ibid (1)

would be lost. In this light, our application of ANN can be viewed as based on learning by examples rather than model based diagnostics (MBD).

5.2.1.4 Two-Spool Turbofan Engine

A modified transient performance prediction code, developed by Maccallum (1984) is used for this case study. The original code has been used to predict the transient processes of Rolls-Royce Spey and the Tay engines with satisfactory results (Maccallum, 1984). Small-time constants, inter-component volume methods as well as bulk metal temperatures were taken into account in the code. Maccallum and Qi (1989) and Pilidis (1983) described details of the transient prediction methods.

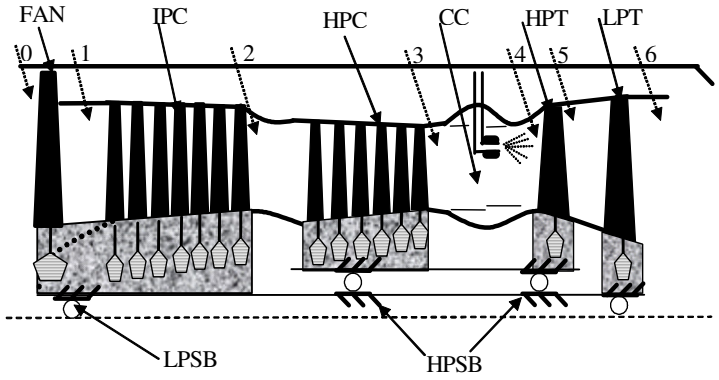

Figure 5.4 Schematic of turbofan engine model and station numbers

A typical schematic of the two-spool turbofan engine and its basic performance parameters are given in Figure 5.4 and Table 5.4 respectively.

Table 5.4 Design parameters for turbofan engine

Total mass flow rate	200 kg/s
Total pressure ratio	19
Bypass ratio	2.7
Turbine entry temperature	1350 K

Table 5.5 Possible instrumentation sets for indicating and isolating combined compressor and turbine faults in a 3-shaft engine with SOP as power-setting parameter

ENGINE: LM1600-PA (3 - SHAFT) | CASE STUDY: L | HANDLE: SHP | FAULT LEVEL: FI = 1%; EI = 1% (EDI = 1%)

VAR.	N1	N2	P2	T2	P3	T3	P4	T4	WFE	P5	T5	P6	T6	P7	T7	SHP	ETAC1	NDMC1	ETAC2	NDMC2	ETAT1	NDMT1	ETAT2	NDMT2	ETAT3	NDMT3	LGPA	NLGPA
1	X	X	X	X		X		X	X	X		X			X		X	X	X	X	X	X	X	X	X	X	1.184	0.285
2	X	X	X		X		X			X	X	X	X		X		X	X	X	X	X	X	X	X	X	X	1.080	0.055
3	X	X	X	X	X	X	X			X		X			X		X	X	X	X	X	X	X	X	X	X	0.635	0.034
4	X	X	X	X	X	X				X			X	X	X		X	X	X	X	X	X	X	X	X	X	0.703	0.495
5	X	X	X	X	X		X	X		X	X			X			X	X	X	X	X	X	X	X	X	X	0.600	0.018
6	X	X			X		X	X		X	X	X		X	X		X	X	X	X	X	X	X	X	X	X	0.663	0.297
7	X	X	X	X		X	X	X	X	X		X					X	X	X	X	X	X	X	X	X	X	0.630	0.015
8	X	X		X	X		X		X	X		X	X	X			X	X	X	X	X	X	X	X	X	X	1.023	0.101
9	X	X	X	X	X		X		X	X		X	X				X	X	X	X	X	X	X	X	X	X	0.573	0.035
10		X	X	X		X	X		X	X		X	X	X			X	X	X	X	X	X	X	X	X	X	2.241	0.054
11	X	X	X	X		X	X	X		X		X		X			X	X	X	X	X	X	X	X	X	X	0.703	0.032
12	X	X	X	X			X	X		X		X	X	X			X	X	X	X	X	X	X	X	X	X	0.722	0.079
13	X	X	X	X		X	X		X	X		X			X		X	X	X	X	X	X	X	X	X	X	0.630	0.015
14	X		X	X	X	X		X	X	X		X			X		X	X	X	X	X	X	X	X	X	X	2.034	0.206
15	X	X	X	X	X			X	X	X		X			X		X	X	X	X	X	X	X	X	X	X	0.626	0.016
16	X	X		X		X	X	X		X		X		X	X		X	X	X	X	X	X	X	X	X	X	0.971	0.076
17	X	X	X	X	X		X	X				X	X	X			X	X	X	X	X	X	X	X	X	X	0.691	0.449
18	X	X	X	X	X	X		X	X	X		X					X	X	X	X	X	X	X	X	X	X	0.632	0.015
19	X	X	X	X	X	X			X	X		X	X				X	X	X	X	X	X	X	X	X	X	0.993	0.205
20	X	X	X	X	X	X	X	X	X			X		X			X	X	X	X	X	X	X	X	X	X	0.716	0.061
21	X	X	X	X		X	X	X	X	X		X					X	X	X	X	X	X	X	X	X	X	0.630	0.015
22	X	X			X		X			X	X	X	X	X	X		X	X	X	X	X	X	X	X	X	X	0.846	0.092
23	X	X	X	X	X	X	X		X	X		X					X	X	X	X	X	X	X	X	X	X	0.636	0.013
24	X	X	X		X	X	X		X	X	X	X					X	X	X	X	X	X	X	X	X	X	0.640	0.054
25	X	X	X	X	X		X		X		X	X	X				X	X	X	X	X	X	X	X	X	X	7.178	0.061
26	X	X	X	X	X	X			X	X			X	X			X	X	X	X	X	X	X	X	X	X	0.679	0.453
27	X	X	X	X	X	X				X		X	X		X		X	X	X	X	X	X	X	X	X	X	0.645	0.020
28	X		X		X	X	X			X	X	X		X	X		X	X	X	X	X	X	X	X	X	X	0.739	0.166
29	X			X	X	X	X			X	X	X		X	X		X	X	X	X	X	X	X	X	X	X	8.951	5.594
30	X	X	X	X	X	X	X	X	X	X	X	X	X	X	X		X	X	X	X	X	X	X	X	X	X	0.673	0.015

INDEPENDENT VARIABLES

RMS

5.2.2 What Sensors?

Several reasons make this question very important. First, the only information available for engine performance estimation is the sensed parameters, and the number of performance parameters to be estimated is often greater than the number of sensors available. For such an underdetermined problem, there exist an infinite number of solutions for the given set of sensor measurements requiring some assumptions to be made in selecting the most probable solution. Secondly, an accurate estimation of performance parameters may not be achieved if sensor locations and combinations are not appropriate. For instance, turbine erosion problems can be better determined by taking measurements within and around the affected component than by relying on measurements further up stream. Finally, like GPA, ANNs in GT diagnosis will perform best when an optimal measurement set is available to undertake the diagnosis (Zedda et al, 1998). The implication of these is that, there is a need to systematically optimise the sensor set observability by optimising the combination, location in the gas-path and numerical quantity for the faults for which it is intended to diagnose.

One approach to obtaining an appropriate sensor set is by deliberately implanting faults in the GT components and observing the simultaneous effects on the measured performance parameters, and thence seeking the optimal combination of dependent variables that can describe such faults. This combination will facilitate the choice of types and locations of the sensors required for the diagnosis of the faults along the gas-path.

Ogaji and Singh (2002b) and Ogaji et al (2002c) have undertaken a study on the optimisation of measurement sets for GPFD in GTs. The studies involved the use of nonlinear GPA techniques to obtain various measurement combinations that demonstrated high degree of observability for the fault combinations implanted on a

thermodynamic engine model. Excerpts from Ogaji et al (2002c) on the description of their technique are included in Appendix A.4.

Table 5.5 presents results from a typical case study (L), involving a 3-shaft engine configuration. Simultaneous multiple faults are implanted in all five components (2 compressors and 3 turbines) of this engine. The implanted faults involved changes to ten health parameters (efficiencies and flow capacity for each component) and thus ten measurements were required by GPA to diagnose the faults. From the Table, L1→L28 are twenty eight possible combinations of the sensors that would be appropriate for the fault diagnosis in the engine gas-path components. L29 is an ineffective diagnostic suite while L30 considers the scenario where all possible sensors (15 in this case) are mounted on the engine. Discussions in Appendix A.4 have shown that a sensor suite such as L30 is not a necessary option.

In general, the optimal instrumentation selection study gave rise to a number of possible combinations of measurement sets with each set equally capable to diagnose the implanted gas-path fault, not withstanding their slight differences in RMS values. From this list, a choice can be made on a suitable combination with applied decision criteria including the cost of installation; ease of accessibility and other operating environmental issues such as working temperatures. In this research, the suites C22 (Table A.4.5) and L19 (Table 5.5) have been chosen as possible sensor combinations for diagnosing the gas-path faults for a 2-shaft and 3-shaft stationary GTs respectively with shaftpower (SOP) as handle. This choice is influenced primarily by data made available from a GT user (British gas Plc). Though the optimal instrumentation selection study required 10 sensors for the gas-path diagnosis of a 3-shaft engine, the company data showed that only 9 of these are mounted on the engine. This research would therefore be restricted to work within the ambit of what is available, that is, gas-path diagnostics for the 3-shaft engine configuration will be carried out with the 9-measurement set.

For the turbofan engine, the focus was limited to the components mounted on the HP and IP shafts that is the IPC, HPC, HPT and IPT. Eight engine measurements were thus considered.

The nomenclature of the chosen measurement sets for all three engine configurations are shown in Tables 5.6 - 5.8.

Table 5.6 Sensors, identity and accuracy ranges for a 2-shaft GT

Sensor	Identity	Unit	(%) Required accuracy over span[5]
N1	GG speed	-	± 0.03
P2	GG compressor delivery pressure	Atms.	± 0.1
T2	GG compressor delivery temperature	K	± 0.4
WFE	GG fuel flow	Kg/s	± 1.0
P4	GG exhaust pressure	Atms.	± 0.1
T4	GG exhaust temperature	K	± 0.4

Table 5.7 Sensors, identity and accuracy ranges for a 3-shaft GT

Sensor	Identity	Unit	(%) Required accuracy over span[6]
N1	GG speed	-	± 0.03
N2	GG (HP) speed	-	± 0.02
P2	IP compressor delivery pressure	Atms.	± 0.1
T2	IP compressor delivery temperature	K	± 0.1
P3	GG compressor delivery pressure	Atms.	± 0.1
T3	GG compressor delivery temperature	K	± 0.4
WFE	GG fuel flow	Kg/s	± 1.0
P6	GG exhaust pressure	Atms.	± 0.1
T6	GG exhaust temperature	K	± 0.4

[5] Source: British gas Plc
[6] Ibid(5)

Table 5.8 Sensors, identity and accuracy ranges for a turbofan GT

Sensor	Identity	Unit	(%) Required accuracy over span
T2	IPC total outlet temperature	K	± 0.4
T3	HPC total outlet temperature	K	± 0.4
T6	LPT total outlet temperature	K	± 0.4
P2	IPC total outlet pressure	KPa	± 0.1
P3	HPC total outlet pressure	KPa	± 0.1
P6	LPT total outlet pressure	KPa	± 0.1
N1	Low pressure relative shaft speed	%	± 0.03
N2	High pressure relative shaft speed	%	± 0.02

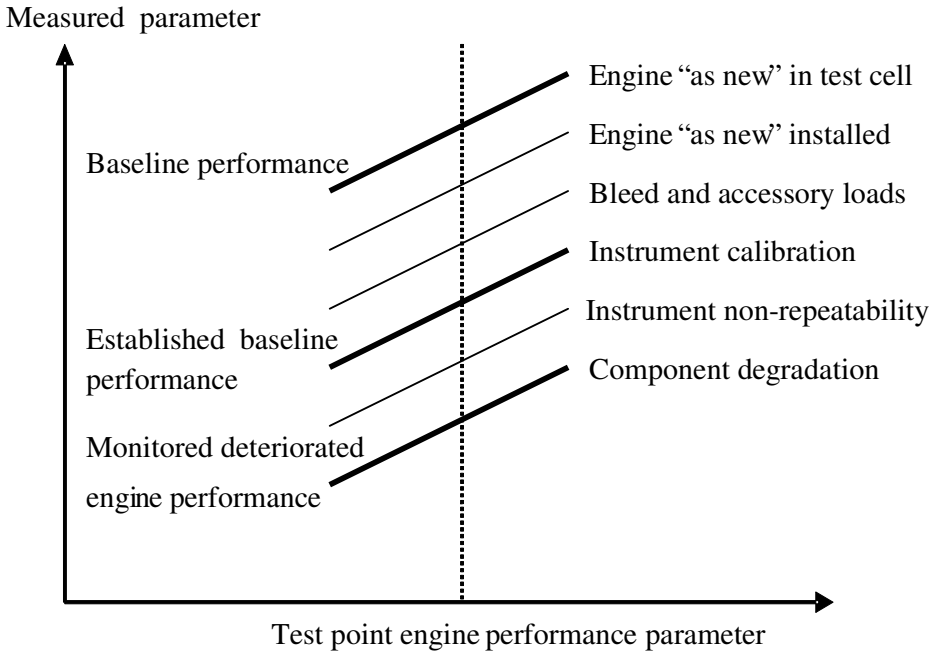

Figure 5.5 Effect of measurement non-repeatability

The analysis of faults, whether sensor or component, requires a baseline from which deviations can be obtained at a given operating point. Dependent and independent delta

variables used in training and testing the networks are computed as percentage deviations from a predetermined baseline using equation (5.1).

$$\Delta Z = \frac{Z - Z_{estbaseline}}{Z_{estbaseline}} * 100 \qquad (5.1)$$

Where:

$Z_{estbaseline}$ is the established baseline condition

Z is the measured or calculated value.

It is noteworthy that the established baseline (Figure 5.5) is obtained after all loses – installation, bleed and accessory loads, calibrations amongst others – except instrument non-repeatability and degradation have been accounted for. These non-repeatability values were applied as white noise with a gaussian distribution to generated engine data and have been determined to be in the range of three standard deviations from the mean value.

5.3 What Diagnostic Approach?

Deterioration is a change in performance of an engine from a previously established acceptable level or baseline. Performance deterioration modelling of engines is predicated on the singular notion that it must provide an adequate representation of the cause of the apparent engine problem.

In order to make explicit the effect of component deterioration on a GT performance, baselines must be established. A proper baseline would help to adjust predictions to be compatible with actual measurements since engine-to-engine tolerances, installation effects and sensor/transducer absolute level inaccuracies are eliminated as error sources (Doel, 1994, Urban, 1975). These baselines are regularly updated as test condition or other events dictate.

Many faults do not have empirical data to enable their investigation/development and so their effect will be subsumed into other faults of similar effects. Such faults include F.O.D, thermal damage amongst others. As an instance, F.O.D. has been shown to have similar effects as fouling on the compressor characteristics (Boyce, 1984).

A number of fault effects can be detected along the gas-path of a GT. These include such faults manifesting in:

- Compressor efficiency and flow capacity changes
- Turbine efficiency and flow function changes
- Cooling and leakage flows

In the face of insufficient instrumentation, in addition to their associated sensor errors, increasing the list of state (independent) variables, which are associated with the fault effects without additional sensors, will reduce considerably the average response of the system to fault identification. On the other hand, when fault effects or state variables of some components are left out from the analysis, for example, non-consideration of combustor faults, the impact is a compounding or translation of faults from such sources to those component state parameters that are considered which again is another restriction on proper fault identification. An improvement in sensor variability, functionality and location would make the otherwise unmodelled faults distinguishable (Doel, 1994a, Ogaji and Singh, 2002a).

Sources of component deterioration are numerous. In a compressor, for instance, these include:

- Engine transients that result in rubs between rotor blades and the shrouds or between the stators and the rotor blades, increasing clearances.
- Salt, sand or other materials ingested by the engine causing erosion of the compressor blades.

- Pollutants that cause blade profile/surface finish changes via corrosion and fouling.
- Rubs resulting in splatter on blades.
- Foreign or domestic object damage causing bending or even break off of compressor blades.

The result of this is a reduction of compressor efficiency as mass flow and pressure ratios are reduced. Power output drops while specific fuel consumption or heat rate (as used in the power industry) is increased.

It is obviously not an easy matter to spot each and every fault in the gas-path of an engine as there is some form of relationship between them with respect to the effects on the component they affect, thus it is usually the case that an identified effect be used as the basis for a maintenance plan.

Diagnosis is both a classification as well as an estimation problem, that is, it aims to determine the faulty element(s) of a system that fail to meet its expected performance with the overall objective of identifying a course of action that will eliminate the problem. The diagnostic task has thus summarily been classified into the following categories (Isermann, 1984; Lakshminarasimha et al, 1994):

- Fault detection – making a binary decision between fault and no fault condition
- Fault diagnosis – isolating the source of the fault
- Fault evaluation – characterising the extent and significance of the failure.

An effective gas-path analysis tool will involve augmentation that possesses the ability to effectively identify faults from the presented signature of the output data of the algorithm. It is necessary at this point to state that the variables needed for the diagnostic purposes, both state and measured, are assumed to be Gaussian, that is, their mean can be taken to be zero. This is achieved by defining these variables as deviations

from a nominal condition. Thus the measured variables as an instance is not the raw measured value but is its deviation from a nominal reference condition (baseline) and likewise, the state variables represent deviations from the same nominal point.

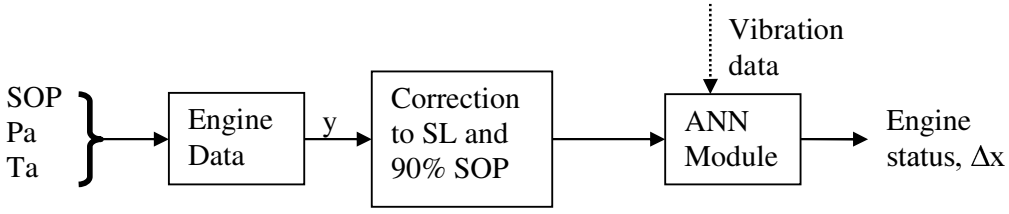

Figure 5.6 Level 1 data flow diagram (DFD)

From Figure 5.6, an engine or engine model to provide data, a parameter correction module and an ANN module are the basic requirements for the proposed diagnostic approach.

5.3.1 Engine Degradation Data

As stated in section 1.4, data required for this research would be obtained primarily from a thermodynamic model of the engine. This is done principally for two reasons:

1. It is difficult to obtain real life data for diagnostic studies in the required quantity and quality.
2. Simulation models can be tuned to meet engine operational conditions and thus data from such process would be close to real life values.

The steady state simulation code, Turbomatch, on which the stationary engines were designed was built at Cranfield University and allows the construction of various engine configurations and the simulation of these under various operating conditions. Sets of faulty and fault free data obtained from such a process are then used to build the diagnostic models having a knowledge database. Faulty data patterns included single, multiple sensor faults as well as single, and multiple component faults for all the engines considered. For the 2-shaft stationary engines, a maximum of 2-sensors can be

simultaneously faulty and for the 3-shaft stationary engine, up to 3-sensors can be faulty at any one time. This implies that the more sensors available on an engine as well as the more correlation between the different measurements, the more faulty sensors that can be diagnosed.

5.3.2 Parameter Correction

Introduction

Three parameters – shaftpower (SOP), ambient temperature (Ta) and ambient pressure (Pa)-, determine the operating point of the stationary engines used in this research. These parameters can never be fully constant at any given time during an engine operation. Thus, to obtain measurement baselines, a diagnostic programme would either require that engine data be generated each time a fault diagnosis is to be conducted or seek alternative approaches of obtaining these baselines.

In this research, a Triple Step Analytic (TSA) approach is developed, following a pattern reported by Volponi (1999), to correct data obtained at operating points other than the point at which the diagnostic networks were set up – the diagnostic point. The approach involves using a database of various operating points on which a 3-dimensional interpolation is carried out to determine the baselines for each of the engine measurements when the user has stipulated the current values for the ambient and power setting parameter. A proper positioning of the baseline is a step towards obtaining a sufficiently accurate value for the deviations of each of the measurements. This process is fast and results show that it is reliable and particularly to regions with operating points spread across good sections of the component maps.

In what follows, we determine if a relationship exists between engine measurements and the operating point setting parameters, define the region to concentrate on in carrying

out a TSA data correction and finally, describe the TSA approach to parameter correction.

Relationship between Operating Point Setting Parameters and Engine Measurements.

Before delving into computing correction exponents for the variables that set the operating point (SOP, Pa, and Ta), it is necessary to establish first, if a relationship exist and the nature of such relationship existing between these variables and the measurements taken from the engine. These pictures are captured in Figure 5.7 for the 3-shaft engine configuration. From Figure 5.7a, there is generally an increase in all measurements as SOP increases. This is obvious since at higher shaftpower and without engine faults, spool speeds, pressures and temperatures should rise. From Figure 5.7b, at constant SOP and Pa, as Ta increased, the engine ran hotter, speed increased, increasing the mass flow and hence station pressures dropped. Fuel flow also dropped slightly as temperature rise across the combustor dropped. In Figure 5.7c, an increase in Pa increased station pressures while other parameters dropped.

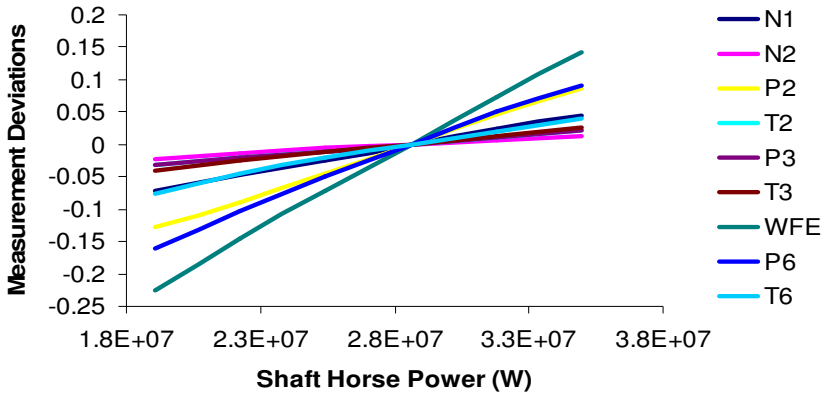

Figure 5.7a

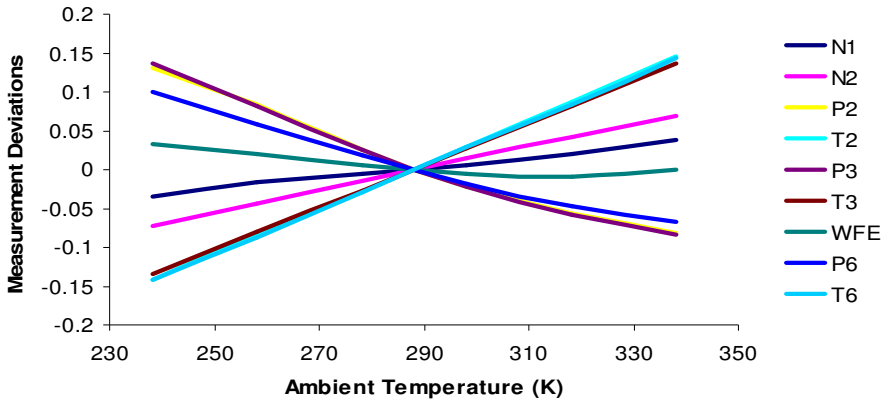

Figure 5.7b

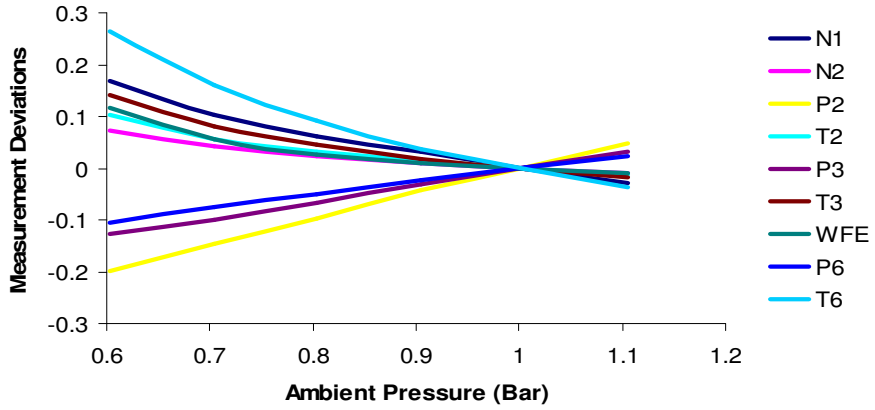

Figure 5.7c

Figure 5.7 (a-c) Variation of SOP, ambient temperature and ambient pressure respectively with engine measurements

In Figure 5.8, the variations of the three parameters setting the operating point are shown simultaneously plotted against the low-pressure relative shaft speed (N1) of a 3-shaft GT. The figure shows that the shaft speed is most increased at low pressures and high temperatures and lowest at points of low temperatures and high pressures. One reason for this is that compressor work varies with the ambient condition, as it is much easier to compress cold air than hot air, thus at hot conditions density drops and the only way to produce the same power level is for mass flow to increase and hence the engine

shaft rotates faster. In addition, the various surfaces (sheets) in the Figure represent various power setting parameter (SOP) levels, nine in this case and show LP speed increasing as SOP increases. The scenario with respect to other engine measurements can be similarly presented.

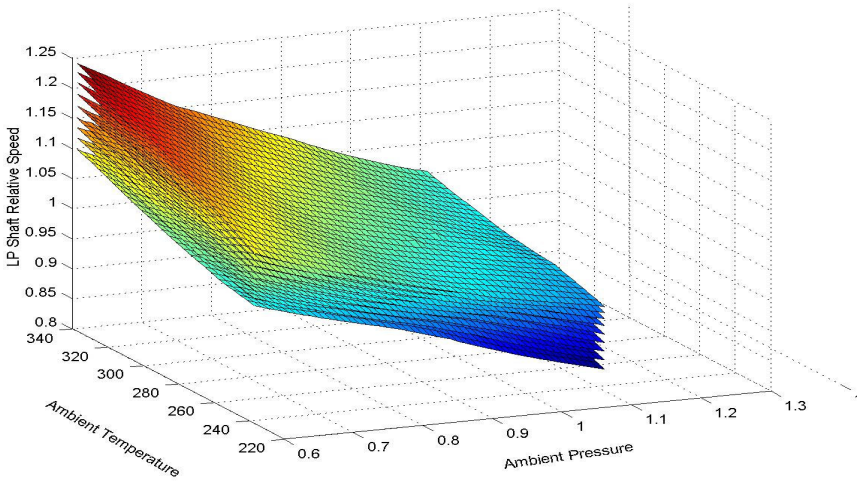

Figure 5.8 Effect of Pa, Ta and SOP variation on LP relative shaft speed (N1).

Given that relationships exist between the engine measurements and the setting parameters, it is evident from Figures 5.7 and 5.8 that these relationships are not linear. In addition, the surface plots in Figure 5.8 show that each surface possesses some form of distortion that makes it non-parallel with its neighbours but identical to them. A regression analysis carried out to map points on these surfaces failed because it was necessary to apply distinct coefficients to each surface. Thus, the TSA approach with adaptive exponents was devised. The TSA approach first determines exponents for each of the measurements from the baseline surface before applying such exponents to the deterioration surface for data correction.

Theory of the Triple Step Analytic (TSA) Approach

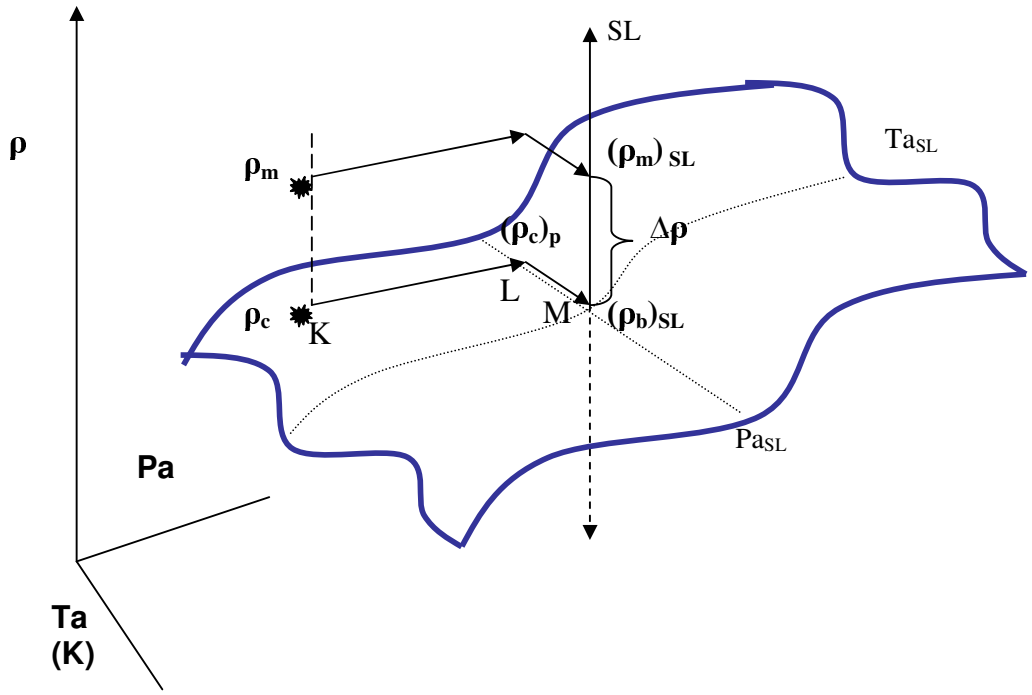

Figure 5.9 The dual step analytic correction approach for various environmental conditions

Visualising the TSA approach can be better understood if we first consider a simple dual step analytic (DSA) approach (Figure 5.9) involving correction for ambient conditions only. For any given engine measurement, ρ, and for any given point on a surface obtained from various combinations of ambient temperature (Ta) and ambient pressure (Pa), it is possible to define some relations that would transform such baseline point to another point termed reference, such as sea level (SL) conditions, as used in this case. By extension, any surface defined by a different engine state, probably induced by deterioration can be sufficiently described by relations developed at the baseline. Because the surfaces are irregular, it is reasonable to consider the fact that different points on the surface would require different correction exponents with a positive slope giving rise to a raised exponent while a negative slope, a decreased exponent.

Basic Assumption

For any given engine state, brought about by changes in component characteristics, the surface obtained when varying ambient temperatures, ambient pressures and shaftpower are considered for a given measurement, is identical to its baseline surface (obtained with no engine fault present) but located on a different plane due to the difference in measurement signatures.

Figures 5.10 to 5.12 present views of the surface obtained from a clean and a deteriorated engine with different operating points. In Figure 5.10, the 3-D surface of the variation of LP shaft speed in clean and deteriorated mode is shown plotted against varying ambient temperatures and pressures but at a fixed 80% SOP. In Figure 5.11, we show a cross-sectional view of the surface. From both Figures, the assumption made on the similarity of various surfaces at different fault levels over the entire operating range may appear justified.

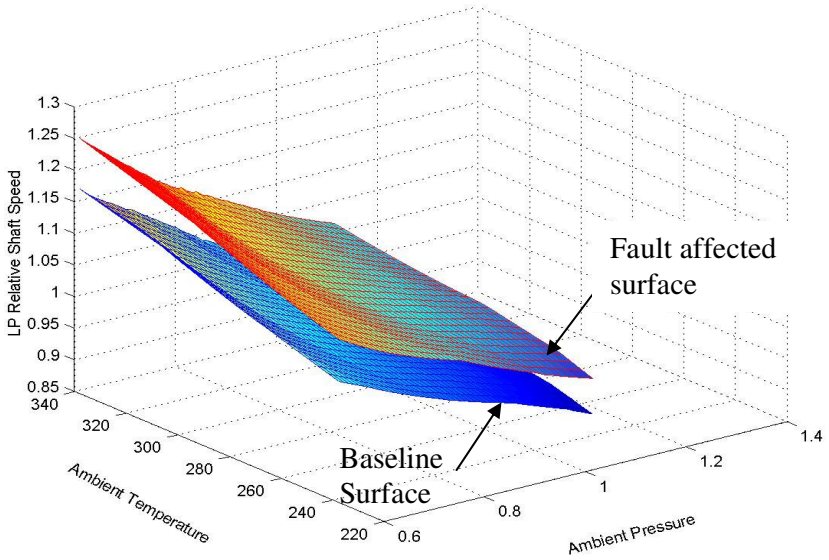

Figure 5.10 Surface view of the effect of IPC fouling (-3%η_{IPC} and -12%Γ_{IPC} drop) on LP relative shaft speed at 80% SOP

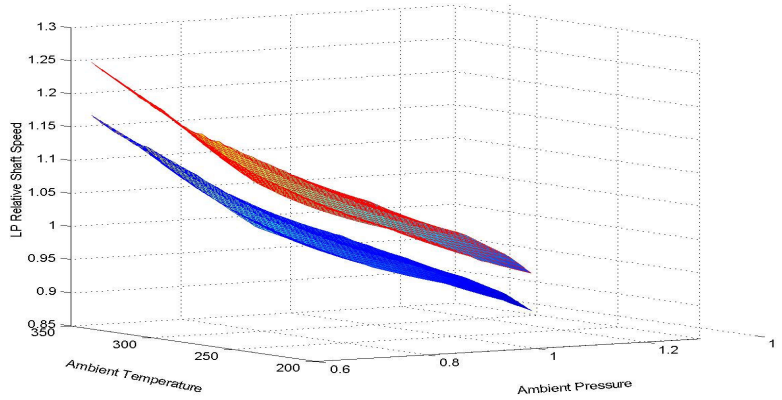

Figure 5.11 Cross sectional view of the effect of IPC fouling (-3% η_{IPC} and -12% Γ_{IPC} drop) on LP relative shaft speed at 80% SOP

Figure 5.12, shows a similar plot for the LPT outlet temperature. Again, the similarity of the surface curvatures is evident, and seems to validate our basic assumption.

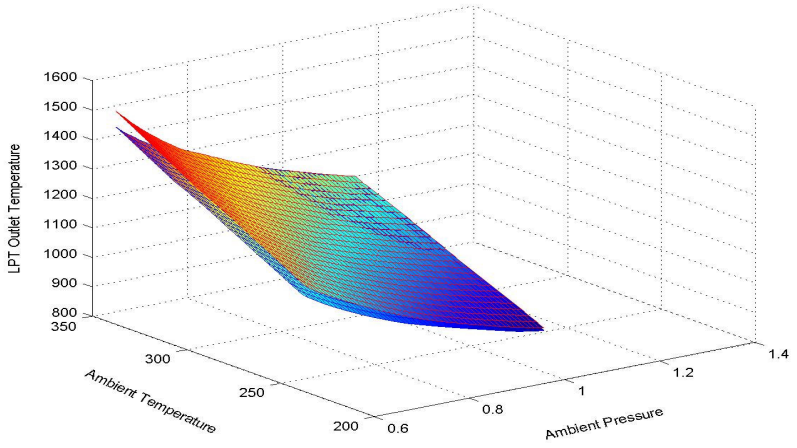

Figure 5.12 Surface view of the effect of IPC fouling (-3% η_{IPC} and -12% Γ_{IPC} drop) on LPT outlet temperature at 80% SOP

One way of validating our assumption is to determine the percentage deviation between the scenario when a fault is present in the engine and when there is no fault, across a given operating range for each parameter, ρ. In this case, we applied equation 5.2.

$$\%\text{Deviation} = \frac{\rho_{\text{Measured}} - \rho_{\text{Baseline}}}{\rho_{\text{Baseline}}} * 100 \qquad (5.2)$$

Equation 5.2 provided a relative comparison, which enabled us to ascertain the constancy of variations across the considered range. Plots obtained by computing the percentage deviations for all measurements under varying operating point setting parameters are shown in Figure 5.13. From Figure 5.13, variation of Pa presents the most distortion on percentage deviation of the measurements. The downward pointing vertical arrow indicates the point at which diagnostics is intended to be carried out. Thus from Figure 5.13, it is shown that the farther we go from the intended diagnostic point the more distortion we should expect and hence the less correct, our corrected measurement would be. The implantation of faults in a down stream component- LPT, with the percentage deviation computed and plotted in Figure 5.14 further indicates the distortions.

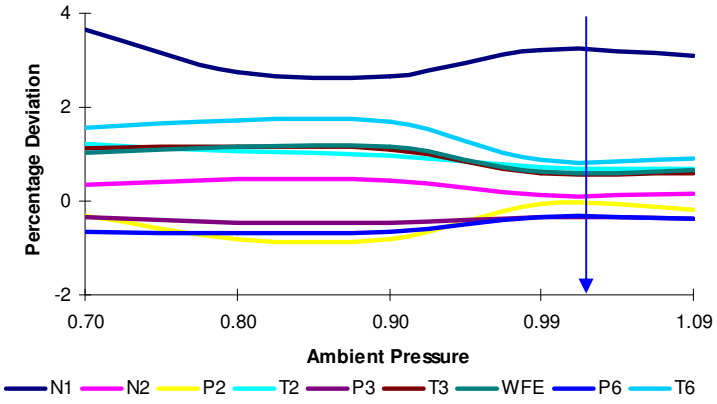

Figure 5.13a

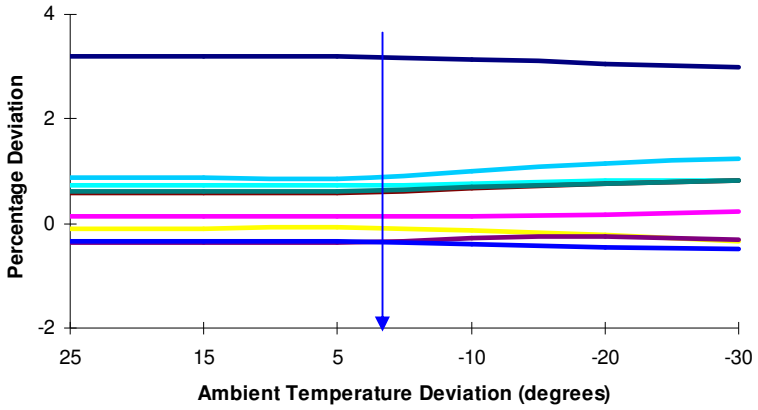

Figure 5.13b

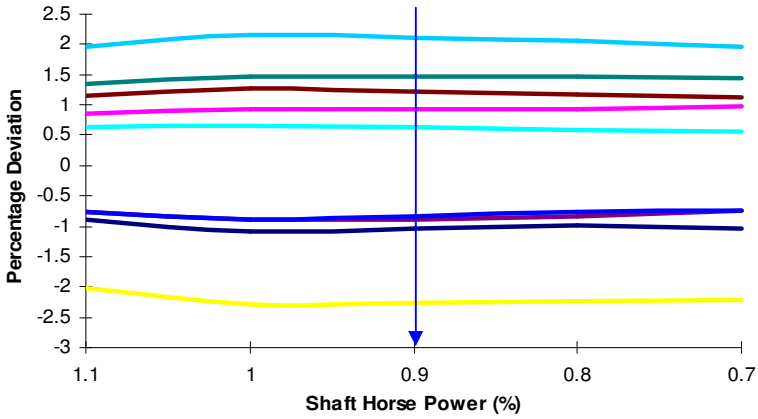

Figure 5.13c

Figure 5.13 (a-c) Percentage deviation of measurement from baseline for deteriorated IPC (-3% η_{IPC} and -6%Γ_{IPC}) with varying ambient pressure, ambient temperature and SOP respectively.

Reasons for this distortion can be traced to model inaccuracies resulting from the use of insufficiently accurate component maps in addition to the errors resulting from the use of scaling factors both to model the engine components and to simulate faults.

In order to minimise the multiplying effect of these errors, a logical approach would be to restrict range of operation to areas just around the intended diagnostic points as presented in Table 5.9, with various networks trained to handle other regions not covered by the current structure. It is necessary to note that this intended approach does not invalidate our initial assumption but provides the best option in the presence of the highlighted limitations.

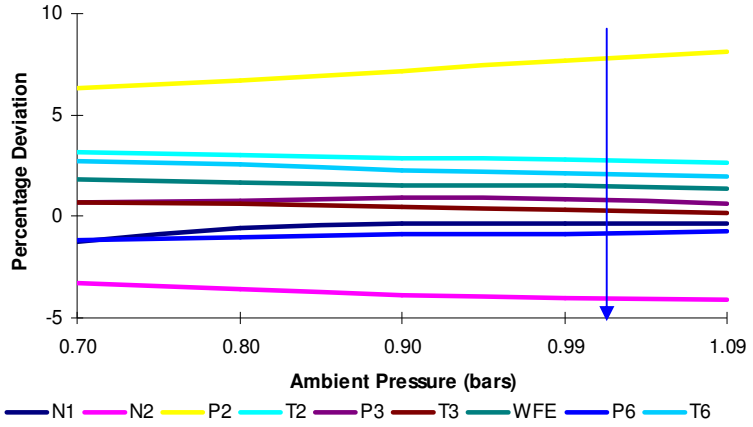

Figure 5.14a

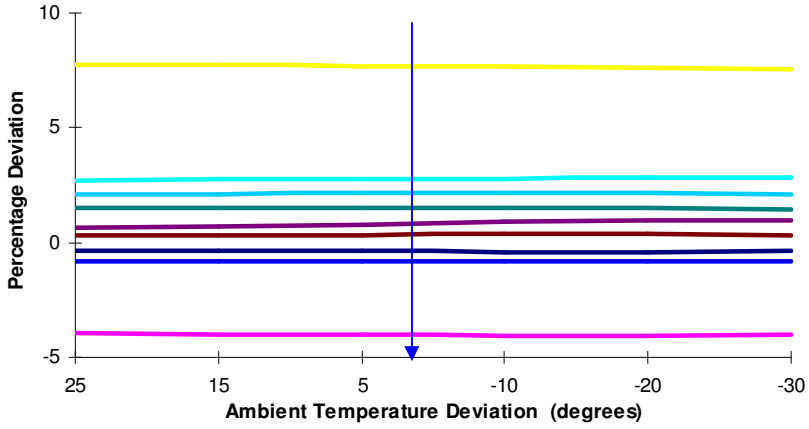

Figure 5.14b

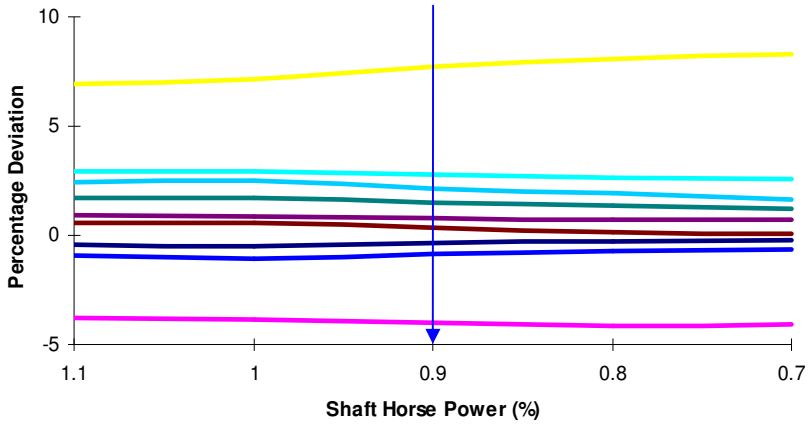

Figure 5.14c

Figure 5.14 (a-c) Percentage deviation of measurement from baseline for deteriorated LPT (-3% η_{LPT} and +6%Γ_{LPT}) with varying ambient pressure, ambient temperature and SOP respectively.

Table 5.9 Operational envelope of diagnostic model

Operating Point Variable	Diagnostic Point	Applicable Range of Model
Ambient pressure, Pa (bar)	1	0.97 to 1.02
Ambient Temp. Deviation, Ta (degrees)	0 (≡ 15 deg. Celsius)	-10 to 10
Shaftpower, SOP (%)	90	85 to 95

Methodology

The processes involved in making parameter corrections can basically be divided into two levels viz.:

LEVEL 1: Determine the correction exponents from baseline surface at prescribed ambient and shaftpower condition. For this multi-dimensional problem, three steps are required.

LEVEL 2: Use the obtained exponents to correct engine measurements to sea level condition – the specified reference point-.

These levels are further elucidated below.

LEVEL 1

The TSA approach can actually be carried out in any one of six possible routes for which we present one, i.e. KLMN, which is a stepwise correction for pressure, then temperature, and finally shaftpower (note that the step for MN is not indicated for simplicity). This is shown in Figures 5.9 and 5.15.

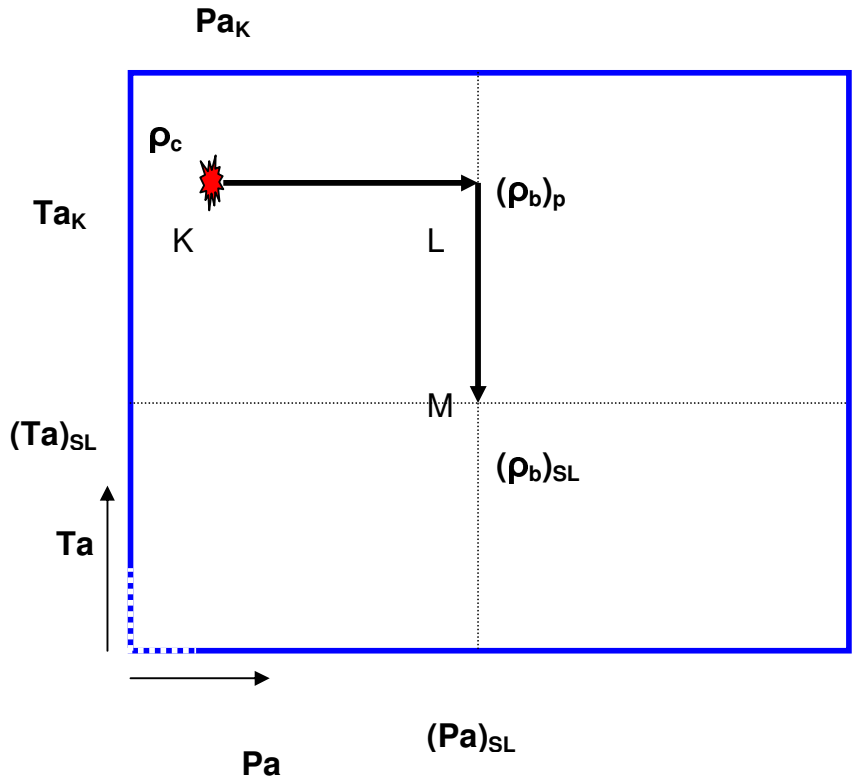

Figure 5.15 The DSA approach on a baseline surface.

Consider the surface in Figure 5.9 with a simplified plan view presented in Figure 5.15. The details of the intended approach are:

1. Given a point K with ambient temperature and pressure coordinates Pa_K and Ta_K respectively, we obtain the computed value of the considered parameter, $\boldsymbol{\rho_c}$, via

interpolation from a database or from an accurate thermodynamic engine model run with ambient temperature and pressure appropriately specified. Both approaches should give approximately the same results because the database was obtained from the engine model with very small steps applied. However, any differences between the results could be due to approximation errors.

2. From the surface plot, via a 2-D interpolation we obtain a baseline value for the parameter at point L, $(\boldsymbol{\rho_b})_{\mathbf{p}}$, i.e. value at SL pressure but temperature remaining at point Ta_K.
3. Next, with the same technique described above, we obtain baseline value at M, $(\boldsymbol{\rho_b})_{\mathbf{SL}}$ which is the value of the parameter with ambient temperature and pressure at reference point i.e. SL.
4. In moving from point K to point M, there is an ambient temperature and pressure influence on the value of the parameter and these have to be accounted for overtly or covertly.

A relation that could be applied for correcting variation of Pa, Ta and SOP in measurements is defined as-

$$(\rho_m)_{SL} = \frac{\rho_m}{\delta^a \theta^b \gamma^c} \tag{5.3}$$

where:

$(\rho_m)_{SL}$ is the parameter corrected to the reference point

ρ_m is the value of the measured parameter at some value of ambient pressure, ambient temperature and shaft output power.

δ is pressure ratio, which is prevailing intake pressure divided by reference point intake pressure

γ is the shaftpower ratio, which is measured shaftpower divided by shaftpower at reference point.

θ is the temperature ratio, which is prevailing ambient temperature divided by reference point ambient temperature.

a δ correction exponent

b θ correction exponent

c γ correction exponent

For this work-

$$\left.\begin{aligned} \theta &= \frac{Ta}{288.15} \\ \delta &= \frac{P_1}{0.99} \\ \gamma &= \frac{SOP}{28601640} \end{aligned}\right\} \qquad (5.4)$$

It is necessary to note that the baseline value for the SOP is equal to 90% of the full power of the RB211 engine and is specific to this engine.

In order to obtain values for the exponent, a, b, and c we apply the TSA approach where the influence of ambient pressure variation is first evaluated and then the influence of ambient temperature is considered and finally the influence of shaftpower is considered. This process was used to determine values for the exponents a, b and c (equations 5.5 to 5.10) with the exponents latter applied to actual measured values for corrections.

Step 1: Pressure correction exponent, a

We define the relation: -

$$(\rho_b)_P = \frac{\rho_c}{\delta^a} \qquad (5.5)$$

making a the subject of the formula gives-

$$a = \frac{\ln\left[\frac{\rho_c}{(\rho_b)_P}\right]}{\ln(\delta)} \qquad (5.6)$$

Step 2: Temperature correction exponent, b

We define the relation:-

$$(\rho_b)_{PT} = \frac{(\rho_b)_P}{\theta^b} \tag{5.7}$$

by a simple algebraic manipulation we have-

$$b = \frac{\ln\left[\frac{(\rho_b)_P}{(\rho_b)_{PT}}\right]}{\ln(\theta)} \tag{5.8}$$

Step 3: Shaftpower correction exponent, c

We define the relation:-

$$(\rho_b)_{SL} = \frac{(\rho_b)_{PT}}{\gamma^c} \tag{5.9}$$

by a simple algebraic manipulation we have-

$$c = \frac{\ln\left[\frac{(\rho_b)_{PT}}{(\rho_b)_{SL}}\right]}{\ln(\gamma)} \tag{5.10}$$

LEVEL 2

With the exponents obtained, we now proceed to correct the measured parameter, ρ_m and this is accomplished using equation 5.3.

$$\Delta\rho = \frac{(\rho_m)_{SL} - (\rho_b)_{SL}}{(\rho_b)_{SL}} * 100 \tag{5.11}$$

Levels 1 and 2 are performed for all the measured parameters to give corrected values at SL and diagnostic SOP, which is the reference point. The corrected parameters are then normalised as shown in equation (5.11) with the delta value introduced into the network for training or testing or diagnosis.

5.3.3 The ANN Module

The ANN module refers to the defined nested network that would be required to perform diagnosis for a given engine configuration. This subject would be addressed in chapter 6.

5.4 What Training Rules/Algorithms?

Whether in classification or regression, it is necessary to employ appropriate training algorithms. For feedforward networks with error backpropagation, various training algorithms such as delta, backpropagation, resilient backpropagation, delta-bar-delta, conjugate gradient algorithms, Levenberg Marquardt, Bayesian regularisation, etc. are available. The choice of which algorithm to apply is usually based on a trade off between many factors such as minimum root mean square (RMS) error obtainable, length of training time or speed of convergence, memory requirements, nature of the problem being learned, etc. There is no laid down procedure as to which algorithm is best for a problem set because pattern sets are different. The onus is then left to the researcher to determine which algorithm is applicable for his situation.

In this research, after several trials with most available algorithms, the scaled conjugate gradient algorithm, a robust variant of the conjugate algorithms that does not required a line search, was chosen. Its speed of convergence and memory economy were key factors that supported this choice. It was also found that Bayesian regularisation-training algorithm and the resilient backpropagation algorithms could have been likely candidates on the choice of learning algorithm. While the former gave better results by improving generalisation especially with classification problems, the latter had the advantage of training faster. However, the large memory requirements of the Bayesian regularisation algorithm and the poor generalisation ability of the resilient backbropagation algorithm necessitated their discontinued implementation.

In all processing elements of the trained networks, the use of hyperbolic tangent sigmoid as the transfer function was preferred because it squashes the inputs to {-1, 1} range thus providing a level of confidence such that network outputs, the tasks not withstanding, are allowed to vary nonlinearly within the defined range.

5.5 What size of Network?

The number of layers and the number of processing elements per layer are important decisions. These parameters to a feedforward, back-propagation topology are also the most ethereal. They are the art of the network designer.

The size of network (number of network free parameters or sum of weights and biases) required for any task depends on the intricacy of the regression problem being handled. The number of processing elements in the input and output layers are fixed by the number of input measurements and required output vectors respectively. This means that the problem is one of determining the adequate number of processing elements in the hidden layers.

There is no quantifiable best answer to the layout of the network for any particular application thus the optimal number of processing elements in the hidden layers is usually based on trial and error. However some general rules have been picked up over time and followed by most researchers and engineers applying this architecture for their problems. These rules include:

Rule One: As the complexity in the relationship between the input data and the desired output increases, then the number of the processing elements in the hidden layer should also increase.

Rule Two: If the process being modelled is separable into multiple stages, then additional hidden layer(s) may be required. If the process is not separable into stages, then additional layers may simply enable memorization and not a true general solution.

Rule Three: The amount of training data available sets an upper bound for the number of processing elements in the hidden layers. To calculate this upper bound, we use the number of input-output pair examples in the training set and divide that number by the total number of input and output processing elements in the network. Then divide that result again by a scaling factor between five and ten. Larger scaling factors are used for relatively noisy data. Extremely noisy data may require a factor of twenty or even fifty, while very clean input data with an exact relationship to the output might drop the factor to around two.

Generally, a less than optimal number of processing elements would mean there are insufficient network parameters (weights and biases) to undertake the required task, which leads to under-learning of the problem domain. In the same vein, a more than necessary processing elements at the hidden layer would lead to poor generalisation as the features of the training patterns are memorised making the network less capable to apply knowledge learned to patterns that were not included in the training process, though within the problem domain. In other words, the network becomes useless on new data sets. In most cases, it is necessary to ensure that the number of network free parameters is less than the number of training patterns.

All the multilayer perceptrons (MLPs) applied in the developed diagnostic structure have at least two hidden neuron layers as these have been empirically proven to give better training results.

5.6 Summary

This chapter has considered the criteria required for building a gas-path fault diagnostic system and these include the engine models, choice of sensors, design of a diagnostic approach and parameter correction.

Three engine models were thermodynamically designed to match their real counterparts. The amount of error evidenced by the difference between the published and predicted design parameters shows that a sufficiently accurate engine model is being used for the diagnostics. The developed diagnostic framework was applied to a fourth engine model – an aeroengine under transient operating condition.

An elaborate approach was developed to determine various possible combinations of sensors that can be implemented in the diagnosis of faults in an engine's gas-path. The choice of the best combinations from the group is decided by economic and maintenance considerations. In this case, the choice was influenced by information made available from a GT user.

Engine measurements can be obtained at operating points other than that at which diagnostics are expected to be carried out. The effect of the ambient conditions and power setting parameters needs to be accounted for. In this research, the TSA approach has been developed to correct parameters within a defined region. The limitation of the correction domain was necessitated by errors inherent in the component maps of the thermodynamic engine model as well as error introduced from the use of scaling factors, which is the only available approach for degradation studies.

In chapter 6, the conceptual model for GPFD would be developed and implemented using ANN. Its applicability to sensor and component fault diagnosis would be discussed.

CHAPTER 6

DEVELOPMENT OF CONCEPTUAL MODELS FOR GPFD

6.1 Introduction

Developing diagnostic approaches would require the consideration of a number of factors. In chapter 5, some of these issues were addressed. They include: (i) the thermodynamic design of the engine models; (ii) the selection of the sensors to monitor; (iii) the definition of the diagnostic approach; and (iv) the outlining of a procedure for correcting measurements taken outside the diagnostic point. Some of these considerations, such as parameter selection, gave rise to the development of novel techniques.

In this chapter, we present the diagnostic approach with developed case studies. The case studies are taken from the 2-shaft and 3-shaft stationary engine configurations including a two-spool aeroengine under transient condition. The nested neural network architectures developed for these engine configurations are not unique, except for the data, to the engine brand name used for the analysis but are generic to GT engines of similar configurations. For complex engine configurations such as those incorporating intercoolers, recuperators or even a bottoming steam turbine, an adjustment would be required in the presented diagnostic structure.

This chapter is structured as follows. Section 6.2 describes the diagnostic philosophy. The conceptual models, using ANN, for the various engine configurations are presented in section 6.3. The procedures for sensor fault and component fault detections are discussed in sections 6.4 and 6.5 respectively. Section 6.6 briefly describes the graphic user interface (GUI) developed to co-ordinate the diagnostic programme execution and finally, a summary of the chapter is given in section 6.7.

6.2 Diagnostic Philosophy

One of the challenges often encountered in the performance estimation problem is the highly nonlinear relation between performance parameters and measured parameters. It is possible that small degradations in performance parameters, which are considered insignificant from an operability perspective, can cause large shifts in the sensor measurements. Likewise, significant degradation in a single performance parameter can result in small measurement shifts relative to the standard noise level. Furthermore, there is a chance that distinct performance degradations will result in indistinguishable shifts in sensor measurements (Urban, 1975). In the light of the foregoing, a preliminary analysis is required to determine what level of performance parameter change can be detected by the sensed measurements under noisy conditions, while simultaneously ensuring that such deviations in the sensed parameters are not limited to just one or two sensors which would hinder the proper distinction of sensor and component faults. This analysis provided the minimum level of fault implanted on the engine models to generate degradation data.

The analysis of faults, whether sensor or component, requires a baseline from which deviations can be obtained at a designated operating point. As previously discussed in section 5.2.2, measurements from an engine are subject to noise and measurement non-repeatability. One of the strong points of neural networks is its ability to perform creditably even in the presence of corrupted/noisy data. In order to build in this robustness into a neural network, the generated data is doused with noise prior to training and testing each network.

Since the system should be able to detect generic single and multiple component faults as well as sensor faults, it is necessary to use a large database. This is made of several couples of measurement-performance parameter vectors, with each called a pattern. This then creates an extensive fault library from which training and testing patterns are drawn. Due to the approach adopted, the initial fault library for the first classifier

network is generic but subsequent networks become more specific or unique being tailored to isolating or assessing the implanted faults.

The philosophy of the proposed approach is such that the presence of a fault is first ascertained (detected), its source is isolated and its impact is assessed or quantified.

6.3 Conceptual Model for GPFD using ANN

The diagnostic philosophy outlined in section 6.2, would require the use of multiple network structures because the presence of a fault would first be diagnosed before it is isolated and assessed. In this section, we present the different developed diagnostic structures, optimised for the gas-path of the three engine configurations - single-spool stationary GT, twin-spool stationary GT and twin spool turbofan engine - within which the case studies fall.

6.3.1 Single-Spool or 2-Shaft Stationary GT

The GPFD framework deemed suitable for this engine configuration required a total of thirteen (13) neural networks architectures. This number is made up of 5 classification networks, one autoassociative network and 7 approximation networks. This structure is shown in Figure 6.1 and the sequel gives a brief description of the structure.

Engine measurements after correction to required operating point are introduced into the network as deviations from a baseline value, the first classification network CLASS1 assesses the patterns and classifies it as not faulty (NF) or faulty (F). If not faulty, the process terminates, but if faulty, the data is passed on to the second classification network, CLASS2, that determines if the faulty pattern is due to sensor bias (fault) or component fault. If the fault is identified as a sensor bias, an auto-associative network, AUTOASSOC1 is called in to determine the magnitude of fault(s) in the biased sensor(s). Should the pattern be classified as a component fault by CLASS2, a third classification network, CLASS3 is called in to determine if the faulty pattern is as a

result of a single component fault (SCF), a dual component fault (DCF) or a multi-component fault (MCF). If the pattern is identified as a SCF by CLASS3 the pattern is passed on to a fourth classification network, CLASS4 to isolate the faulty single component which could either be the compressor, the gas generator turbine or the power turbine. When the faulty component has been isolated, the pattern is passed on to an approximation network which determines the magnitude of deterioration in the affected component. In this way we determine faults affecting two simultaneous components or even all three components.

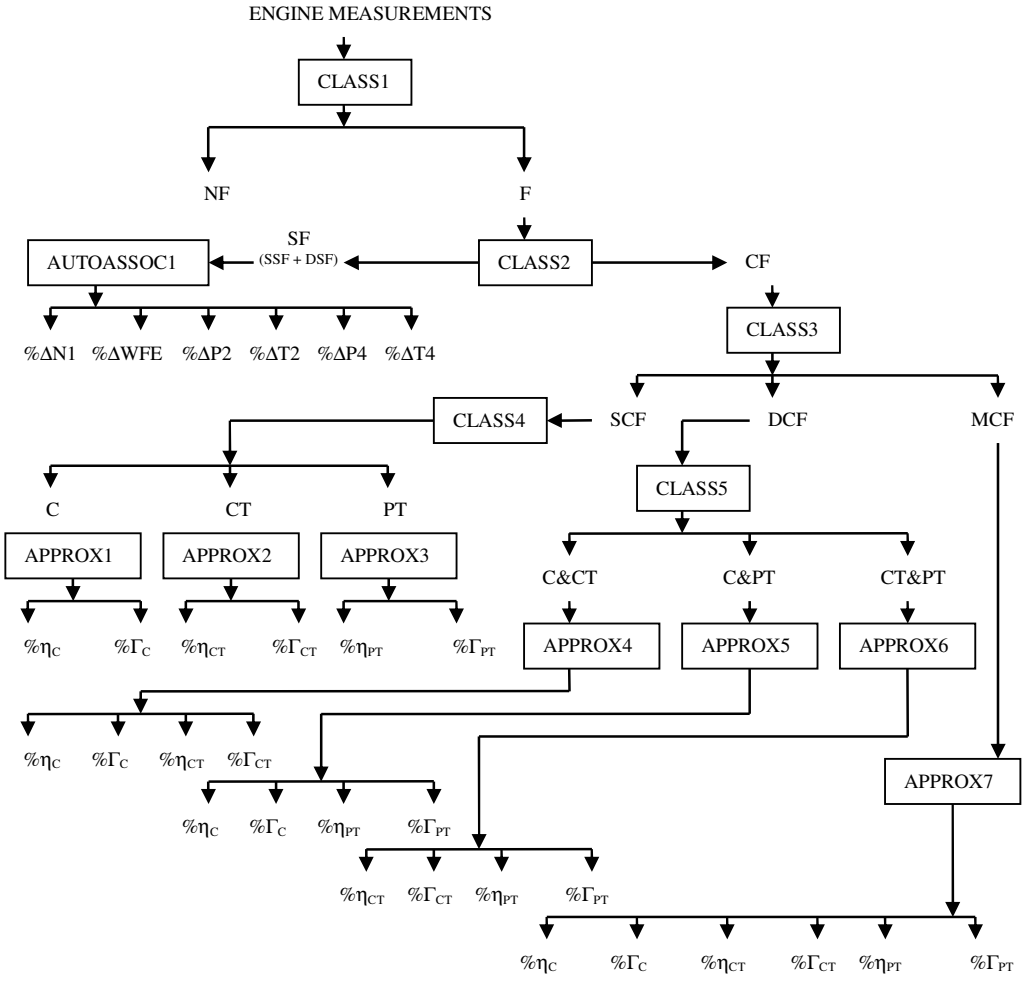

Figure 6.1 ANN module for GPFD in a single spool GT

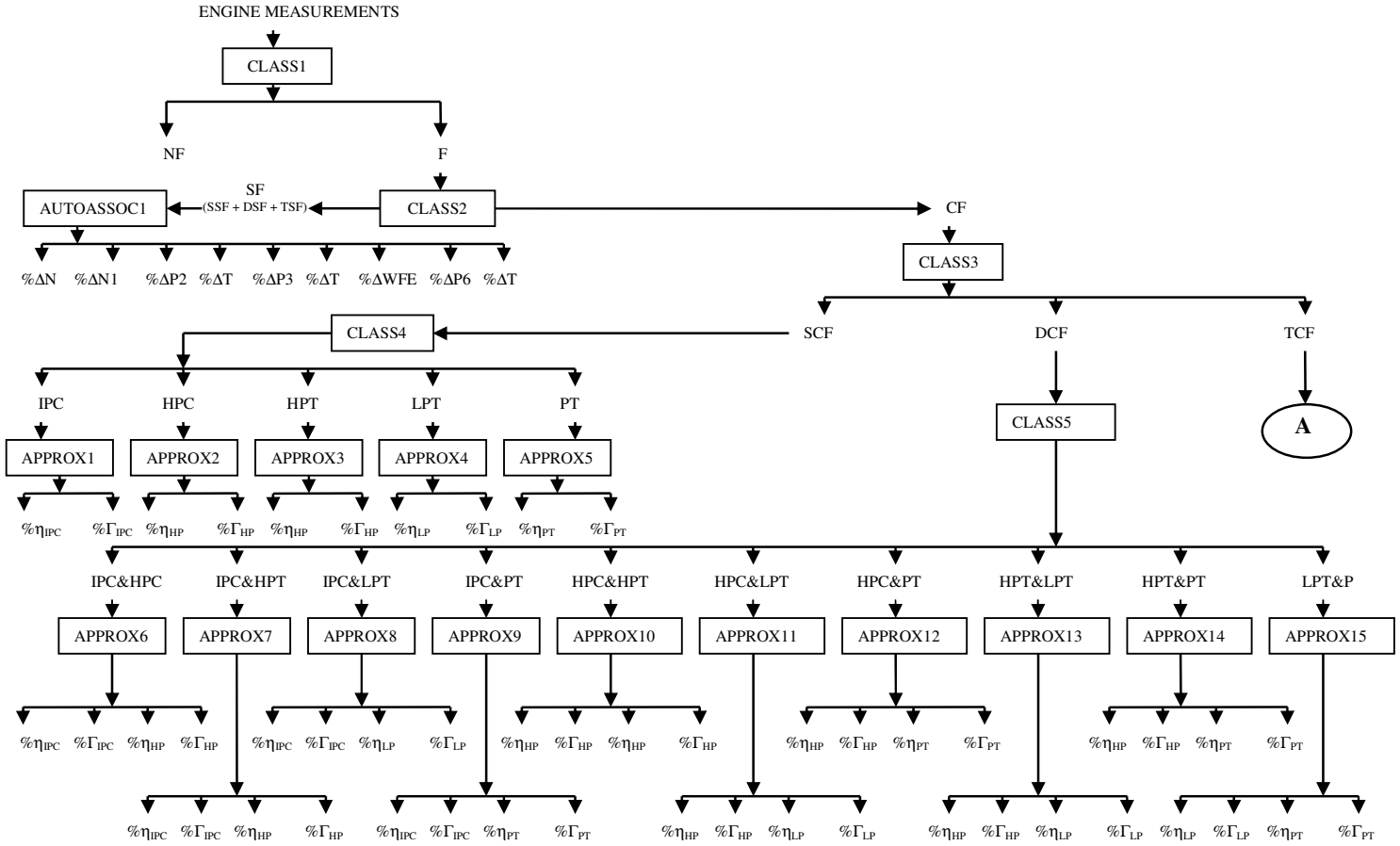
ENGINE MEASUREMENTS
CLASS1
NF
F
SF
(SSF + DSF + TSF)
AUTOASSOC1
CLASS2
CF
%ΔN %ΔN1 %ΔP2 %ΔT %ΔP3 %ΔT %ΔWFE %ΔP6 %ΔT
CLASS3
SCF
DCF
TCF
CLASS4
IPC
HPC
HPT
LPT
PT
CLASS5
A
APPROX1
APPROX2
APPROX3
APPROX4
APPROX5
%ηIPC %ΓIPC %ηHP %ΓHP %ηHP %ΓHP %ηLP %ΓLP %ηPT %ΓPT
IPC&HPC
IPC&HPT
IPC&LPT
IPC&PT
HPC&HPT
HPC&LPT
HPC&PT
HPT&LPT
HPT&PT
LPT&P
APPROX6
APPROX7
APPROX8
APPROX9
APPROX10
APPROX11
APPROX12
APPROX13
APPROX14
APPROX15
%ηIPC %ΓIPC %ηHP %ΓHP
%ηIPC %ΓIPC %ηLP %ΓLP
%ηHP %ΓHP %ηHP %ΓHP
%ηHP %ΓHP %ηPT %ΓPT
%ηHP %ΓHP %ηPT %ΓPT
%ηIPC %ΓIPC %ηHP %ΓHP
%ηIPC %ΓIPC %ηPT %ΓPT
%ηHP %ΓHP %ηLP %ΓLP
%ηHP %ΓHP %ηLP %ΓLP
%ηLP %ΓLP %ηPT %ΓPT

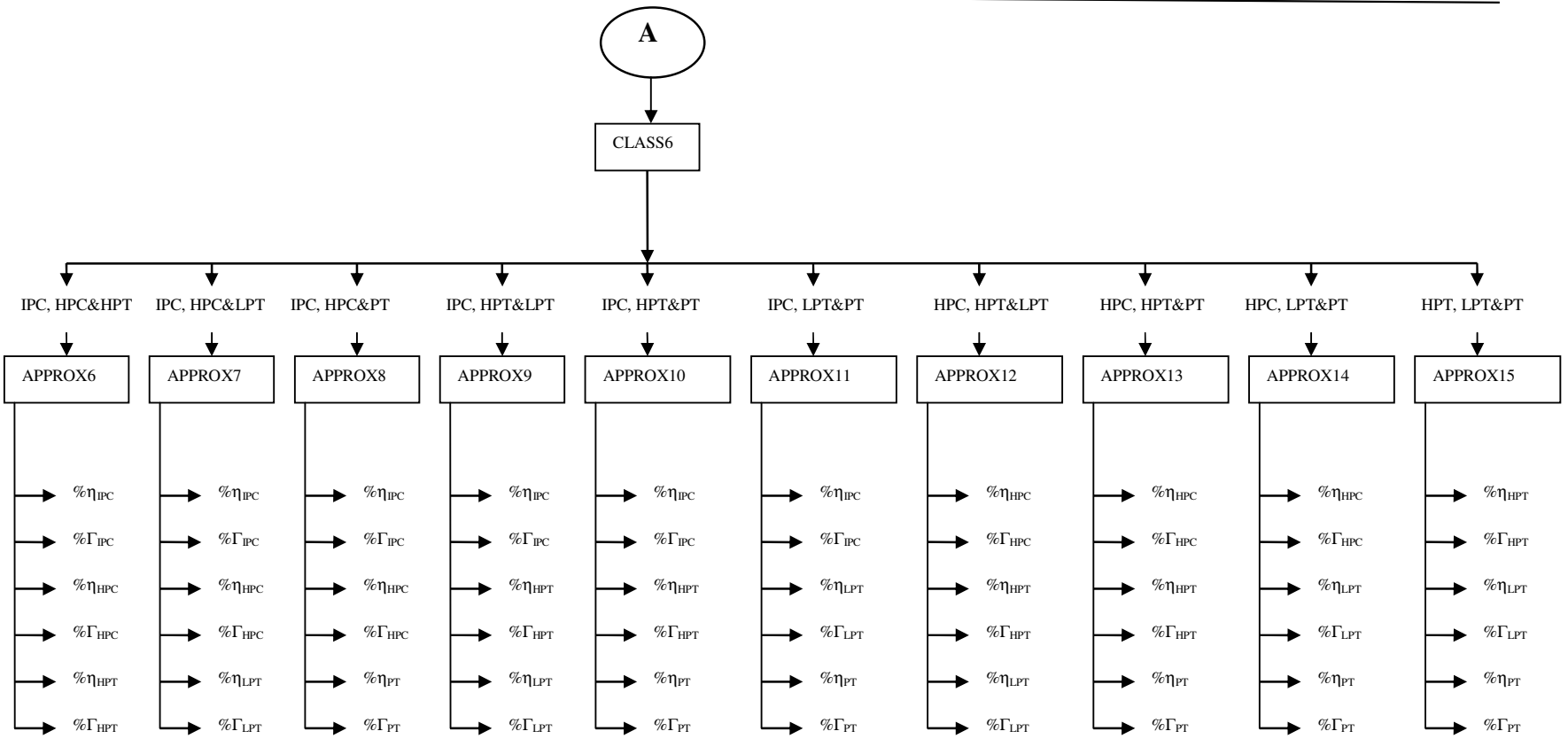

Figure 6.2 ANN module for GPFD in a 3-shaft stationary GT

6.3.2 Twin-Spool or 3-Shaft Stationary GT

For this case, the developed ANN module is presented in Figure 6.2 where it is shown that 32 networks are involved in gas-path fault diagnoses with faults simultaneously affecting any three components considered a possibility. This diagnostic system is made up of 6 classification networks, 1 autoassociative network and 25 approximation networks. The paths traced in the process of fault diagnosis in this engine configuration are equivalent to those presented for the 2-shaft engine.

6.3.3 Twin-Spool Turbofan GT

This section considers the diagnosis of a turbofan engine under transient conditions. More materials that are descriptive are included here because the engine and its condition of operation are different from those of stationary applications. Further information however is available from Ogaji et al (2003).

Transient Diagnosis

Diagnostic analysis has traditionally been conducted under steady state conditions; unfortunately, good steady state data may not be available under every operating condition especially for military aircraft engines that operate for up to 70% of the total mission time in unsteady state conditions (Merrington, 1988).

Steady state operation can simply be defined as that condition wherein engine parameters are relatively time invariant. Conversely, when engine operations require that such parameters as speed and firing temperature vary with time, a transient condition exists. White (1988) summarized some of the main differences between steady state and transient operations as follows:

1. Shaft inertia demands or produces power during transient depending on whether it is accelerated or decelerated.

2. Differential mass flows into and out of components resulting from pressure and temperature gradient occur during transients and depends on the rate of change of the transient.
3. Non-adiabatic conditions exist as heat balances are no longer satisfied during transients. Engine components adjacent to the gas stream either transfer to or give out heat from the gas stream.
4. Dimensions of engine components can change during transients due to expansion and strain from temperature and centrifugal forces. The result of this is change in tip clearance and leakage of bleed air flows which can be detrimental to engine operation.

Engine diagnostics from transient data has been discussed by a number of authors. Areas considered include:

1) Application of a parameter estimation scheme to extract information from engine dynamic characteristics and correlating changes with particular engine faults (Merrington, 1988, 1994).
2) Use of test cell fault implantation to obtain fault signatures from some selected measurements (Eustace el al, 1994).
3) Use of genetic algorithms (GA) to diagnose SCFs and mechanical faults from transient data (Li, 2003).

Most of these works are qualitative in that they aim at establishing the presence or absence of a fault and not the assessment of the fault magnitude. The current analysis applies ANN to turbofan fault detection, isolation and quantification. The analysis is limited to four of the gas-path components (IPC, HPC, HPT and LPT) with the possibility of any two of these being simultaneously considered, if faulty.

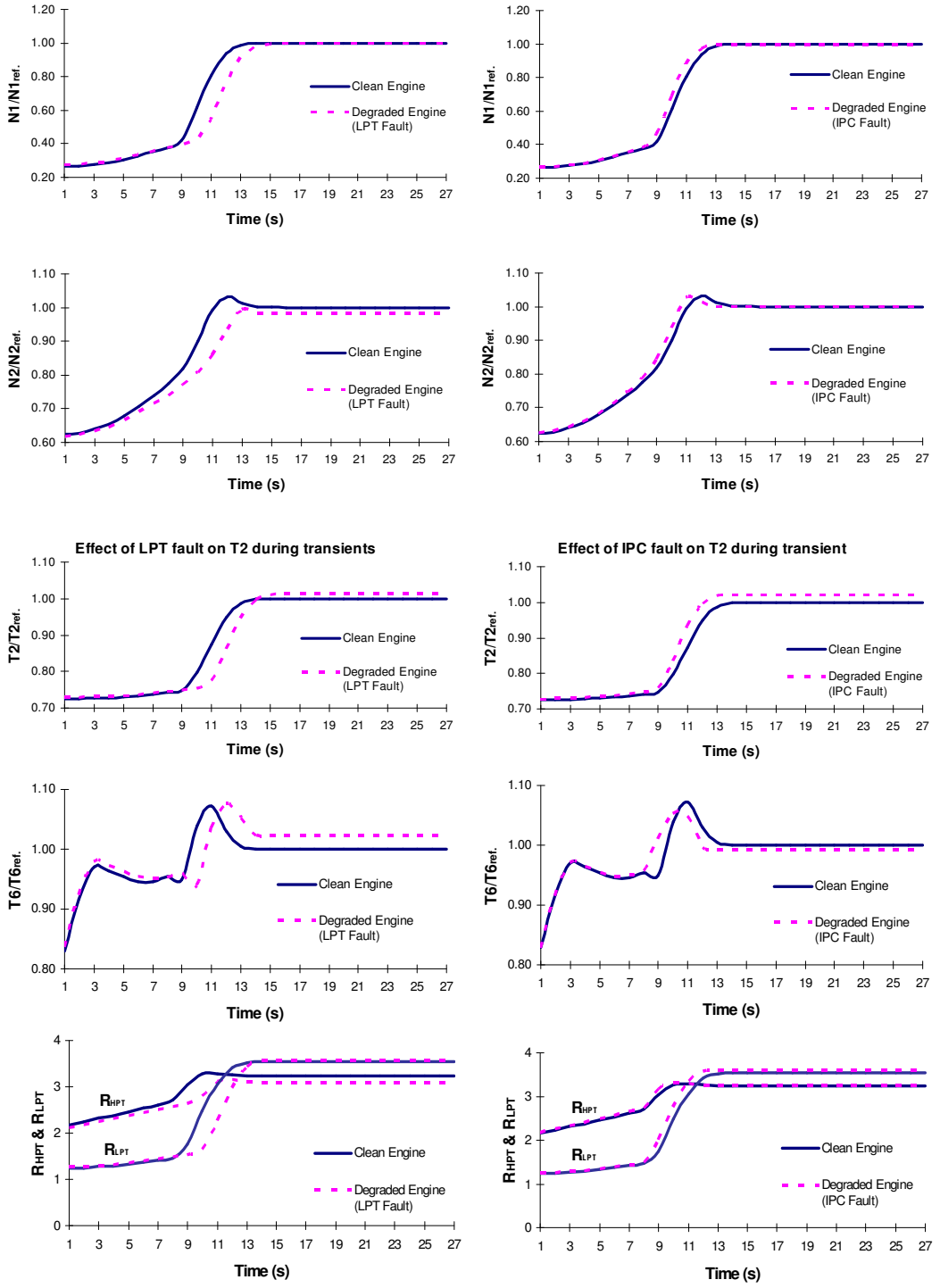

Figure 6.3 Trajectories of clean and degraded engine measurable parameters during transient

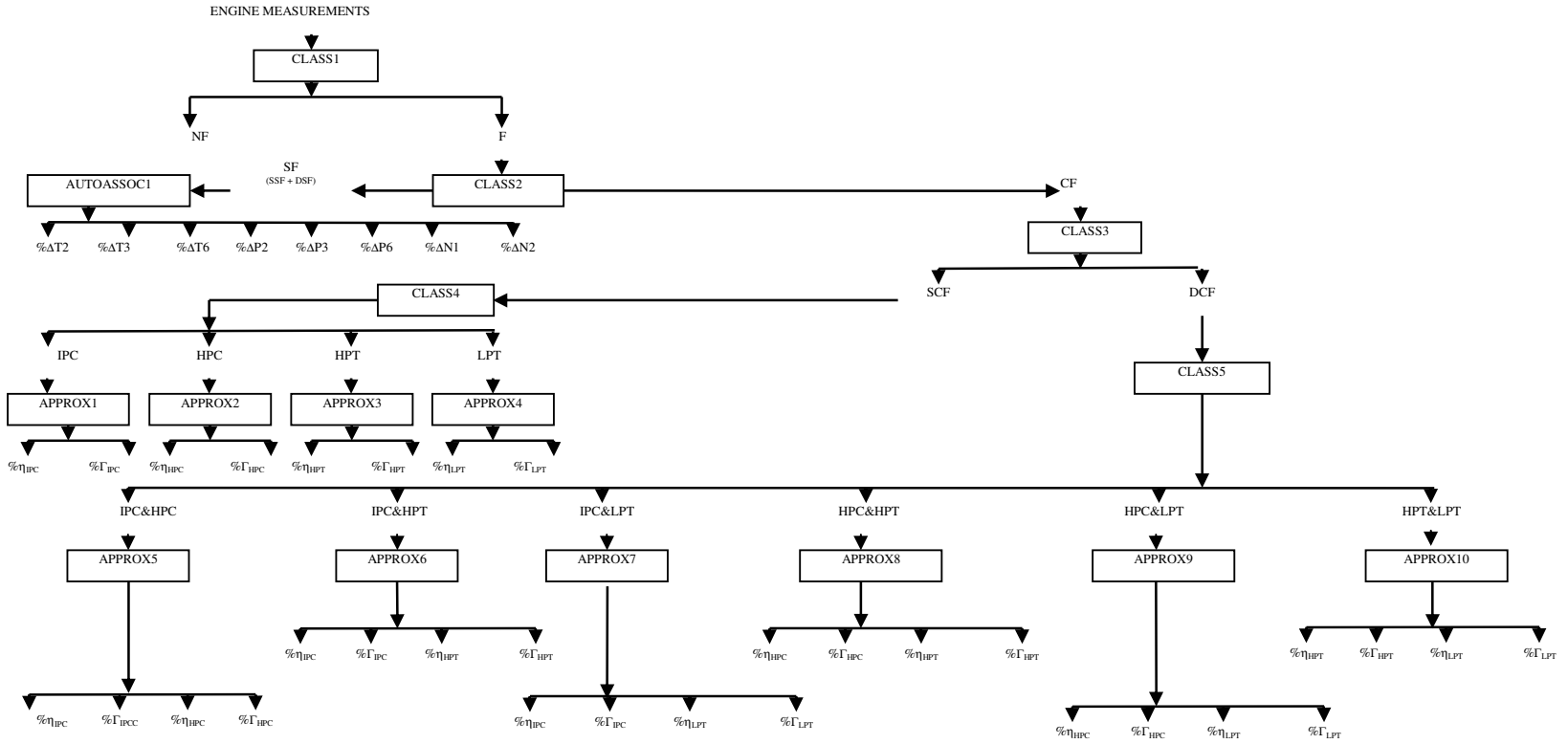

Figure 6.4 ANN module for GPFD in turbofan GT

Fault Characteristics in Transients

In Figure 6.3, we present the trajectories for a clean and deteriorated engine during an acceleration process. The deteriorated engine had SCFs LPT (-2% efficiency and +4% flow capacity change) and IPC (-2% efficiency and -6% flow capacity change) implanted respectively. Of the eight measurable parameters, four are shown including the pressure ratio across the HPT and LPT. All the plots on the left hand of Figure 6.3 have LPT faults while those on the right hand have IPC faults for corresponding measurable parameters. It is clear from this Figure why we should expect a pattern difference from faults originating from different components, in addition, parameter deviations obtained during transients are shown to be more than those from a steady state process. Features (bulges) on the N2 and T6 plots are the result of control system response to HP shaft acceleration (experiencing some over-acceleration) and system regulation of the fuel flow into the combustor, which in this case is restricted by the HPC map, respectively.

ANN Module

Some faults, such as foreign object damage (FOD) would require the consideration of vibration data before prognostic decisions can be made because fault signatures with respect to its effects on the estimated independent variable could be similar with other gas-path faults such as fouling. However, without the inclusion of networks that would fuse data from vibration and oil analysis for some category of faults diagnostic and prognostic purposes, the presented ANN module for this engine configuration (Figure 6.4) had 16 independent network units made up of 5 CLASS, 1 AUTOASSOC and 10 APPROX. Here, again, the genericity of the diagnostic philosophy applies, that is, the current state of the engine is first ascertained and faults, if detected, isolated and quantified at the module level.

Transient Data Processing

Before the engine data is introduced into the transient ANN module, it is normalized and an accumulated deviation is computed using equation (6.1), introduced by Li (2003). The concept of accumulated deviation is applied here because the trajectories of a nominal (clean) engine measurement is different from that of a faulty engine (Figure 6.4) and because the transient process takes place over a given time interval, the area between both trajectories needs to be computed for each of the measurable parameters at appropriate time steps.

$$\Delta\tilde{z} = \frac{\int_0^t [z(t) - z_{estBaseline}(t)]dt}{\int_0^t z_{estBaseline}(t)dt} * 100 \qquad (6.1)$$

Equation (6.1) in the limit tends to equation (5.1) which was applied to steady state processes.

6.4 Sensor Fault Detection, Isolation and Quantification

When measurements from a failed sensor are used as input for engine diagnostics, the consequences could be grave. Sensor failures are a major cause of concern in engine-performance monitoring as they can result in false alarms and, in some cases, lead to the condemnation of a non-offending component or section of the engine. This condition has the potential to increase engine downtime and thus incur higher operational costs. The fact that more than a single sensor could be faulty simultaneously should also not be overlooked.

A partial list of theoretical SFDI techniques (Napolitano et al, 1996) can be given by:

- Generalised Likelihood Ratio (GLR)
- Multiple Model Kalman Filtering (MMKF)
- Sequential Probability Likelihood Ratio Test (SPLRT)
- Generalised Likelihood Test/Maximum Likelihood Detector (GLT/MLD)

These techniques, which are all based on the use of Kalman filter models, feature a continuous monitoring of measurements from the sensors such that failures create conditions where the observable output is different from the predictable trajectories. However, the limitations of the KF approach to fault diagnosis, whether sensor or component, have been discussed in chapter 2.

Based on the level of fault, sensor failures can be classified into two categories:

1. Hard-over failures: these are catastrophic but easy to detect.
2. Soft failures: these are difficult to detect and if uncompensated, potentially catastrophic.

For pattern-association tasks, AANN's are appropriate. This network requires that the number of neurons in the bottleneck be greater than or equal to the number of principal components required in reconstructing the output in the case of failed sensor(s) or noisy inputs. In addition, the dimensionalities of the input and output patterns are equal and various input sets may be required to give a particular output pattern. This makes it distinct from the heteroassociative networks, where various input patterns are mapped to various output sets with the dimensionalities of the input and output not necessarily being identical.

Training as well as test patterns for AUTOASSOC network (networks obtained from AANN) was generated in four basic groups with a fifth group considered for engines with more sensors such as the 2-spool stationary GT. The groups are those with

(i) No noise or bias;

(ii) Gaussian noise of zero means;

(iii) implanted single-sensor faults; this produces fault classes equal to the number of sensors,

(iv) Implanted dual-sensor faults: Using the combination relation in equation (6.2), fifteen sensor fault classes were obtained for the single-spool stationary GT, twenty-eight sensor fault classes for the turbofan engine with

eight measurements, and thirty-six sensor fault classes for the 2-spool stationary GT with nine measurements.

(v) Implanted triple-sensor faults. This was only considered for the 2-spool stationary GT with nine engine measurements and gave rise to eighty-four sensor fault classes.

$$\text{Fault Classes} = {}^{n}Cr_{bias} = \binom{n}{r_{bias}} = \frac{n!}{r_{bias}!(n - r_{bias})!} \tag{6.2}$$

where: n is the number of engine measurements

r_{bias} is the number of measurements that could be considered biased.

AUTOASSOC networks for the single-spool stationary GTs and the turbofan engine were thus trained to isolate and quantify single and dual-sensor faults: in addition to noise filtering, while the AUTOASSOC network for the 2-spool stationary GT was trained to perform these tasks with a capability to handle three simultaneously faulty sensors.

The magnitude of sensor faults implanted varied from soft (twice the noise level) to hard limits (up to $\pm$ 10% deviation from normal readings, for all sensors).

The data for this network were uniquely pre- and post- processed following training to provide a sufficiently accurate output reconstitution. Equations (6.3) to (6.6) were used in this regard.

$$I_i = \frac{(Z_{ki} - Z_{bki})}{Z_{bki}} * 100 \tag{6.3}$$

$$O_i = \frac{(Z_{cki} - Z_{bki})}{Z_{bki}} * 100 \tag{6.4}$$

$$\% \, \Delta \text{ Sensor fault or noise} = I_i - O_i \tag{6.5}$$

$$Z_{cki} = Z_{bki} + \frac{O_i Z_{bki}}{100} \quad (6.6)$$

Equations (6.3) and (6.4) were used to generate the input and output for training and testing the network. Equation (6.5) was used to determine the levels of faults or noise inherent in any input set. This is the result of the AUTOASSOC fault isolation and quantification process. Equation (6.6) was applied to reconstruct the approximate output of the sensor, once the noise had been filtered off. The network output during training was restricted to remain within the clean/corrected (i.e. no noise or bias) range.

6.5 Component Fault Detection, Isolation and Quantification

For the purpose of component fault diagnosis, data was generated in classes. The fault classes for the three engine configurations are shown in Tables 6.1 to 6.3.

Table 6.1 Component fault classes for single-spool stationary GT

Fault Class	Component(s)
1	C.
2	CT.
3	PT.
4	C, CT.
5	C, PT.
6	CT, PT.
7	C, CT, PT.

In Table 6.1, it is shown that seven fault classes are possible in a 2-shaft stationary engine configuration- three-single component, three-dual component and one-triple component. Any one of these could be the result of such an engine's component fault. The ANN module in Figure 6.1 presents how the path is traced and the faulty component(s) isolated. Thereafter, the amount of fault is quantified. For each of these fault classes, training and test data that cover all the possible permutations involving expected changes in independent parameters are generated. A typical pattern generation process for SCFs is shown in Figure 6.5.

Fault levels considered for components were in the range of 0.7% to 3.5% efficiency drop at various mass flow capacity levels. The reason for the minimum detected level placed at 0.7% was that at levels lower than this, it was statistically difficult to differentiate sensor faults from component faults. This is because faults in some components such as HPT and LPT for a two-spool engine configuration produced only significant pattern changes in one sensor, GG exhaust pressure (P6), and there is the likelihood that for our diagnostic system, this would be classified as a sensor fault rather than a component fault.

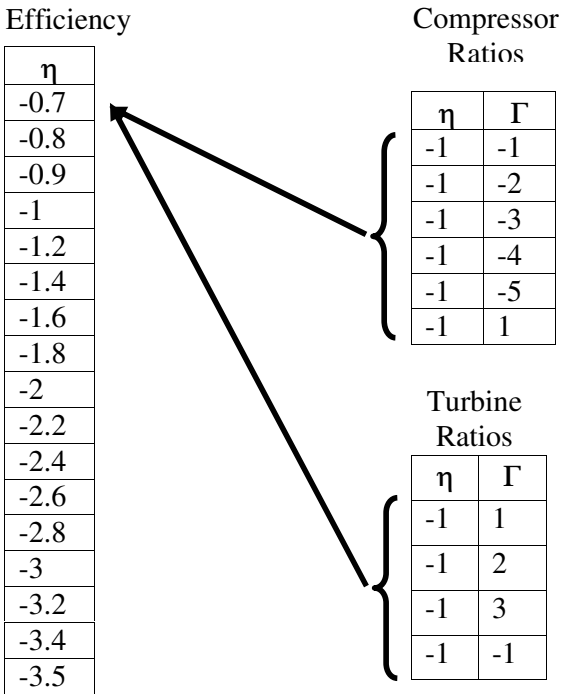

Figure 6.5 Pattern generation for SCF

From Figure 6.5, if we consider the compressor, each level of efficiency drop is combined with different ratios of flow capacity as shown in the compressor ratios. Typically, patterns generated according to the outline above would produce about 102 for the compressor with 68 for a turbine; however, this number can be increased by a factor since each pattern after being combined with white noise of Gaussian distribution becomes different from any other pattern.

Table 6.2 Component fault classes for twin-spool stationary GT

Fault Class	Component(s)	Fault Class	Component(s)
1	IPC.	**14**	HPT, PT.
2	HPC.	**15**	LPT, PT.
3	HPT.	**16**	IPC, HPC, HPT.
4	LPT.	**17**	IPC, HPC, LPT.
5	PT.	**18**	IPC, HPC, PT.
6	IPC, HPC.	**19**	IPC, HPT, LPT.
7	IPC, HPT.	**20**	IPC, HPT, PT.
8	IPC, LPT.	**21**	IPC, LPT, PT.
9	IPC, PT.	**22**	HPC, HPT, LPT.
10	HPC, HPT.	**23**	HPC, HPT, PT.
11	HPC, LPT.	**24**	HPC, LPT, PT.
12	HPC, PT.	**25**	HPT, LPT, PT.
13	HPT, LPT.		

The fault classes for a three-shaft stationary GT such as the RB211-24GT is shown in Table 6.2. The maximum combinations of simultaneously faulty components were limited to three. Though it is possible to consider faults affecting four and five components simultaneously, it was not undertaken in this research because:

- it was not deemed a technologically feasible scenario
- Even if it does occur, an identified TCF when corrected and the diagnostic programme re-run, the remaining faulty component(s) would be identified and their faults corrected
- Any technique developed for the considered cases can be applied for varying other scenarios with little fuss.

Twenty-five fault classes were considered and comprised five SCFs; ten DCFs and ten TCFs. Training and test patterns generated for the various classes followed a permutation process in which order was essential.

The turbofan engine was included in the research process as one of the ways of validating the diagnostic capabilities of the developed framework to a different operating regime – transient process. Table 6.3 shows that ten component fault classes

were considered involving four SCFs, and six DCFs. The generation of training and test patterns followed a similar process as the previous engine configurations.

Table 6.3 Component fault classes for twin-spool turbofan GT

Fault Class	Component(s)	Fault Class	Component(s)
1	IPC.	**6**	IPC, HPT.
2	HPC.	**7**	IPC, LPT.
3	HPT.	**8**	HPC, HPT.
4	LPT.	**9**	HPC, LPT.
5	IPC, HPC.	**10**	HPT, LPT

The network type, structure and total training patterns for this diagnostic framework are given in Table 6.4. Unlike the stationary applications where MLP was used in the CLASS networks to give the maximum possible classification accuracy, the PNN was used in this case. The PNN is easily set up and provides acceptable classification accuracy.

Table 6.4 Network structures and training patterns for a 2-spool turbofan engine

NETWORK	**TYPE**	**STRUCTURE**	**TTRP.**
CLASS1	PNN	8-21860-2	21860
CLASS2	PNN	8-19860-2	19860
CLASS3	PNN	8-16260-2	16260
CLASS4	PNN	8-1460-4	1460
CLASS5	PNN	8-14800-6	14800
APPROX1	MLP	8-10-10-2	438
APPROX2	MLP	8-10-10-2	438
APPROX3	MLP	8-10-10-2	292
APPROX4	MLP	8-10-10-2	292
APPROX5	MLP	8-25-25-4	3600
APPROX6	MLP	8-25-25-4	2400
APPROX7	MLP	8-25-25-4	2400

APPROX8	MLP	8-25-25-4	2400
APPROX9	MLP	8-25-25-4	1600
APPROX10	MLP	8-25-25-4	3600
AUTOASSOC1	AANN	8-30-3-30-8	3600

6.6 Diagnostic Programme Structure

A number of analytical procedures and networks were required to perform the GT fault detection, isolation and assessment. To undertake these processes mechanically each time a diagnosis is to be carried out would be rather clumsy, laborious and time consuming. Hence, the networks were programmed to operate in a batch process and this in turn was included in a wider program that considers completely, the diagnostic process from inputting test data to providing diagnosis results. The macro view of the diagnostic structure is outlined in the flowchart of Figure 6.6. When the programme called ANNDIAG is started, the user selects an engine from the included choices. An interface for entering engine measurements taken or simulated for the engine pops up. When the programme is run, a 3-D interpolation is carried out on a stored database to determine measurement baselines at the current operating point. This process is a prelude to computing the correction exponents that are eventually used to correct the measurements to SL conditions. The corrected measurements are then normalised to produce a signature that is introduced into the ANN diagnostic module for fault isolation and diagnosis. Some views of the GUI that implements this structure are shown in APPENDIX A.5. It should be noted that Figure 6.6 is an expansion of the level one DFD presented in Figure 5.6.

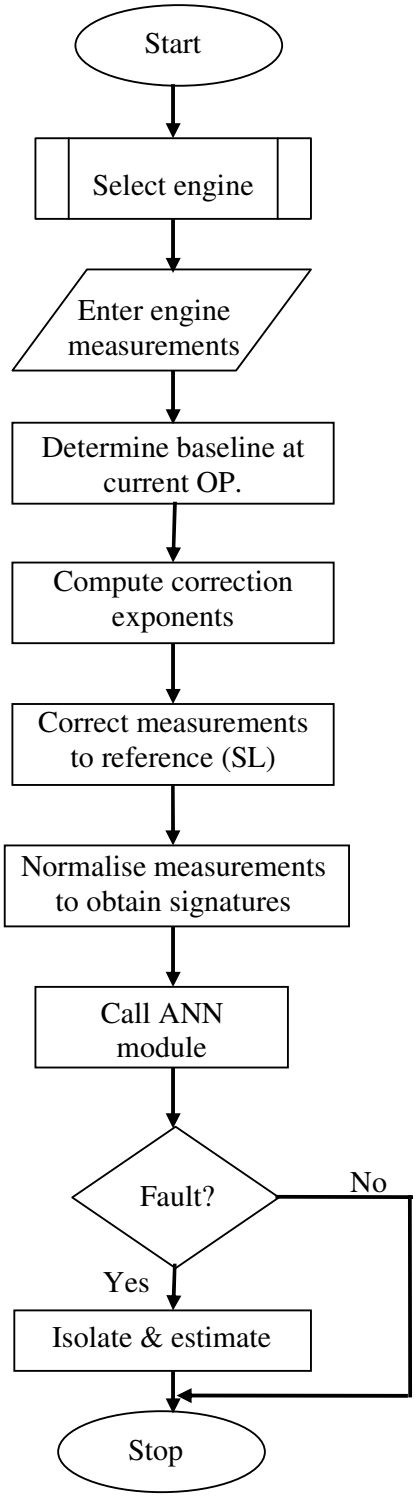

Figure 6.6 Programme structure

6.7 Conclusion

Fault diagnosis processes require a systematic approach. For the case of the gas-path of a GT, ANN has been applied to ascertain the presence of a fault before isolating and quantifying the amount of fault. Advantages of such an approach include the following:

- Much time and resources are saved when a non-faulty engine is allowed to continue operation. This condition is established by the first level of diagnosis.
- Subsequent networks after the first classification become more specialised in their task which makes for better understanding of the task.
- These latter networks could require smaller sizes to undertake their intended task.
- Smaller network sizes would imply shorter training time, though this may not be the case for complex and less separable data sets.
- Maintenance of the diagnostic structure is made much easier.

Four engine modules, thermodynamically similar to RR Avon, LM2500+, RB211 and Turbofan engine, and drawn from three engine configurations – single-spool stationary GT, twin-spool stationary GT and twin-spool turbofan GT, have been considered in this research. The ANN modules for the considered components of these engines were presented in addition to the classes of faults –sensor and component.

Interesting results were obtained from the application of the developed approach and these are presented and discussed in chapter 7.

CHAPTER 7

DISCUSSION OF RESULTS

7.1 Introduction

In chapter 6, the model for GPFD was developed and implemented on a number of engine configurations. The diagnostic philosophy was such that the presence or not of a fault is ascertained before diagnosis. The process of diagnosis required the use of several networks performing tasks such as classification, auto-association and approximation. This chapter will discuss results obtained from tests carried out with the various diagnostic frameworks in order to bring out their significance.

The chapter is organised as follows: Section 7.2 presents results from testing carried out on the CLASS networks of the stationary diagnostic models and discusses them. Similarly, the results and discussion of tests on the APPROX networks are presented in sections 7.3, with a comparison of the APPROX results across the engines undertaken in section 7.4. In section 7.5, results for the special case of diagnosing GPFs in a turbofan engine under transient is presented. Section 7.6 considers in a bit more detail results from sensor fault estimation process. Comparison of results from the ANN approach and other diagnostic techniques such as GPA and fuzzy logic is considered in section 7.7. Finally, section 7.8 gives a summary of the chapter's findings.

7.2 Discussion of Results from Classification Networks

The diagnostic framework developed in chapter 6 was subjected to a battery of tests and the results obtained from the classification networks of the three stationary GTs considered i.e. the RR Avon, the LM2500+ and the RB211 are summarised in Tables 7.1 to 7.3.

In explaining network classification results, it is possible to determine the relative contribution of each input to a network to the terminal nodal output by applying the concept of causal importance (Feraud and Clerot, 2002) or by input removal techniques. This would give the degree to which each nodal output can be explained off by the various network inputs. In GT diagnostics, GPA can handle such tasks to a reasonable degree of accuracy during instrumentation set selection thus our explanation of classification results would be based on which neurons are firing and which are not and the implication of these. Discussion of results from function approximation would be based on the statistical comparison with the expected values or target.

In Table 7.1, results from the RR Avon CLASS networks are shown.

Table 7.1 Results from CLASS networks for RR Avon diagnostic program

CLASS1	**NF**	**F**	
TTP	1500	12016	
%CCP	100	99.9	
CLASS2	**SF**	**CF**	
TTP	2100	9901	
%CCP	99.2	99.8	
CLASS3	**SCF**	**DCF**	**MCF**
TTP	1330	4096	4500
%CCP	99.0	94.2	89.7
CLASS4	**C**	**CT**	**PT**
TTP	570	380	380
%CCP	100	100	100
CLASS5	**C&CT**	**C&PT**	**CT&PT**
TTP	1536	1536	1024
%CCP	99.3	98.2	97.6

CLASS1 indicates that measurements taken from an engine with - (sensor(s) and component(s)) - and without faults, were adequately identified. This is a critical task in engine diagnosis as there is no need to look for a fault where it does not exist, thus

engines should be allowed to continue operation if they are identified as healthy. About 13516 simulated patterns comprising 1500 no-fault (NF) patterns with uncertainty (noise) built into them, 12016 faulty patterns made up of sensor, and component faults with uncertainty considered were introduced into the CLASS1 network. While the CLASS1 network identified all NF patterns, the network identified 99.9% of the faulty data. A careful consideration of the 12 misclassified patterns showed that 1 of the patterns belonged to the component fault class but had very minor fault while the remaining 11 patterns were from the sensor fault category with minimal sensor fault present. This low fault levels gave rise to fault signatures that were similar to a NF condition, hence, the misclassifications. However, the results from CLASS1 indicate that the possibility of isolating a faulty measurement from a non-faulty one can be adequately handled by a trained network.

CLASS2 network, designed to distinguish a pattern that has a sensor fault from one that has a component fault, performed very well. A problem with most GT diagnostic packages is their inability to distinguish between faulty component(s) and faulty sensor(s), as such sensor faults (SF) are interpreted as engine component faults and this results in uneconomic long downtimes taken to trace faults that would otherwise have been corrected in a short time. The results from CLASS2 show that a well-trained network can achieve over 99% classification accuracy for such a task. Patterns with low multiple sensor faults, presented signatures that were similar to those obtained from low component faults thus giving rise to regions where both classes are equiprobable. The natural outcome of this is a misclassification, but the result indicates this problem to be minimal.

CLASS3 presents the least accuracy amongst the CLASS networks. The reason for this lies mainly in the complexity of the task performed as even an increase in network size beyond that used did not improve accuracy but rather poor generalisation emanating from overfitting was experienced. A number of overlaps were observed amongst the three classes considered but most especially between the DCF and TCF as shown in

Figure 7.1. Of the 1330 SCF patterns tested, Figure 7.1 shows that 1316 representing about 99% were correctly classified while 11 patterns representing 0.83% were incorrectly classified as DCF and the remaining 2 patterns or 0.15% incorrectly classified as TCF. A similar explanation can be given for the DCF and TCF.

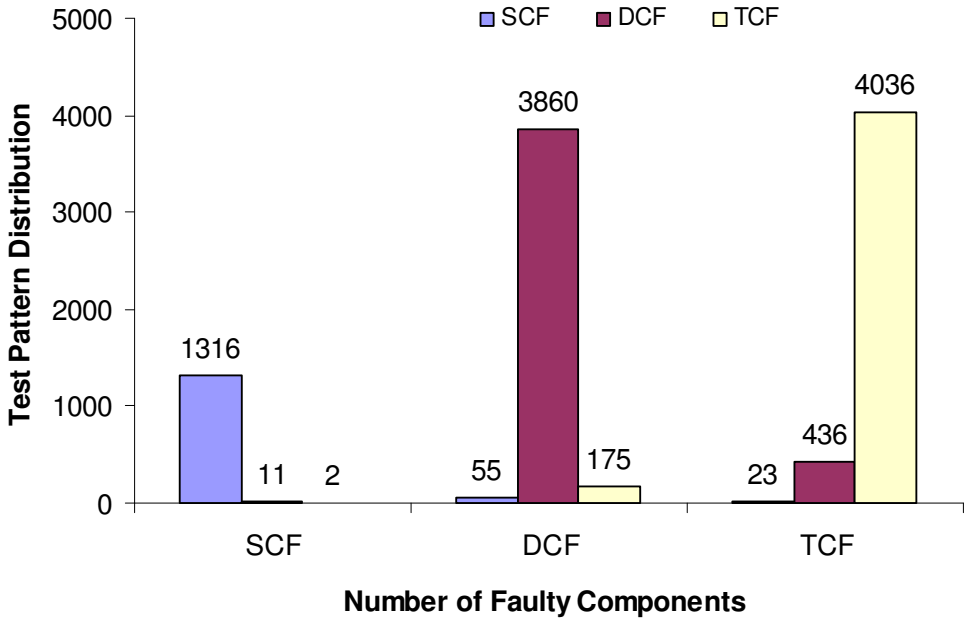

Figure 7.1 Classification of component faults for CLASS3 based on number of faulty components.

Investigation of the misclassified patterns reveals that some SCF patterns with high levels of fault had similar fault signatures to those from DCFs where one of the components has a high fault level and the other a low fault level. In a similar way, fault signatures obtained from patterns with high levels of DCFs on both components are likely to be classified as TCFs because of similarity in signatures while signatures obtained from TCFs having high levels of faults on two of the components and very low faults on the third are very likely to be classified as DCFs. However, the misclassifications does not detract from the usefulness of the results, as empirical studies revealed that when a SCF is classified as a DCF, the amount of fault in the component that is actually faulty is quantified while the stray component is assigned a

less that realistic fault level. This is also true if the reverse occurs, that is, a DCF being classified as a SCF. Here, the component with the higher fault is isolated and the amount of fault quantified. If this fault is corrected and the measurements re-taken and introduced into the network, the previously unidentified component would be isolated and its fault level assessed.

The classification accuracy obtained from CLASS4, demonstrates the high level of distinction that exist between the three classes of faults hence training time as well as network size was small. CLASS4 isolates the fault to the component level before assessment is carried out for the faulty component.

It is possible to have two components simultaneously faulty in an engine. Based on this fact, CLASS5 network was designed to isolate any of the three possible combinations of DCFs obtainable from this engine configuration. The classification accuracy over the test range is deemed high. As with some of the previously presented networks, some levels of misclassifications exist and a pattern study showed that these were unavoidable because of the similarities of signatures obtained for such cases. The level of misclassification however, did not warrant an increase in the CLASS5 network size as no appreciable degree of generalisation was experienced beyond the presented values when the network size was increased.

In Table 7.2, the CLASS results obtained from testing the LM2500+ diagnostic framework is shown. A careful consideration of this Table vis-à-vis Table 7.1 shows that similar results are obtained. This is not unexpected as the engine configurations are similar though of different overall pressure ratios and shaftpower. Slight differences in %CCP can be attributed to the ANN training process, as it is unlikely that the same final network weights can be obtained each time a given network is trained though networks may converge to the same minimum. Also, the magnitudes of measured parameters are higher for the LM2500+ than for the RR Avon, and thus their deviations are more

pronounced. In any case, the discussion presented for the RR Avon CLASS networks equally apply to these networks.

Table 7.2 Results from CLASS networks for LM2500+ diagnostic program

CLASS1	**NF**	**F**	
TTP	1500	12017	
%CCP	99.9	99.9	
CLASS2	**SF**	**CF**	
TTP	2100	9906	
%CCP	99.1	99.9	
CLASS3	**SCF**	**DCF**	**MCF**
TTP	1330	4096	4500
%CCP	99.5	94.1	92.0
CLASS4	**C**	**CT**	**PT**
TTP	570	380	380
%CCP	100	100	100
CLASS5	**C&CT**	**C&PT**	**CT&PT**
TTP	1536	1536	1024
%CCP	99.5	99.0	98.5

Table 7.3 Results from CLASS networks for RB211 diagnostic program

CLASS1	**NF**	**F**								
TTP	1500	9456								
%CCP	99.3	99.7								
CLASS2	**SF**	**CF**								
TTP	1290	8179								
%CCP	99.7	100								
CLASS3	**SCF**	**DCF**	**TCF**							
TTP	1224	1150	5805							
%CCP	100	76.2	97.2							

CLASS4	**IPC**	**HPC**	**HPT**	**LPT**	**PT**					
TTP	306	306	204	204	204					
%CCP	100	100	100	100	100					
CLASS5	**IPC& HPC**	**IPC& HPT**	**IPC& LPT**	**IPC& PT**	**HPC& HPT**	**HPC& LPT**	**HPC& PT**	**HPT& LPT**	**HPT& PT**	**LPT& PT**
TTP	160	120	120	120	120	120	120	90	90	90
%CCP	100	99.2	99.2	100	99.2	98.3	99.2	98.9	98.9	98.9
CLASS6	**IPC, HPC& HPT**	**IPC, HPC& HPT**	**IPC, HPC& LPT**	**IPC, HPC& PT**	**IPC, HPT& LPT**	**IPC, HPT& PT**	**IPC, LPT& PT**	**HPC, HPT& LPT**	**HPC, LPT& PT**	**HPT, LPT& PT**
TTP	720	720	720	540	540	540	540	540	540	405
%CCP	99.7	98.6	99.0	99.1	98.3	99.1	99.6	96.7	98.0	95.8

Table 7.3 presents results for RB211 CLASS networks. It should be recalled that the RB211 is a 3-shaft aeroderivative GT having five gas-path components that require examination for the presence of faults. Because ten possible combinations of the condition of three components being simultaneously faulty are included, this engine configuration has one more CLASS network than the two previously considered. Generally, the results from these CLASS networks are comparable to those obtained from the simpler engine configuration. Apart from CLASS3 that produced about 76% of CCP on one of its fault classes, all other CLASS networks gave values of %CCP above 95. The implications of this are that well-trained networks can be applied to isolate faults to the component(s) level, the engine configuration notwithstanding.

All the network architectures implemented in the CLASS are multilayer perceptrons (MLPs) trained with the scaled conjugate gradient algorithm. A worthy alternative would have been the use of probabilistic neural network (PNN). As previously discussed in section 4.3.2.6, the PNN does not require an explicit training and thus can be set up in less than 2 minutes when processed network data is available. This is unlike the MLP that could typically require anything from a couple of seconds to several days of training before it can be put to use. In addition, the PNN has excellent classification ability especially when the classes in the problem domain are easily separable. But with

the possibility of interference/overlapping occurring amongst members of different classes, a structure such as the MLP with nonlinear activation functions would be required to provide better definition of class boundaries and hence better classification. For the RB211 CLASS networks, a comparison was made between results obtained from the use of MLPs and PNNs. The $\%CCP_{av}$. (which is the mean of the sum of %CCP from a CLASS network) calculated from equation (7.1), was plotted against the different CLASS networks as shown in Figure 7.2.

$$\%CCP_{av} = \frac{1}{N}\sum_{i=1}^{N} \%CCP_i \qquad (7.1)$$

From Figure 7.2, CLASS1, CLASS2 and CLASS4 give similar results for MLP and PNN. Decision boundaries can easily be constructed to separate patterns in these classes. However in CLASS3, CLASS5 and CLASS6, an increased complexity is experienced in the problem domain. In order to make the most of any performance improvement, the MLP is chosen in preference to the PNN as it affords a better overall classification accuracy in these classes. In any case, the PNN was still implemented on the turbofan diagnosis framework, as the idea behind the development of this case study was to ascertain the workability of the diagnostic philosophy in transient conditions.

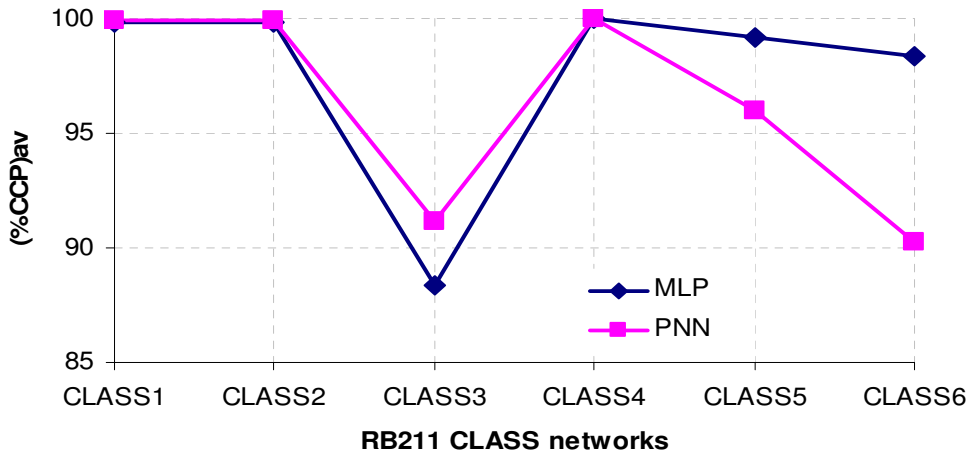

Figure 7.2 Comparison of classification accuracy using MLP and PNN for RB211 fault isolation.

7.3 Discussion of Results from Approximation Networks

The GPFD philosophy requires that faults be isolated to the component(s) level before an assessment or quantification of the fault is carried out. The diagnostic process begins with a detection of a fault by the first CLASS network with the second CLASS network discriminating this faulty pattern into either a sensor fault or a component fault. Thereafter, patterns identified as originating from component faults are passed through a number of CLASS networks to isolate the faulty component(s). Determining what component(s) is/are responsible for performance drops is only one aspect of the problem, with the other aspect being the estimation of the amount of fault. Knowledge of the fault level would aid planning for resource scheduling and maintenance.

In Tables 7.4 to 7.9, results of fault estimation from APPROX networks for the RR Avon, LM2500+ and RB211 are presented. These results comprise estimations from random fault implant tests and two-standard deviation of errors obtained from a range of test patterns.

In Table 7.4, seven test cases, each drawn from the seven APPROX networks of RR Avon, are considered. The first three of these test cases are for SCFs; the next three were drawn from DCFs while the final test case considers a TCF. Bearing in mind

Table 7.4 Results from random fault implant test cases for RR Avon APPROX networks.

TEST CASES	IMPLANTED FAULT (%)						PREDICTED FAULT (%)						ABSOLUTE ESTIMATION ERROR (%)					
	Component 1		Component 2		Component 3		Component 1		Component 2		Component 3		Component 1		Component 2		Component 3	
SINGLE COMPONENT FAULTS (SCFs)																		
Case 1	η_C -2	Γ_C -6					η_{IC} -2.05	Γ_{IC} -5.98					η_C 0.05	Γ_C 0.02				
Case 2	η_{CT} -2	Γ_{CT} +4					η_{CT} -2.20	Γ_{CT} 4.20					η_{CT} 0.20	Γ_{CT} 0.20				
Case 3	η_{PT} -2	Γ_{PT} +4					η_{PT} -1.77	Γ_{PT} 4.16					η_{PT} 0.23	Γ_{PT} 0.16				
DUAL COMPONENT FAULTS (DCFs)																		
Case 4	η_C -2.2	Γ_C -6.6	η_{CT} -2.2	Γ_{CT} +4.4			η_C -2.35	Γ_C -6.55	η_{CT} -2.08	Γ_{CT} 4.18			η_C 0.15	Γ_C 0.05	η_{CT} 0.12	Γ_{CT} 0.22		
Case 5	η_C -2.2	Γ_C -6.6	η_{PT} -2.2	Γ_{PT} +4.4			η_C -2.06	Γ_C -6.59	η_{PT} -1.68	Γ_{PT} 4.69			η_C 0.14	Γ_C 0.01	η_{PT} 0.52	Γ_{PT} 0.29		
Case 6	η_{CT} -2.2	Γ_{CT} +4.4	η_{PT} -2.2	Γ_{PT} +4.4			η_{CT} -2.18	Γ_{CT} 4.38	η_{PT} -1.73	Γ_{PT} 4.60			η_{CT} 0.02	Γ_{CT} 0.02	η_{PT} 0.47	Γ_{PT} 0.20		
TRIPLE COMPONENT FAULT (TCF)																		
Case 7	η_C -2.2	Γ_C -6.6	η_{CT} -2.2	Γ_{CT} +4.4	η_{PT} -2.2	Γ_{PT} +4.4	η_C -2.37	Γ_C -6.34	η_{CT} -1.98	Γ_{CT} 4.11	η_{PT} -1.85	Γ_{PT} 4.33	η_C 0.17	Γ_C 0.26	η_{CT} 0.27	Γ_{CT} 0.29	η_{PT} 0.35	Γ_{PT} 0.07

that the presented case studies were randomly selected, the accuracy of prediction indicated by the absolute estimation error is good. A number of isolated points such as the grayed cells of cases 5 and 6 gave estimation errors that were regarded as high, that is being more than 20% in estimation error. These points not withstanding, the fact that a substantial amount of fault exist in the component, PT in this case, is established.

A better picture of the network performance can be obtained if the network response over a range of test data is assessed. Ascertaining the standard deviation (σ) of error would give an indication of how far in the error space we need to go in order to encompass a given percentage of the test data. For instance, one standard deviation (1-σ) of error is known to include about 68% of the test data; 2-σ includes about 95% of test data while 3-σ includes about 99% of the test data. For the present analysis, a 2-σ error level would be used to specify a sufficiently accurate range. The mean errors in all cases were approximately equal to zero.

Table 7.5 2-σ error levels from fault assessment using APPROX networks of RR Avon.

NETWORK	2-σ ERROR FOR GIVEN PARAMETER (%)					
	Component 1		Component 2		Component 3	
APPROX1	η_C 11.23	Γ_C 6.49				
APPROX2	η_{CT} 5.13	Γ_{CT} 6.07				
APPROX3	η_{PT} 11.91	Γ_{PT} 6.11				
APPROX4	η_C 26.21	Γ_C 12.28	η_{CT} 25.48	Γ_{CT} 10.82		
APPROX5	η_C 20.67	Γ_C 16.17	η_{PT} 15.67	Γ_{PT} 13.15		
APPROX6	η_{CT} 18.16	Γ_{CT} 14.13	η_{PT} 22.26	Γ_{PT} 17.00		
APPROX7	η_C 34.55	Γ_C 31.82	η_{CT} 35.08	Γ_{CT} 37.53	η_{PT} 36.62	Γ_{PT} 43.00

In order to distinguish between error magnitudes originating from different fault levels, the relative error is introduced and defined by equation 7.2.

$$E_{rel} = \left(\frac{\hat{\rho} - \rho_{actual}}{\rho_{actual}} \right) \qquad 7.2$$

Table 7.6 Results of random fault implant test cases for LM2500+ approximation networks.

TEST CASES	IMPLANTED FAULT (%)						PREDICTED FAULT (%)						ABSOLUTE ESTIMATION ERROR (%)					
	Component 1		Component 2		Component 3		Component 1		Component 2		Component 3		Component 1		Component 2		Component 3	
SINGLE COMPONENT FAULTS (SCFs)																		
Case 1	η_C -2	Γ_C -6					η_{IC} -2.00	Γ_{IC} -5.99					η_C 0.00	Γ_C 0.01				
Case 2	η_{CT} -2	Γ_{CT} +4					η_{CT} -1.99	Γ_{CT} 3.97					η_{CT} 0.01	Γ_{CT} 0.03				
Case 3	η_{PT} -2	Γ_{PT} +4					η_{PT} -1.99	Γ_{PT} 4.01					η_{PT} 0.01	Γ_{PT} 0.01				
DUAL COMPONENT FAULTS (DCFs)																		
Case 4	η_C -2.2	Γ_C -6.6	η_{CT} -2.2	Γ_{CT} +4.4			η_C -2.32	Γ_C -6.59	η_{CT} -2.22	Γ_{CT} 4.40			η_C 0.12	Γ_C 0.01	η_{CT} 0.02	Γ_{CT} 0.00		
Case 5	η_C -2.2	Γ_C -6.6	η_{PT} -2.2	Γ_{PT} +4.4			η_C -2.21	Γ_C -6.64	η_{PT} -2.20	Γ_{PT} 4.39			η_C 0.01	Γ_C 0.04	η_{PT} 0.00	Γ_{PT} 0.01		
Case 6	η_{CT} -2.2	Γ_{CT} +4.4	η_{PT} -2.2	Γ_{PT} +4.4			η_{CT} -2.19	Γ_{CT} 4.41	η_{PT} -2.19	Γ_{PT} 4.36			η_{CT} 0.01	Γ_{CT} 0.01	η_{PT} 0.01	Γ_{PT} 0.04		
TRIPLE COMPONENT FAULT (TCF)																		
Case 7	η_C -2.2	Γ_C -6.6	η_{CT} -2.2	Γ_{CT} +4.4	η_{PT} -2.2	Γ_{PT} +4.4	η_C -2.20	Γ_C -6.52	η_{CT} -2.19	Γ_{CT} 4.43	η_{PT} -2.15	Γ_{PT} 4.41	η_C 0.00	Γ_C 0.08	η_{CT} 0.01	Γ_{CT} 0.03	η_{PT} 0.05	Γ_{PT} 0.01

The standard deviation is computed from the relative error with the relation shown in equation 7.3.

$$\sigma = \sqrt{\frac{\sum_{i=1}^{N} \left(E_{rel(i)} - \overline{E}_{rel}\right)^2}{N-1}} \qquad 7.3$$

where N is the number of test patterns.

It therefore follows that the network estimate would be in the defined range given by equation 7.4 for 95% of the time.

$$\hat{\rho} = \rho_{actual} \mp 2\sigma \qquad 7.4$$

In Table 7.5, 2-σ estimation error for efficiency and flow capacity for the different APPROX networks of RR Avon are presented. The implication of these results for APPROX1 as an instance is that, given an actual fault scenario of -2% drop in efficiency and -6% drop in flow capacity of the compressor, the network would give values in the range of -2 ∓ 0.1123 for efficiency and -6 ∓ 0.0649 for flow capacity 95% of the time. This level of error bounding the correct prediction of about 95% of the test data is considered acceptable. As expected, the error level increases with complexity of the problem set, that is, as more components are presumed faulty, the prediction ability of the ANN diminishes, albeit slowly.

Table 7.7 2-σ error levels from fault assessment using APPROX networks of LM2500+.

NETWORK	**2-σ ERROR FOR GIVEN PARAMETER (%)**					
	Component 1		**Component 2**		**Component 3**	
APPROX1	η_C 12.82	Γ_C 6.03				
APPROX2	η_{CT} 4.44	Γ_{CT} 5.06				
APPROX3	η_{PT} 5.99	Γ_{PT} 4.35				
APPROX4	η_C 26.37	Γ_C 14.18	η_{CT} 21.64	Γ_{CT} 13.59		
APPROX5	η_C 22.00	Γ_C 17.12	η_{PT} 13.78	Γ_{PT} 14.38		
APPROX6	η_{CT} 13.24	Γ_{CT} 16.65	η_{PT} 19.36	Γ_{PT} 12.81		
APPROX7	η_C 32.27	Γ_C 30.79	η_{CT} 27.57	Γ_{CT} 41.68	η_{PT} 31.15	Γ_{PT} 39.18

Table 7.8 Results of random fault implant test cases for RB211 approximation networks.

TEST CASES	IMPLANTED FAULT (%)						PREDICTED FAULT (%)						ABSOLUTE ESTIMATION ERROR (%)					
	Component 1		Component 2		Component 3		Component 1		Component 2		Component 3		Component 1		Component 2		Component 3	
SINGLE COMPONENT FAULTS (SCFs)																		
Case 1	η_{IPC} -2	Γ_{IPC} -6					η_{IPC} -1.99	Γ_{IPC} -6.01					η_{IPC} 0.01	Γ_{IPC} 0.01				
Case 2	η_{HPC} -2	Γ_{HPC} -6					η_{HPC} -2.02	Γ_{HPC} -6.03					η_{HPC} 0.02	Γ_{HPC} 0.03				
Case 3	η_{HPT} -2	Γ_{HPT} +4					η_{HPT} -2.48	Γ_{HPT} 5.47					η_{HPT} 0.48	Γ_{HPT} 1.47				
Case 4	η_{LPT} -2	Γ_{LPT} +4					η_{LPT} -2.00	Γ_{LPT} 4.00					η_{LPT} 0.00	Γ_{LPT} 0.00				
Case 5	η_{PT} -2	Γ_{PT} +4					η_{PT} -2.03	Γ_{PT} 4.03					η_{PT} 0.03	Γ_{PT} 0.03				
DUAL COMPONENT FAULTS (DCFs)																		
Case 6	η_{IPC} -2.2	Γ_{IPC} -6.6	η_{HPC} -2.2	Γ_{HPC} -6.6			η_{IPC} -2.14	Γ_{IPC} -6.58	η_{HPC} -2.14	Γ_{HPC} -6.59			η_{IPC} 0.06	Γ_{IPC} 0.02	η_{HPC} 0.06	Γ_{HPC} 0.01		
Case 7	η_{IPC} -2.2	Γ_{IPC} -6.6	η_{HPT} -2.2	Γ_{HPT} +4.4			η_{IPC} -2.23	Γ_{IPC} -6.62	η_{HPT} -2.22	Γ_{HPT} 4.44			η_{IPC} 0.03	Γ_{IPC} 0.02	η_{HPT} 0.02	Γ_{HPT} 0.04		

Case 8	η_{IPC} -2.2	Γ_{IPC} -6.6	η_{LPT} -2.2	Γ_{LPT} +4.4			η_{IPC} -2.24	Γ_{IPC} -6.61	η_{LPT} -1.72	Γ_{LPT} 4.15			η_{IPC} 0.04	Γ_{IPC} 0.01	η_{LPT} 0.48	Γ_{LPT} 0.25		
Case 9	η_{IPC} -2.2	Γ_{IPC} -6.6	η_{PT} -2.2	Γ_{PT} +4.4			η_{IPC} -2.19	Γ_{IPC} -6.57	η_{PT} -2.21	Γ_{PT} 4.40			η_{IPC} 0.01	Γ_{IPC} 0.03	η_{PT} 0.01	Γ_{PT} 0.00		
Case 10	η_{HPC} -2.2	Γ_{HPC} -6.6	η_{HPT} -2.2	Γ_{HPT} +4.4			η_{HPC} -2.48	Γ_{HPC} -6.55	η_{HPT} -1.99	Γ_{HPT} 4.46			η_{HPC} 0.28	Γ_{HPC} 0.05	η_{HPT} 0.01	Γ_{HPT} 0.06		
Case 11	η_{HPC} -2.2	Γ_{HPC} -6.6	η_{LPT} -2.2	Γ_{LPT} +4.4			η_{HPC} -2.01	Γ_{HPC} -6.58	η_{LPT} -2.26	Γ_{LPT} 4.51			η_{HPC} 0.19	Γ_{HPC} 0.02	η_{LPT} 0.06	Γ_{LPT} 0.11		
Case 12	η_{HPC} -2.2	Γ_{HPC} -6.6	η_{PT} -2.2	Γ_{PT} +4.4			η_{HPC} -2.23	Γ_{HPC} -6.61	η_{PT} -2.21	Γ_{PT} 4.41			η_{HPC} 0.03	Γ_{HPC} 0.01	η_{PT} 0.01	Γ_{PT} 0.01		
Case 13	η_{HPT} -2.2	Γ_{HPT} +4.4	η_{LPT} -2.2	Γ_{LPT} +4.4			η_{HPT} -2.30	Γ_{HPT} 4.33	η_{LPT} -2.20	Γ_{LPT} 4.52			η_{HPT} 0.10	Γ_{HPT} 0.07	η_{LPT} 0.00	Γ_{LPT} 0.12		
Case 14	η_{HPT} -2.2	Γ_{HPT} +4.4	η_{PT} -2.2	Γ_{PT} +4.4			η_{HPT} -2.19	Γ_{HPT} 4.40	η_{PT} -2.21	Γ_{PT} 4.40			η_{HPT} 0.01	Γ_{HPT} 0.00	η_{PT} 0.01	Γ_{PT} 0.00		
Case 15	η_{LPT} -2.2	Γ_{LPT} +4.4	η_{PT} -2.2	Γ_{PT} +4.4			η_{LPT} -2.13	Γ_{LPT} 4.70	η_{PT} -1.83	Γ_{PT} 4.46			η_{LPT} 0.07	Γ_{LPT} 0.30	η_{PT} 0.37	Γ_{PT} 0.06		
TRIPLE COMPONENT FAULTS (TCFs)																		
Case 16	η_{IPC} -2.2	Γ_{IPC} -6.6	η_{HPC} -2.2	Γ_{HPC} -6.6	η_{HPT} -2.2	Γ_{HPT} +4.4	η_{IPC} -2.11	Γ_{IPC} -6.52	η_{HPC} -1.75	Γ_{HPC} -6.55	η_{HPT} -2.04	Γ_{HPT} 4.34	η_{IPC} 0.09	Γ_{IPC} 0.08	η_{HPC} 0.45	Γ_{HPC} 0.05	η_{HPT} 0.16	Γ_{HPT} 0.06
Case 17	η_{IPC} -2.2	Γ_{IPC} -6.6	η_{HPC} -2.2	Γ_{HPC} -6.6	η_{LPT} -2.2	Γ_{LPT} +4.4	η_{IPC} -2.20	Γ_{IPC} -6.53	η_{HPC} -2.14	Γ_{HPC} -6.46	η_{LPT} -1.92	Γ_{LPT} 4.40	η_{IPC} 0.00	Γ_{IPC} 0.07	η_{HPC} 0.06	Γ_{HPC} 0.14	η_{LPT} 0.28	Γ_{LPT} 0.00

Case 18	η_{IPC} -2.2	Γ_{IPC} -6.6	η_{HPC} -2.2	Γ_{HPC} -6.6	η_{PT} -2.2	Γ_{PT} +4.4	η_{IPC} -1.84	Γ_{IPC} -6.60	η_{HPC} -2.36	Γ_{HPC} -6.91	η_{PT} -1.54	Γ_{PT} 4.64	η_{IPC} 0.36	Γ_{IPC} 0.00	η_{HPC} 0.16	Γ_{HPC} 0.31	η_{PT} 0.66	Γ_{PT} 0.24
Case 19	η_{IPC} -2.2	Γ_{IPC} -6.6	η_{HPT} -2.2	Γ_{HPT} +4.4	η_{LPT} -2.2	Γ_{LPT} +4.4	η_{IPC} -2.25	Γ_{IPC} -6.56	η_{HPT} -2.11	Γ_{HPT} 4.32	η_{LPT} -2.07	Γ_{LPT} 4.31	η_{IPC} 0.05	Γ_{IPC} 0.04	η_{HPT} 0.09	Γ_{HPT} 0.08	η_{LPT} 0.13	Γ_{LPT} 0.09
Case 20	η_{IPC} -2.2	Γ_{IPC} -6.6	η_{HPT} -2.2	Γ_{HPT} +4.4	η_{PT} -2.2	Γ_{PT} +4.4	η_{IPC} -2.07	Γ_{IPC} -6.46	η_{HPT} -1.93	Γ_{HPT} 4.32	η_{PT} -1.97	Γ_{PT} 4.41	η_{IPC} 0.13	Γ_{IPC} 0.14	η_{HPT} 0.27	Γ_{HPT} 0.08	η_{PT} 0.23	Γ_{PT} 0.01
Case 21	η_{IPC} -2.2	Γ_{IPC} -6.6	η_{LPT} -2.2	Γ_{LPT} +4.4	η_{PT} -2.2	Γ_{PT} +4.4	η_{IPC} -2.25	Γ_{IPC} -6.55	η_{LPT} -1.81	Γ_{LPT} 4.42	η_{PT} -2.01	Γ_{PT} 4.40	η_{IPC} 0.05	Γ_{IPC} 0.05	η_{LPT} 0.39	Γ_{LPT} 0.02	η_{PT} 0.19	Γ_{PT} 0.00
Case 22	η_{HPC} -2.2	Γ_{HPC} -6.6	η_{HPT} -2.2	Γ_{HPT} +4.4	η_{LPT} -2.2	Γ_{LPT} +4.4	η_{HPC} -1.84	Γ_{HPC} -6.49	η_{HPT} -2.28	Γ_{HPT} 4.30	η_{LPT} -2.21	Γ_{LPT} 4.43	η_{HPC} 0.36	Γ_{HPC} 0.11	η_{HPT} 0.08	Γ_{HPT} 0.10	η_{LPT} 0.01	Γ_{LPT} 0.03
Case 23	η_{HPC} -2.2	Γ_{HPC} -6.6	η_{HPT} -2.2	Γ_{HPT} +4.4	η_{PT} -2.2	Γ_{PT} +4.4	η_{HPC} -2.13	Γ_{HPC} -6.60	η_{HPT} -1.83	Γ_{HPT} 4.39	η_{PT} -2.00	Γ_{PT} 4.37	η_{HPC} 0.07	Γ_{HPC} 0.00	η_{HPT} 0.37	Γ_{HPT} 0.01	η_{PT} 0.20	Γ_{PT} 0.03
Case 24	η_{HPC} -2.2	Γ_{HPC} -6.6	η_{LPT} -2.2	Γ_{LPT} +4.4	η_{PT} -2.2	Γ_{PT} +4.4	η_{HPC} -1.54	Γ_{HPC} -6.52	η_{LPT} -2.12	Γ_{LPT} 4.67	η_{PT} -1.82	Γ_{PT} 4.52	η_{HPC} 0.66	Γ_{HPC} 0.08	η_{LPT} 0.08	Γ_{LPT} 0.27	η_{PT} 0.38	Γ_{PT} 0.12
Case 25	η_{HPT} -2.2	Γ_{HPT} +4.4	η_{LPT} -2.2	Γ_{LPT} +4.4	η_{PT} -2.2	Γ_{PT} +4.4	η_{HPT} -2.04	Γ_{HPT} 4.60	η_{LPT} -2.11	Γ_{LPT} 4.58	η_{PT} -1.79	Γ_{PT} 4.47	η_{HPT} 0.16	Γ_{HPT} 0.20	η_{LPT} 0.09	Γ_{LPT} 0.18	η_{PT} 0.41	Γ_{PT} 0.07

In Tables 7.6 and 7.7, a similar test scenario to that of the RR Avon but involving the LM2500+ is presented. The absolute estimation errors in Table 7.6 may appear better than what was presented for RR Avon in Table 7.4 but this does not give the overallpicture of the LM2500+ APPROX network performance. Table 7.7 shows that the application of a range of test data to the APPROX networks of the LM2500+ gives a similar level of performance as those of the RR Avon, this point will be clearer when the average root mean square (RMS) error for each of the APPROX network is considered in section 7.4.

In Tables 7.8 and 7.9, the performance of the APPROX networks as it pertains to the RB211 is presented. Twenty-five fault classes made up of all possible combinations of single, dual and triple component faults gave rise to twenty-five APPROX networks. The first five APPROX networks were designed to estimate SCFs for the five considered components; the next ten APPROX networks are to estimate DCFs while the last ten were designed to estimate TCFs. Here again, the grayed cells in Table 7.8 indicate points with absolute errors exceeding 20% of implanted values. From Table 7.9, it can be observed that a much-improved estimation of the amount of fault is achieved as the possible fault combinations increase. The reason for this will be discussed in section 7.4.

Table 7.9 2-σ error levels from fault assessment using APPROX networks of RB211.

NETWORK	**2-σ ERROR FOR GIVEN PARAMETER (%)**					
	Component 1		**Component 2**		**Component 3**	
APPROX1	η_{IPC} 9.19	Γ_{IPC} 4.89				
APPROX2	η_{HPC} 32.03	Γ_{HPC} 6.74				
APPROX3	η_{HPT} 9.41	Γ_{HPT} 11.71				

APPROX4	η_{LPT} 5.97	Γ_{LPT} 3.55				
APPROX5	η_{PT} 10.89	Γ_{PT} 4.61				
APPROX6	η_{IPC} 11.85	Γ_{IPC} 7.02	η_{HPC} 15.03	Γ_{HPC} 6.98		
APPROX7	η_{IPC} 10.78	Γ_{IPC} 6.99	η_{HPT} 8.76	Γ_{HPT} 9.31		
APPROX8	η_{IPC} 15.16	Γ_{IPC} 8.75	η_{LPT} 8.74	Γ_{LPT} 7.16		
APPROX9	η_{IPC} 8.03	Γ_{IPC} 6.96	η_{PT} 7.27	Γ_{PT} 6.38		
APPROX10	η_{HPC} 43.37	Γ_{HPC} 12.36	η_{HPT} 26.97	Γ_{HPT} 16.69		
APPROX11	η_{HPC} 25.54	Γ_{HPC} 14.03	η_{LPT} 19.56	Γ_{LPT} 15.96		
APPROX12	η_{HPC} 12.00	Γ_{HPC} 5.96	η_{PT} 6.78	Γ_{PT} 4.89		
APPROX13	η_{HPT} 33.10	Γ_{HPT} 12.17	η_{LPT} 40.50	Γ_{LPT} 26.99		
APPROX14	η_{HPT} 7.19	Γ_{HPT} 9.90	η_{PT} 6.12	Γ_{PT} 4.87		
APPROX15	η_{LPT} 38.68	Γ_{LPT} 6.07	η_{PT} 12.48	Γ_{PT} 9.08		
APPROX16	η_{IPC} 17.81	Γ_{IPC} 14.64	η_{HPC} 74.78	Γ_{HPC} 18.66	η_{HPT} 44.12	Γ_{HPT} 19.51
APPROX17	η_{IPC} 27.45	Γ_{IPC} 13.14	η_{HPC} 50.39	Γ_{HPC} 16.39	η_{LPT} 61.96	Γ_{LPT} 36.71
APPROX18	η_{IPC} 22.91	Γ_{IPC} 15.83	η_{HPC} 43.68	Γ_{HPC} 16.45	η_{PT} 25.24	Γ_{PT} 12.83
APPROX19	η_{IPC} 23.71	Γ_{IPC} 13.54	η_{HPT} 43.04	Γ_{HPT} 13.87	η_{LPT} 54.16	Γ_{LPT} 34.88
APPROX20	η_{IPC} 24.67	Γ_{IPC} 11.36	η_{HPT} 15.47	Γ_{HPT} 14.92	η_{PT} 14.51	Γ_{PT} 8.92

APPROX21	η_{IPC} 31.78	Γ_{IPC} 14.56	η_{LPT} 29.12	Γ_{LPT} 11.65	η_{PT} 17.57	Γ_{PT} 12.78
APPROX22	η_{HPC} 44.13	Γ_{HPC} 16.68	η_{HPT} 24.45	Γ_{HPT} 17.57	η_{LPT} 67.77	Γ_{LPT} 32.02
APPROX23	η_{HPC} 88.80	Γ_{HPC} 9.45	η_{HPT} 39.96	Γ_{HPT} 19.55	η_{PT} 16.78	Γ_{PT} 6.13
APPROX24	η_{HPC} 52.48	Γ_{HPC} 14.76	η_{LPT} 41.03	Γ_{LPT} 39.04	η_{PT} 21.37	Γ_{PT} 14.11
APPROX25	η_{HPT} 51.38	Γ_{HPT} 22.40	η_{LPT} 56.11	Γ_{LPT} 45.80	η_{PT} 26.03	Γ_{PT} 15.29

The diagnostic framework for all the stationary applications were exposed to tests from different operating conditions in order to validate its applicability. Results for the case of RB211 are included in APPENDIX A.6. The tests was conducted for ambient temperature deviations of -7^{o}C (281.15K) and -7^{o}C (295.15K); ambient pressures of 0.98bar and 1.01bar; shaft power of 86% and 94%. These points are close to the bounds set for the diagnostic programme. Faults were implanted on single, dual and triple components with the faults varying between soft and hard levels. All the changes in efficiencies were grouped in a single column separated by semicolons with flow capacities done in a similar way. The components with faults implanted on them are presented in the first column while the components isolated by the diagnostic programme as faulty are listed in the seventh column. The predicted faults are also presented for each of the isolated components.

The results show that SCFs were properly classified and the fault level quantified to a high degree of accuracy. However, some of the DCFs and TCFs, indicated by the grayed rows, were misclassified. A close look at the misclassified patterns shows that components with the least faults were either omitted (i.e. when a DCF is classified as a SCF or a TCF as a DCF) or included (when an inexistent third component fault is included in a DCF scenario). In any case, the level of overall accuracy obtained, points to the suitability of the correction process to provide representative results of the engine condition. Our analysis shows that, obtaining a range of signatures over a number of

power settings and tracking the results of diagnosis would zero down on the best possible result describing the engine condition.

7.4 Comparison of Results from Stationary Applications

A crucial part of the GPFD process is the estimation of an isolated fault. In section 7.3, estimation results from three aeroderivative GTs were presented and discussed. In this section, the APPROX results from these engines are compared in order to make adequate deductions. In addition, the strength of the relationship between the implanted and estimated fault is considered.

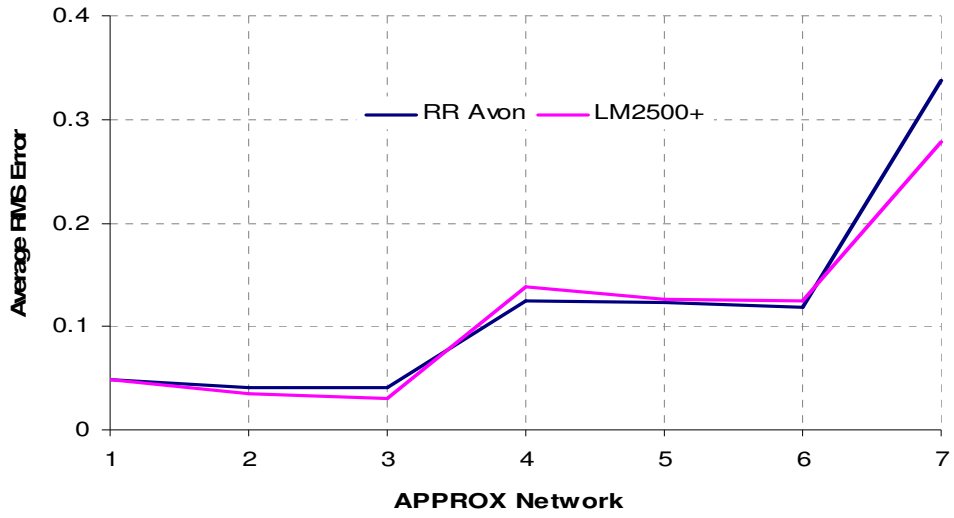

Figure 7.3 RMS_{av} error for RR Avon and LM2500+ APPROX networks

The RR Avon and LM2500+ are engines of the same basic configuration (2-shaft) but designed to meet different performance requirements. The LM2500+ operates at a much higher-pressure ratio and produces a much higher shaft power. The same network architecture and training parameters has been applied to the various aspects of both engines fault diagnosis process. Figure 7.3 shows a comparison of the average root mean square error (RMS_{av}) obtained from the APPROX networks of the two engines. The RMS_{av} is computed from equation 7.5.

$$RMS_{av} = \frac{1}{n}\sum_{j=1}^{n}\sqrt{\frac{1}{P}\sum_{i=1}^{P}(a_i - t_i)^2} \qquad 7.5$$

where RMS_{av} is the mean of the RMS computed for each of the test pattern

n is the number of test patterns

P is the number of estimated performance variables in each test pattern

a_i is the output of the ith neuron of the network output layer for test pattern j.

t_i is the true/target value of the ith neuron for test pattern j.

As shown in Figure 7.3, approximately the same error level is achieved for trained network from both engine configurations. This is to be expected if network architectures are similar and data credibility is guaranteed.

The RMS_{av} for the RB211 shown in Figure 7.4 does not present a clearly defined layout that distinguishes the various combinations of faulty components being considered, but some important observations that can be drawn from Figure 7.4 vis-à-vis Figure 7.3 includes:

- As the number of possible combinations of faulty components increase, the RMS error resulting from estimating the fault increases.

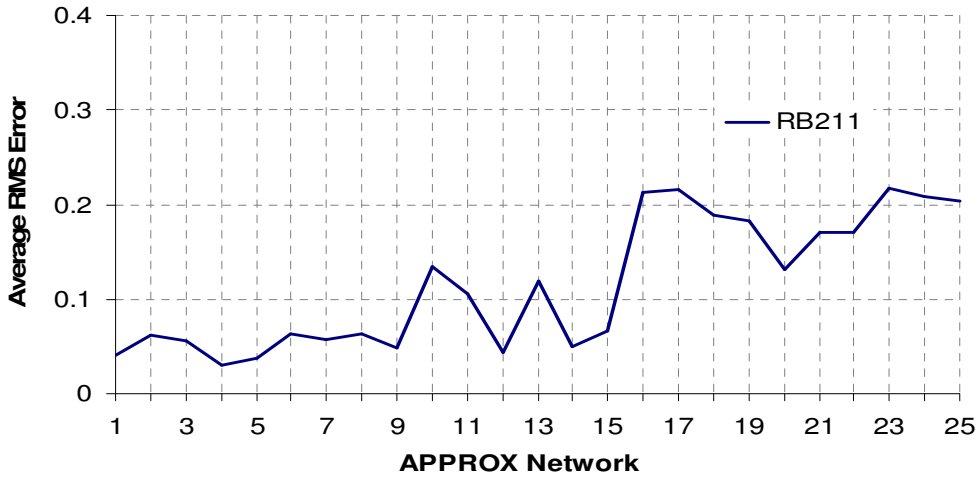

Figure 7.4 RMS_{av} error for RB211 APPROX networks

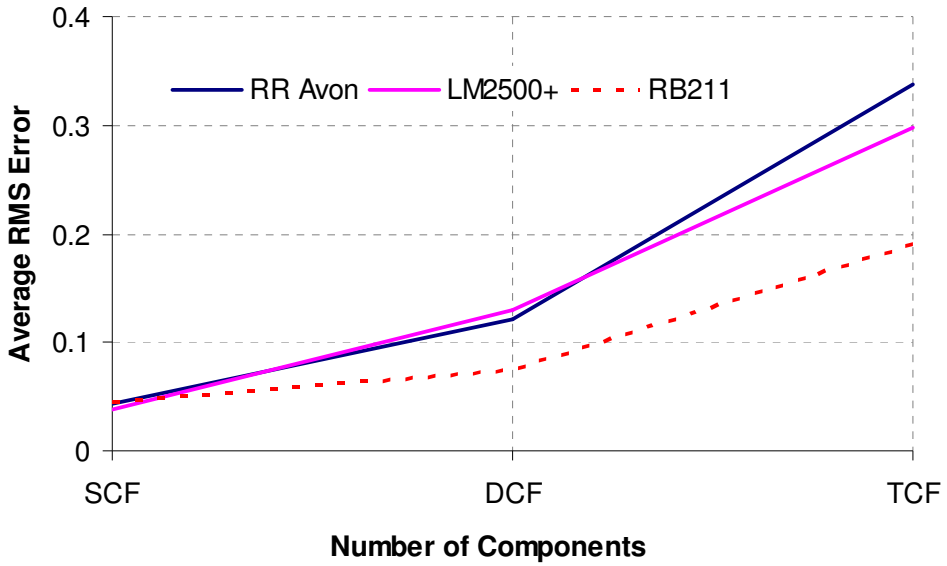

Figure 7.5 Average RMS for APPROX networks based on number of faulty components

- The average RMS levels resulting from multiple component fault estimation are much lower for the RB211 than for the RR Avon and LM2500+. This fact is captured in Figure 7.5 where the RMS is plotted based on the number of faulty components. The reason for this can be traced directly to what is termed *observability*. Observability refers to the ability of available instrumentation set to estimate the detected faults with minimal smearing. RB211 uses nine optimised measurement sets while the 2-shaft engines have six optimised sensors respectively. Thus, the more relevant measurements we have, as possible fault combinations increase, the better positioned we are to provide better fault estimation.

In order that 95% of test patterns be approximately estimated, some level of errors equivalent to 2-σ from the mean would be involved. In section 7.3, 2-σ for each of the performance parameters making up the various APPROX networks outputs have been computed and presented. In Figures 7.6 and 7.7, averaged values of these relative errors

have been plotted to present a broad perspective of the level of errors being considered. To adequately predict 95% of SCF in the 2-shaft engine, relative error level would typically be about 8%, this would rise to about 18% for DCFs and to 37% for TCFs. For the 3-shaft engine, predicting 95% of SCF faults would have error of about 10%, for DCFs this would be about 14% and about 29% for TCFs. In Figure 7.8, these mean values of 2-σ has been computed and plotted for each of the engines.

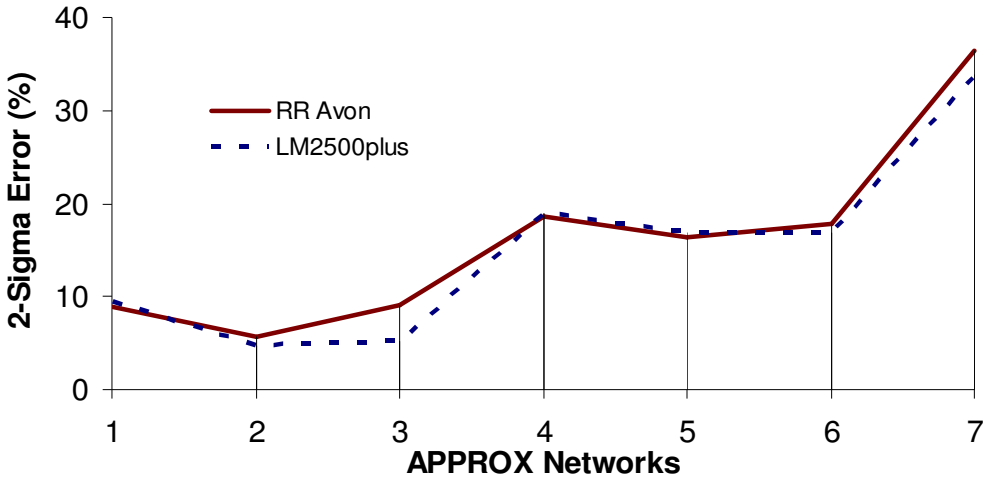

Figure 7.6 Plots of 2-sigma error for RR Avon and LM2500+ APPROX networks

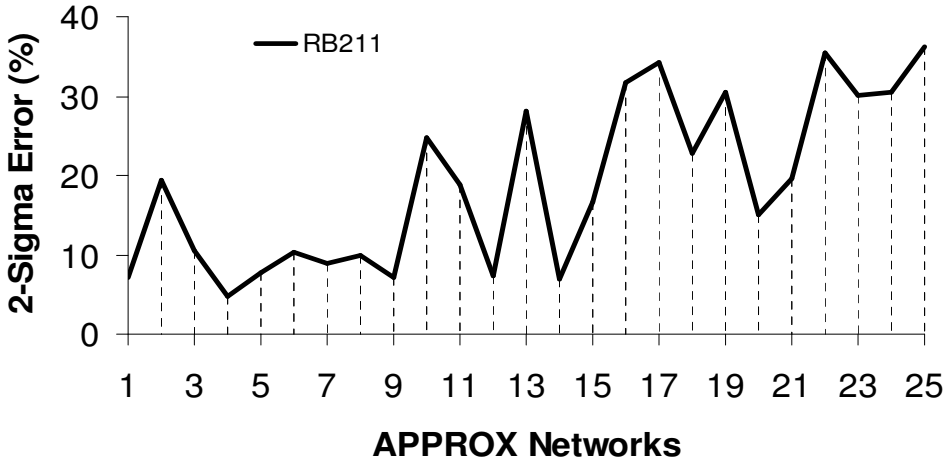

Figure 7.7 Plots of 2-sigma error for RB211 APPROX networks

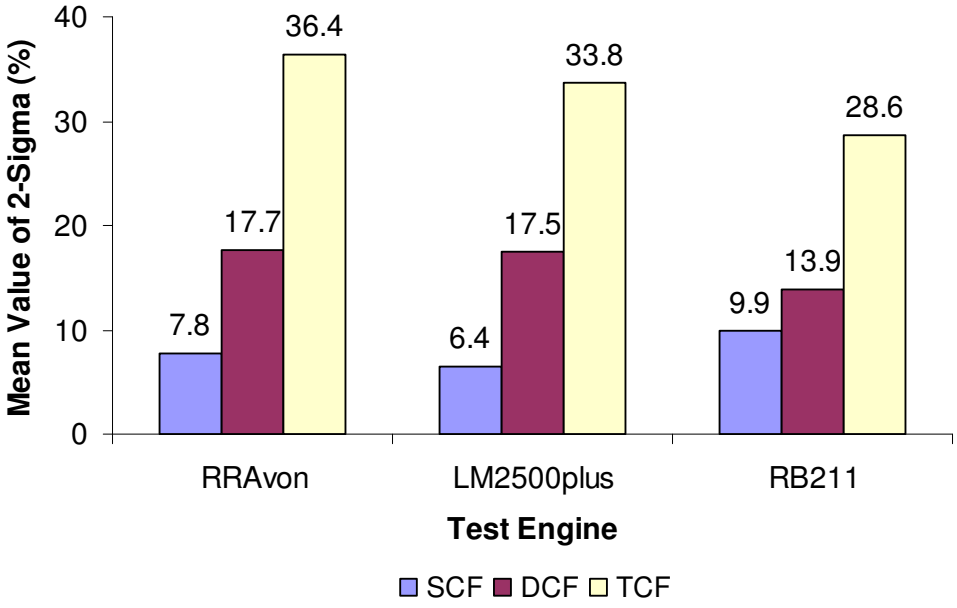

Figure 7.8 Comparison of mean values for 2-sigma error based on number of faulty components

Another approach applied in analysing the APPROX results is by the use of correlation coefficients (CoC). The CoC is a measure of how well trends in a predicted value agree with trends in the actual/target values. The CoC in this case was computed from equation 7.6.

$$\text{CoC} = r = \frac{n\sum at - \sum a \sum t}{\sqrt{\left[n\sum a^2 - \left(\sum a\right)^2\right] * \left[n\sum t^2 - \left(\sum t\right)^2\right]}} = \frac{\text{COV}(a,t)}{\sigma_a \sigma_t} \qquad 7.6$$

$$-1 \le r \le 1$$

where a is the network prediction of a performance parameter

t is the target or actual value of the performance parameter

n is the number of data points

COV is the covariance between network output and target

As the strength in relationship between a predicted and actual value grows, so does the CoC tend to 1 while a weakened relationship tends through zero to -1 for reversed trends.

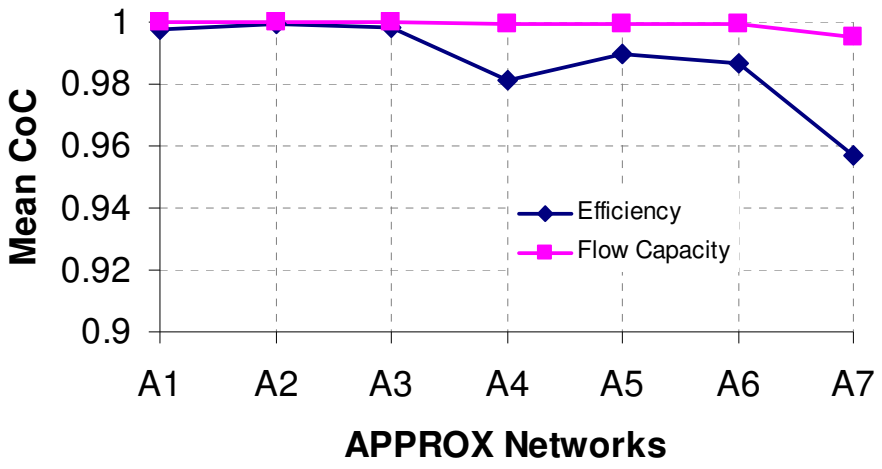

Figure 7.9 Mean coefficient of correlation for RR Avon APPROX networks

CoC computed for each of the performance parameter in the various APPROX networks are included in APPENDIX A.7. However, a mean value obtained by grouping efficiencies and flow capacities respectively for the different APPROX networks is shown in Figures 7.9 to 7.11. The CoC from the flow capacity indicates a much stronger relationship between the network prediction and target than that of the efficiency. This simply implies that the APPROX networks better predicts the flow capacities than the efficiencies. In terms of absolute errors obtained by direct comparison between estimate and true levels of faults, magnitudes are equivalent, but relative to the values of faults being estimated, the errors in the flow capacity are smaller than those obtained from efficiency estimation. In a compressor, the fault range considered for efficiency is -3.5% → -0.5% while the flow capacity changes were from -17.5% → +3.5%. In the turbine, efficiency changes were similar to those of the compressor but flow capacity changes ranged form -3.5% → +10.5%. These ranges were chosen to cover a wide range of possible faults.

In APPENDIX A.8, the distributions of percentage relative error for all the APPROX networks are presented. In obtaining these distributions, it was ensured that every single point involved in the test was plotted, the level of relative error not withstanding, however, the main area of interest is the range defined by the majority of test patterns. The percentage relative errors were computed from equation 7.2. An important observation here is that the CoC patterns presented in Figures 7.9 to 7.11 is in agreement with these distributions. The relative error margins presented in APPENDIX A.8 for the efficiencies are wider in most cases than their corresponding flow capacity margins and this fact is more established by the values of 2-σ given in Tables 7.5, 7.7 and 7.9. In addition, the CoC from the prediction of efficiency on the TCFs of RB211 (Figure7.11) are low for most points due to high estimation errors. Training of more networks or the reassessment of the data set may provide better results for these points.

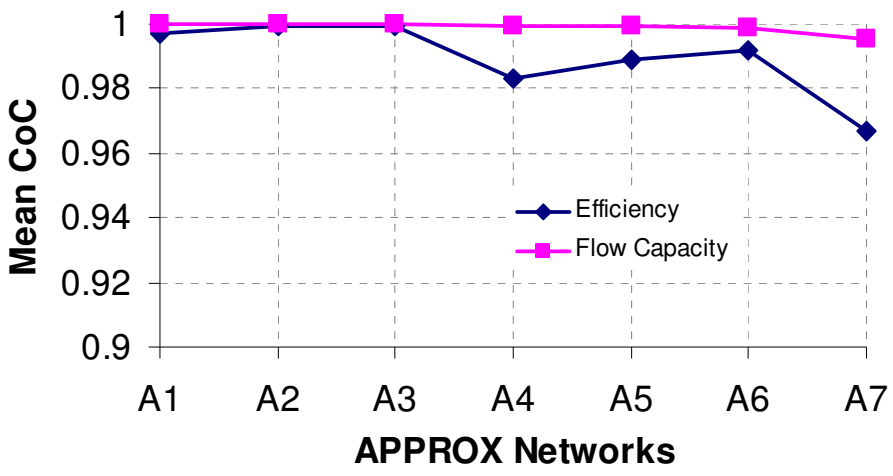

Figure 7.10 Mean coefficient of correlation for LM2500+ APPROX networks

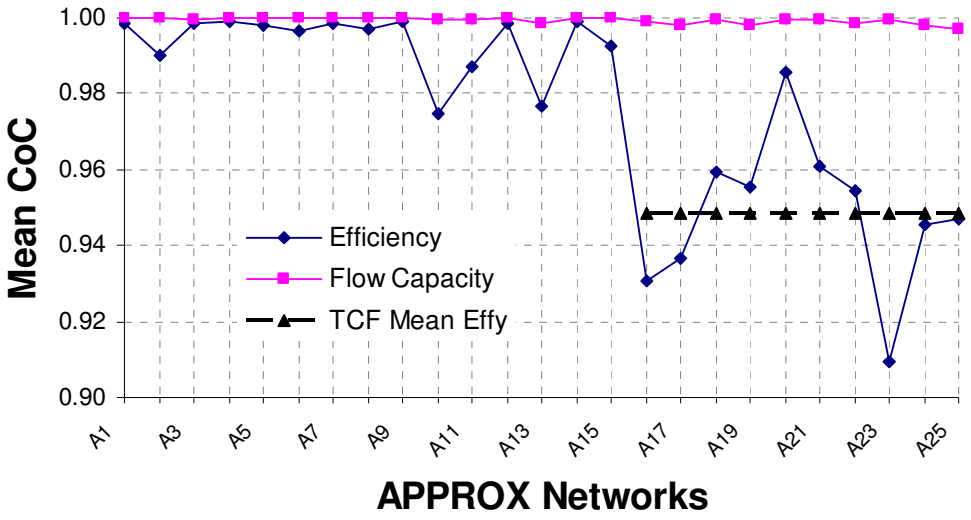

Figure 7.11 Mean coefficient of correlation for RB211 APPROX networks

7.5 Discussion of Results from 2-Spool Turbofan Diagnostics

The previous sections of this chapter have discussed results from the diagnostic technique developed for stationary GTs operating in steady state. In this section, the diagnostic philosophy is applied to a turbofan engine under transient conditions. The network structure and peculiarities have initially been outlined in section 6.3.3, the results obtained and their discussions are now considered.

A rigorous test was carried out on the developed diagnostic framework in the batch process mode to validate its robustness. This involved the generation of various noised test patterns with the various network units broadly represented in the test space. Table 7.10 shows the classification results obtained from passing about 21,860 test patterns through the diagnostic program. It is clear from the Table that the ANN abilities seem reduced as the complexity in the fault combinations increase. An objective look at the misclassified fault signatures obtained for dual component faults however indicates a high similarity between patterns of different fault classes hence the result given by the

PNN. In general, CLASS1-CLASS4 networks achieved a high success rate, which in any case represents the range of problems most often encountered as GT GPFs.

Table 7.10 Results from CLASS networks for Turbofan diagnostic program

CLASS1	**NF**	**F**				
TTP	2000	19860				
%CCP	100	99.8				
CLASS2	**SF**	**CF**				
TTP	3600	16260				
%CCP	100	100				
CLASS3	**SCF**	**DCF**				
TTP	1460	14800				
%CCP	99.5	96.2				
CLASS4	**IPC**	**HPC**	**HPT**	**LPT**		
TTP	438	438	292	292		
%CCP	100	100	100	100		
CLASS5	**IPC& HPC**	**IPC& HPT**	**IPC& LPT**	**HPC& HPT**	**HPC& LPT**	**HPT& LPT**
TTP	3600	2400	2400	2400	2400	1600
%CCP	85	90.4	90.8	86.7	90.1	88

Table 7.11 Results of random fault implant test cases for Turbofan APPROX networks.

TEST CASES	IMPLANTED FAULT (%)				PREDICTED FAULT (%)				ABS. ESTIMATION ERROR (%)			
	Component 1		Component 2		Component 1		Component 2		Component 1		Component 2	
SINGLE COMPONENT FAULTS												
Case 1	η_{IPC} -2	Γ_{IPC} -6			η_{IPC} -2.023	Γ_{IPC} -5.989			η_{IPC} 0.023	Γ_{IPC} 0.011		
Case 2	η_{HPC} -2	Γ_{HPC} -6			η_{HPC} -2.035	Γ_{HPC} -5.867			η_{HPC} 0.035	Γ_{HPC} 0.133		
Case 3	η_{HPT} -2	Γ_{HPT} +4			η_{HPT} -1.978	Γ_{HPT} +3.965			η_{HPT} 0.022	Γ_{HPT} 0.035		
Case 4	η_{LPT} -2	Γ_{LPT} +4			η_{LPT} -1.993	Γ_{LPT} +3.991			η_{LPT} 0.007	Γ_{LPT} 0.009		
DUAL COMPONENT FAULTS												
Case 5	η_{IPC} -2.2	Γ_{IPC} -6.6	η_{HPC} -2.2	Γ_{HPC} -6.6	η_{IPC} -2.042	Γ_{IPC} -6.528	η_{HPC} -2.126	Γ_{HPC} -6.752	η_{IPC} 0.158	Γ_{IPC} 0.072	η_{HPC} 0.074	Γ_{HPC} 0.152
Case 6	η_{IPC} -2.2	Γ_{IPC} -6.6	η_{HPT} -2.2	Γ_{HPT} +4.4	η_{IPC} -2.248	Γ_{IPC} -7.311	η_{HPT} -2.097	Γ_{HPT} +4.439	η_{IPC} 0.048	Γ_{IPC} 0.711	η_{HPT} 0.103	Γ_{HPT} 0.039
Case 7	η_{IPC}	Γ_{IPC}	η_{LPT}	Γ_{LPT}	η_{IPC}	Γ_{IPC}	η_{LPT}	Γ_{LPT}	η_{IPC}	Γ_{IPC}	η_{LPT}	Γ_{LPT}

	-2.2	-6.6	-2.2	+4.4	-2.265	-6.552	-2.176	+4.386	0.065	0.048	0.024	0.014
Case 8	η_{HPC} -2.2	Γ_{HPC} -6.6	η_{HPT} -2.2	Γ_{HPT} +4.4	η_{HPC} -2.307	Γ_{HPC} -6.281	η_{HPT} -2.207	Γ_{HPT} +4.599	η_{HPC} 0.107	Γ_{HPC} 0.319	η_{HPT} 0.007	Γ_{HPT} 0.199
Case 9	η_{HPC} -2.2	Γ_{HPC} -6.6	η_{LPT} -2.2	Γ_{LPT} +4.4	η_{HPC} -2.181	Γ_{HPC} -6.858	η_{LPT} -2.113	Γ_{LPT} +4.391	η_{HPC} 0.019	Γ_{HPC} 0.258	η_{LPT} 0.087	Γ_{LPT} 0.009
Case 10	η_{HPT} -2.2	Γ_{HPT} +4.4	η_{LPT} -2.2	Γ_{LPT} +4.4	η_{HPT} -2.439	Γ_{HPT} +4.365	η_{LPT} -2.100	Γ_{LPT} +4.415	η_{HPT} 0.239	Γ_{HPT} 0.035	η_{LPT} 0.100	Γ_{LPT} 0.015

Table 7.12 2-σ error levels from fault assessment using APPROX networks of Turbofan.

NETWORK	**2-σ ERROR FOR GIVEN PARAMETER (%)**			
	Component 1		**Component 2**	
APPROX1	η_{IPC} 3.91	Γ_{IPC} 1.85		
APPROX2	η_{HPC} 8.73	Γ_{HPC} 8.90		
APPROX3	η_{HPT} 4.11	Γ_{HPT} 9.16		
APPROX4	η_{LPT} 3.39	Γ_{LPT} 2.98		
APPROX5	η_{IPC} 41.4	Γ_{IPC} 34.0	η_{HPC} 12.7	Γ_{HPC} 21.7
APPROX6	η_{IPC} 31.1	Γ_{IPC} 53.4	η_{HPT} 14.6	Γ_{HPT} 15.9
APPROX7	η_{IPC} 16.8	Γ_{IPC} 23.5	η_{LPT} 9.4	Γ_{LPT} 14.3
APPROX8	η_{HPC} 20.7	Γ_{HPC} 29.7	η_{HPT} 24.7	Γ_{HPT} 20.8
APPROX9	η_{HPC} 17.8	Γ_{HPC} 26.6	η_{LPT} 35.8	Γ_{LPT} 21.4
APPROX10	η_{HPT} 17.5	Γ_{HPT} 26.3	η_{LPT} 20.4	Γ_{LPT} 19.1

In Table 7.11, estimation results for typical case studies of fouling (compressor) and erosion (turbine) affecting single and dual components are shown. The absolute estimation errors (unsigned difference between prediction and target) show the high level of accuracy obtainable from the diagnostic framework in terms of the extent of degradation present in the engine. As is applicable to most diagnostic programs, some test patterns do not give the level of accuracy desired. The grayed cell of Case 6 and Case 10 for example, show estimation error that is relatively high where compared to the level of fault. In any case, the predicted results are still indicative of the possible

fault(s) present in the engine. In addition, it is obvious from Table 7.11 that as the fault complexity increases from SCF to DCF, the estimation error increases, this being more apparent when the test is conducted over a wider range of patterns and the standard deviation computed as shown in Table 7.12.

Table 7.12 shows results obtained when the approximation networks were tested with much data comparable to that given in Table 7.10. This data varied from -0.5% to -4% change in efficiency for all components while flow capacities for compressors varied from -20% $\rightarrow$ +4% and for turbines from -4% $\rightarrow$ +12%. This range covered all possible combinations of faults that might affect the gas-path of the gas turbine though in practice we may not expect such large flow capacity drops. The results displayed represent 2-standard deviation (2- σ) values of relative estimation errors within which it is expected that about 95% of the test data fall. Typical mean errors are about zero and thus the level of accuracy reported by the 2-σ error values is obviously within limits expected from diagnostic programs as it would provide a good knowledge of the engine status and thus enhance the development of an effective condition based maintenance scheme. This level of accuracy is not, however, the same for all the networks as APPROX6 presents a high level of error component for the inclusion of 95% of its flow capacity test data for the IPC under a dual component fault scenario. As stated earlier, estimation accuracy reduces with the complexity of the problem and this, amongst other reasons, informed the choice of nested approach to the diagnostic problem so that each network unit is configured for a specific task.

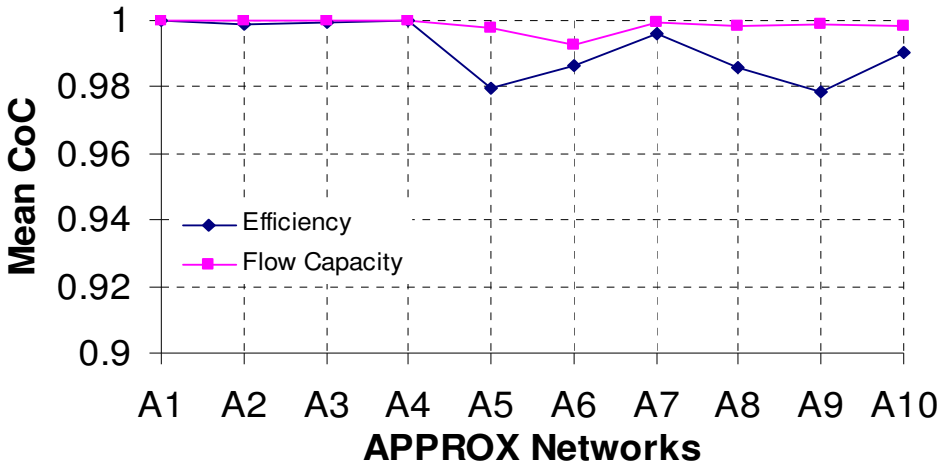

Figure 7.12 Mean coefficient of correlation for Turbofan APPROX networks

The CoC for each of the estimated parameters from this diagnostic framework were computed and reported in Table A.7.4 of APPENDIX A.7. Figure 7.12 shows the mean values of these CoC plotted for each APPROX network and differentiated into efficiency and flow capacity. Here again a better prediction of the flow capacities is experienced and the reasons for this are as given in section 7.4.

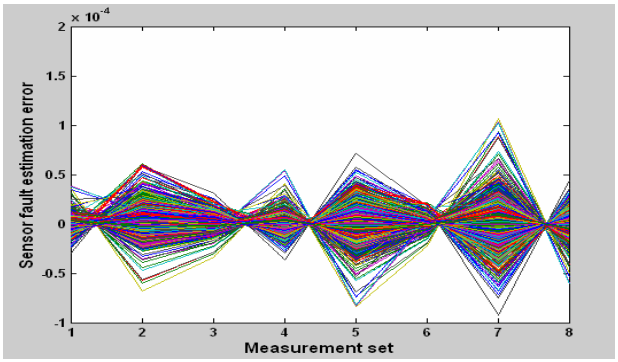

Figure 7.13 Error (noise) levels from turbofan sensor fault(s) estimation

From CLASS2 of the diagnostic framework, patterns identified as originating from sensor fault are passed on to an AANN to isolate the faulty sensor(s) while placing a

value on the amount of fault. The process involved is such that the input to the network is the accumulated deviations of the respective sensors with network output restrained to a non-faulty range for different faulty inputs. Thus, a difference between the network input and output gives values for the fault or noise present in the sensor(s). The errors involved in the fault estimation process are typically in the order of $x10^{-4}$ as shown in Figure 7.13 where the x-axis indicates the measurement set. Figure 7.13 shows error levels for series of tests (3600) conducted on this network with various combinations of single and dual sensor fault(s).

7.6 Discussion of Results from Sensor Fault Diagnosis

The task of sensor fault(s) isolation and estimation in all the diagnostic frameworks have been handled by the use of autoassociative (AUTOASSOC) networks. For the 2-shaft engine configuration a maximum of two simultaneously faulty sensors can be isolated and estimated while for the 3-shaft engine configuration, the number increases to three. The number of diagnosable faulty sensors is indirectly proportional to the number of neurons required in the bottleneck to reconstruct the output in the case of failed sensor(s) or noisy inputs. Thus, the more neurons required in the bottleneck (that is, less correlation between measurements) the smaller number of faulty sensors that can be diagnosed and vice versa. Because of the similarities in sensor fault diagnosis for the stationary engines, some results for the 3-shaft engine scenario that are presented here, would be taken as representative of those of other engines.

Sensor fault detection and estimation for the RB211 engine was performed with the AUTOASSOC1 network. This network was designed to isolate single, dual and triple sensor faults while quantifying the amount of faults in such biased sensors.

No corrections were made on the training patterns because they were generated at SL conditions. The baseline values for the nine measured parameters used in this analysis are the same as those used for other networks in this engine. The sensor non-repeatability values formed the level of noise added to the sensor readings for training

the networks while we defined our minimum magnitude for which a given sensor's reading is identified as faulty to be twice the level of noise for that sensor. This difference is required to create some gap/distinction between a faulty and non-faulty sensor class.

White noise with a normal distribution was added to all the generated training and testing data. Implanted sensor faults ranged from twice the noise level to about 20% for all sensors. The pre- and post-processing of data was conducted as presented in section 6.4. The network outputs during training were suppressed to remain within a wholly clean range using the AANN.

Figures 7.14 presents the test patterns prior to and results obtained when simulated with a trained network as it affects a single sensor fault. In this case, ten test patterns are used and the faulty sensor is the LP shaft speed, N1, of the 3-shaft engine.

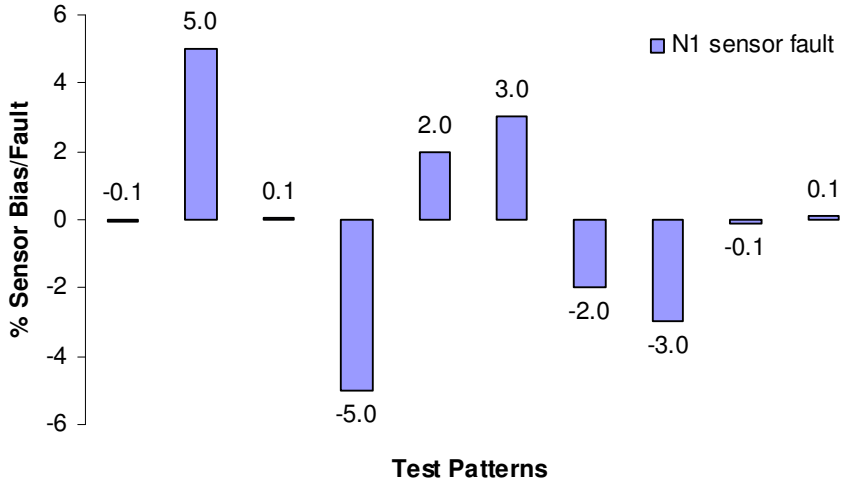

Figure 7.14a Random fault implanted on LP shaft speed (N1) indicating a single sensor fault

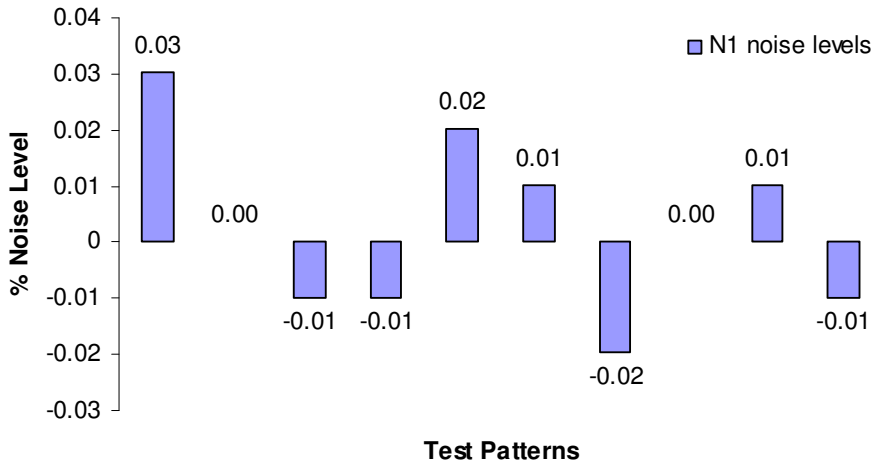

Figure 7.14b: Random noise levels applied to N1

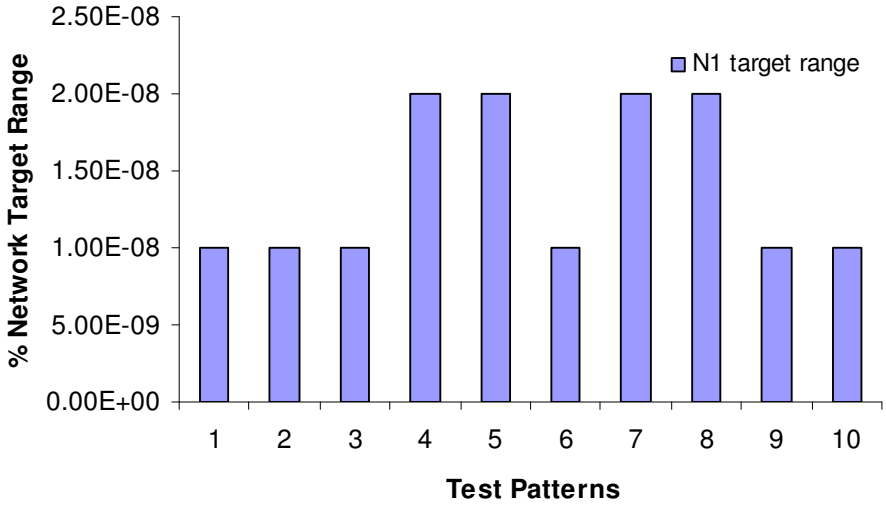

Figure 7.14c Expected output range for N1 from network

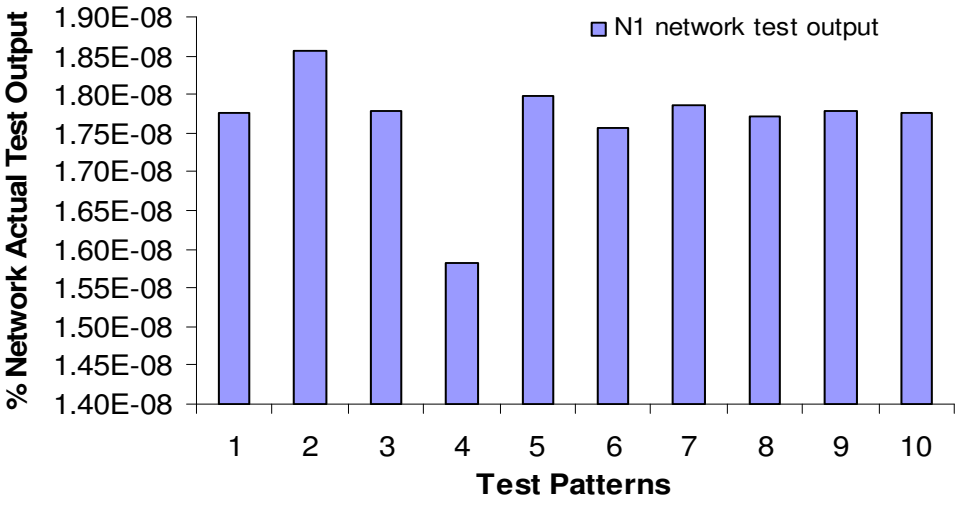

Figure 7.14d Actual network output for N1

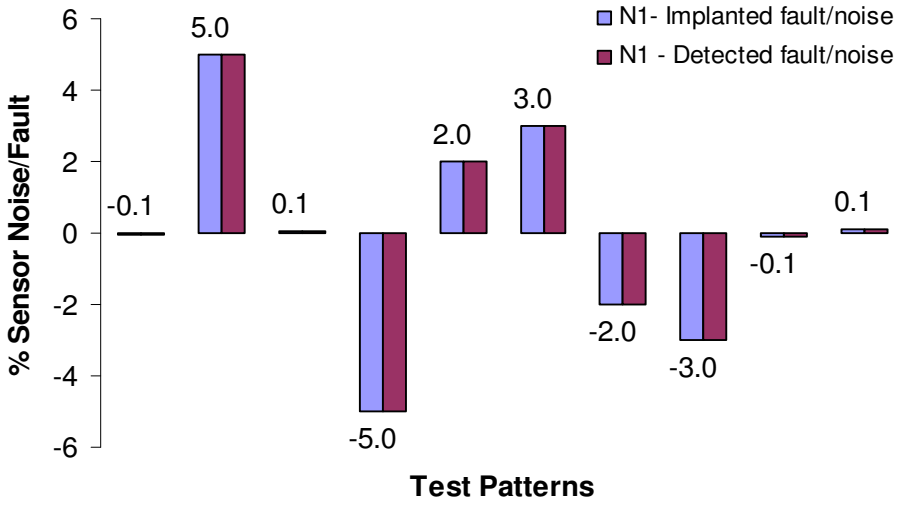

Figure 7.14e Comparison of implanted and detected Single sensor fault on N1

In Figure 7.14a, ten SSF patterns are shown. These pre-processed deviation values indicate the percentage by which a sensor reading differs from a clean baseline value. In this case, the faults are in the range ± 5%. The noise level applied to the N1 sensor is shown in Figure 7.14b. The expected output from the network is suppressed to be within the clean range, which in this case is approximately zero as shown in Figure

7.14c. The trained AANN adjusts its output (Figure 7.14d) to the required target, which then allows us to determine the quantity of fault by computing the difference between the network input and output. Figure 7.14e shows that the implanted and detected sensor faults forms a perfect fit.

The approach to isolating and quantifying DSF and TSF indicated in APPENDIX A.9 are similar to what has been described above.

If a measured pattern is correctly identified by CLASS2 as having a sensor fault, then the foregoing shows that the amount of fault can be accurately determined.

7.7 Comparison of ANN Approach and Other Techniques

In this section, we carry out a brief comparison of typical results obtained using ANN systems, developed after the presented approach and diagnostic results from (1) two techniques in gas-path analysis – linear and nonlinear, and (2) results from fuzzy logic (FL) diagnostic system. The degree of accuracy of each approach is based on the consideration of the mean value of the root mean square (RMS) over the range of test patterns.

7.7.1 Comparison of Results from ANN Diagnostic Approach with GPA

Tables 7.13 and 7.14 shows the comparison between the diagnostic results from two gas-path analysis (GPA) techniques with those of the trained networks for compressor and gas generator turbine faults respectively. Urban (1972) initially introduced GPA as a tool for engine diagnostics. It involves the thermo-mathematical matching of engine measurements (dependent variables) to health parameter (independent variables) changes. This is based on the premise that faults in the gas-path of a gas turbine cause changes in efficiencies and flow capacities, which are not directly measurable. Because relationship exists between some of the measurements such as pressures, temperatures, speeds etc. taken from different stations of an engine and the health parameters, it is

exploited to determine the magnitude of changes in the independent variables. Urban (1972) considered this relationship from a linear perspective and his work is now more commonly termed the linear gas-path analysis (LGPA). In reality, gas turbine parameter interrelationships are highly nonlinear hence, Escher and Singh (1995) developed an iterative approach to the problem with the principles based on Urban's formulation. This new approach is termed the nonlinear gas-path analysis (NLGPA).

Two components – C and CT- of the RR Avon are considered for this analysis. In Table 7.13, the implanted fault in the compressor component and the diagnostic results from three (3) diagnostic techniques, LGPA, NLGPA and ANN are compared. It should be noted that the presence of a fault is indicated by a change in the independent variables which would thus affect the measurements taken from the engine. The following observations can be made from the analysis:

1. Noting that the ANN module involved in estimating the fault in the compressor (C) is APPROX1, the mean RMS errors from the three techniques show that the estimation accuracy depreciates from NLGPA through ANN to LGPA; the mean error from the ANN is twice that from NLGPA. A similar conclusion can be drawn from Table 7.14 where APPROX2 is called to estimate compressor turbine fault from the ANN module.
2. In Table 7.14 however, NLGPA failed to converge on some fault scenarios. This non-convergence is due to a convergence feature in the NLGPA algorithm that causes instability when it is perceived that a solution is not possible with the current instrumentation suite. This is in contrast with the ANN results, which shows that the instrumentation suite is sufficient.
3. Finally, it should be noted that the results from the GPA techniques (LGPA and NLGPA) do not include measurement noise unlike those from ANN. Had noise been included in the NLGPA measurements, the ANN diagnostic results may have compared favourably with those from NLGPA or even better since no noise filtering algorithm exist in the NLGPA tool.

Table 7.13 Comparison of diagnostic results from ANN and GPA for RR Avon C.

IMPLANTED FAULTS		**LINEAR GPA**			**NON-LINEAR GPA**			**ANN**		
η_c	Γ_c	η_c	Γ_c	**RMS**	η_c	Γ_c	**RMS**	η_c	Γ_c	**RMS**
-0.5	-0.5	-0.81	-0.33	**0.251**	-0.50	-0.47	**0.022**	-0.59	-0.50	**0.062**
-0.5	-1.0	-0.83	-0.86	**0.253**	-0.50	-1.00	**0.003**	-0.53	-0.94	**0.045**
-0.5	-1.5	-0.92	-1.50	**0.299**	-0.50	-1.55	**0.037**	-0.55	-1.49	**0.034**
-0.5	-2.0	-1.22	-1.69	**0.555**	-0.62	-1.53	**0.340**	-0.59	-2.04	**0.071**
-1.0	-1.0	-1.62	-0.65	**0.503**	-1.00	-0.98	**0.012**	-1.04	-1.00	**0.030**
-1.0	-2.0	-1.66	-1.72	**0.506**	-1.00	-2.00	**0.002**	-0.80	-1.83	**0.189**
-1.0	-3.0	-2.07	-2.52	**0.832**	-1.13	-2.49	**0.373**	-1.01	-3.03	**0.020**
-1.0	-4.0	-2.46	-3.42	**1.111**	-1.01	-3.97	**0.025**	-1.02	-4.04	**0.032**
-1.5	-1.5	-2.46	-0.88	**0.811**	-1.50	-1.47	**0.019**	-1.34	-1.40	**0.130**
-1.5	-3.0	-2.46	-0.88	**1.647**	-1.49	-3.00	**0.007**	-1.54	-3.04	**0.042**
-1.5	-4.5	-3.13	-3.81	**1.251**	-1.50	-4.48	**0.015**	-1.35	-4.35	**0.151**
-1.5	-6.0	-3.72	-5.11	**1.693**	-1.51	-5.99	**0.006**	-1.81	-6.29	**0.302**
-2.0	-2.0	-3.51	-0.80	**1.365**	-2.00	-1.99	**0.008**	-1.79	-1.87	**0.177**
-2.0	-4.0	-3.49	-3.09	**1.236**	-2.08	-3.73	**0.201**	-1.81	-3.85	**0.170**
-2.0	-6.0	-4.19	-5.11	**1.673**	-2.00	-6.00	**0.005**	-1.93	-5.99	**0.048**
-2.0	-8.0	-5.01	-6.88	**2.270**	-2.01	-7.99	**0.012**	-1.91	-7.93	**0.080**
-2.5	-2.5	-4.30	-1.02	**1.648**	-2.50	-2.48	**0.015**	-2.74	-2.74	**0.243**
-2.5	-5.0	-4.24	-4.07	**1.393**	-2.53	-4.96	**0.038**	-2.59	-5.10	**0.097**
-2.5	-7.5	-5.28	-6.24	**2.156**	-2.50	-7.49	**0.010**	-2.62	-7.55	**0.090**
-2.5	-10.0	-6.33	-8.69	**2.862**	-2.52	-9.99	**0.014**	-2.48	-9.87	**0.093**
-3.0	-3.0	-5.25	-0.98	**2.138**	-3.01	-2.99	**0.006**	-2.81	-2.97	**0.137**
-3.0	-6.0	-5.09	-4.85	**1.690**	-3.04	-5.96	**0.039**	-3.14	-6.05	**0.107**
-3.0	-9.0	-6.37	-7.45	**2.623**	-3.01	-8.99	**0.009**	-3.08	-9.00	**0.054**
-3.0	-12.0	-7.60	-10.41	**3.440**	-2.99	-11.99	**0.006**	-3.06	-12.05	**0.057**
		Mean Error		1.425	**Mean Error**		0.051	**Mean Error**		0.102

Table 7.14 Comparison of Diagnostic Results from ANN and GPA for RR Avon CT.

IMPLANTED FAULTS		**LINEAR GPA**			**NON-LINEAR GPA**			**ANN**		
η_{CT}	Γ_{CT}	η_{CT}	Γ_{CT}	**RMS**	η_{CT}	Γ_{CT}	**RMS**	η_{CT}	Γ_{CT}	**RMS**
-0.5	0.5	-0.99	0.38	**0.358**	-0.51	0.47	**0.021**	-0.53	0.55	**0.038**
-0.5	1.0	-1.01	0.86	**0.373**	-0.51	0.97	**0.023**	-0.53	1.13	**0.098**
-0.5	1.5	-1.04	1.30	**0.403**	-0.51	1.44	**0.041**	-0.60	1.61	**0.109**
-0.5	2.0	-1.06	1.75	**0.434**	-0.49	1.97	**0.023**	-0.59	1.97	**0.065**
-1.0	1.0	-2.11	0.69	**0.814**	-1.01	1.01	**0.007**	-1.00	1.06	**0.040**
-1.0	1.5	-2.17	1.13	**0.866**	-0.99	1.48	**0.014**	-1.06	1.59	**0.075**
-1.0	2.0	-2.37	1.55	**1.021**	-1.00	1.99	**0.008**	-0.94	1.96	**0.053**
-1.0	2.5	-2.58	1.95	**1.184**	-1.00	2.50	**0.003**	-0.94	2.39	**0.085**
-1.5	1.5	-3.96	1.01	**1.775**	-1.51	1.50	**0.004**	-1.47	1.49	**0.020**
-1.5	2.5	-4.32	1.73	**2.069**	-1.67	2.48	**0.118**	-1.50	2.45	**0.033**
-1.5	3.5	-4.36	2.46	**2.152**	-1.52	3.48	**0.023**	-1.53	3.53	**0.028**
-1.5	4.5	-4.65	3.16	**2.421**	-1.49	4.49	**0.008**	-1.44	4.38	**0.097**
-2.0	2.0	-5.45	1.17	**2.507**	-2.01	2.00	**0.006**	-2.04	1.95	**0.042**
-2.0	3.0	-5.76	1.89	**2.770**	-2.02	2.99	**0.013**	-2.00	3.06	**0.041**
-2.0	4.0	-6.07	2.58	**3.048**	-2.01	4.00	**0.006**	-2.01	4.02	**0.018**
-2.0	4.5	-6.22	2.91	**3.190**	-2.01	4.49	**0.011**	-1.91	4.39	**0.096**
-2.5	2.5	-6.82	1.34	**3.166**	NC	NC	**-**	-2.42	2.39	**0.097**
-2.5	3.0	-7.01	1.69	**3.318**	NC	NC	**-**	-2.43	2.95	**0.061**
-2.5	3.5	-7.18	2.03	**3.469**	NC	NC	**-**	-2.56	3.55	**0.059**
-2.5	4.5	-7.79	2.69	**3.951**	NC	NC	**-**	-2.55	4.56	**0.055**
-3.0	3.0	-11.53	1.42	**6.134**	NC	NC	**-**	-2.95	3.07	**0.057**
-3.0	3.5	-12.23	1.70	**6.648**	NC	NC	**-**	-3.04	3.63	**0.095**
-3.0	4.0	-11.44	1.98	**6.139**	NC	NC	**-**	-3.02	4.16	**0.111**
-3.0	4.5	-12.37	2.21	**6.822**	NC	NC	**-**	-2.99	4.61	**0.081**
		Mean Error		2.710	**Mean Error**		0.021	**Mean Error**		0.065

7.7.2 Comparison of Results from ANN Diagnostic Approach with FL

Fuzzy logic (FL) has been introduced in section 2.3.2.2 as one of the evolving approaches for GPFD. No information was found in the public literature on the use of FL for quantitative fault diagnosis in GTs thus the gas turbine research group at Cranfield University, in the paper *Engine Diagnostics-A Fuzzy Logic approach* (Marinai et al, 2003) have begun considering this possibility. Ogaji et al (2003b) have also published some results from this study compared against results from the use of ANN.

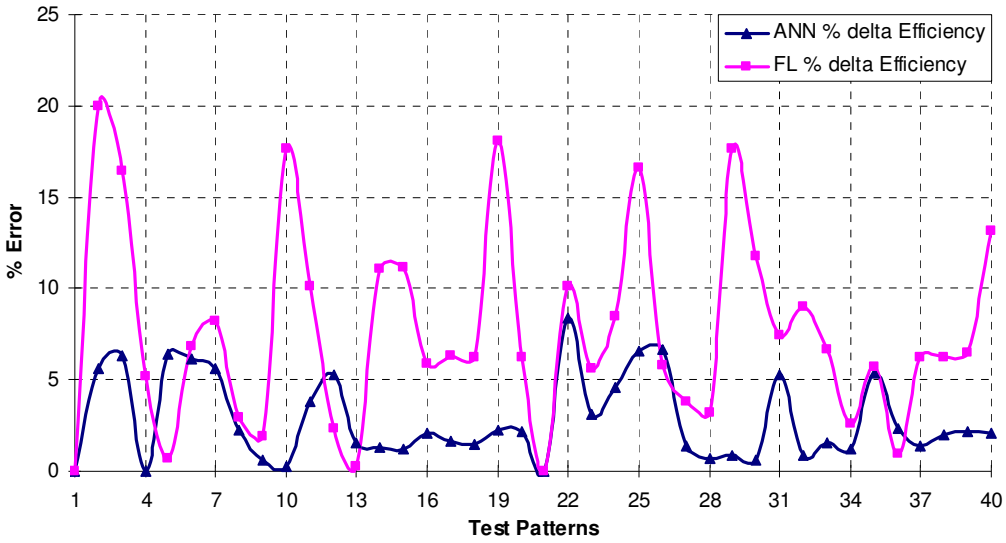

Figure 7.15 Percentage error from prediction of IPC efficiency using ANN and FL

In the current tests, diagnostic systems using ANN and FL were built for a 3-spool military turbofan engine thermodynamical similar to the Rolls Royce RB199. Uncertainties (noise) with a Gaussian distribution were added during the creation of the membership functions (MFs) of the fuzzy variables and the inputs for the ANN training. Forty IPC test patterns were passed through the diagnostic programmes and the percentage deviation of the programme's output from the implanted faults for the IPC efficiency and IPC flow capacity were plotted as shown in Figures 7.15 and 7.16. It

should be noted that Fault levels considered during the design of the diagnostic system as well as testing ranged from -0.5% to -3.5% for efficiency and flow capacities.

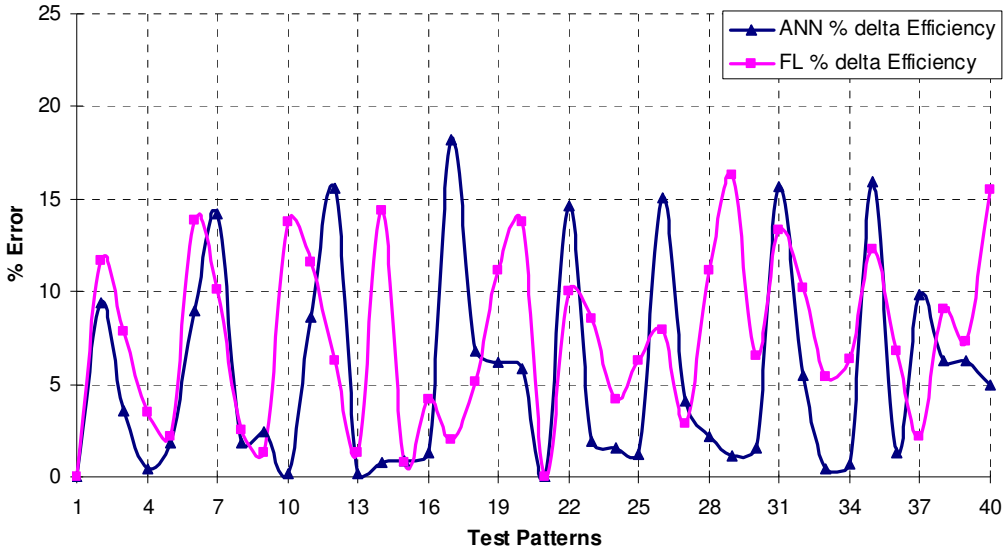

Figure 7.16 Percentage error from prediction of IPC flow capacity using ANN and FL

In Figure 7.15, it is clearly seen that the ANN performs a much better prediction of the IPC's efficiency than the FL. In the case of the flow capacity prediction shown in Figure 7.16, results from ANN are similar to those of FL. Computation of the mean RMS shows that while the ANN had a value of 0.076, the FL had 0.163, indicating a much better performance of the ANN than the FL. It is thought that there may be some improvement in the FL accuracy if the number of rules was increased, but this was not verified.

ANN is not only favoured in the prediction accuracy but also in the time required to obtain results in the recall mode. However, in the time required to set up the diagnostic system, FL may be the favourite, especially scenarios where the ANN is a complex one that will require a lengthy period to learn properly, though this will depend on if explicit rules can be found for the FL system.

Finally, the use of both approaches to GPFD has the potential to increase confidence in results since it is unlikely that both would provide simultaneously wrong estimates for a particular engine condition.

7.8 Summary

One sure way of validating the effectiveness of a diagnostic setup, especially one that involves the use of ANN is to determine its generalization ability with respect to fault patterns hitherto unseen but within the range of the training patterns. Results from such tests as well as discussions of the implications have been presented for the various engines used as case studies in this work. The results included those from classification, approximation and autoassociative networks. Single and multiple components as well as single and multiple sensor faults were considered. Comparisons of results across engine platforms as well as with other diagnostic techniques were made.

An ANN is as good as the data from which it is trained and its performance in some cases is determined by the intricacy of the problem set. Just as performance of components degrades, the performance of ANN also degrades gradually as the problem becomes more complicated, for instance, the inclusion of dual and triple component fault in this case. Another possible reason for degradation in network performance is the reduction in the amount of information available from the fixed sensor set as well as compounding errors introduced from the engine simulation programme.

One way of increasing confidence in diagnostic results and hence enhancing the diagnostic capability of the developed framework is to perform the diagnostics under multiple operating points, which fall within the diagnostic interval defined earlier. Measurements can be taken from the engine at two different power settings and introduced into the diagnostic model. Reproduction of the same results increases confidence in those results. This is possible because very little time is required in undertaking this diagnostic task as the programme produces results in seconds once the networks have been set up.

CHAPTER 8

CONCLUSIONS

8.1 Conclusions

The aim of this research was to develop a framework for the application of advanced GPFD to GTs. The aim, decomposed into research objectives amongst other things, provided a task map.

A literature search showed that while GPFs are varied, their effect on the performance of the GT could be devastating (economically and otherwise), if not checked. The literature also showed that most of the work carried out in GPFD, the tools used notwithstanding, has been qualitative – isolating the faulty component without consideration given to the level of fault. The few that have tried to consider the quantitative aspect of this problem were restricted to looking at one component or the other or just limited to a single sensor in case of sensor faults. Only one group of authors (Zedda and Singh, 1998) attempted a consideration of more than one-component fault.

In view of the identified gaps in contemporary research, this investigation applied ANN as a tool that could possibly move the frontiers of GPFD forward especially when one notes that conventional techniques are plagued with such drawbacks as noise, measurement bias, model inaccuracies, non-linearity between parameters, and inability to utilise the limited available sensory information optimally. The literature showed critical features that must be taken into account in order to achieve the set objectives from an ANN application.

The engine models used in this research had thermodynamic semblance to their prototypes. Sensors were chosen based on their quality, that is, with respect to the observability of the faults being diagnosed. A developed parameter correction approach

was useful in enabling fault diagnoses over a number of operating points without having to retrain the networks. In addition, the application of these corrections would enable the use of degradation measurements from two or more different operating points, which will improve the confidence in results obtained from the diagnostic process.

The diagnostic process utilised a philosophy that has received commendations from several researchers and paper reviewers alike in their comments. It required the determination of the presence of a fault before any further action is taken to isolate and quantify the fault. A nested ANN structure proved useful in fragmenting the task. This structure would allow easy maintenance of each unit, quick retraining in scenarios where this may be required as well as better diagnosis since each network is *specialised*.

Substantial tests, applied to the developed case studies, showed the high quality of results derivable from the application of ANN. A high degree of accuracy was obtained with the various processes involving classifications, approximations and autoassociations. Results from collaborating researchers, validating various aspects of this research, support the effectiveness of the developed approach. In addition, several publications in refereed journals and conference have arisen from this work, some of which are included amongst the references.

Finally, other impacts of this research can be envisaged in:

- The application of the developed framework by GT users and OEMs for GPFD
- Synergetic application of ANN and other techniques, such as GA. On the one hand, ANN, because of its speed of convergence to a solution, can be applied to isolate a fault class while GA would be used to provide an estimate of the faults. On the other hand, GA can be applied to optimise the weights of ANN, while the ANN is used for fault diagnosis. This latter approach could prevent the ANN from settling in a local minimum, and so provide better generalisation results.
- The application of the described technique to obtain actual values for failed sensor(s) when they have been isolated and their faults quantified.

8.2 Major Contributions of Research

ANNs have been successfully applied to other domains (medicine, finance etc) and even to aspects of engine diagnostics as discussed in section 2.3.2.4 but very little information is available on its application to the gas-path of the GT. The research presented in this thesis has significantly improved understanding about the worthwhileness of the application of ANN to GPFD of GTs. Results presented in chapters 5 to 7 indicate the novelty of the developed technique. The research has identified GPFs as one of the major causes of engine life-loss as well as life-cycle-cost increases. Amongst the contributions made by this research in diagnosing GPFs are:

- Developing a parameter correction approach that would enable fault diagnosis to be achieved under various operating points, with the limit being the level of accuracy of either the training data or of the model being used for the data generation.
- Developing an approach for selecting optimal measurement sets, for fault diagnosis. This is particularly useful for scenarios where they do not exist or where OEMs or GT users desire to know what quality measurements to monitor in order to improve the observability of particular faults.
- Distinguishing effectively between a faulty engine and non-faulty engine from the measured patterns.
- Isolating sensor faults from component faults, which in actual application would go a long way to prevent false alarms, which are characteristic of most traditional diagnostic techniques.
- Assessing the level of faults in single or simultaneously multiple faulty sensors
- Isolating faulty component(s) to the class level.
- Assessing the magnitude of faults in the isolated faulty component(s).
- Introduction of a wholistic approach involving nested ANN for GPFD

8.3 Limitations of Research

Due to the nature of the tool used in developing the diagnostic framework, the thermo-mathematical software for simulating engine performances at different operating conditions and some approaches developed in the process of the research, limitations exist.

In section 4.6, the strengths and weaknesses of the main tool used in developing the diagnostic framework, ANN, were presented. Some of these weaknesses formed part of the limitations of this study. Because an ANN cannot perform outside the range of data for which it is trained, much training data are required. Long training times are a common feature and often a network may be repeatedly trained before it can be certified as ready for the intended task. These limitations are manageable if avenues of data generation or collection are available and if sufficient processing capacity is available for large networks.

A trained network is only as good as the data from which it has been trained. This research was conducted with data generated wholly with a simulation program. Approximation errors exist in this program and component maps are inconsistent at some points, so resulting in non-convergences. In addition, the process of fault implantation, which involves the use of scaling factors, has its own accompanying errors. Since measurement changes due to faults are very small, high data accuracy is required. Thus, the degree of accuracy of the diagnostic program is bound to be affected by the compounding of errors inherent in the set-up.

A methodology has been described for correcting measurements taken at operating points other than the point at which the diagnostic program was set up. Within the limits defined for the three operating-point setting parameters, namely ambient temperature, ambient pressure and shaftpower, the correcting process is adequate, but beyond these points, errors occur. These errors are partly due to irregularities in the component map and partly due to the non-sophistication of the correction algorithm. Improving the

potency of the correction algorithm may increase the range of operating points that can be considered for a given diagnostic module via the use of the developed approach.

8.4 Future Desirable Research

The validity of the results obtained in this research has been established. Nevertheless, further research could be conducted in this area. Indeed the scope of application of ANN to GPFD can be extended if some of the following issues are addressed:

- Simultaneous analysis of two sets of measurement otherwise known as multiple operating point analysis should be considered. Measurements are taken from two or more independent operating points and analysed without recourse to correction. This may have the advantage of increasing sensory information, an approach that may be of great benefit for poorly instrument engines.
- The use of parallel processing to speed up the network-training task. Some networks typically take several days to set up and in scenarios such as this, where multiple networks are required in batch, the use of a number of processors can be instrumental in ensuring a quick set-up.
- Problems with one degree of freedom that is, problems that cause a change of just one health parameter i.e. efficiency or flow capacity respectively, should be included. As an instance, a problem in turbine cooling is said to result in a change in turbine flow capacity alone. The current work considered performance faults that used two degrees of freedom.
- Noise and biases should be considered in the parameters setting the operating point of the engine (i.e. power-setting parameter and environmental variables) as the possibility of such a scenario occurring cannot be ruled out.
- The possibility of incorporating GA and ANNs, such that the former optimises the weights, learning rates, momentum factor and such like, that are required by the neural networks, should be investigated. This will reduce the ANN training time as well as limit the possibility of sub-optimisation via convergence in a local minimum.

- The possibility of fault isolation and assessment in scenarios with sensor and component fault existing simultaneously should be considered.
- The possibility of obtaining online-trained networks should be investigated. We note that it is possible to obtain networks that are trained online, that is, having continuous update of the networks weights and biases. The attendant problems that would need attention for this approach include:
  - ⇒ Determining the length of time required for training.
  - ⇒ Ascertaining when the network is deemed to be well trained
  - ⇒ Determining the computational effort required, especially for scenarios with multiple-network structures.

REFERENCES

Agrawal, R. K., MacIsaac, B. D., and Saravanamuttoo, H. I. H. 1978**. An Analysis Procedure for Validation of On-Site Performance Measurements of Gas Turbines**. ASME Journal of Engineering for Power (78-GT-152).

Aker, G. F., and Saravanamuttoo, H. I. H. 1989. **Predicting Gas turbine Performance Behaviour Due to Compressor Fouling Using Computer Simulation Techniques**. ASME Journal of Engineering for Gas Turbines and Power Volume 111: pp 343-50.

Ali, M., and Gupta, U. 1990. **An Expert System for Fault Diagnosis in a Space Shuttle Main Engine**. 26th AIAA/SAE/ASME/ASEE Joint Propulsion Conference, Orlando, FL ,July 16 - 18,AIAA 90-1890.

Allwood, R. J., Kings, S. P., and Pitts, N. J. 1996. **The Automatic Interpretation of Vibration Data**. Aeronautical Journal Volume 100, no. 993: pp 99-107.

Anderson, D. and McNeill, G. 1992. **Artificial Neural Networks Technology**. Data and analysis centre for software (DACS), Technical Reports. Contract No. F30602-89-C-0082.

Angelakis, C., Loukis, E.N., Pouliezos, A.D. and Stavrakakis, G.S. 2001 **A Neural Network Based Method for Gas Turbine Blading Fault Diagnosis** International Journal of Modelling and Simulation, Volume 21, No 1.

Bakal, B.; Adali, T.; Fakory, R.; Sonmez, M. K., and Tsaoi, O. 1995 **Neural Network Simulation of Real Time Core Neutronic Model.** Proceedings of the SCS Simulation Multiconference. Phoenix, AZ, USA.

Barlett, E. B. and Uhrig, R. E. 1992 **Power Plant Status Diagnostics Using Artificial Neural Network**. Nuclear Technology. Volume 97:pp.272-281.

Barschdorff, D. 1991 **Comparison of Neural and Classical Decision Algorithms** IFAC/IMACS Symposium on Fault Detection, Supervision and Safety for Technical Processes. September 10-13. Baden-Baden, Germany.

Batcho, P. F., Moller, J. C., Padova, C., and Dunn, M. G. **Interpretation of Gas Turbine Response Due to Dust Ingestion**. ASME Journal of Engineering for Gas Turbines and Power Volume 109: pp 344-52.

Berenblut, and Masom. **Radiation Pyrometry for Gas Turbine Engines- An Introduction**. The British Journal of Non- Destructive Testing Volume 24(5): pp 268-69.

Boyce, M. P. 1984. **Gas Turbine Engineering Handbook**. Gulf Publishing.

Brotherton, T. and Johnson, T. 2001 **Anomaly Detection for Advanced Military Aircraft Using Neural Networks.** IEEE Proceedings on Aerospace Conference.; Volume 6:pp.3113-3123.

Brotherton, T.; Jahns, G.; Jacobs, J., and Wroblewski, D. 2000 **Prognosis of Faults in Gas Turbine Engines**. IEEE Aerospace Conference Proceedings. Volume 6:pp. 163-171.

Brownell, T. A. 1992 **Neural Networks for Sensor Management and Diagnostics**. Aerospace and Electronics Conference, Proceedings of the IEEE. Volume 3. pp. 923-929.

Cheng, B, and Titterington, D. M. 1994. **Neural Networks: a review from a statistical perspective**. Statistical Science Volume 9.

Cifaldi, M. L., and Chokani, N. 1998. **Engine Monitoring Using Neural Networks**. American Institute of Aeronautics and Astronautics,AIAA-98-3548.

Costandy, S. S. 1995. **Advances in Aerospace Lubricant and Wear Metal Analysis**. Lubrication Engineer Volume 51: pp 777-83.

Cue, R. W., and Muir, D. E. 1991. **Engine Performance Monitoring and Troubleshooting Techniques for the CF-18 Aircraft**.

Demuth, H and Beale, M. 2001. **Matlab Neural Networks Users Guide** Version 4, MathWorks, Inc.

Denney, G. 1993 **F16 Jet Engine Trending and Diagnostics with Neural Networks** SPIE Applications of Artificial Neural Networks IV. Volume 1965, pp 419-422.

DePold, H.R. and Gass, F.D. 1999 **The Application of Expert Systems and Neural Networks to Gas Turbine Prognostics and Diagnostics** Journal of Engineering for Gas Turbines and Power, Volume 121, pp 607-612.

Dietz, W.E., Kiech, E.L. and Ali, M. 1989 **Jet and Rocket Engine Fault Diagnosis in Real Time**. Journal of Neural Network Computing. Volume 1, No 1, pp 5-18.

Doel, D. L. 1990. **The Role of Expert Systems in Gas Turbine Engine Monitoring**. Gas Turbine and Aeroengine Congress and Exposition, Brussels. Belgium. June 11-14 (90 - GT – 374).

Doel, D. L. 1994a. TEMPER - **A Gas-path Analysis Tool for Commercial Jet Engines**. ASME Journal of Engineering for Gas Turbines and Power Volume 116: pp82-89.

Doel, D. L. 1994b. **An Assessment of Weighted-Least-Squares- Based Gas-path Analysis**. ASME Journal of Engineering for Gas Turbines and Power Volume 116: pp 366-73.

Doel, D.L. and Lapierre, L.R. 1989 **Diagnostic Expert System for Gas Turbine Engines-Status & Prospects** AIAA/ASME/SAE/ASEE 25th Joint Propulsion Conference, Monterey, CA. July 10-12. (AIAA-89-2585).

Dong, D.W., Hopfield, J.J. and Unnikrishnan, K.P. 1997 **Neural Networks for Engine Fault Diagnostics** Neural Networks for Signal Processing VII. pp 636-644.

Dupuis, R.J., Saravanamuttoo, H.I.H. and Rudnitski, D.M. 1985 **The Use of Fault Matrices in On Condition Health Monitoring** Proceedings of the TH NRCC Conference on Gas Turbine Operations & Maintenance. September.

Escher, P.C., 1995 **Pythia: An Object-Oriented Gas-path Analysis Computer Program for General Applications.** Ph.D. Thesis, School of Mechanical Engineering, Cranfield University. United Kingdom.

Eustace, R., and Merrington, G. 1995. **Fault Diagnosis of Fleet Engines Using Neural Networks.** Twelfth International Symposium on Air Breathing Engines, Melbourne, Australia ,September 10-15,ISABE 95-7085.

Eustace, R.W., Woodyatt, B.A., Merrington, G.L. and Runacres, A., 1994 **Fault Signatures Obtained From Fault Implant Tests on an F404 Engine**, Journal of Engineering for Gas Turbines and Power, Volume 116, pp 178-183.

Fantoni, P. F. and Mazzola, A. 1996 **Multiple Failure Signal Validation in Nuclear Power Plants Using Artificial Neural Networks**. Nuclear Technology. Volume 113(No. 3).

Feraud, R. and Clerot, F. A 2002. **Methodology to Explain Neural Network Classification.** Neural Networks. Volume 15:pp. 237-246.

Fuh-Eau, W. 1994. **Aero Engine Life Calculated From Combined Creep and Fatigue, and Extended By Trading off excess Thrust**. Cranfield University. UK.

Fukuzaki, T.; Ohga, Y., and Kobayashi, Y. 1992. **Feasibility Studies on Applying Neural Network Techniques in Nuclear Power Plants**. Proceedings of the OECD-NEA/IAEA International Symposium on NPP Instrumentation and Control; Tokyo, Japan.

Ganguli, R. 2001a **Application of Fuzzy Logic for Fault Isolation of Jet Engines** Proceedings of ASME Turbo Expo. New Orleans, Louisiana. June 4-7. (2001-GT-0013).

Ganguli, R. 2001b **Data Rectification and Detection of Trend Shifts in Jet Engine Gas-path Measurements Using Median Filters and Fuzzy Logic**. Proceedings of ASME Turbo Expo. New Orleans, Louisiana. June 4-7. (2001-GT-0014).

Gas Turbine World Handbook. 1998-1999, Volume 19A Requot Publication.

Gauss K.G., 1963 **Theory of Motion of the Heavenly Bodies.** New York: Dover.

Green, A, and Allen, D. 1997. **Artificial Intelligence for Real Time Diagnostics and Prognostics of Gas Turbine Engines**. (AIAA 97 – 2899) 33rd AIAA/ASME/SAE/ASEE Joint Propulsion Conference and Exhibition, Seatle, WA ,July 6 – 9.

Grenstad, P. E, and Smith, M. J. Duncan R. L. 1982. **A Base Load Gas Turbine To Meet Utility Requirements for Reliability and Availability**. ASME Journal of Engineering for Power Volume 104.

Grewal, S. M. 1988. **Gas Turbine Engine Performance Deterioration and Analysis**. Ph.D. Thesis, Cranfield University. UK.

Gulati, A., Zedda, M., and Singh, R. 2000. **Gas Turbine Engine and Sensor Multiple Operating Point Analysis Using Optimization Techniques**. 36th AIAA/ASME/SAE/ASEE Joint Propulsion Conference and Exhibit. (AIAA-2000-3716)

Guo, T. H., Saus, J., Lin, C. F., and Ge, J. H. 1996. **Sensor Validation for Turbofan Engines Using an Autoassociative Neural Network**. AIAA Guidance Navigation and Control Conference ,San Diego, CA. July 29-31, (AIAA-96-3926),

Guo, T.H and Nurre, J. 1991 **Sensor Failure Detection and Recovery by Neural Networks.** NASA Technical Memorandum 104484.

Guo, Z and Uhrig, R. E. 1992 **Use of Artificial Neural Networks to Analyze Nuclear Power Plant Performance**. Nuclear Technology. Volume 99:pp. 36-42.

Hall, D. L., Hansen, R. J., and Lang, D. C. 1997. **The Negative Information Problem in Mechanical Diagnostics**. ASME Journal of Engineering for Gas Turbines and Power Volume 119: pp 370-377.

Haykin, S. 1999 **Neural Networks: A Comprehensive Foundation.** Prentice Hall; ISBN: 0-13-908385-5.

Hebb, D. O., 1949. **The Organization of Behaviour**, Wile, New York, New York.

Hopfield, J. J., 1982 **Neural Networks and Physical Systems with Emergent Collective Computational Abilities**, Proceedings of the National Academy of Sciences, Volume 79, April.

Huang, H.; Vian, J.; Choi, J.; Carlson, D., and Wunsch, D. 2001 **Neural Network Inverse Models for Propulsion Vibration Diagnostics**. Proceedings of SPIE. Volume 4390:pp. 12-21.

Illi, O.J., Greitzer, F.L., Kangas, L.J. and Reeve, T.J. 1994 **An Artificial Neural Network System for Diagnosing Gas Turbine Engine Fuel Faults**, 48th Meeting of the Mechanical Failure Group (MFPG 48), April 19-21. Wakefield, MA.

Isermann, R. 1984. **Process Fault Detection Based on Modeling and Estimation Methods - A Survey**. Automatica Volume 20: pp 387-404.

Isik, C. 1991 **Fuzzy Logic: Principles, Applications and Perspectives**. SAE Transactions, Journal of Aerospace, Volume 100 pp 393-396. (SAE-91/1148).

Ismail, I. H., and Bhinder, F. S. 1991. **Simulation of Aircraft Gas Turbine Engines**. ASME Journal of Engineering for Gas Turbines and Power Volume 113: pp 95-99.

Jacobs, R.A., 1988. **Increased Rates of Convergence Through Learning Rate Adaptation**, Neural Networks, Volume 1.

Javed, M. A.; Hope, A. D.; Little fair, G.; Adradi, D.; Smith, G. T., and Rao, B. K. N. 1996 **On-line Tool Condition Monitoring Using Artificial Neural Networks**. Insight. Volume 38(No. 5):pp.351-354.

Jouse, W. C. and Williams, J. G. **Neural Control of Temperature and Pressure during PWR Start-up**. 1990 American Nuclear Society Transactions. Volume 61:pp. 219-220.

Kalman, R.E. 1960. **A New Approach to Linear Filtering and Prediction Problems.** Journal of Basic Engineering, Series 82D, p35-45. March.

Kamboukos, Ph., and Mathioudakis, K. 2003. **Comparison of Linear and Non-linear Gas Turbine Performance Diagnostics**. Ptoceedings of ASME Turbo Expo, Atlanta, Georgia, June 16-19, GT2003-38518.

Kanelopoulos, K., Stamatis, A., and Mathioudakis, K. 1997. **Incorporating Neural Networks into Gas turbine Performance Diagnostics**. International Gas Turbine and Aeroengine Congress and Exhibition, Orlando, Florida, June 2-5, 97-GT-35.

Kevin, G. 1997. **An introduction to Neural Networks**. UCL Press Limited.

Kobayashi, T. and Simon, D. L. **A Hybrid Neural Network-Genetic Algorithm Technique for Aircraft Engine Performance Diagnostics** 2001 (AIAA-2001-3763). 37th AIAA/ASME/SAE/ASEE Joint Propulsion Conference and Exhibit; Salt lake City, Utah. .

Kohonen, T., 1982. **Self-Organization Formation of Topologically Correct Feature Maps**, Biological Cybernetics, Volume 43.

Kramer, M. A. **Nonlinear Principal Component Analysis Using Autoassociative neural Networks**. AIChE. 1991; Volume 37(No. 2):pp.233-243.

Lakshminarasimha, A. N., Boyce, M. P., and Meher-Homji, C. B. 1994. **Modelling and Analysis of Gas Turbine Performance Deterioration**. ASME Journal of Engineering for Gas Turbines and Power Volume 116: pp46-52.

Li, Y.G., 2003. **A Gas Turbine Diagnostic Approach with Transient Measurements**, ImechE Journal of Power and Energy, Volume 217, A2.

Lifson, A., Quentin, G. H., Smalley, A. J., and Knauf, C. L. 1989. **Assessment of Gas Turbine Vibration Monitoring**. ASME Journal of Engineering for Gas Turbine and Power Volume 111: pp 257-63.

Lowrance, J. D., and Garvey, T. D. 1982 **Evidential Reasoning: A Developing Concept**. Proc. International Conference on Cybernetics and Society.

Lu, P., Hsu, T., Zhang, M., and Zang, J. 2000. **An Evaluation of Engine Faults Diagnostics Using Artificial Neural Networks**. Proceedings of ASME Turbo Expo 2000: Land, Sea and Air, Munich, Germany. May 8-11 (2000-GT-0029).

Lucas, M., and Anderson, D. P. 1997. **Lubricant Analysis for Gas Turbine Condition Monitoring.** ASME Journal of Engineering for Gas Turbine and Power Volume 119: pp 225-30.

Luppold, R.H., Roman, J.R., Gallops, G.W. and Kerr, L.J. 1989 **Estimating In-Flight Engine Performance Variations Using Kalman Filter Concepts** (AIAA-89-2584) AIAA/ASME/SAE/ASEE 25th Joint Propulsion Conference, Monterey, CA. July 10-12.

MacIsaac, B. D. **Engine Performance and Health Monitoring Models Using Steady State and Transient Prediction Methods**. Advisory Group for Aerospace Research and Development AGARD-LS-183: pp 9.1-9.21.

MacLeod, J. D. 1991. **Computer Modelling of Implanted Component Faults in a Gas Turbine Engine**. *AIAA/SAE/ASME/ASEE 27th Joint Propulsion Conference*, Sacramento , CA , June 24-26,

Macmillan, W. L. 1974. **Development of a Modular Type Computer Program for the Calculation of Gas Turbine off Design Performance**. Cranfield Institute of Technology, School of Mechanical Engineering. UK.

Marinai, L, Ogaji, S., Sampath, S. and Singh, R. 2003 **Engine Diagnostics-A Fuzzy Logic Approach** Proceedings of the Seventh International Conference on Knowledge-

Based Intelligent Information Engineering Systems & Allied Technologies, 16-18 September, Oxford, UK.

Mathioudakis, K. 2003 **Neural Networks in Gas Turbine Fault Diagnostics** Von Karman Institute Lecture Series 2003-01 on Gas Turbine Condition Monitoring & Fault Diagnosis, 13-17 January. Belgium.

Mathioudakis, K. and Sieverding, C.H. 2003 **Gas Turbine Condition Monitoring & Fault Diagnosis** Von Karman Institute Lecture Series 2003-01, 13-17 January. Belgium.

Mathioudakis, K, and Stamatis, A. 1994. **Compressor Fault Identification from Overall Performance Data Based on Adaptive Stage Stacking**. ASME Journal of Engineering for Gas Turbines and Power, Volume 116: pp 156-64.

Meher-Homji, C. B. 1990. **Gas turbine Axial Compressor Fouling - A Unified Treatment of its Effects, Detection and Control**. ASME IGTI Volume 5.

Meher-Homji, C. B., Boyce, M. P., Lakshminarasimha, A. N., Whitten, J. A., and Meher-Homji, F. J. 1993. **Condition Monitoring and Diagnostic Approaches for Advanced Gas Turbines**. ASME Proceedings of 7th Congress & Exposition on Gas Turbine Cogeneration and Utility, Industrial and Independent Power Generation, Bournemouth, England, pp 347-354.

Merrington, G., Kwon, O., and Goodwin, b. Carlsson B. 1991. **Fault Detection and Diagnosis in Gas Turbines**. ASME Journal of Engineering for Gas Turbines and Power Volume 113: pp 276-286.

Merrington, G.L. 1989. **Fault Diagnosis of Gas Turbine Engines from Transient Data**. ASME Journal of Engineering for Gas Turbines and Power Volume 111: pp 237-243.

Merrington, G.L., 1988 **Identification of Dynamic Characteristics for Fault Isolation Purposes in a Gas Turbine Using Closed-Loop Measurements**, Engine Condition Monitoring-Technology and Experience, AGARD-CP-448, Oct.
Merrington, G.L., 1994 **Fault Diagnosis in Gas Turbines Using a Model-Based Technique**, Journal of Engineering for Gas Turbines and Power, Volume 116, pp 374-380.

Michalewicz, Z., 1996 **Genetic algorithms + data structures = evolution programs,** Springer Verlag, 3rd Edition, Berlin**.**

Minai, A.A., and Williams, R.D., 1990. **Acceleration of Back-Propagation through Learning Rate and Momentum Adaptation**, International Joint Conference on Neural Networks, Volume 1, January.

Minsky, M. L., and Papert, S. S., 1969. **Perceptrons: An Introduction to Computational Geometry**, MIT Press, Cambridge, MA.

Miur, D. E., Saravanamuttoo, H. I. H, and Marshall, D. J. 1989. **Health Monitoring of Variable Geometry Gas Turbines for the Canadian Navy**. ASME Journal of Engineering for Gas Turbines and Power Volume 111: pp. 244-250.

Moller, M.F., 1993, **A Scaled Conjugate Gradient Algorithm for Fast Supervised Learning**. Neural Networks, Volume 6, pp. 525-534.

Myrick, S. T. 1982**. Survey Results of Condition Monitoring in the Petrochemical Industry**. Proceedings of the Vibration Monitoring and Analysis Meeting.

Napolitano, M, Windon, D., Casanova, J., and Innocenti, M. 1996. **A Comparison between Kalman Filter and Neural Network Approaches for Sensor Validation**. AIAA Guidance Navigation and Control Conference, San Diego, CA, July 29-31, (AIAA-96-3894).

Ogaji, S., Sampath, S. and Singh, R. 2002d **Gas Turbine Faults: Detection, Isolation and Assessment Using Neural Networks.** Proceedings of the Sixth International Conference on Knowledge-Based Intelligent Information Engineering Systems & Allied Technologies, 16-18 September, Crema, Italy.

Ogaji, S., Sampath, S., Singh, R., and Probert, D. 2002b **Novel Approach for Improving Power-Plant Availability Using Advanced Engine Diagnostics**. Applied Energy 72 pp 389-407.

Ogaji, S.O.T. and Singh, R. 2002a **Study of the Optimisation of Measurement Sets for Gas-path Fault Diagnosis in Gas Turbines**, Proceedings of the ASME Turbo Expo, June 3-6, Amsterdam, The Netherlands. (GT-2002-30050).

Ogaji, S.O.T. and Singh, R. 2002b **Advanced Engine Diagnostics Using Artificial Neural Networks**. Proceedings of the IEEE International Conference on Artificial Intelligence Systems, 5-10 September, Gelendzhik. Black Sea Coast, Russia.

Ogaji, S.O.T. and Singh, R. 2002c **Neural Network Technique for Gas Turbine Fault Diagnosis** International Journal of Engineering Intelligent Systems, Volume 10, no. 4. pp 209-214.

Ogaji, S.O.T., and Singh, R. 2003 **Gas-path Fault Diagnoses Framework for a 3-Shaft Gas Turbine.** ImechE Journal of Power and Energy, Volume 217, A3.

Ogaji, S.O.T., Li, Y.G., Sampath, S and Singh, R. 2003 **Gas-path Fault Diagnosis of a Turbofan Engine from Transient Data Using Artificial Neural Networks.** Proceedings of the ASME Turbo Expo 2003, June 16-19, Atlanta, Georgia. USA (GT2003-38423).

Ogaji, S.O.T., Marinai, L., Sampath, S. and Singh, R. 2003b **Comparison of Artificial Neural Networks and Fuzzy Logic Approaches to Engine Diagnostics.** Paper submitted for publication in the International Journal of Engineering Intelligent Systems.

Ogaji, S.O.T., Sampath, S., Singh, R. and Probert, S. D. 2002c **Parameter Selection for Diagnosing Gas-Turbine Performance Deterioration**. Applied Energy 73(1) pp25-46.

Ogaji, S.O.T., Singh, R., and Probert, S.D. 2002a **Multiple-sensor fault-diagnoses for a 2-shaft stationary gas-turbine**. Applied Energy. Volume 71:pp. 321-339.

Parlos, A.G.; Muthusami, J., and Atiya, A. F. 1994 **Incipient Fault Detection and Identification in Progress Systems Using Accelerated Neural Network Learning**. Nuclear Technology. Volume 105:pp. 145.

Perz, E. 1991. **Computer Method for Thermal Power Cycle Calculation**. ASME Journal of Engineering for Gas Turbines and Power Volume 113: pp 184-89.

Provost, M.J. 1994. **The Use of Optimal Estimation Techniques in the Analysis of Gas Turbine Turbines**. Ph.D. Thesis, School of Mechanical Engineering, Cranfield University. United Kingdom.

Rao, B.V.A. 1996. **Condition Monitoring -Condition-Based Maintenance**. Journal of the Institution of Engineers (India), Part ME: Mechanical Engineering Division 66, no. 5: pp 123-129.

Rosenblatt, F., 1958. **The Perceptron: A Probabilistic Model for Information Storage and Organization in the Brain**, Psychological Review, Volume 65.

Rumelhart, D.E., Hinton, G.E., and Williams, R.J., 1985 **Learning Internal Representations by Error Propagation**, in D.E. Rumelhart, and J.L. McClelland, eds, Volume 1, Chapter 8, Cambridge, MA: MIT Press.

Sampath, S, Li, Y.G., Ogaji, S.O.T. and Singh, R. 2003 **Fault Diagnosis of a Two Spool Turbo-Fan Engine using Transient Data: A Genetic Algorithm Approach**. Proceedings of the ASME Turbo Expo 2003, June 16-19, Atlanta, Georgia. USA (GT2003-38300).

Sampath, S., Ogaji, S., Singh, R. 2002c **Advanced Fault Diagnosis Using Genetic Algorithm for Gas Turbine Engines**. Paper presented at the Sixth International Conference on Knowledge-Based Intelligent Information Engineering Systems & Allied Technologies, 16-18 September, Crema, Italy.

Sampath, S., Ogaji, S., Singh, R. and Probert, D. 2002b **Engine-Fault Diagnostics: an Optimisation Procedure**, Applied Energy 73(1) pp.47-70.

Sampath, S., Ogaji, S.O.T. and Singh, R. 2002a **Improving Power Plant Availability Through Advanced Engine Diagnostic Techniques.** Proceedings of the International Joint Power Generation Conference, June 24-26, Phoenix, AZ, USA. (IJPGC2002-26080).

Saravanamuttoo, H. I. H. 1992. **Overview on Basis and Use of Performance Prediction Methods**. Advisory Group for Aerospace Research and Development AGARD-LS-183: pp 1.1-1.18.

Sellers, J., and Daniele, C. 1975. **DYNGEN-A Program for Calculating Steady-State and Transient Performance of Turbojet and Turbofan Engines**. NASA TN D-7901.

Simani, S. and Fantuzzi, C. 2000 **Fault Diagnosis in Power Plant Using Neural Networks**. Information Sciences. Volume 127:pp.125-136.

Simmon, H. R., and Lifson, A. 1985. **Vibration Measurement for Determining Plant Component Reliability**. Proceedings of American Power Conference, Chicago, IL ,Apr. 23-25.

Singh, R. 1999**. Managing Gas Turbine Availability, Performance and Life Usage via Advanced Diagnostics**. 44th Gas Turbine Users Association Annual Conference, Dubai, UAE, 9-14 May.

Singh, R. 1996. **Fifty Years of Civil Aero Gas Turbines**. Paper Presented at Cranfield University's Fiftieth Anniversary. UK.

Singh, R. and Escher, P.C. 1995. **Gas Turbine Diagnostics and Availability**. Invited Paper Presented at Industrial & Power Gas Turbine Operations & Maintenance Conference, London. 26-27th September.

Sofa, T.; Eryurek, E.; Uhrig, R. E.; Dodds, H. L., and Cook, D. H. 1990 **Estimation of HFIR Core Flow Rate Using a Backpropagation Network**. American Nuclear Society Transactions. Volume 61.

Sorenson, H.W. 1970 **Least-squares Estimation: from Gauss to Kalman** IEEE Spectrum, Volume 7, pp63-68. July.

Specht, D.F., 1988 **Probabilistic Neural Networks for Classification, Mapping or Associative Memory**, ICNN-88 Conference Proceedings.

Specht, D.F., 1990 **Probabilistic Neural Networks**, Neural Networks, November.

Spector, R. B. 1989. **A Method of Evaluating Life Cycle Cost Of Industrial Gas Turbines**. ASME Journal of Engineering for Gas Turbines and Power Volume 111: pp 637-641.

Spina, P.R., Torella, G. and Venturini, M. 2002. **The Use of Expert Systems for Gas Turbine Diagnostics and Maintenance**. Proceedings of the ASME Turbo Expo. Amsterdam, The Netherlands. June 3-6.

Stamatis, A., Mathioudakis, K, and Papailiou, K. D. 1990. **Adaptive Simulation of Gas Turbine Performance**. ASME Journal of Engineering for Gas Turbines and Power Volume 112: pp168-175.

Stamatis, A., Mathioudakis, K, and Papailiou, K. D. 1992. **Optimal Measurement and Health Index Selection for Gas Turbine Performance Status and Fault Diagnosis**. ASME Journal of Engineering for Gas Turbines and Power Volume 114: pp209-216.

Tabakoff, W., and Balan, C. 1983. **A Study of the Surface Deterioration due to Erosion**. ASME Journal of Engineering for Power Volume 105: pp 834-38.

Torella, G. 1993. **Expert Systems for the Simulation of Turbofan Engines.** International Society for Air Breathing Engines (ISABE), Tokyo, Japan, September 20 - 24, ISABE 93-7133.

Torella, G. 1997. **Expert Systems and Neural Networks for Fault Isolation in Gas Turbines**. International Society of Air Breathing Engines, (ISABE 97-7148).

Torella, G., and Blasi, L. 2000**. Artificial Intelligence Tools for Gas Turbine Engine Utilisation Problems**. 36th AIAA/ASME/SAE/ASEE Joint Propulsion Conference, Huntsville, Alabama, July 16 - 19, (AIAA 2000-3502).

Torella, G., and Torella, R. 1999. **Probabilistic Expert Systems for the Diagnostics and Trouble-shooting of Gas Turbine Apparatuses**. 35th AIAA/ASME/SAE/ASEE Joint Propulsion Conference, LA. California, June 20 -24, (AIAA 99-2942).

Tsai, T. M. and Chou, H. P. 1996 **Recurrent Neural Networks for Fault Detection and Isolation**. Proceedings of the 1996 American Nuclear Society International Topical Meeting on Nuclear Plant Instrumentation, Control and Human-Machine Interface Technologies; Pennsylvania, USA. pp. 921-926.

Tsalavoutas, A, Arekatis, N., Mathioudakis, K., and Stamatis, A. 2000. **Combining Advanced Data Analysis Methods for the Constitution of an Integrated Gas Turbine Condition Monitoring and Diagnostic System**. Proceeding of ASME TURBOEXPO 2000, Munich, Germany, May 8-11, (2000-GT-0034).

Tsoukalas, L. H. 1994 **Virtual Measurement and Prediction in Human-Centered Automation**. Proceedings of the Topical Meeting on Computer-Based Human Support Systems: Technology, Methods, and Future, The American Nuclear Society's Human Factors Division; Pennsylvania, USA. pp. 235-241.

Upadhyaya, B. R. and Eryurek, E. 1992 **Application of Neural Networks for Sensor Validation and Plant Monitoring.** Nuclear Technology. Volume 97(No. 2):pp. 170-176.

Upton, A. W. J. 1974. **Axial Flow Compressor and Turbine Blade Fouling: Some Causes, Effects and Cleaning Methods**. First Symposium on Gas Turbine Operations and Maintenance, National Research Council of Canada.

Urban, L. A. 1972. **Gas-path Analysis Applied to Turbine Engine Condition Monitoring**, (AIAA 72-1082). AIAA/SAE 8th Joint Propulsion Specialist Conference; New Orleans, LA. November 29 - December 1.

Urban, L. A. 1975. **Parameter Selection for Multiple Fault Diagnostics of Gas Turbine Engines**. ASME Journal of Engineering for Power: pp 225-30.

Volponi, A. J. 1982. **A Large Measurement Error Recovery Algorithm for Gas turbine Module Performance Analysis**, 3430. Hamilton Standard.

Volponi, A. J. 1999. **Gas Turbine Parameter Corrections**, Transaction of the ASME, Journal of Engineering for Gas Turbines and Power, Vol 121, No 4, pp. 613-621.

Walsh, P. P., and Fletcher, P. 1998. **Gas Turbine Performance.** Blackwell Science Ltd.

Weidong, H., Kechang, W., and Qizhi, C. 1996. **Sensor Failure Detection and Data Recovery Based on Neural Network**. 32nd AIAA/ASME/SAE/ASEE Joint Propulsion Conference, Lake Buena Vista, FL ,July 1-3, (AIAA-96-2932).

Yangping, Z., Bingquan, Z., and DongXin, W. 2000 **Application of Genetic Algorithms to Fault Diagnosis in Nuclear Power Plants** Reliability Engineering and System Safety, Volume 67 pp 153-160**.**

Zadeh, L.A. 1988 **Fuzzy Logic** Computer, Volume 21 Issue 4, pp 83-93.

Zaita, A. V., Buley, G., and Karlsons, G. 1998. **Performance Deterioration Modelling in Aircraft Gas Turbine Engines**. ASME Journal of Engineering for Gas Turbines and Power Volume 120: pp 344-49.

Zedda, M., and Singh, R. 1998**. Fault Diagnosis of a Turbofan Engine using Neural Networks: A Quantitative Approach**. 34th AIAA/ASME/SAE/ASEE Joint Propulsion Conference & Exhibit, Cleveland, OH, July 13-15, (AIAA 98-3602).

Zedda, M., and Singh, R. 1999a. **Gas Turbine Engine and Sensor Fault Diagnosis Using Optimisation techniques**. 35th AIAA/ASME/SAE/ASEE Joint Propulsion Conference and Exhibit, Los Angeles, California, June 20-24, (AIAA 99-2530).

Zedda, M., and Singh, R. 1999b. **Gas Turbine Engine and Sensor Diagnostics**. IS10/UNK010, XIV International Symposium on Air-Breathing Engines (ISABE). Florence, Italy. 5-10 September.

APPENDIX A.1

MATHEMATICAL FORMULATION OF NON LINEAR GPA

(ESCHER, 1995)

The basic relationship between a dependent variable Y and an independent variable X is:

$$Y = F(X)$$

(A.1.1)

If we assume a small change in X, then a corresponding change in Y would, from equation (A.1.1), give: -

$$F(X + \delta X) = Y + \delta Y$$

or

$$F(X + \delta X) = F(X) + \delta Y$$

(A.1.2)

Given a small change **w** for a single variable function Z (a), the Taylor series expansion would be:

$$Z(a + w) = Z(a) + wZ'(a) + \frac{w^2}{2!}Z''(a) + \frac{w^3}{3!}Z'''(a) + \ldots\ldots$$

(A.1.3)

Thus equation (A.1.2) can be written as-

$$F(X + \delta X) = F(X) + J\delta X + HOT$$

(A.1.4)

where the Jacobian notation here stands for the first derivative in the Taylor series expansion of the matrix $F(X + \delta X)$,

$$\text{that is} \quad J = \begin{bmatrix} \frac{\partial f_1(X)}{\partial x_1} & \frac{\partial f_1(X)}{\partial x_2} & \cdots & \frac{\partial f_1(X)}{\partial x_m} \\ \frac{\partial f_2(X)}{\partial x_1} & \frac{\partial f_2(X)}{\partial x_2} & \cdots & \frac{\partial f_2(X)}{\partial x_m} \\ \vdots & \vdots & \vdots & \vdots \\ \frac{\partial f_n(X)}{\partial x_1} & \frac{\partial f_n(X)}{\partial x_2} & \cdots & \frac{\partial f_n(X)}{\partial x_m} \end{bmatrix}$$

$$\text{and} \qquad \delta X = \begin{bmatrix} \delta x_1 \\ \delta x_2 \\ \vdots \\ \delta x_m \end{bmatrix}$$

For small changes in X, we can neglect the higher-order terms (HOTs), and equation (A.1.4) thus becomes

$$F(X + \delta X) = F(X) + J\,\delta X \tag{A.1.5}$$

and from equations (A.1.2) and (A.1.5) we have –

$$\delta Y = F(X + \delta X) - F(X) = J\,\delta X \tag{A.1.6}$$

The solution of equation (A.1.6) is made easier if the Jacobian is inverted (Donaghy, 1991). This gives

$$J^{-1}\,\delta Y = \delta X \tag{A.1.7}$$

δX signifies correction on the independent variable and this is added to the solution vector viz.:

$$X_{New} = X_{Old} + \delta X \tag{A.1.8}$$

Each execution of the process indicated in equation (A.1.8) creates a new baseline to which further corrections are made until a defined convergence criterion that minimises the error (i.e. difference between measured and prediction) is attained, or the process is stopped after a given number of iterations. For each linear GPA calculation, an appropriate baseline is required. In the first iteration, a measured baseline is used and subsequent iterations use a calculated baseline derived from the implanted faults that are detected in the previous iteration. It is necessary to note that the first solution vector is the LGPA.

APPENDIX A.2

MATHEMATICAL FORMULATION OF THE WEIGHTED LEAST-SQUARES ALGORITHM

A typical model of this technology is given as (Doel, 1994a & 1994b):

$$z = h(x) + v \qquad \text{(A.2.1)}$$

where:

z is the measurement vector comprising the independent measurement on which the model is based: it is often called the dependent variable and comprises such parameters as shaft speed, temperature or pressure. It has a dimension of 'p'.

x is the state vector composed of the characteristics (of the engine) which are expected to vary with time. It is also called the independent variable and includes such parameters as component efficiencies and flow functions. It has a dimension of 'n'.

$h(x)$ is a 'p x n' matrix describing the effects of the state variables upon the measurements and is often called the influence-coefficient matrix. It is derived from the cycle model. For all practical purposes, it is necessary that $p \geq n$, since, outside this range, measured variables cannot sufficiently match the state variables to isolate faults as different faults may have similar signatures. In addition, this will allow for any redundancy in the system.

v is a vector of measurement noise and biases. It is meant to include the influence of state variables not included in the state vector, x, and any random imperfections in the model.

The analysis of equation (A.2.1) is simplified by the following modifications/assumptions:

- Replacing the nonlinear model $h(x)$ by a linear approximation Hx
- The measurement error is gaussian with a zero mean.
- State variables, x, are considered to be Gaussian in their distribution

With these assumptions, the objective of the weighted least-square analysis is to determine a "best estimate" of the state of the system given a set of measurements, z. The resulting approximation to equation (A.2.1) is:

$$z = Hx + v \qquad \text{(A.2.2)}$$

The probability-density function for the likelihood of z being obtained from an initial state vector x, whose designation would be $P(x|z)$ where $P(x|z)$ is a decreasing monotonic function of the quadratic form J, where:

$$J = 1/2 \{x^T M^{-1} x + (z-Hx)^T R^{-1} (z-Hx)\} \qquad \text{(A.2.3)}$$

where M is a covariance matrix for the state vector

R is a covariance matrix of the measurement error

T stands for transpose

Solving by minimizing J with respect to x will give the state vector estimate with the highest probability. The optimal solution x_o is:

$$x_o = (M^{-1} + H^T R^{-1} H)^{-1} H^T R^{-1} z \qquad \text{(A.2.4)}$$

The true measurement z_o for the engine state x_o is:

$$z_o = Hx_o \qquad \text{(A.2.5)}$$

Using these true values, from equations (A.2.4) and (A.2.5) the estimated measurement error can also be computed as follows:

$$v_o = [I - H(M^{-1} + H^T R^{-1} H)^{-1} H^T R^{-1}] z \qquad \text{(A.2.6)}$$

The corresponding residual solution J_o, is obtained by using x_o in equation (A.2.4). The implication of this is that the greater the value of J_o, the less likely that the assumed statistical model is correct for the particular data sample.

The algorithm is linear in z and therefore the solution error is proportional to the measurement deviation. In case the turbine efficiency is doubled, the solution error would also be doubled, as the percent error remains fixed. Hence, the weighted least-squares algorithm provides best result when measurement deviations are small.

APPENDIX A.3

PRINCIPLES OF THE SCG ALGORITHM

The processes involved in the SCG algorithm as developed by Moller (1993) are:

1. Choose weight vector w_1 and scalars $\sigma > 0$, $\lambda_1 > 0$ and $\bar{\lambda}_1 = 0$.

   Set $p_1 = r_1 = -E'(w_1)$, $k = 1$ and success = true.

2. if success = true then calculate second order information:

$$\sigma_k = \frac{\sigma}{|p_k|}$$

$$s_k = \frac{E'(w_k + \sigma_k p_k) - E'(w_k)}{\sigma_k}$$

$$\delta_k = p_k^T s_k$$

3. Scale δ_k:

$$\delta_k = \delta_k + (\lambda_k - \bar{\lambda}_k)|p_k|^2$$

4. If $\delta_k \leq 0$ then make the Hessian matrix positive definite:

$$s_k = s_k + \left(\lambda_k - 2\frac{\delta_k}{|p_k|^2}\right)p_k,$$

$$\bar{\lambda}_k = 2\left(\lambda_k - \frac{\delta_k}{|p_k|^2}\right)$$

$$\delta_k = -\delta_k + \lambda_k |p_k|^2$$

$$\lambda_k = \bar{\lambda}_k$$

5. Calculate step size:

$$\mu_k = p_k^T r_k$$

$$\alpha_k = \frac{\mu_k}{\delta_k}$$

6. Calculate the comparison parameter:

$$\Delta_k = \frac{2\delta_k [E(w_k) - E(w_k + \alpha_k p_k)]}{\mu_k^2}$$

7. If $\Delta_k \geq 0$, then successful reduction in error can be made:

$$\tilde{w}_{k+1} = \tilde{w}_k + \alpha_k \tilde{p}_k$$

$$\tilde{r}_{k+1} = -E'\left(\tilde{w}_{k+1}\right)$$

$\bar{\lambda}_k = 0$, success = true

If k mod N = 0 then restart algorithm:

$$\tilde{p}_{k+1} = \tilde{r}_{k+1}$$

else create new conjugate direction:

$$\beta_k = \frac{\left(\left|\tilde{r}_{k+1}\right|^2 - \tilde{r}_{k+1}^T \tilde{r}_k\right)}{\mu_k}$$

APPENDIX A.4

OPTIMAL INSTRUMENTATION SELECTION (OGAJI ET AL, 2002C).

It is sometimes possible to make intuitive guesses about dependent variables that would be relevant in detecting particular types of gas-path faults, but using an analytical approach based on techniques, such as GPA, is usually preferable. In addition, gas-path faults are detectable as long as there are discernible patterns in the dependent variables, and by extension, in the independent variables.

Compressor fouling and turbine erosion have high probabilities of occurring in a GT. The power turbine, by virtue of its position in the gas stream, coupled with its physical design is much less likely to experience gas-path damage than other components upstream. In this study, we have considered the power turbine on an equal footing with other components in the analysis of faulty components because any appropriate choice of instrumentation may be shown to operate under various fault levels.

The minimum requirement to determine a set of **n** unknowns in simultaneous-equation analysis is to use a set of **n** equations. The task is then to seek the **n** (i.e. the optimum number of sensors) set of dependent variables, optimised in types and locations, which would effectively estimate the changes in the set of **n** independent variables, which describe the signatures of the desired faults. In other words, the aim is to obtain a non-redundant set of sensors for a given fault scenario. The approach requires a prior knowledge of the independent variables that would be affected by the presence of any particular fault or fault combinations, and the signatures imposed by these faults on the performance parameters. For given levels of each fault, an attempt is then made to obtain the most appropriate instrumentation that can effectively diagnose the fault(s). As noted by Urban (1975), a poor choice of instrumentation first becomes obvious with

the presence of large coefficients in the inverted matrix, or FCM, which is brought to the fore by the occurrence of non-convergence of the iterative process or by large RMS error values.

The processes applied in choosing the instrumentation selection for a given set of performance parameters are: -

- Devising a model of the behaviour of the engine to be used
- Evaluating the degree of relevance (observability) of each possible measurement to a given change in each independent variable
- Determining the possible combinations of instruments, that would accurately quantify changes in a given set of independent variables

What follows, elaborates the application of these processes.

An engine that compares favourably with its real operational counterpart was thermodynamically modelled using nonlinear GPA (NLGPA). This engine has been chosen to represent the class of two-shaft stationary GTs for this study. A similar approach can be used for any engine configuration.

The engine model was run on a NLGPA program to obtain an order of sensitivity for each individual measurement to each independent variable, when perturbed by a given amount through varying its scaling factor. What is implied here is that, each of the independent variables was changed by some amount to simulate a fault, and all the possible measurements along the engine's gas-path applied, one at a time, to determine the degree of their effectiveness in quantifying the implanted fault. The results in Table A.4.1 show those parameters that respond most to a given independent variable change with an error less than a NLGPA RMS value of 0.7 using a SOP as power setting parameter, while Table A.4.2 was obtained with COT as power setting parameter. It should be noted that this threshold value of RMS, was subjectively chosen to specify the minimum level of accuracy, required for any sensor to fit in as a possible candidate in the choice of sensors to quantify changes in the considered independent variable. The

combustor's outlet temperature (COT) and the shaft power (SOP) are the only engine power setting parameters used in this study.

This final step required seeking various combinations of these parameter measurements that respond to faults implanted on component(s) with an NLGPA RMS of less than 0.5. Note, here again, the RMS indicated is subjective and specifies the minimum level of accuracy, required for any combination of sensors to fit in as possible candidates in the choice of sensors to estimate changes in implanted faults. The aim here is to ensure that at least, each sensor, present in the combination, represents one of the independent variables whose implanted fault we seek to quantify.

Table A.4.1 Order of sensitivity of dependent to independent parameter changes using an NLGPA programme and SOP as power setting parameter

POWER SETTING PARAMETER: SOP ENGINE: RR AVON (2-SHAFT)										
	→ → → → → direction of decreasing observability									
ETAC1	T3	T6	T8	T9	P6	P3	WFE	N1		
NDMC1	N1	P9								
ETAT1	N1	T9	T6	T8	WFE	P3	P6	T3	P8	
NDMT1	P6	P3	WFE	T9	T8	T3	P9	P8	T6	N1
ETAT2	WFE	T3	P3	P6	N1	T6	T9	T8	P8	
NDMT2	T8	P6	N1							

Table A.4.2 Order of sensitivity of dependent to independent parameter changes using an NLGPA programme and COT as power setting parameter

POWER SETTING PARAMETER: COT ENGINE: RR AVON (2-SHAFT)										
	→ → → → → direction of decreasing observability									
ETAC1	SOP	N1	P8	WFE	P6	P3	T9	T8	T3	

NDMC1	N1	SOP								
ETAT1	T9	SOP	T3	P8	WFE	P3	P6	N1	T8	
NDMT1	SOP	P6	P3	P8	WFE	T9	N1	T3	P9	T8
ETAT2	SOP	P8	N1	WFE	T9	P3	P6	T8	T3	
NDMT2	SOP	WFE	P3	P6	N1	T3	P9	T8	P8	T9

This approach proved useful in helping avoid situations where randomly-selected sensors do not completely represent all possible independent variables, which would be affected by a fault. Components were initially grouped into 'likes', that is to say, all compressors were put into one group and similarly all turbines were put into a

Table A.4.3 Possible instrumentation sets for isolating compressor faults in a 2-shaft engine

CASE STUDY: A							ENGINE: RR AVON (2 - SHAFT)						
POWER SETTING PARAMETER: SHP							FAULT LEVEL: FI = 1%						
DEPENDENT	1	2	3	4	5	6	7	8	9	10	11	12	13
N1	X	X	X	X	X	X	X					X	X
P2						X							X
T2	X												X
P3					X								X
T3		X						X					X
WFE							X				X		X
P4													X
T4			X						X				X
P5								X	X	X	X	X	X
T5				X						X			X
SHP													
					INDEPENDENT VARIABLES								
ETAC1	X	X	X	X	X	X	X	X	X	X	X	X	X
NDMC1	X	X	X	X	X	X	X	X	X	X	X	X	X
ETAT1													
NDMT1													
ETATPT													
NDMPT													
					RMS								
LGPA	0.767	0.652	0.629	0.621	0.724	0.730	0.575	2.213	2.124	2.122	2.086	0.978	0.678
NLGPA	0.108	0.097	0.123	0.124	0.219	0.214	0.108	0.091	0.086	0.197	0.118	1.523	0.053

separate group with various levels of fault index applied to determine suitable instrumentation sets. A fouling index (FI) of unity indicates a drop in efficiency of 1% with a simultaneous drop in flow capacity of 4% to simulate compressor fouling for

each compressor on the engine. An erosion index (EI) of unity represents a drop in efficiency of 1% and an increase in flow capacity of 2% to simulate turbine erosion for each turbine on the engine. The engine was then considered as a whole under a multi-component fault-scenario and, a search was made for suitable instrumentation sets that would enable an effective diagnosis to be achieved. Sample results from this step are presented in Tables A3.3 → A3.6 for the 2-shaft engine considered. Also presented are the RMS values obtained when a linear GPA (LGPA) and the NLGPA were sequentially used. The relation in equation (A.4.1) defines the GPA RMS sensitivity used. Its units depend on the specific parameter in use, but in this study, the independent parameter errors are expressed as percentages.

$$RMS = \sqrt{\frac{\sum_{j=1}^{n} (e_j)^2}{n}} \qquad (A.4.1)$$

Table A.4.4 Possible instrumentation sets for isolating turbine faults in a 2-shaft engine

CASE STUDY: B	POWER SETTING PARAMETER: SHP	DEPENDENT	N1	P2	T2	P3	T3	WFE	P4	T4	P5	T5	SHP	INDEPENDENT VARIABLES	ETAC1	NDMC1	ETAT1	NDMT1	ETATPT	NDMPT	RMS	LGPA	NLGPA
ENGINE: RR AVON (2 - SHAFT)	FAULT LEVEL: EI = 1%	1	X			X		X		X							X	X	X	X		0.628	0.160
		2				X		X	X	X							X	X	X	X		0.068	0.143
		3	X	X				X		X							X	X	X	X		0.630	0.401
		4	X		X			X		X							X	X	X	X		0.736	0.424
		5	X					X		X	X						X	X	X	X		0.233	0.083
		6	X					X	X	X							X	X	X	X		0.108	0.171
		7	X				X	X		X							X	X	X	X		0.862	0.126
		8		X				X	X	X							X	X	X	X		0.068	0.143
		9			X			X	X	X							X	X	X	X		0.127	0.140
		10					X	X	X	X							X	X	X	X		0.161	0.140
		11	X		X	X				X							X	X	X	X		0.939	0.195
		12	X	X		X				X							X	X	X	X		0.897	0.313
		13	X			X			X	X							X	X	X	X		0.082	0.142
		14		X		X			X	X							X	X	X	X		0.061	0.145
		15				X			X	X		X					X	X	X	X		0.060	0.146
		16			X	X			X	X							X	X	X	X		1.158	0.278
		17				X			X	X	X						X	X	X	X		0.059	0.385
		18				X	X		X	X							X	X	X	X		1.185	0.218
		19	X	X					X	X							X	X	X	X		0.083	0.142
		20	X		X				X	X							X	X	X	X		0.159	0.143
		21	X		X					X	X						X	X	X	X		0.253	0.288
		22	X	X						X	X						X	X	X	X		0.114	0.229
		23	X			X				X	X						X	X	X	X		0.110	0.290
		24	X				X			X	X						X	X	X	X		0.323	0.226
		25	X							X	X	X					X	X	X	X		0.533	0.133
		26	X				X		X	X							X	X	X	X		0.200	0.138
		27	X						X	X		X					X	X	X	X		0.217	0.138
		28		X					X	X		X					X	X	X	X		0.060	0.145
		29		X	X				X	X							X	X	X	X		9.117	1.234
		30	X	X	X	X	X	X	X	X	X	X					X	X	X	X		0.076	0.052

Table A.4.5: Possible instrumentation sets for isolating combined compressor and turbine faults in a 2-shaft engine with SOP as the power setting parameter

CASE STUDY: C

POWER SETTING PARAMETER: SHP

ENGINE: RR AVON (2 - SHAFT)

FAULT LEVEL: FI = 1% ; EI = 1% (EDI = 1%)

INDEPENDENT VARIABLES

RMS

DEPENDENT	N1	P2	T2	P3	T3	WFE	P4	T4	P5	T5	SHP	ETAC1	NDMC1	ETAT1	NDMT1	ETATPT	NDMPT	LGPA	NLGPA
1	X	X	X	X			X	X				X	X	X	X	X	X	0.416	0.014
2	X	X		X	X		X	X				X	X	X	X	X	X	0.427	0.014
3	X	X		X			X	X		X		X	X	X	X	X	X	0.320	0.019
4	X	X		X		X	X	X				X	X	X	X	X	X	0.344	0.015
5		X	X	X			X	X	X			X	X	X	X	X	X	0.617	0.075
6		X		X	X		X	X	X			X	X	X	X	X	X	0.622	0.042
7		X		X			X	X	X	X		X	X	X	X	X	X	0.554	0.086
8		X		X		X	X	X	X			X	X	X	X	X	X	0.573	0.076
9	X		X	X			X	X		X		X	X	X	X	X	X	0.406	0.013
10	X		X	X		X	X	X				X	X	X	X	X	X	0.408	0.013
11	X			X	X		X	X		X		X	X	X	X	X	X	0.412	0.011
12	X			X	X	X	X	X				X	X	X	X	X	X	0.417	0.014
13	X		X	X	X		X	X				X	X	X	X	X	X	0.409	0.015
14	X			X		X	X	X		X		X	X	X	X	X	X	0.406	0.013
15	X		X	X			X	X	X			X	X	X	X	X	X	0.635	0.251
16			X	X			X	X	X	X		X	X	X	X	X	X	0.594	0.087
17			X	X		X	X	X	X			X	X	X	X	X	X	0.602	0.077
18		X	X	X			X	X	X			X	X	X	X	X	X	0.617	0.100
19				X	X		X	X	X	X		X	X	X	X	X	X	0.597	0.086
20				X	X	X	X	X	X			X	X	X	X	X	X	0.605	0.086
21		X		X	X		X	X	X			X	X	X	X	X	X	0.622	0.103
22	X	X	X			X	X	X				X	X	X	X	X	X	0.409	0.014
23	X	X	X				X	X		X		X	X	X	X	X	X	0.407	0.013
24	X	X				X	X		X	X		X	X	X	X	X	X	0.608	0.095
25	X	X			X	X	X	X				X	X	X	X	X	X	0.418	0.016
26	X	X			X		X	X		X		X	X	X	X	X	X	0.416	0.013
27		X	X				X	X	X	X		X	X	X	X	X	X	0.593	0.073
28		X	X			X	X	X	X			X	X	X	X	X	X	0.601	0.083
29	X	X				X	X	X	X			X	X	X	X	X	X	7.913	NC
30	X	X	X	X	X	X	X	X	X	X		X	X	X	X	X	X	0.410	0.012

Important deductions from the study are now presented. Firstly, except for the last two columns on Tables A3.3 → A3.6, all the presented combinations are considered to be optima because they are able to detect, isolate and quantify the implanted faults to a high degree of accuracy, as indicated by the RMS values. Generally, the lower the RMS value, the lower the smearing effect and the better the capability of the instrumentation set employed to detect changes in the independent variables. Again, it needs to be emphasised that, the optimal instrumentation set, as used in the current analysis, involves the appropriate number, effective combination, and the optimal locations of sensors on the GT, so enabling the detection and isolation of single, dual and simultaneous multiple component faults.

Table A.4.6 Possible instrumentation sets for indicating and isolating combined compressor and turbine faults in a 2-shaft engine with COT as the power-setting parameter

CASE STUDY: D — POWER SETTING PARAMETER: COT (T3)

ENGINE: RR AVON (2- SHAFT) — FAULT LEVEL: FI = 1%; EI = 1% (EDI = 1%)

INDEPENDENT VARIABLES

RMS

DEPENDENT	N1	P2	T2	P3	T3	WFE	P4	T4	P5	T5	SHP	ETAC1	NDMC1	ETAT1	NDMT1	ETATPT	NDMPT	LGPA	NLGPA
1	X			X		X	X			X	X	X	X	X	X	X	X	0.527	0.009
2	X	X		X		X	X			X		X	X	X	X	X	X	0.549	0.004
3	X			X		X	X	X		X		X	X	X	X	X	X	0.547	0.007
4	X		X	X		X	X			X		X	X	X	X	X	X	0.548	0.007
5	X	X		X		X	X				X	X	X	X	X	X	X	0.553	0.007
6	X	X		X		X	X	X				X	X	X	X	X	X	0.654	0.238
7	X			X		X	X	X			X	X	X	X	X	X	X	0.552	0.003
8	X		X	X		X	X				X	X	X	X	X	X	X	0.553	0.007
9	X	X				X	X	X			X	X	X	X	X	X	X	0.552	0.007
10	X	X		X			X	X			X	X	X	X	X	X	X	0.549	0.007
11	X		X	X		X	X				X	X	X	X	X	X	X	0.553	0.006
12	X	X	X			X	X				X	X	X	X	X	X	X	0.553	0.006
13	X	X	X	X			X				X	X	X	X	X	X	X	0.551	0.004
14	X	X	X	X			X			X		X	X	X	X	X	X	0.548	0.007
15	X	X		X			X			X	X	X	X	X	X	X	X	0.505	0.005
16	X	X		X		X	X			X		X	X	X	X	X	X	0.549	0.005
17	X	X		X			X	X		X		X	X	X	X	X	X	0.546	0.006
18	X			X			X	X		X	X	X	X	X	X	X	X	0.508	0.007
19	X	X					X	X		X	X	X	X	X	X	X	X	0.511	0.007
20	X	X				X	X			X	X	X	X	X	X	X	X	0.528	0.007
21	X	X	X				X			X	X	X	X	X	X	X	X	0.511	0.008
22	X	X					X		X	X	X	X	X	X	X	X	X	5.305	0.013
23	X		X	X			X			X	X	X	X	X	X	X	X	0.509	0.008
24	X		X	X		X				X	X	X	X	X	X	X	X	7.865	7.603
25	X	X	X	X		X	X	X	X	X	X	X	X	X	X	X	X	0.553	0.012

In Tables A.4.1 and A.4.2, the order of relevance of measurements to independent variable changes is shown for the two power-setting parameters used. This highlights the requirements of some key measurements, such as shaft speed and fuel flow in fault diagnosis, as well as the pre-eminence of pressure and temperature measurements in flow and efficiency determination when SOP is used as the power setting parameter (Table A.4.1). The scenario is different when COT is the power-setting parameter as SOP turns out to be one of the most significant parameters for diagnostics, while temperature measurement plays a slightly lesser role except in the efficiency of the first turbine.

In Table A.4.3 or case study A, implanted compressor faults for a 2-shaft engine were used to obtain suitable instrumentation sets for the compressor-fault diagnosis. Because the engine was taken to be of fixed design, it was assumed that faults would affect the efficiencies and flow capacities of the components, thus requiring at least two

measurements to diagnose fault levels. The study initially used an FI of 1%, which represents simultaneous drops of 1% efficiency and 4% flow capacity for each compressor of the engine. Eleven possible combinations (A1 → A11) of such sensors were identified. The combination in A12 shows a choice of instrumentation set that is deficient in identifying compressor faults, though each of the sensors involved can be at least assigned to one of the independent variables. A13 shows the use of a redundant set involving all possible sensors (10 in this case) on the engine. A careful consideration of A13's RMS value, vis-à-vis those of A1 → A11, shows that not much is gained in terms of accuracy of predictions from over-instrumenting an engine. In fact, there is the danger of running at higher operational costs. The point being made here is that both a representation of each independent variable by a sensor and a careful choice of the participating sensors in the set are required for a comprehensive fault-diagnosis. Using a few sensors that are optimally selected and located could be as good as over-instrumenting the engine, but would obviously be better than the latter in terms of installation and maintenance costs. Finally, some combinations may appear unrealistic to the reader at first glance, such as A9, but our simulation shows them to be effective in quantifying compressor gas-path faults.

In Table A.4.4 or case study B, the scenario of fault diagnoses for all the turbines in the engine is presented. Initially, an EI of 1%, representing a simultaneous drop of 1% efficiency and increase of 2% flow capacity for all turbines on the engine was used. This level was gradually increased to 4% drop in efficiency, which is matched by a corresponding increase of 8% in flow capacity simultaneously for all the turbines. As in case study A, combinations B1 → B28 show different sets of instrumentation that can be used to simultaneously diagnose faults in all the turbines (two in this case) present on the 2-shaft engine. B29 shows a possible combination of sensors that is not diagnostically useful for turbine fault isolation: the reasons for this are as given in case study A. Again, the RMS value of B30 obtained from a redundant set does not justify over-instrumenting an engine.

In case study C (Table A.4.5), a combined fault scenario involving the compressor and all turbines on the engine was analysed. An EDI (engine deterioration index) of 1%, indicating a combination of FI = 1% and EI = 1%, was used initially and incremented. As before, C1→C28 are different instrumentation sets that can be used in fault diagnoses for faults that affect both the compressor and turbines simultaneously, as well as affect individual components. C29 indicates a possible combination that is not optimised for such tasks; this being portrayed by the non-convergence of the NLGPA and the high value of the LGPA. C30 shows the set involving redundant instrumentation.

In case study D (Table A.4.6), the same scenario is presented as in case study C but this time with the COT as the engine's power-setting parameter.

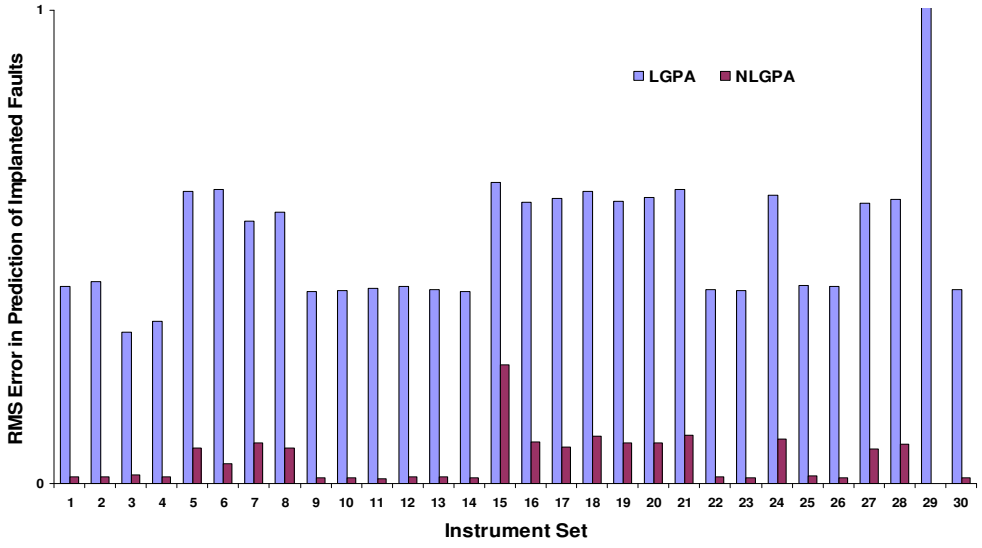

Figure A.4.1 Comparison of NLGPA and LGPA RMS values for various instrumentation choices

One major point being highlighted in this study is the improvement obtained by using NLGPA over LGPA. The successive iteration to an appropriate convergence domain

using LGPA as the first solution provides a better approach to dealing with the non-linear problem of parameter inter-relationships. Figure A.4.1, which is the bar chart format of the RMS of Table A.4.5, shows some relative benefits of the NLGPA approach. The degree of estimation accuracy involved when NLGPA is used is higher than that obtainable from LGPA, and for combinations that were deemed inappropriate such as C29. LGPA still provides an answer, though with a large RMS error, while NLGPA simply did not converge. It should be noted that the value of the RMS is indirectly proportional to the degree of optimality of the given set.

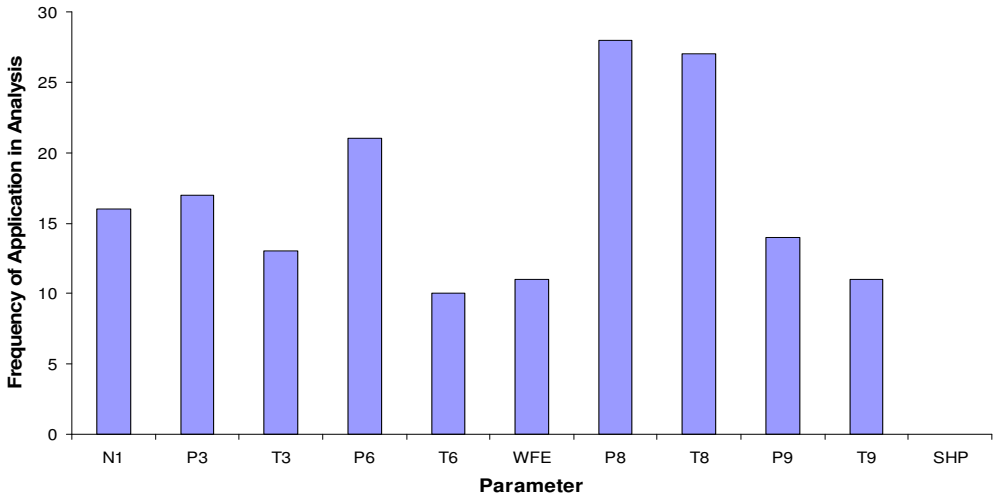

Figure A.4.2 Usage frequency of sensors for optimal instrumentation set selection for a 2-shaft engine with SOP as the power-setting parameter and faults implanted on all compressors and turbines

In the twenty-eight optimal combinations considered for the 2-shaft engine under multiple fault scenarios, with SOP as the power-setting parameter and twenty-three optimal combinations obtained with COT as the power-setting parameter, the usage frequencies of the various sensors are given in Figures A.4.2 and A.4.3. It is worthwhile to recall that, a rigorous approach was adopted to determine the selection and location of the sensors on the engine. This is because a poorly positioned or inappropriate sensor in a given set could result in high RMS values, which indicates an unwise choice. This being the case, sensors were randomly removed and others added into the set with the

program re-run until a better combination was obtained. From Figures A.4.2 and A.4.3, it is shown that some sensors, such as N1, P3, T3, P6, P8, WFE and T9, are crucial to a proper fault-diagnosis irrespective of the control parameter chosen. This assertion is made, based on the grounds that, for all the optimal instrumentation sets generated, these sensors were found repeatedly useful in the diagnostic process. On the other hand, some sensors, such as T6, T8, P9, and SOP, are power-setting parameter-dependent. This is obvious for the T6 and SOP sensors.

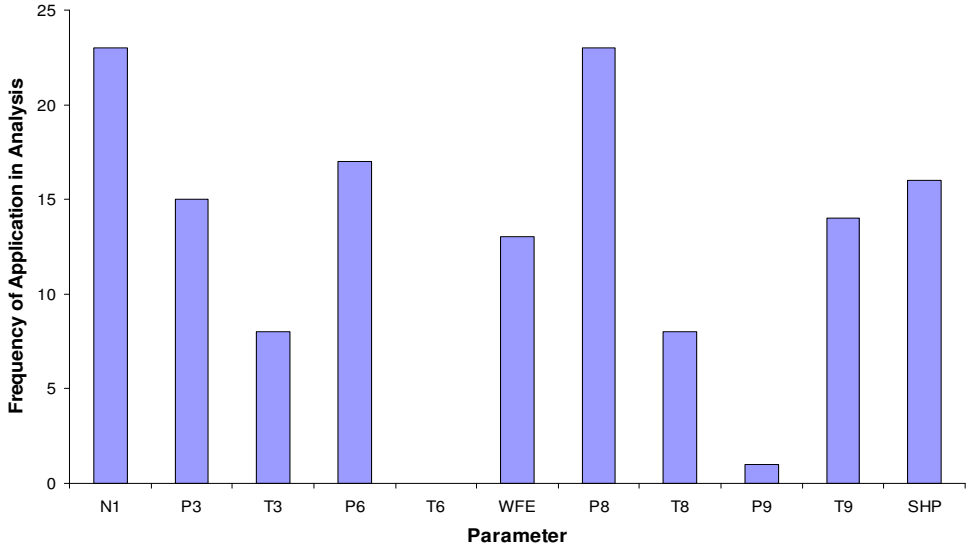

Figure A.4.3 Usage frequency of sensors for optimal instrumentation set selection for a 2-shaft engine with COT as the power-setting parameter and faults implanted on all compressors and turbines

The authors have considered various case studies and various possible combinations. This was motivated by the cost of installation and maintenance for each sensor varying according to sensor type and its location on the GT: therefore it was deemed wise to provide a wide range of possible combinations from which to choose.

In real applications, especially for industrial GTs, the available instrumentation set placed by the OEMs could be well below that recommended by this study. These

provided sets nevertheless may still be sufficient for isolating most engine faults, but in the case of simultaneous multiple-component faults, they could prove ineffective.

In conclusion, the use of the NLGPA approach to instrumentation set selection provides a significant improvement when compared with the LGPA method, because it addresses the nonlinear nature of the problem. Successive application of LGPA either diverges from or converges to an exact solution depending on the choice of instrumentation used. Finally, the results presented show that over-instrumenting the engine may not necessarily provide better diagnosis, but rather, could lead to an increase in cost arising from installation and maintenance of such redundant instruments.

APPENDIX A.5

DIAGNOSTIC GUI

Figures A.5.1 to A.5.4 demonstrate a typical application of the graphic user interface (GUI), developed to test the diagnostic process. The GUI is relatively simple and seeks to make the diagnostic process user friendly. The GUI is designed and programmed in Matlab.

In Figure A.5.1 and A4.2, the introductory GUI and the current GT engines included in this version of the programme are shown. Some of the programme's capabilities are briefly highlighted.

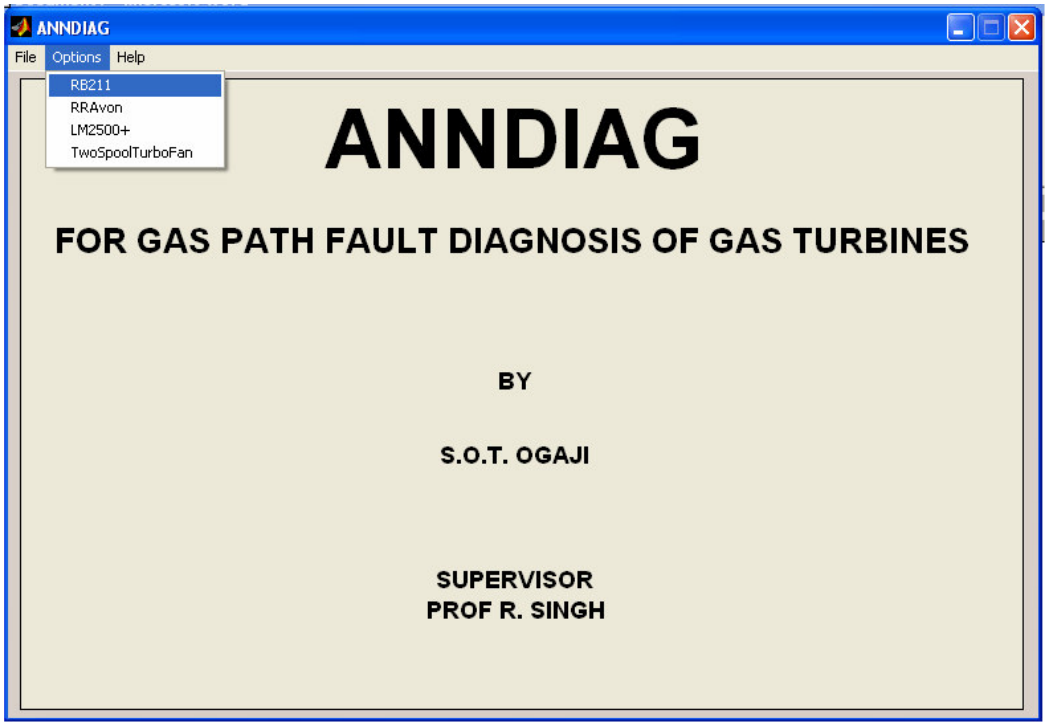

Figure A.5.1 Credits and GTs included.

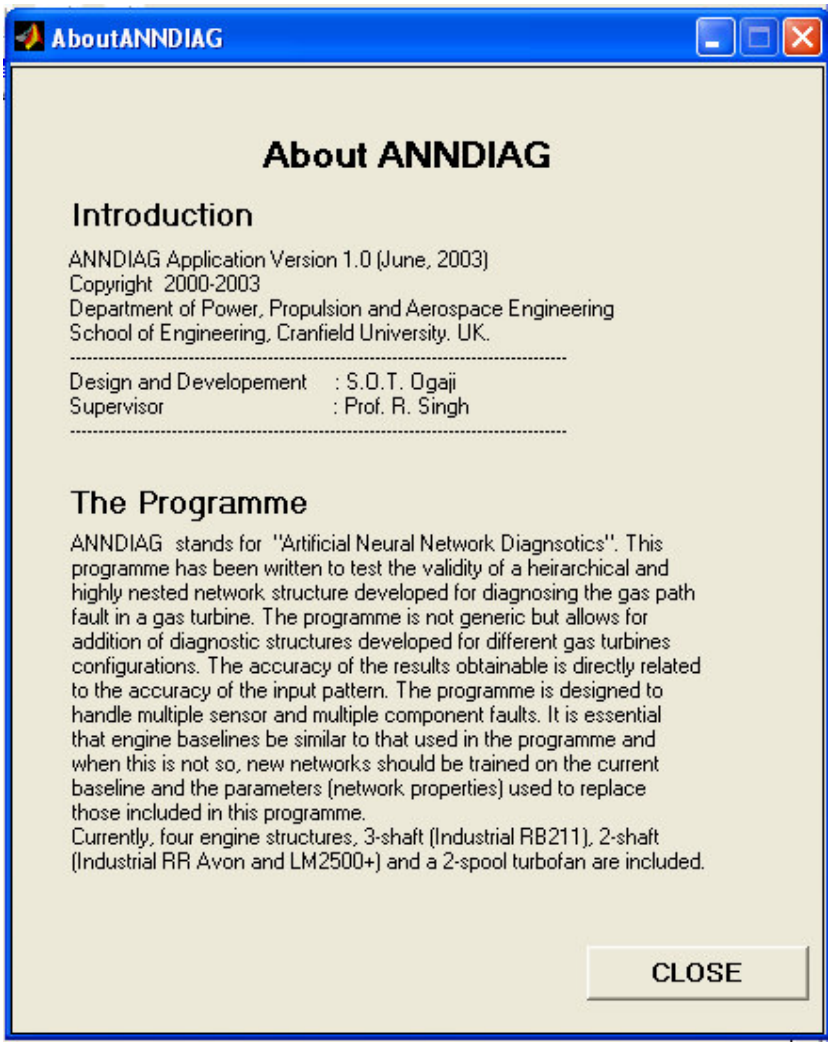

Figure A.5.2 Programme introduction.

Selecting the RB211 engine from the possible options in Figure A.5.1 provides the diagnostic interface shown in Figure A.5.3. In this interface, the operating point is set by entering in values for the ambient pressure, ambient temperature and haft output power. These values should lie within the range earlier stipulated in Table 5.9, else, an

error message is displayed. Next, the engine measurements are entered in their respective slots and the programme is run.

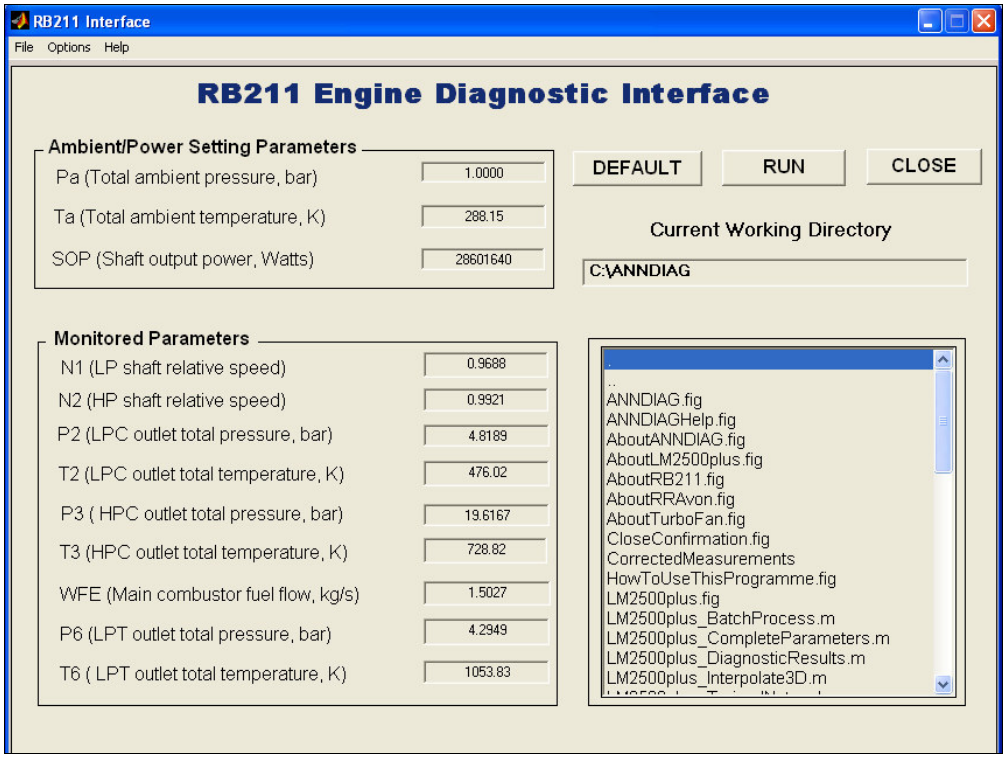

Figure A.5.3 RB211 diagnostic interface

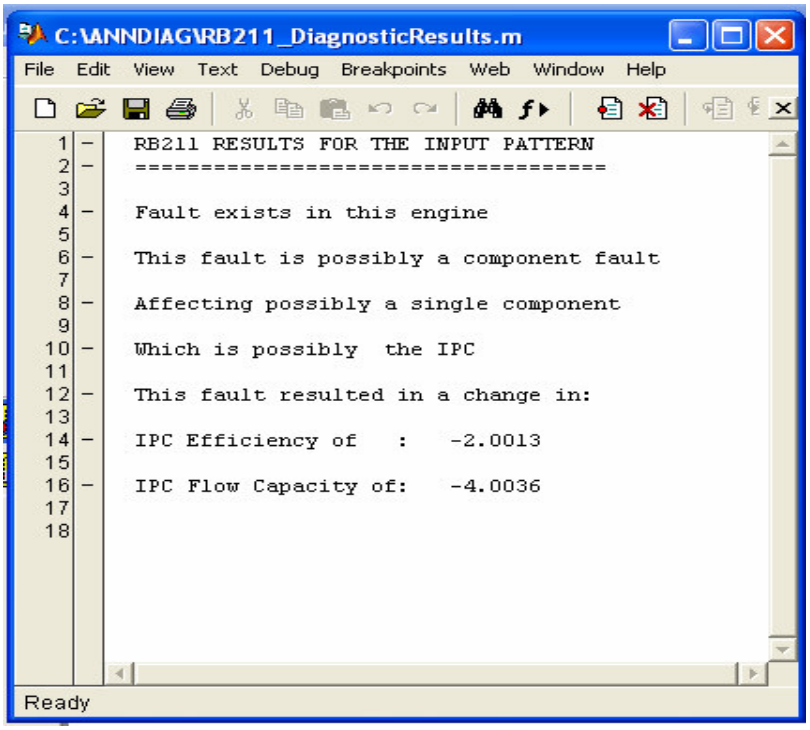

Figure A.5.4 Results from an input pattern

A typical example run on the RB211 diagnostic setup with measured pattern generated from implanting a -2%η and -4%Γ fault on the IPC produced the result shown in Figure A.5.4. The results shows the steps traversed during the programme execution. Firstly, the existence or not of a fault is ascertained, the nature of the fault –i.e. sensor or component, spelt out, the number of components affected is defined, the faulty component is identified and finally the amount of fault via the changes in efficiency and flow capacity is computed. The word "possibly" is used because diagnosis could be inexact.

APPENDIX A.6

RB211 TEST RESULTS FROM VARYING OPERATING POINTS

Faulty Component(s)	Ta (dev)	Pa (bar)	SOP (%)	Implanted faults		Isolated Components	Detected Faults	
				Efficiency (%)	Flow Capacity (%)		Efficiency (%)	Flow Capacity (%)
SINGLE COMPONENT FAULTS								
IPC	7	0.98	0.94	-3	-12	IPC	-3.5	-11.9
IPC	-7	1.01	0.86	-0.5	-2	IPC	-0.5	-1.9
HPC	7	0.98	0.94	-3	-12	HPC	-3.0	-12.2
HPC	-7	1.01	0.86	-0.5	-2	HPC	-0.5	-2.1
HPT	7	0.98	0.94	-3.0	6	HPT	-3.0	6.1
HPT	-7	1.01	0.86	-0.5	1	HPT	-0.5	0.9
LPT	7	0.98	0.94	-3.0	6	LPT	-3.0	5.8
LPT	-7	1.01	0.86	-0.5	1	LPT	-0.5	1.0
PT	7	0.98	0.94	-3.0	6	PT	-3.0	6.0

PT	-7	1.01	0.86	-0.5	1	PT	-0.5	0.9
DUAL COMPONENT FAULTS								
IPC/HPC	7	0.98	0.94	-3; -0.5	-12; -2	IPC/HPC	-3.5; -0.6	-11.7; -2.1
IPC/HPC	-7	1.01	0.86	-0.5; -3	-2; -12	HPC	-2.2	-10.4
IPC/HPT	7	0.98	0.94	-3; -0.5	-12; 1	IPC/HPT	-3.5; -0.5	-11.7; 1.1
IPC/HPT	-7	1.01	0.86	-0.5; -3	-2; 6	IPC/HPT	-0.5; -3.0	-2.0; 5.9
IPC/LPT	7	0.98	0.94	-3; -0.5	-12; 1	IPC/LPT	-3.5; -0.5	-11.5; 1.0
IPC/LPT	-7	1.01	0.86	-0.5; -3	-2; 6	IPC/HPT/LPT	-0.5; -0.5; -2.6	-1.9; -0.5; 5.6
IPC/PT	7	0.98	0.94	-3; -0.5	-12; 1	IPC/PT	-3.5; -0.5	-11.8; 1.0
IPC/PT	-7	1.01	0.86	-0.5; -3	-2; 6	PT	-0.6	3.9
HPC/HPT	7	0.98	0.94	-3; -0.5	-12; 1	HPC/HPT	-2.2; -0.8	-12.3; 1.0
HPC/HPT	-7	1.01	0.86	-0.5; -3	-2; 6	HPC/LPT/HPT	-1.3; -2.6	-2.1; 6.2
HPC/LPT	7	0.98	0.94	-3; -0.5	-12; 1	HPC/LPT	-2.9; -0.6	-12.1; 1.2
HPC/LPT	-7	1.01	0.86	-0.5; -3	-2; 6	HPC/LPT	-0.5; -0.5; -3.3	-1.8; -0.5; 6.4
HPC/PT	7	0.98	0.94	-3; -0.5	-12; 1	HPC/PT	-2.9; -0.5	-12.1; 1.0
HPC/PT	-7	1.01	0.86	-0.5; -3	-2; 6	HPC/PT	-0.5; -3.0	-1.9; 5.9
HPT/LPT	7	0.98	0.94	-3; -0.5	6; 1	HPC/HPT/LPT	-0.5; -3.2; -0.5	0.5; 6.1; 0.4

HPT/LPT	-7	1.01	0.86	-0.5; -3	1; 6	HPT/LPT	-1.1; -2.2	1.0; 5.7
HPT/PT	7	0.98	0.94	-3; -0.5	6; 1	HPT/PT	-3.0; -0.5	6.1; 1.0
HPT/PT	-7	1.01	0.86	-0.5; -3	1; 6	PT	2.9	5.8
LPT/PT	7	0.98	0.94	-3; -0.5	6; 1	IPC/LPT/PT	-0.5; -2.6; -0.5	0.5; 6.1; 1.1
LPT/PT	-7	1.01	0.86	-0.5; -3	1; 6	LPT/PT	-0.5; -3.0	1.1; 6.1
TRIPLE COMPONENT FAULTS								
IPC/HPC/HPT	7	0.98	0.94	-3; -1; 0.5	-12; -4; 1	IPC/HPC/HPT	-3.5; -1.2; -0.5	-11.2; -4.0; 1.2
IPC/HPC/HPT	-7	1.01	0.86	-1; -0.5; -3	-4; -2; 6	IPC/HPC/HPT	-1.0; -1.9; -2.1	-3.9; -2.0; 6.3
IPC/HPC/HPT	0	1.01	0.94	-0.5; -3; -1	-2; -12; 2	IPC/HPC/HPT	-0.5; -2.5; -1.3	-2.1; -11.9; 1.9
IPC/HPC/LPT	7	0.98	0.94	-3; -1; 0.5	-12; -4; 1	IPC/HPC/LPT	-3.5; -1.1; -0.5	-11.5; -3.9; 1.1
IPC/HPC/LPT	-7	1.01	0.86	-1; -0.5; -3	-4; -2; 6	IPC/HPC/LPT	-0.9; -0.6; -2.7	-3.9; -1.9; 5.8
IPC/HPC/LPT	0	1.01	0.94	-0.5; -3; -1	-2; -12; 2	IPC/HPC/LPT	-0.5; -2.4; -1.1	-2.1; -11.9; 2.4
IPC/HPC/PT	7	0.98	0.94	-3; -1; 0.5	-12; -4; 1	IPC/HPC/PT	-3.5; -0.9; -0.5	-11.7; -4.0; 1.0
IPC/HPC/PT	-7	1.01	0.86	-1; -0.5; -3	-4; -2; 6	IPC/HPC/PT	-0.7; -0.5; -2.3	-4.0; -2.2; 6.4
IPC/HPC/PT	0	1.01	0.94	-0.5; -3; -1	-2; -12; 2	IPC/HPC/PT	-0.5; -2.4; -0.8	-1.9; -12.0; 1.9
IPC/HPT/LPT	7	0.98	0.94	-3; -1; 0.5	-12; 2; 1	IPC/HPT/LPT	-3.5; -0.8; -0.8	-11.5; 2.0; 1.3
IPC/HPT/LPT	-7	1.01	0.86	-1; -0.5; -3	-4; 1; 6	IPC/HPT/LPT	-0.8; -0.8; -2.6	-3.8; 0.9; 5.7

IPC/HPT/LPT	0	1.01	0.94	-0.5; -3; -1	-2; 6; 2	IPC/HPT/LPT	-0.5; -2.4; -1.4	-2.0; 6.0; 2.6
IPC/HPT/PT	7	0.98	0.94	-3; -1; 0.5	-12; 2; 1	IPC/PT	-3.3; -0.6	-11.0; 0.33
IPC/HPT/PT	-7	1.01	0.86	-1; -0.5; -3	-4; 1; 6	IPC/HPT/PT	-1.1; -0.5; -2.8	-4.1; 1.1; 6.0
IPC/HPT/PT	0	1.01	0.94	-0.5; -3; -1	-2; 6; 2	IPC/HPT/PT	-0.5; -2.7; -0.9	-1.9; 5.8; 2.0
IPC/LPT/PT	7	0.98	0.94	-3; -1; 0.5	-12; 2; 1	IPC/LPT/PT	-3.5; -0.6; -0.5	-11.8; 2.0; 0.9
IPC/LPT/PT	-7	1.01	0.86	-1; -0.5; -3	-4; 1; 6	IPC/LPT/PT	-1.2; -0.5; -2.9	-4.0; 0.9; 6.3
IPC/LPT/PT	0	1.01	0.94	-0.5; -3; -1	-2; 6; 2	IPC/LPT/PT	-0.6; -2.4; -0.9	-1.9; 6.0; 2.1
HPC/HPT/LPT	7	0.98	0.94	-3; -1; 0.5	-12; 2; 1	HPC/HPT/LPT	-2.6; -1.0; -0.6	-12.2; 2.0; 1.1
HPC/HPT/LPT	-7	1.01	0.86	-1; -0.5; -3	-4; 1; 6	HPC/HPT/LPT	-1.1; -0.5; -3.2	-4.2; 1.1; 6.3
HPC/HPT/LPT	0	1.01	0.94	-0.5; -3; -1	-2; 6; 2	HPC/HPT/LPT	-0.6; -3.0; -1.0	-2.0; 6.1; 2.1
HPC/HPT/PT	7	0.98	0.94	-3; -1; 0.5	-12; 2; 1	HPC/HPT/PT	-3.2; -0.9; -0.5	-12.2; 2.2; 1.0
HPC/HPT/PT	-7	1.01	0.86	-1; -0.5; -3	-4; 1; 6	HPC /PT	-0.6; -3.0	-3.9; -3.9; 6.0
HPC/HPT/PT	0	1.01	0.94	-0.5; -3; -1	-2; 6; 2	HPC/HPT/PT	-0.8; -2.8; -0.9	-1.9; 6.1; 2.0
HPC/LPT/PT	7	0.98	0.94	-3; -1; 0.5	-12; 2; 1	HPC/LPT/PT	-2.5; -2.1; -0.5	-12.2; 2.3; 0.9
HPC/LPT/PT	-7	1.01	0.86	-1; -0.5; -3	-4; 1; 6	HPC/LPT/PT	-0.6; -0.6; -2.7	-3.9; 1.2; 6.2
HPC/LPT/PT	0	1.01	0.94	-0.5; -3; -1	-2; 6; 2	HPC/LPT/PT	-0.9; -2.5; -0.9	-2.1; 5.5; 2.0
HPT/LPT/PT	7	0.98	0.94	-3; -1; 0.5	6; 2; 1	HPT/LPT/PT	-2.9; -1.5; -0.5	6.1; 2.1; 0.9

HPT/LPT/PT	-7	1.01	0.86	-1; -0.5; -3	2; 1; 6	HPT/PT	-2.8; -3.5	2.5; 4.9
HPT/LPT/PT	0	1.01	0.94	-0.5; -3; -1	1; 6; 2	HPT/LPT /PT	-0.8; -2.6; -0.9	1.2; 5.7; 2.1

APPENDIX A.7

COEFFICIENT OF CORRELATION FOR APPROX NETWORKS

Table A.7.1 Coefficient of correlation for RR Avon APPROX tests.

NETWORK	CoC. Between Network Output and Target					
	Component 1		Component 2		Component 3	
APPROX1	η_C 0.9978	Γ_C 0.9999				
APPROX2	η_{CT} 0.9992	Γ_{CT} 0.9998				
APPROX3	η_{PT} 0.9984	Γ_{PT} 0.9999				
APPROX4	η_C 0.9783	Γ_C 0.9997	η_{CT} 0.9837	Γ_{CT} 0.9996		
APPROX5	η_C 0.9864	Γ_C 0.9995	η_{PT} 0.9931	Γ_{PT} 0.9994		
APPROX6	η_{CT} 0.9894	Γ_{CT} 0.9993	η_{PT} 0.9843	Γ_{PT} 0.9990		
APPROX7	η_C 0.9592	Γ_C 0.9974	η_{CT} 0.9632	Γ_{CT} 0.9951	η_{PT} 0.9481	Γ_{PT} 0.9923

Table A.7.2 Coefficient of correlation for LM2500plus APPROX tests.

NETWORK	CoC. Between Network Output and Target					
	Component 1		Component 2		Component 3	
APPROX1	η_C 0.9973	Γ_C 0.9999				
APPROX2	η_{CT} 0.9995	Γ_{CT} 0.9999				
APPROX3	η_{PT} 0.9993	Γ_{PT} 0.9999				
APPROX4	η_C 0.9770	Γ_C 0.9994	η_{CT} 0.9898	Γ_{CT} 0.9994		
APPROX5	η_C 0.9839	Γ_C 0.9995	η_{PT} 0.9944	Γ_{PT} 0.9993		
APPROX6	η_{CT} 0.9946	Γ_{CT} 0.9989	η_{PT} 0.9894	Γ_{PT} 0.9989		
APPROX7	η_C 0.9629	Γ_C 0.9977	η_{CT} 0.9791	Γ_{CT} 0.9944	η_{PT} 0.9586	Γ_{PT} 0.9945

Table A.7.3 Coefficient of correlation for RB211 APPROX tests.

NETWORK	CoC. Between Network Output and Target					
	Component 1		Component 2		Component 3	
APPROX1	η_{IPC} 0.9985	Γ_{IPC} 0.9999				
APPROX2	η_{HPC} 0.9902	Γ_{HPC} 0.9999				
APPROX3	η_{HPT} 0.9984	Γ_{HPT} 0.9996				
APPROX4	η_{LPT} 0.9991	Γ_{LPT} 0.9999				
APPROX5	η_{PT} 0.9980	Γ_{PT} 0.9999				
APPROX6	η_{IPC} 0.9970	Γ_{IPC} 0.9999	η_{HPC} 0.9960	Γ_{HPC} 0.9999		
APPROX7	η_{IPC} 0.9981	Γ_{IPC} 0.9999	η_{HPT} 0.9989	Γ_{HPT} 0.9997		
APPROX8	η_{IPC} 0.9947	Γ_{IPC} 0.9998	η_{LPT} 0.9989	Γ_{LPT} 0.9999		
APPROX9	η_{IPC} 0.9985	Γ_{IPC} 0.9999	η_{PT} 0.9991	Γ_{PT} 0.9999		
APPROX10	η_{HPC} 0.9641	Γ_{HPC} 0.9997	η_{HPT} 0.9855	Γ_{HPT} 0.9993		
APPROX11	η_{HPC} 0.9844	Γ_{HPC} 0.9998	η_{LPT} 0.9899	Γ_{LPT} 0.9990		
APPROX12	η_{HPC} 0.9973	Γ_{HPC} 0.9999	η_{PT} 0.9994	Γ_{PT} 0.9999		
APPROX13	η_{HPT} 0.9768	Γ_{HPT} 0.9996	η_{LPT} 0.9766	Γ_{LPT} 0.9979		
APPROX14	η_{HPT} 0.9988	Γ_{HPT} 0.9997	η_{PT} 0.9995	Γ_{PT} 0.9999		
APPROX15	η_{LPT} 0.9875	Γ_{LPT} 0.9999	η_{PT} 0.9977	Γ_{PT} 0.9998		

APPROX16	η_{IPC} 0.9910	Γ_{IPC} 0.9994	η_{HPC} 0.8933	Γ_{HPC} 0.9995	η_{HPT} 0.9081	Γ_{HPT} 0.9982
APPROX17	η_{IPC} 0.9683	Γ_{IPC} 0.9996	η_{HPC} 0.8987	Γ_{HPC} 0.9994	η_{LPT} 0.9434	Γ_{LPT} 0.9958
APPROX18	η_{IPC} 0.9794	Γ_{IPC} 0.9994	η_{HPC} 0.9296	Γ_{HPC} 0.9992	η_{PT} 0.9689	Γ_{PT} 0.9992
APPROX19	η_{IPC} 0.9739	Γ_{IPC} 0.9995	η_{HPT} 0.9495	Γ_{HPT} 0.9993	η_{LPT} 0.9422	Γ_{LPT} 0.9952
APPROX20	η_{IPC} 0.9720	Γ_{IPC} 0.9996	η_{HPT} 0.9912	Γ_{HPT} 0.9990	η_{PT} 0.9936	Γ_{PT} 0.9993
APPROX21	η_{IPC} 0.9225	Γ_{IPC} 0.9996	η_{LPT} 0.9677	Γ_{LPT} 0.9996	η_{PT} 0.9927	Γ_{PT} 0.9994
APPROX22	η_{HPC} 0.9361	Γ_{HPC} 0.9995	η_{HPT} 0.9656	Γ_{HPT} 0.9990	η_{LPT} 0.9624	Γ_{LPT} 0.9968
APPROX23	η_{HPC} 0.7845	Γ_{HPC} 0.9998	η_{HPT} 0.9529	Γ_{HPT} 0.9988	η_{PT} 0.9912	Γ_{PT} 0.9998
APPROX24	η_{HPC} 0.8983	Γ_{HPC} 0.9996	η_{LPT} 0.9539	Γ_{LPT} 0.9952	η_{PT} 0.9837	Γ_{PT} 0.9993
APPROX25	η_{HPT} 0.9437	Γ_{HPT} 0.9985	η_{LPT} 0.9177	Γ_{LPT} 0.9934	η_{PT} 0.9796	Γ_{PT} 0.9991

Table A.7.4 Coefficient of correlation for Turbofan APPROX tests.

NETWORK	**CoC. Between Network Output and Target**			
	Component 1		**Component 2**	
APPROX1	η_{IPC} 0.9999	Γ_{IPC} 1.0000		
APPROX2	η_{HPC} 0.9991	Γ_{HPC} 0.9998		
APPROX3	η_{HPT} 0.9997	Γ_{HPT} 0.9998		
APPROX4	η_{LPT} 0.9999	Γ_{LPT} 1.0000		
APPROX5	η_{IPC} 0.9620	Γ_{IPC} 0.9970	η_{HPC} 0.9970	Γ_{HPC} 0.9986
APPROX6	η_{IPC} 0.9769	Γ_{IPC} 0.9871	η_{HPT} 0.9957	Γ_{HPT} 0.9986
APPROX7	η_{IPC} 0.9933	Γ_{IPC} 0.9988	η_{LPT} 0.9985	Γ_{LPT} 0.9996

APPROX8	η_{HPC} 0.9860	Γ_{HPC} 0.9984	η_{HPT} 0.9857	Γ_{HPT} 0.9977
APPROX9	η_{HPC} 0.9914	Γ_{HPC} 0.9987	η_{LPT} 0.9660	Γ_{LPT} 0.9986
APPROX10	η_{HPT} 0.9928	Γ_{HPT} 0.9984	η_{LPT} 0.9880	Γ_{LPT} 0.9985

APPENDIX A.8

PERCENTAGE RELATIVE ERROR OF APPROX NETWORKS

A.8.1 RR Avon APPROX Networks Error Distribution

APPROX1

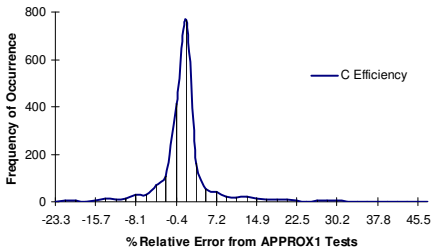

Figure A.8.1a Distribution of relative error from APPROX1 prediction of C. efficiency

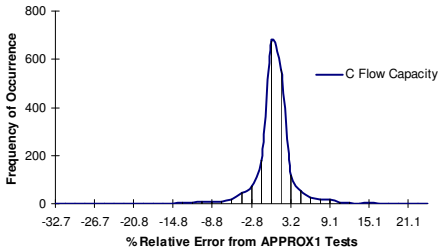

Figure A.8.1b Distribution of relative error from APPROX1 prediction of C. flow capacity

APPROX2

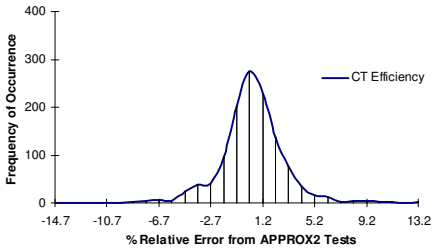

Figure A.8.2a Distribution of relative error from APPROX2 prediction of CT. efficiency

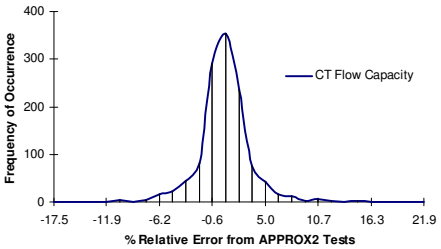

Figure A.8.2b Distribution of relative error from APPROX2 prediction of CT. flow capacity

APPROX3

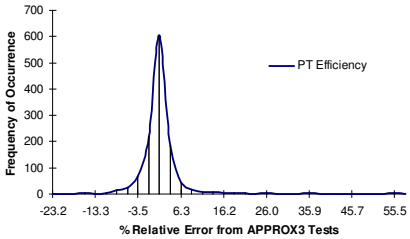

Figure A.8.3a Distribution of relative error from APPROX3 prediction of PT. efficiency

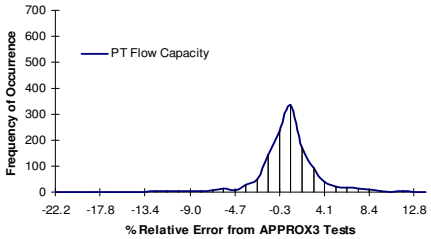

Figure A.8.3b Distribution of relative error from APPROX3 prediction of PT. flow capacity

APPROX4

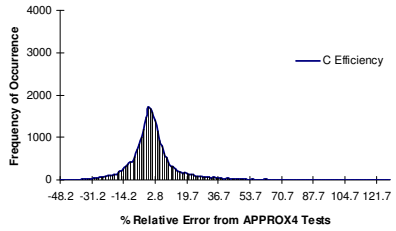

Figure A.8.4a Distribution of relative error from APPROX4 prediction of C. efficiency

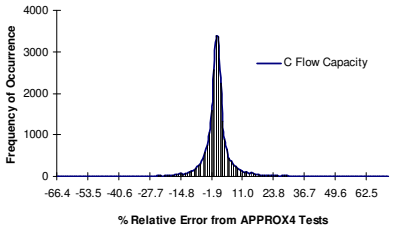

Figure A.8.4b Distribution of relative error from APPROX4 prediction of C. flow capacity

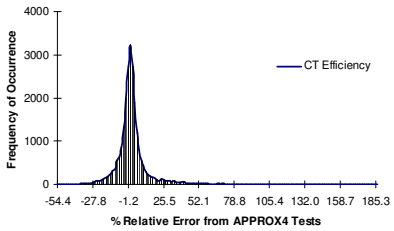

Figure A.8.4c Distribution of relative error from APPROX4 prediction of CT. efficiency

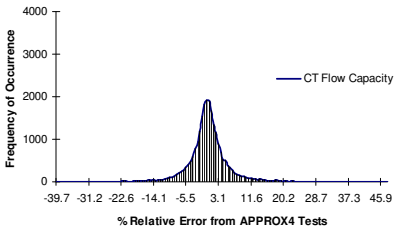

Figure A.8.4d Distribution of relative error from APPROX4 prediction of CT. flow capacity

APPROX5

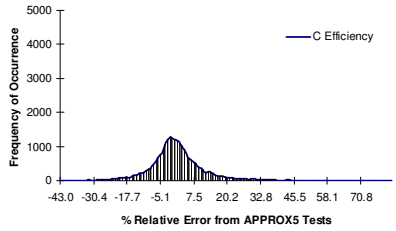

Figure A.8.5a Distribution of relative error from APPROX5 prediction of C. efficiency

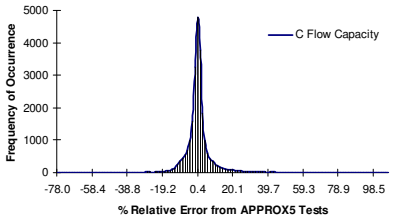

Figure A.8.5b Distribution of relative error from APPROX5 prediction of C. flow capacity

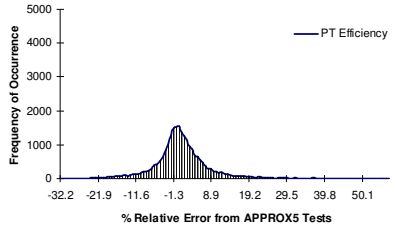

Figure A.8.5c Distribution of relative error from APPROX5 prediction of PT. efficiency

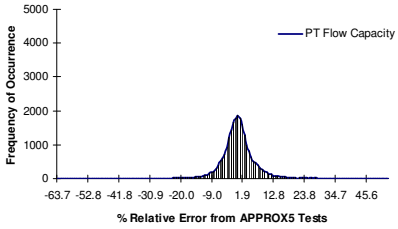

Figure A.8.5d Distribution of relative error from APPROX5 prediction of PT. flow capacity

APPROX6

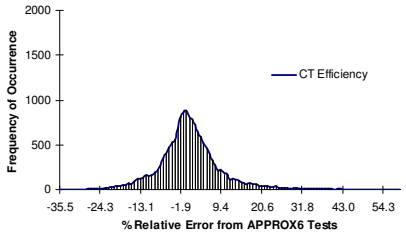

Figure A.8.6a Distribution of relative error from APPROX6 prediction of CT. efficiency

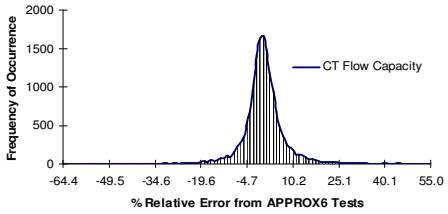

Figure A.8.6b Distribution of relative error from APPROX6 prediction of CT. flow capacity

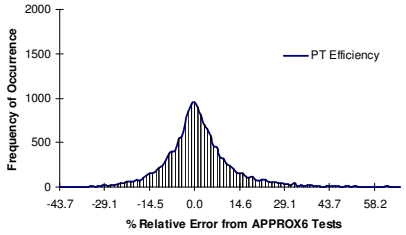

Figure A.8.6c Distribution of relative error from APPROX6 prediction of PT. efficiency

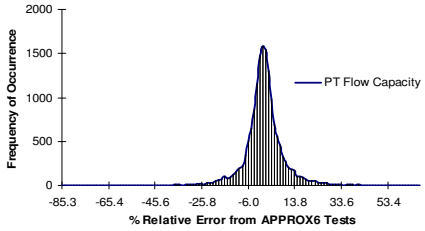

Figure A.8.6d Distribution of relative error from APPROX6 prediction of PT. flow capacity

APPROX7

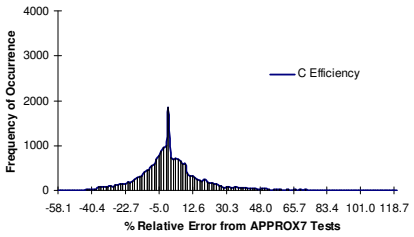

Figure A.8.7a Distribution of relative error from APPROX7 prediction of C. efficiency

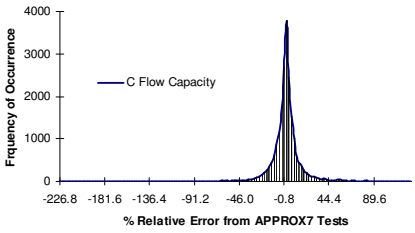

Figure A.8.7b Distribution of relative error from APPROX7 prediction of C. flow capacity

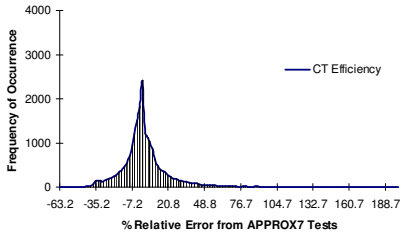

Figure A.8.7c Distribution of relative error from APPROX7 prediction of CT. efficiency

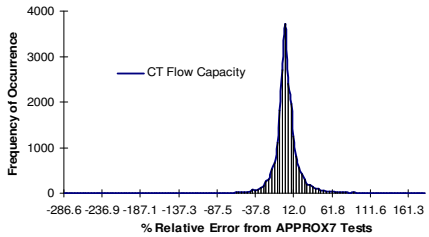

Figure A.8.7d Distribution of relative error from APPROX7 prediction of CT. flow capacity

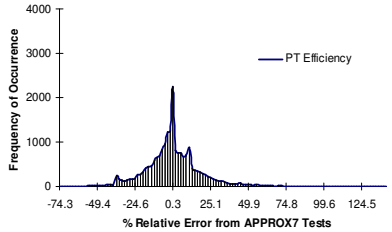

Figure A.8.7e Distribution of relative error from APPROX7 prediction of PT. efficiency

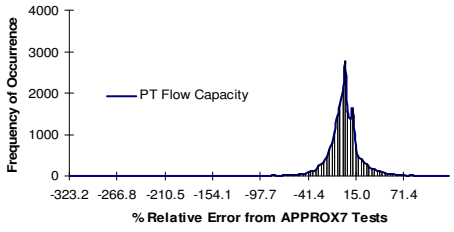

Figure A.8.7f Distribution of relative error from APPROX7 prediction of PT. flow capacity

A.8.2 LM2500+ APPROX Networks Error Distribution

APPROX1

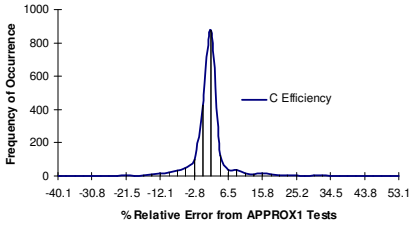

Figure A.8.8a Distribution of relative error from APPROX1 prediction of C. efficiency

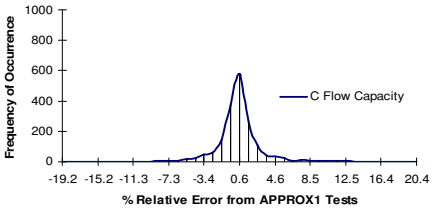

Figure A.8.8b Distribution of relative error from APPROX1 prediction of C. flow capacity

APPROX2

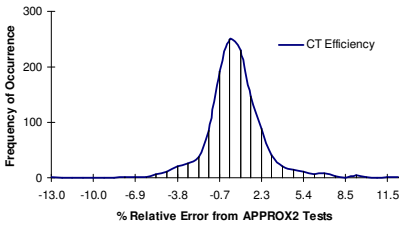

Figure A.8.9a Distribution of relative error from APPROX2 prediction of CT. efficiency

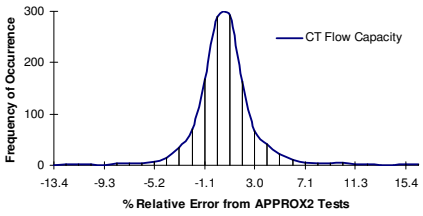

Figure A.8.9b Distribution of relative error from APPROX2 prediction of CT. flow capacity

APPROX3

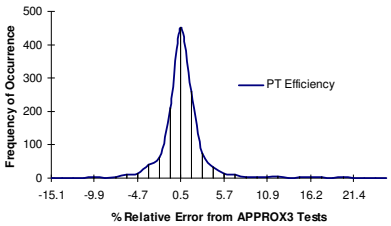

Figure A.8.10a Distribution of relative error from APPROX3 prediction of PT. efficiency

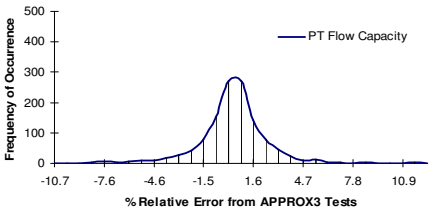

Figure A.8.10b Distribution of relative error from APPROX3 prediction of PT. flow capacity

APPROX4

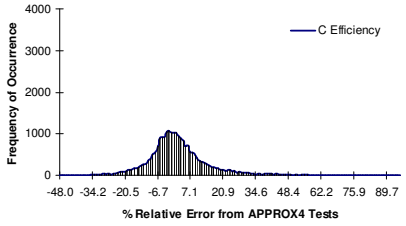

Figure A.8.11a Distribution of relative error from APPROX4 prediction of C. efficiency

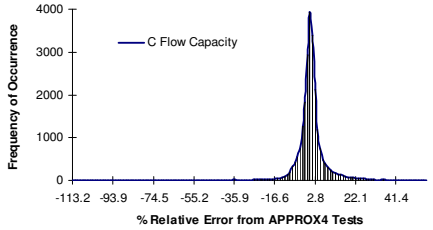

Figure A.8.11b Distribution of relative error from APPROX4 prediction of C. flow capacity

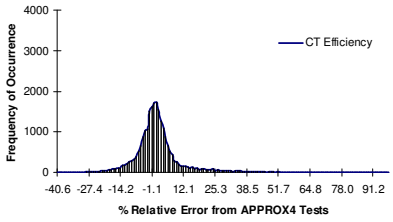

Figure A.8.11c Distribution of relative error from APPROX4 prediction of CT. efficiency

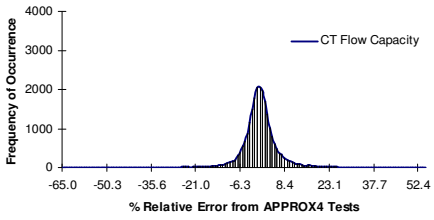

Figure A.8.11d Distribution of relative error from APPROX4 prediction of CT. flow capacity

APPROX5

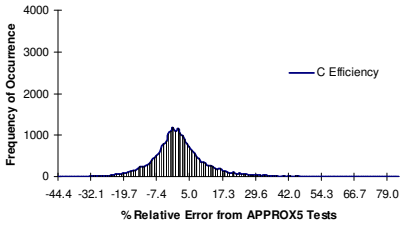

Figure A.8.12a Distribution of relative error from APPROX5 prediction of C. efficiency

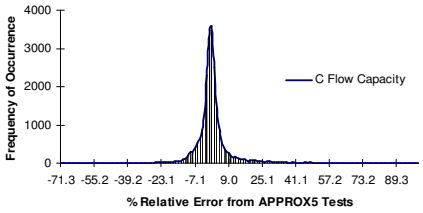

Figure A.8.12b Distribution of relative error from APPROX5 prediction of C. flow capacity

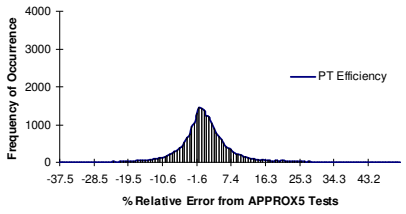

Figure A.8.12c Distribution of relative error from APPROX5 prediction of PT. efficiency

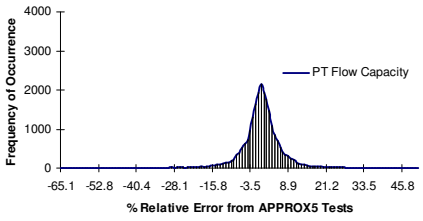

Figure A.8.12d Distribution of relative error from APPROX5 prediction of PT. flow capacity

APPROX6

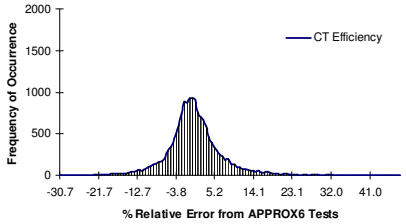

Figure A.8.13a Distribution of relative error from APPROX6 prediction of CT. efficiency

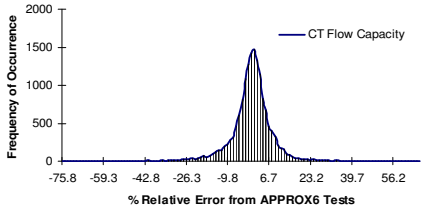

Figure A.8.13b Distribution of relative error from APPROX6 prediction of CT. flow capacity

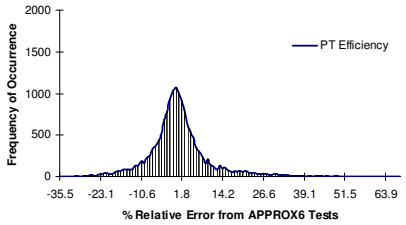

Figure A.8.13c Distribution of relative error from APPROX6 prediction of PT. efficiency

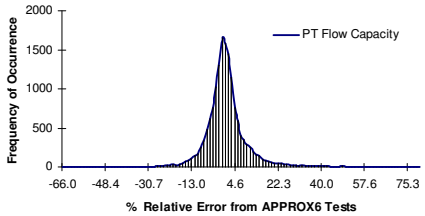

Figure A.8.13d Distribution of relative error from APPROX6 prediction of PT. flow capacity

APPROX7

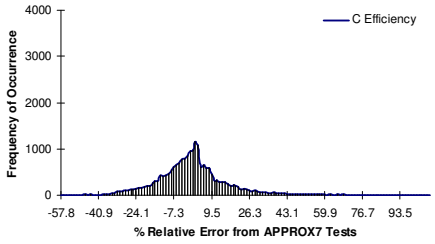

Figure A.8.14a Distribution of relative error from APPROX7 prediction of C. efficiency

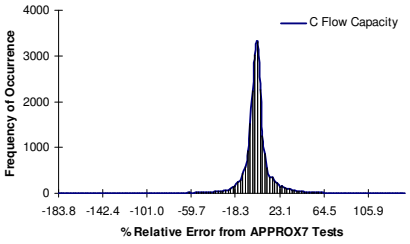

Figure A.8.14b Distribution of relative error from APPROX7 prediction of C. flow capacity

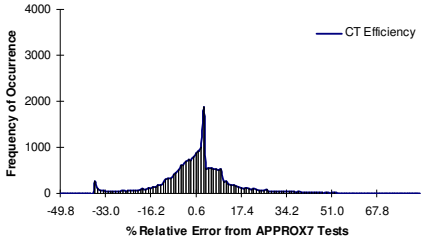

Figure A.8.14c Distribution of relative error from APPROX7 prediction of CT. efficiency

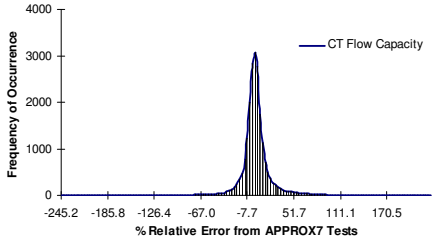

Figure A.8.14d Distribution of relative error from APPROX7 prediction of CT. flow capacity

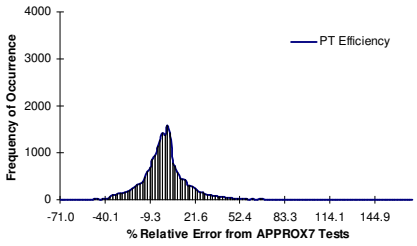

Figure A.8.14e Distribution of relative error from APPROX7 prediction of PT efficiency

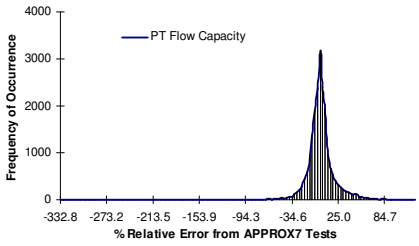

Figure A.8.14f Distribution of relative error from APPROX7 prediction of PT flow capacity

A.8.3 RB211 APPROX Networks Error Distribution

APPROX1

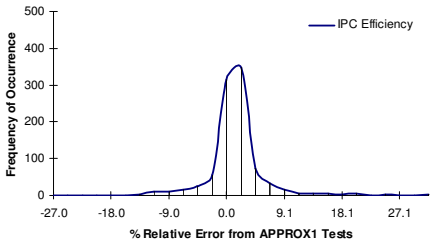

Figure A.8.15a Distribution of relative error from APPROX1 prediction of IPC efficiency

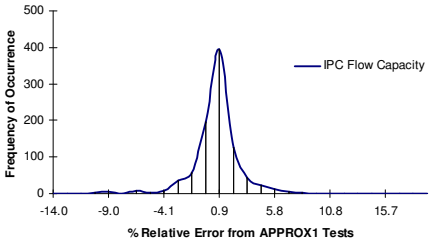

Figure A.8.15b Distribution of relative error from APPROX1 prediction of IPC flow capacity

APPROX2

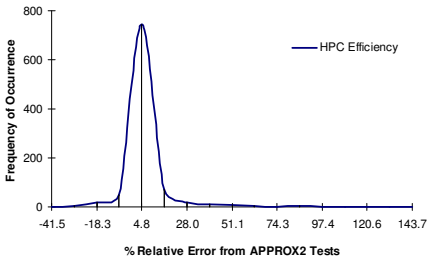

Figure A.8.16a Distribution of relative error from APPROX2 prediction of HPC efficiency

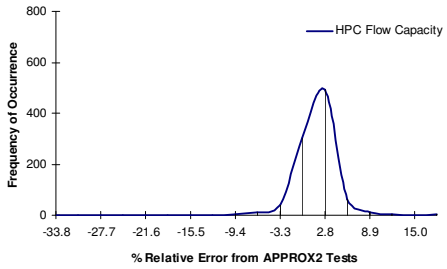

Figure A.8.16b Distribution of relative error from APPROX2 prediction of HPC flow capacity

APPROX3

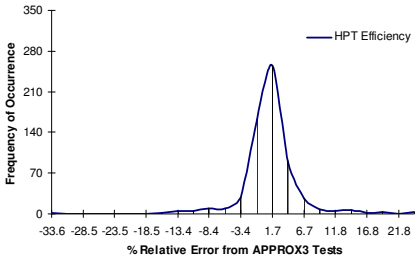

Figure A.8.17a Distribution of relative error from APPROX3 prediction of HPT efficiency

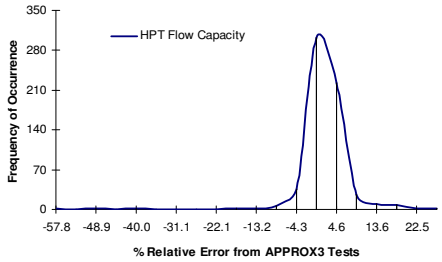

Figure A.8.17b Distribution of relative error from APPROX3 prediction of HPT flow capacity

APPROX4

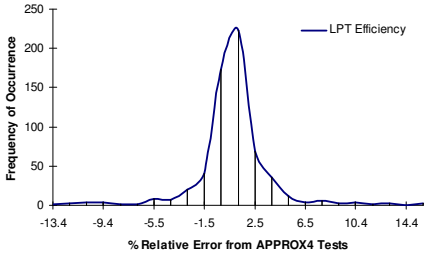

Figure A.8.18a Distribution of relative error from APPROX4 prediction of LPT. efficiency

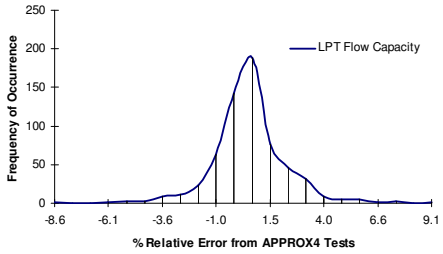

Figure A.8.18b Distribution of relative error from APPROX4 prediction of LPT flow capacity

APPROX5

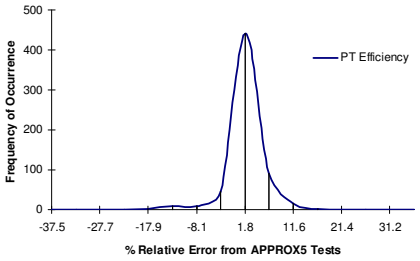

Figure A.8.19a Distribution of relative error from APPROX5 prediction of PT efficiency

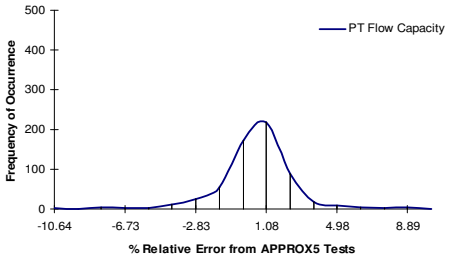

Figure A.8.19b Distribution of relative error from APPROX5 prediction of PT flow capacity

APPROX6

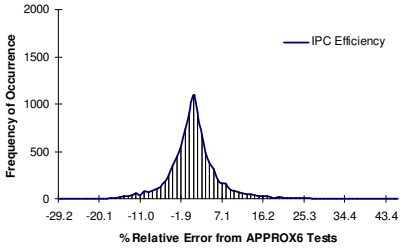

Figure A.8.20a Distribution of relative error from APPROX6 prediction of IPC efficiency

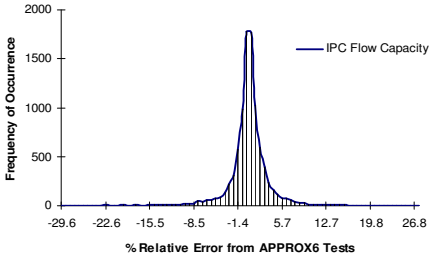

Figure A.8.20b Distribution of relative error from APPROX6 prediction of IPC flow capacity

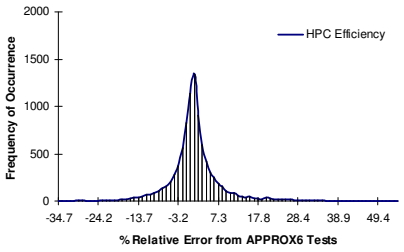

Figure A.8.20c Distribution of relative error from APPROX6 prediction of HPC efficiency

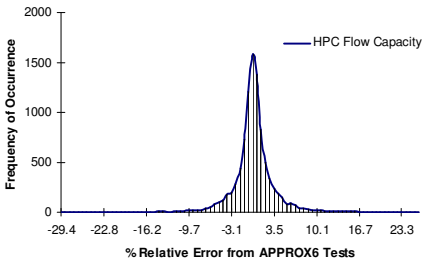

Figure A.8.20d Distribution of relative error from APPROX6 prediction of HPC flow capacity

APPROX7

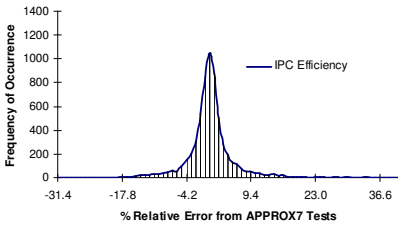

Figure A.8.21a Distribution of relative error from APPROX7 prediction of IPC efficiency

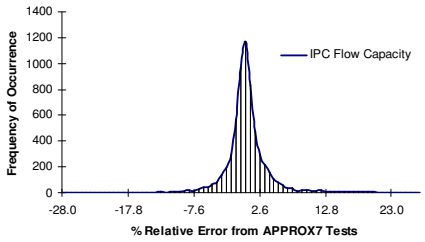

Figure A.8.21b Distribution of relative error from APPROX7 prediction of IPC flow capacity

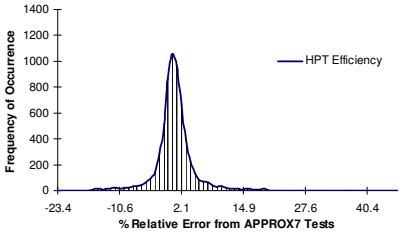

Figure A.8.21c Distribution of relative error from APPROX7 prediction of HPT efficiency

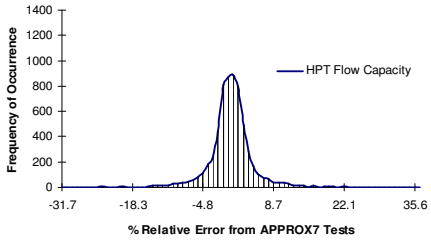

Figure A.8.21d Distribution of relative error from APPROX7 prediction of HPT flow capacity

APPROX8

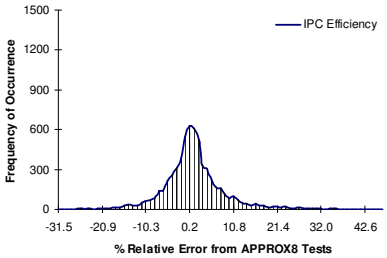

Figure A.8.22a Distribution of relative error from APPROX8 prediction of IPC efficiency

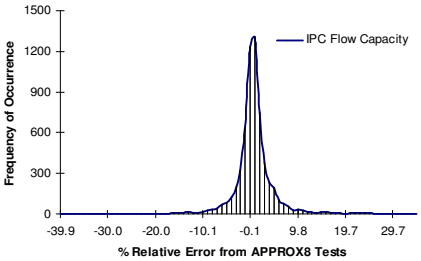

Figure A.8.22b Distribution of relative error from APPROX8 prediction of IPC flow capacity

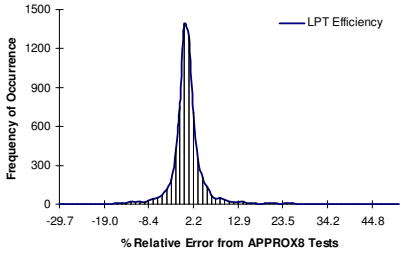

Figure A.8.22c Distribution of relative error from APPROX8 prediction of LPT efficiency

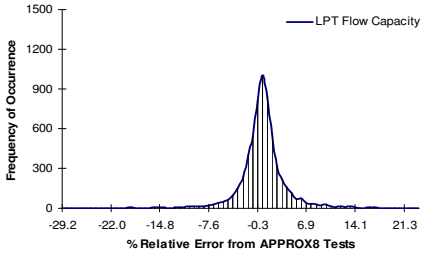

Figure A.8.22d Distribution of relative error from APPROX8 prediction of LPT flow capacity

APPROX9

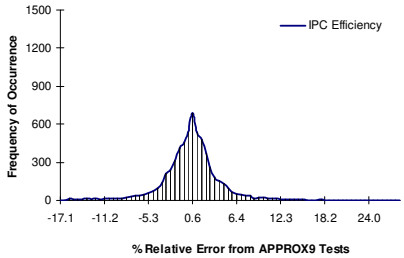

Figure A.8.23a Distribution of relative error from APPROX9 prediction of IPC efficiency

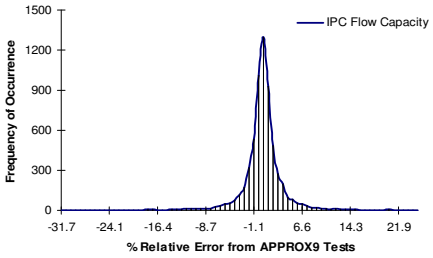

Figure A.8.23b Distribution of relative error from APPROX9 prediction of IPC flow capacity

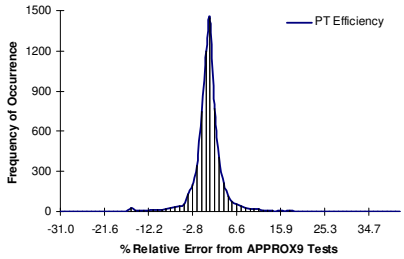

Figure A.8.23c Distribution of relative error from APPROX9 prediction of PT efficiency

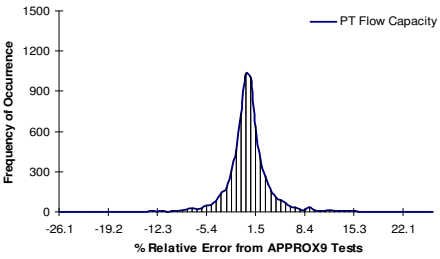

Figure A.8.23d Distribution of relative error from APPROX9 prediction of PT flow capacity

APPROX10

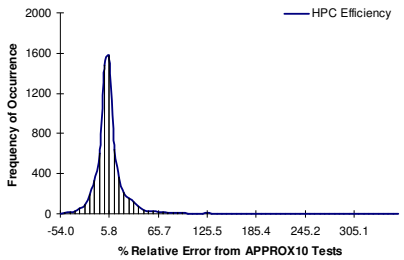

Figure A.8.24a Distribution of relative error from APPROX10 prediction of HPC efficiency

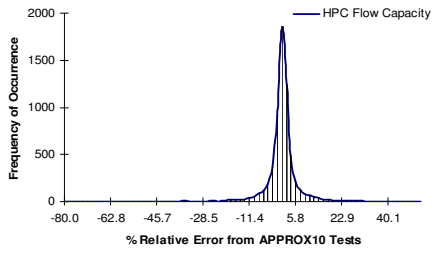

Figure A.8.24b Distribution of relative error from APPROX10 prediction of HPC flow capacity

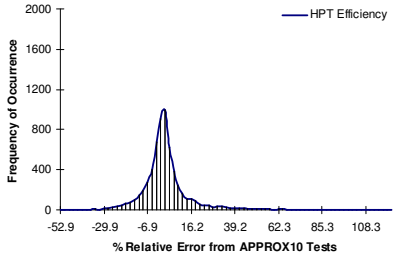

Figure A.8.24c Distribution of relative error from APPROX10 prediction of HPT efficiency

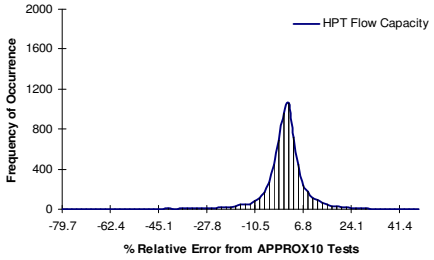

Figure A.8.24d Distribution of relative error from APPROX10 prediction of HPT flow capacity

APPROX11

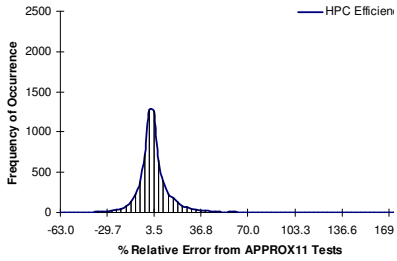

Figure A.8.25a Distribution of relative error from APPROX11 prediction of HPC efficiency

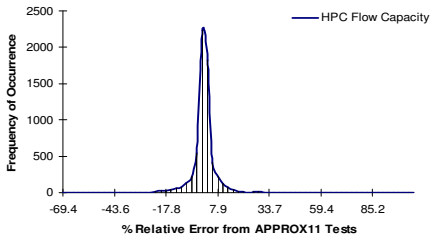

Figure A.8.25b Distribution of relative error from APPROX11 prediction of HPC flow capacity

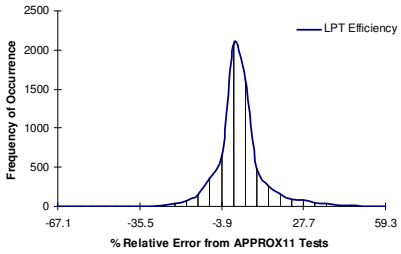

Figure A.8.25c Distribution of relative error from APPROX11 prediction of LPT efficiency

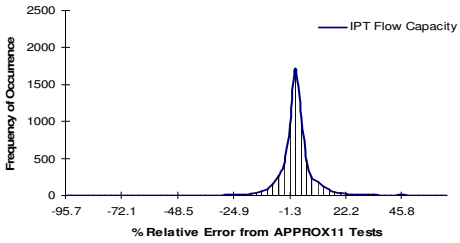

Figure A.8.25d Distribution of relative error from APPROX11 prediction of LPT flow capacity

APPROX12

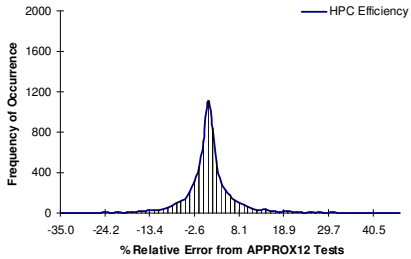

Figure A.8.26a Distribution of relative error from APPROX12 prediction of HPC efficiency

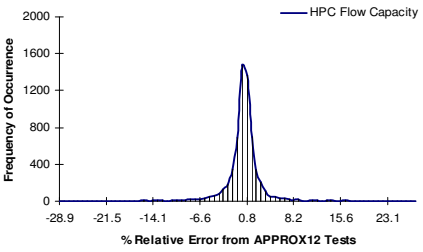

Figure A.8.26b Distribution of relative error from APPROX12 prediction of HPC flow capacity

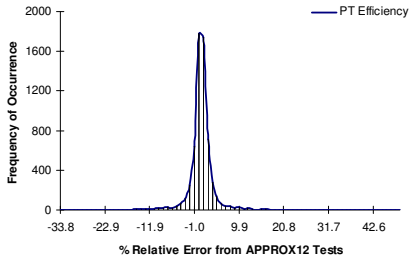

Figure A.8.26c Distribution of relative error from APPROX12 prediction of PT efficiency

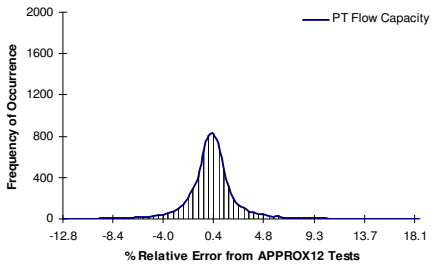

Figure A.8.26d Distribution of relative error from APPROX12 prediction of PT flow capacity

APPROX13

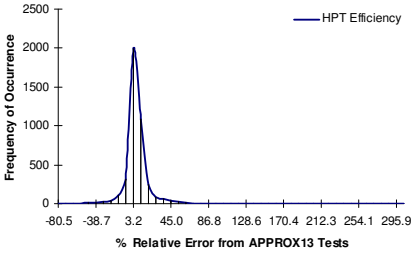

Figure A.8.27a Distribution of relative error from APPROX13 prediction of HPT efficiency

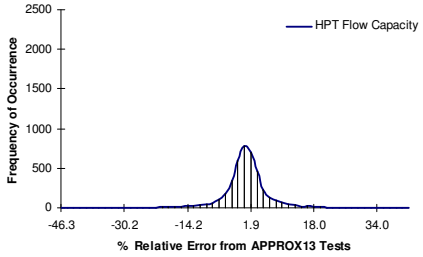

Figure A.8.27b Distribution of relative error from APPROX13 prediction of HPT flow capacity

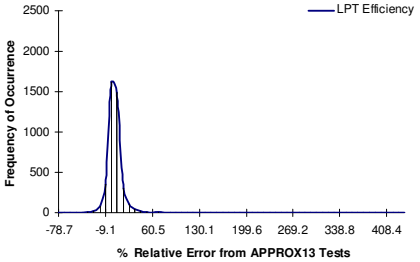

Figure A.8.27c Distribution of relative error from APPROX13 prediction of LPT efficiency

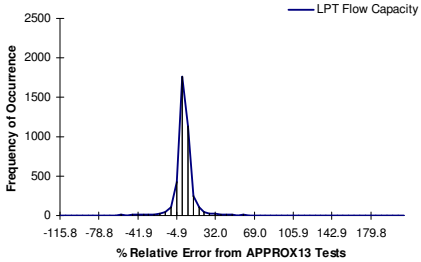

Figure A.8.27d Distribution of relative error from APPROX13 prediction of LPT flow capacity

APPROX14

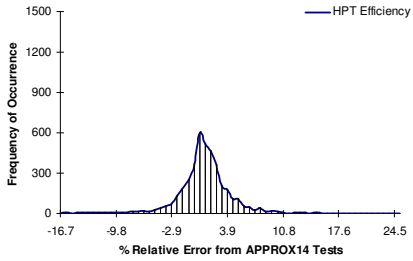

Figure A.8.28a Distribution of relative error from APPROX14 prediction of HPT efficiency

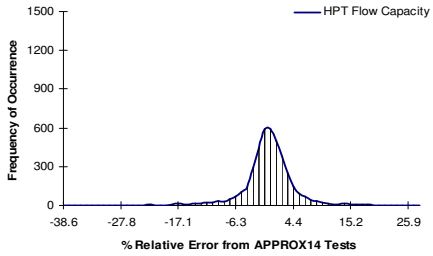

Figure A.8.28b Distribution of relative error from APPROX14 prediction of HPT flow capacity

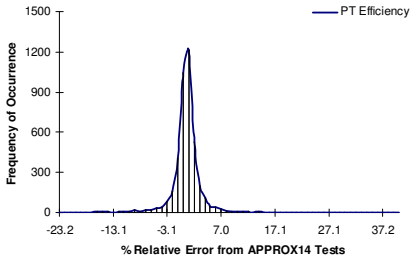

Figure A.8.28c Distribution of relative error from APPROX14 prediction of PT efficiency

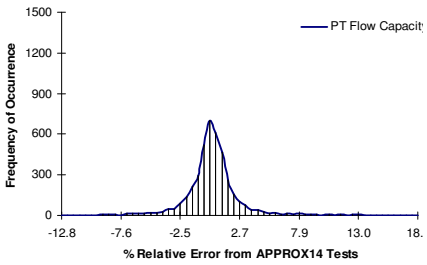

Figure A.8.28d Distribution of relative error from APPROX14 prediction of PT flow capacity

APPROX15

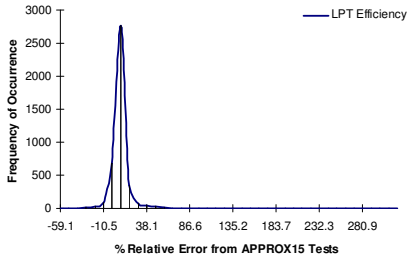

Figure A.8.29a Distribution of relative error from APPROX15 prediction of LPT efficiency

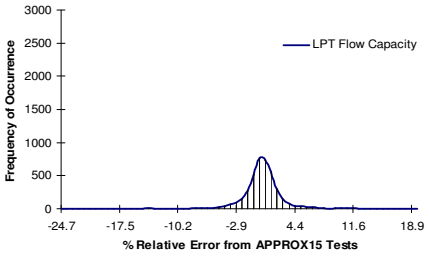

Figure A.8.29b Distribution of relative error from APPROX15 prediction of LPT flow capacity

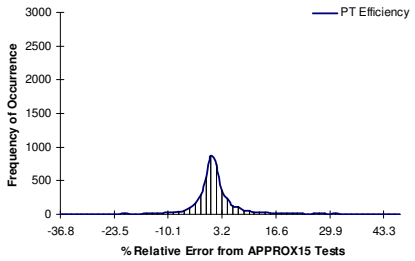

Figure A.8.29c Distribution of relative error from APPROX15 prediction of PT efficiency

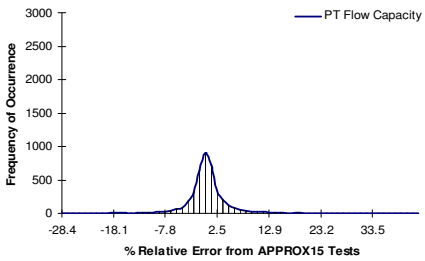

Figure A.8.29d Distribution of relative error from APPROX15 prediction of PT flow capacity

APPROX16

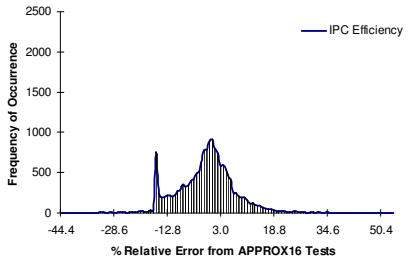

Figure A.8.30a Distribution of relative error from APPROX16 prediction of IPC efficiency

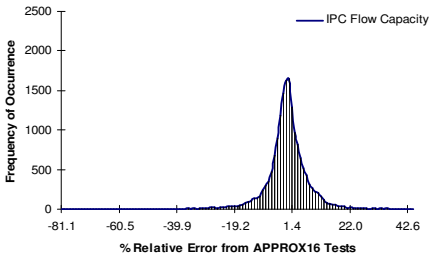

Figure A.8.30b Distribution of relative error from APPROX16 prediction of IPC flow capacity

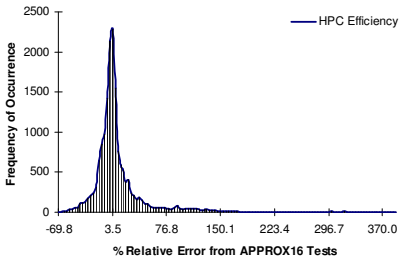

Figure A.8.30c Distribution of relative error from APPROX16 prediction of HPC efficiency

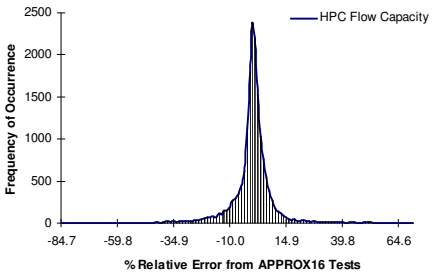

Figure A.8.30d Distribution of relative error from APPROX16 prediction of HPC flow capacity

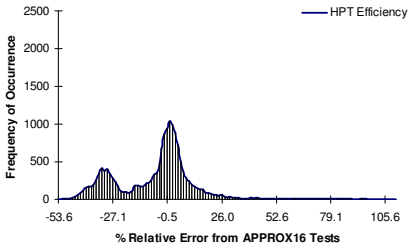

Figure A.8.30e Distribution of relative error from APPROX16 prediction of HPT efficiency

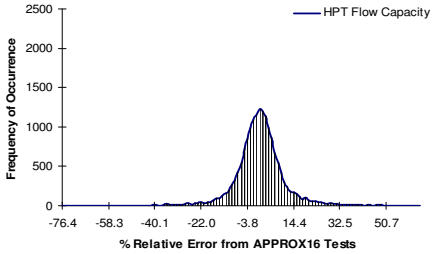

Figure A.8.30f Distribution of relative error from APPROX16 prediction of HPT flow capacity

APPROX17

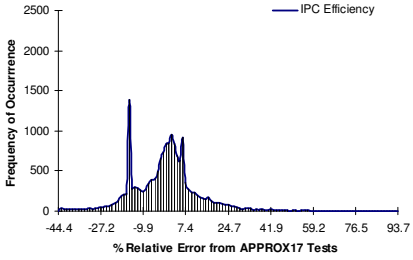

Figure A.8.31a Distribution of relative error from APPROX17 prediction of IPC efficiency

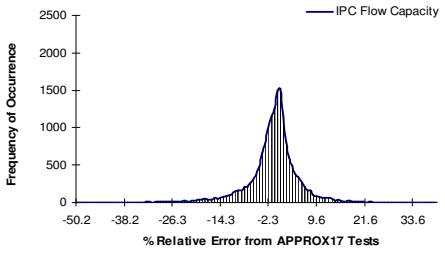

Figure A.8.31b Distribution of relative error from APPROX17 prediction of IPC flow capacity

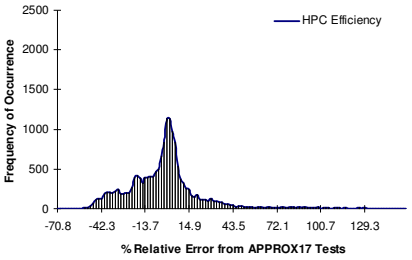

Figure A.8.31c Distribution of relative error from APPROX17 prediction of HPC efficiency

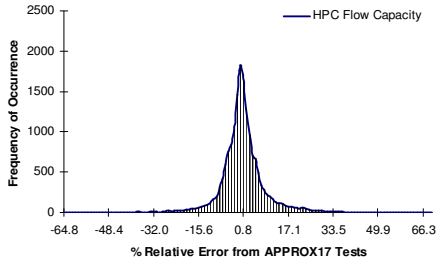

Figure A.8.31d Distribution of relative error from APPROX17 prediction of HPC flow capacity

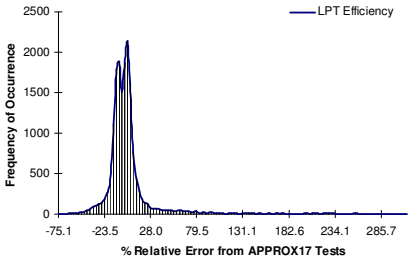

Figure A.8.31e Distribution of relative error from APPROX17 prediction of LPT efficiency

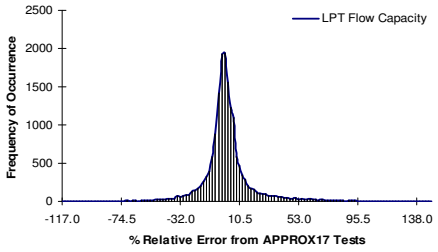

Figure A.8.31f Distribution of relative error from APPROX17 prediction of LPT flow capacity

APPROX18

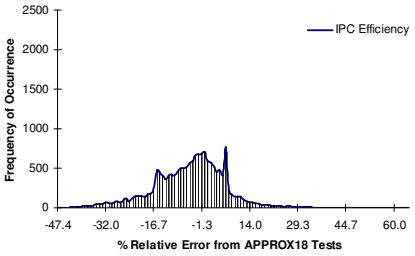

Figure A.8.32a Distribution of relative error from APPROX18 prediction of IPC efficiency

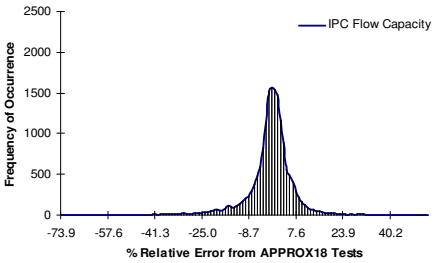

Figure A.8.32b Distribution of relative error from APPROX18 prediction of IPC flow capacity

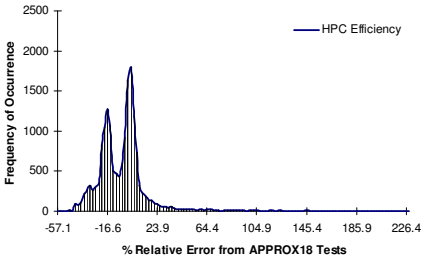

Figure A.8.32c Distribution of relative error from APPROX18 prediction of HPC efficiency

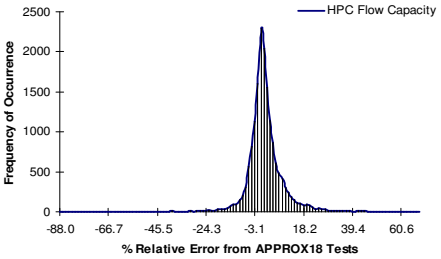

Figure A.8.32d Distribution of relative error from APPROX18 prediction of HPC flow capacity

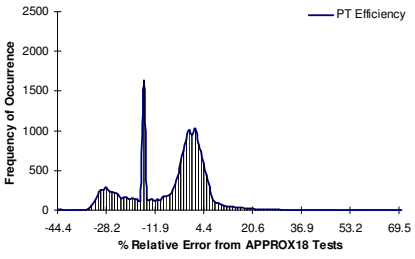

Figure A.8.32e Distribution of relative error from APPROX18 prediction of PT efficiency

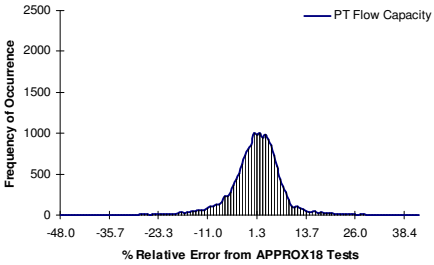

Figure A.8.32f Distribution of relative error from APPROX18 prediction of PT flow capacity

APPROX19

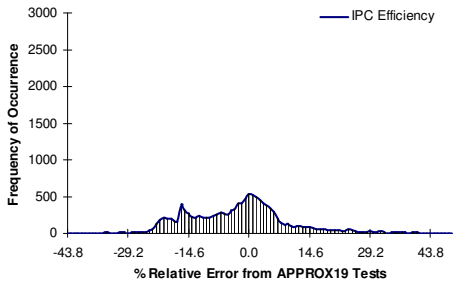

Figure A.8.33a Distribution of relative error from APPROX19 prediction of IPC efficiency

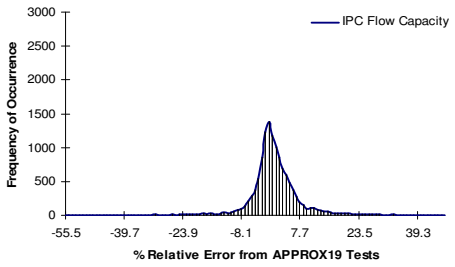

Figure A.8.33b Distribution of relative error from APPROX19 prediction of IPC flow capacity

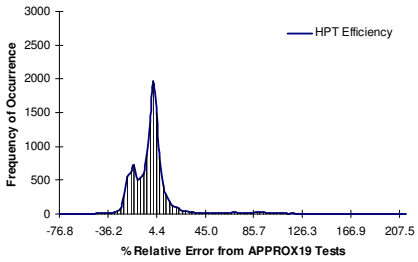

Figure A.8.33c Distribution of relative error from APPROX19 prediction of HPT efficiency

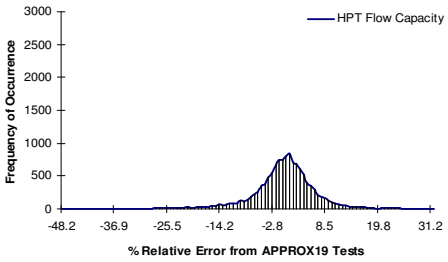

Figure A.8.33d Distribution of relative error from APPROX19 prediction of HPT flow capacity

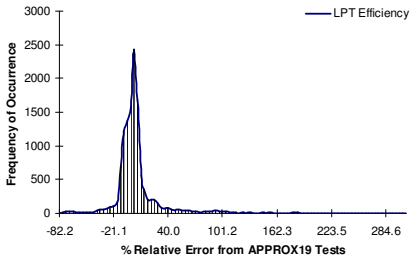

Figure A.8.33e Distribution of relative error from APPROX19 prediction of LPT efficiency

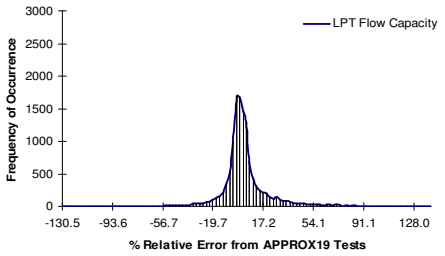

Figure A.8.33f Distribution of relative error from APPROX19 prediction of LPT flow capacity

APPROX20

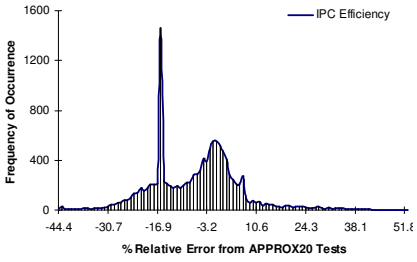

Figure A.8.34a Distribution of relative error from APPROX20 prediction of IPC efficiency

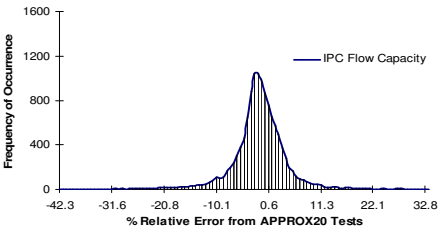

Figure A.8.34b Distribution of relative error from APPROX20 prediction of IPC flow capacity

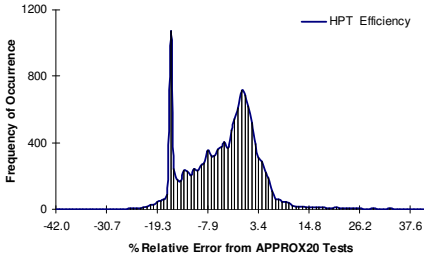

Figure A.8.34c Distribution of relative error from APPROX20 prediction of HPT efficiency

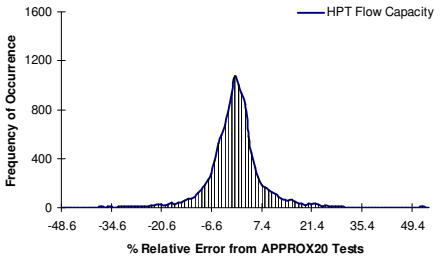

Figure A.8.34d Distribution of relative error from APPROX20 prediction of HPT flow capacity

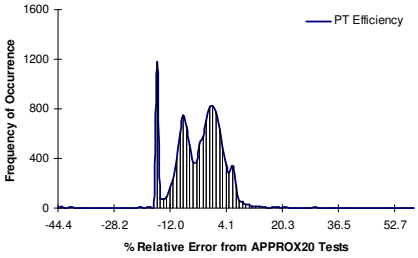

Figure A.8.34e Distribution of relative error from APPROX20 prediction of PT efficiency

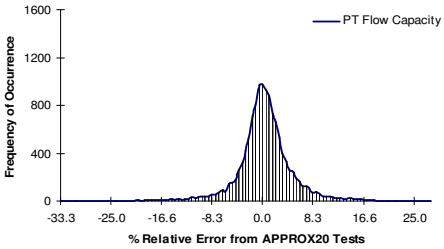

Figure A.8.34f Distribution of relative error from APPROX20 prediction of PT flow capacity

APPROX21

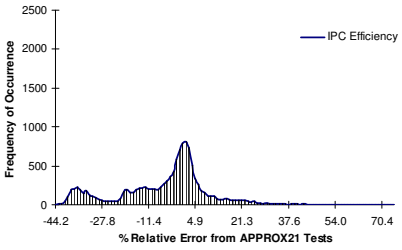

Figure A.8.35a Distribution of relative error from APPROX21 prediction of IPC efficiency

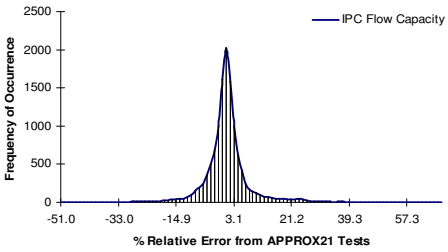

Figure A.8.35b Distribution of relative error from APPROX21 prediction of IPC flow capacity

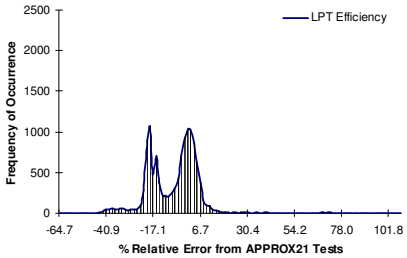

Figure A.8.35c Distribution of relative error from APPROX21 prediction of LPT efficiency

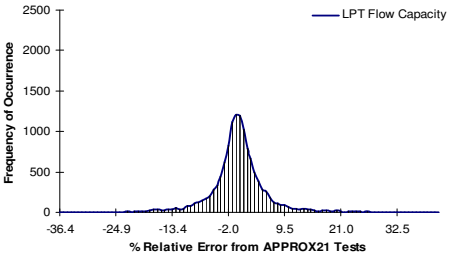

Figure A.8.35d Distribution of relative error from APPROX21 prediction of LPT flow capacity

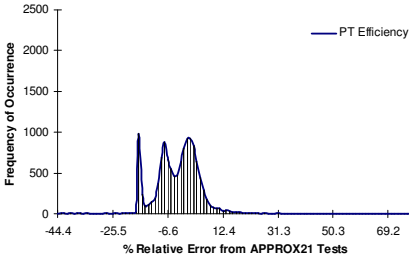

Figure A.8.35e Distribution of relative error from APPROX21 prediction of PT efficiency

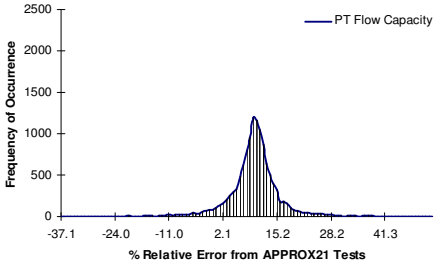

Figure A.8.35f Distribution of relative error from APPROX21 prediction of PT flow capacity

APPROX22

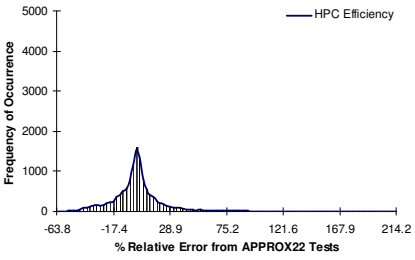

Figure A.8.36a Distribution of relative error from APPROX22 prediction of HPC efficiency

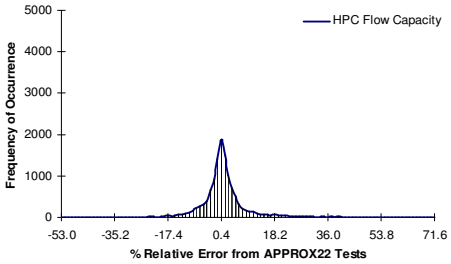

Figure A.8.36b Distribution of relative error from APPROX22 prediction of HPC flow capacity

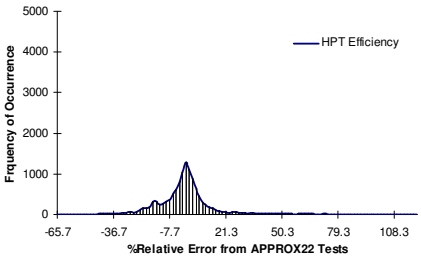

Figure A.8.36c Distribution of relative error from APPROX22 prediction of HPT efficiency

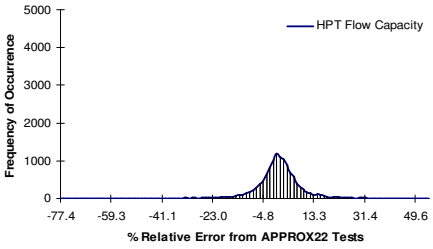

Figure A.8.36d Distribution of relative error from APPROX22 prediction of HPT flow capacity

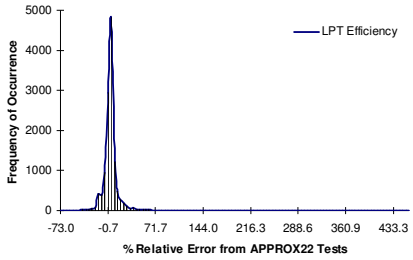

Figure A.8.36e Distribution of relative error from APPROX22 prediction of LPT efficiency

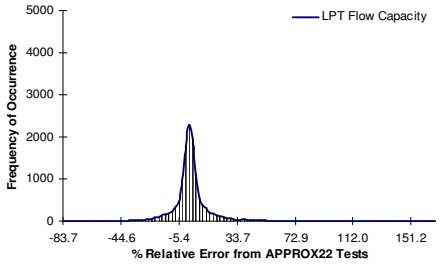

Figure A.8.36f Distribution of relative error from APPROX22 prediction of LPT flow capacity

APPROX23

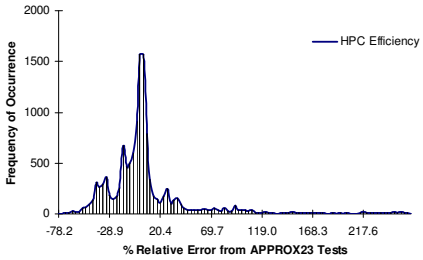

Figure A.8.37a Distribution of relative error from APPROX23 prediction of HPC efficiency

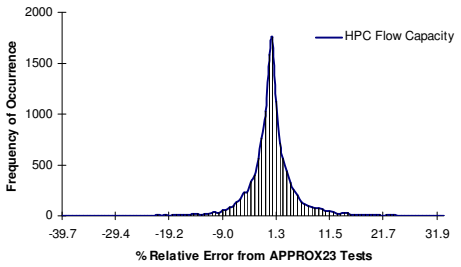

Figure A.8.37b Distribution of relative error from APPROX23 prediction of HPC flow capacity

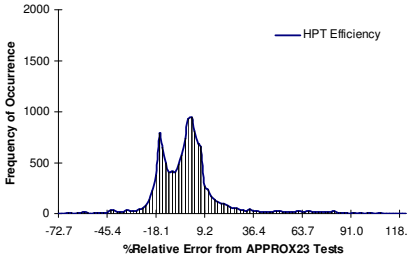

Figure A.8.37c Distribution of relative error from APPROX23 prediction of HPT efficiency

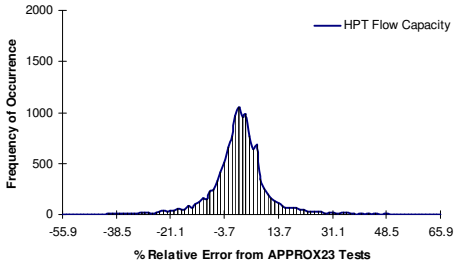

Figure A.8.37d Distribution of relative error from APPROX23 prediction of HPT flow capacity

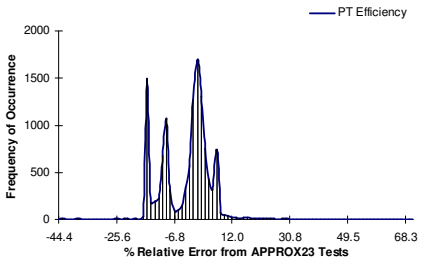

Figure A.8.37e Distribution of relative error from APPROX23 prediction of PT efficiency

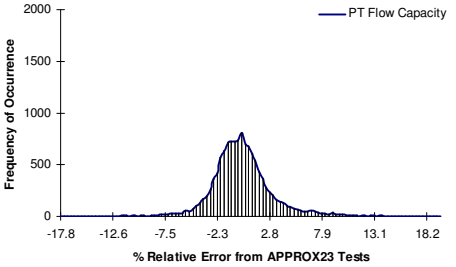

Figure A.8.37f Distribution of relative error from APPROX23 prediction of PT flow capacity

APPROX24

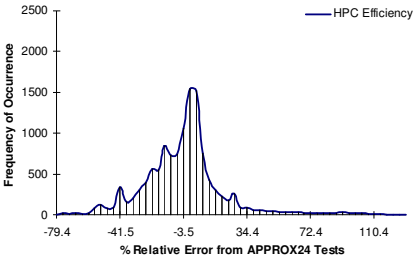

Figure A.8.38a Distribution of relative error from APPROX24 prediction of HPC efficiency

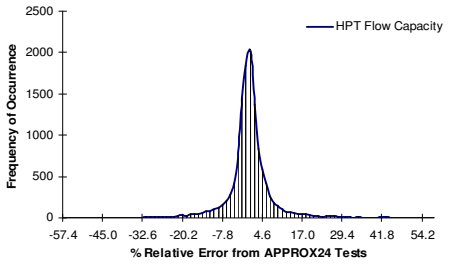

Figure A.8.38b Distribution of relative error from APPROX24 prediction of HPC flow capacity

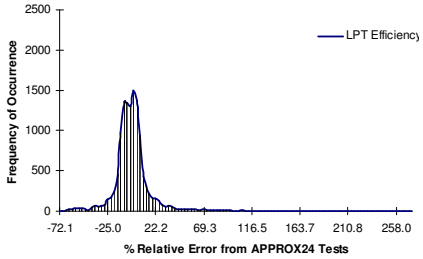

Figure A.8.38c Distribution of relative error from APPROX24 prediction of LPT efficiency

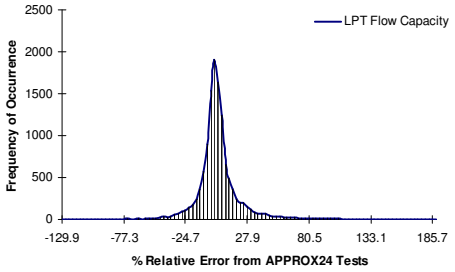

Figure A.8.38d Distribution of relative error from APPROX24 prediction of LPT flow capacity

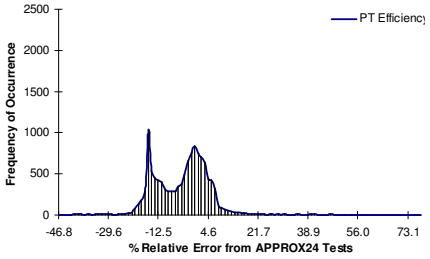

Figure A.8.38e Distribution of relative error from APPROX24 prediction of PT efficiency

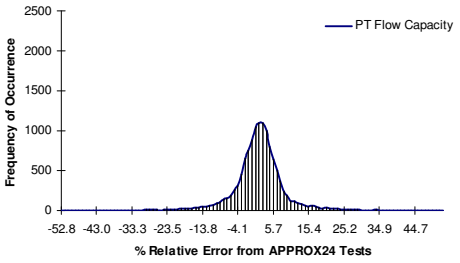

Figure A.8.38f Distribution of relative error from APPROX24 prediction of PT flow capacity

APPROX25

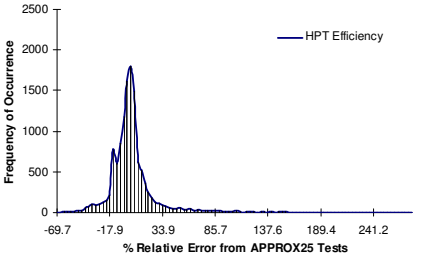

Figure A.8.39a Distribution of relative error from APPROX25 prediction of HPT efficiency

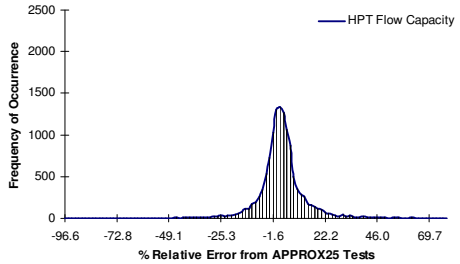

Figure A.8.39b Distribution of relative error from APPROX25 prediction of HPT flow capacity

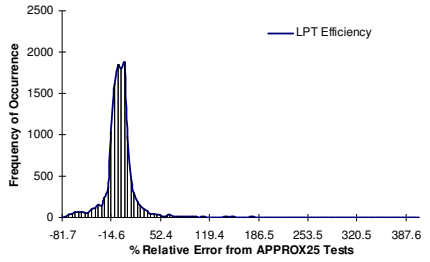

Figure A.8.39c Distribution of relative error from APPROX25 prediction of LPT efficiency

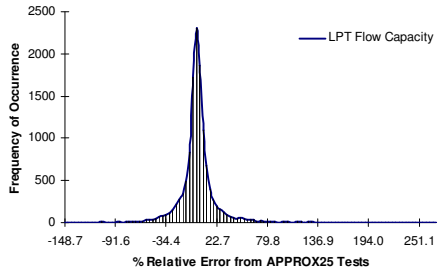

Figure A.8.39d Distribution of relative error from APPROX25 prediction of LPT flow capacity

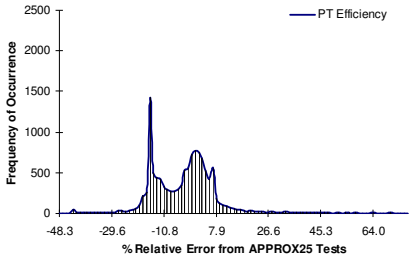

Figure A.8.39e Distribution of relative error from APPROX25 prediction of PT efficiency

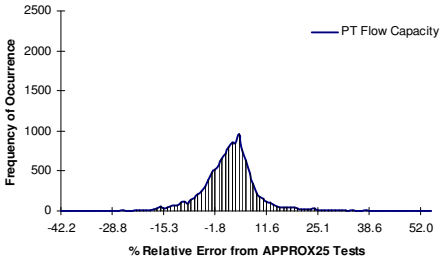

Figure A.8.39f Distribution of relative error from APPROX25 prediction of PT flow capacity

APPENDIX A.9

DSF AND TSF ESTIMATION RESULTS

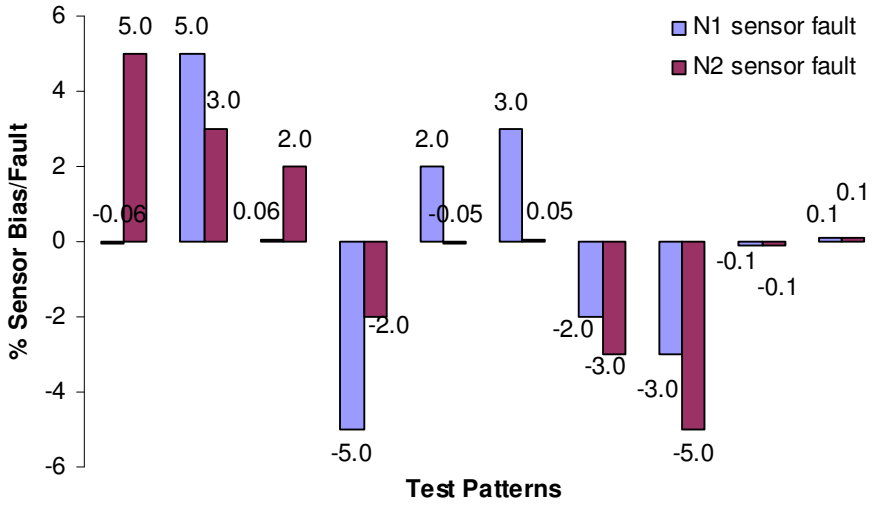

Figure A.9.1 Random fault implanted on LP shaft speed (N1) and HP shaft speed (N2) indicating a dual sensor fault

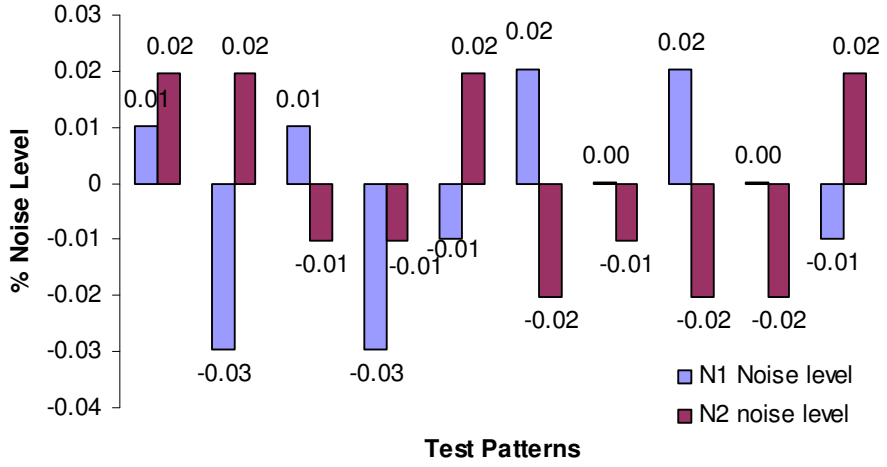

Figure A.9.2 Random noise levels applied to N1 and N2

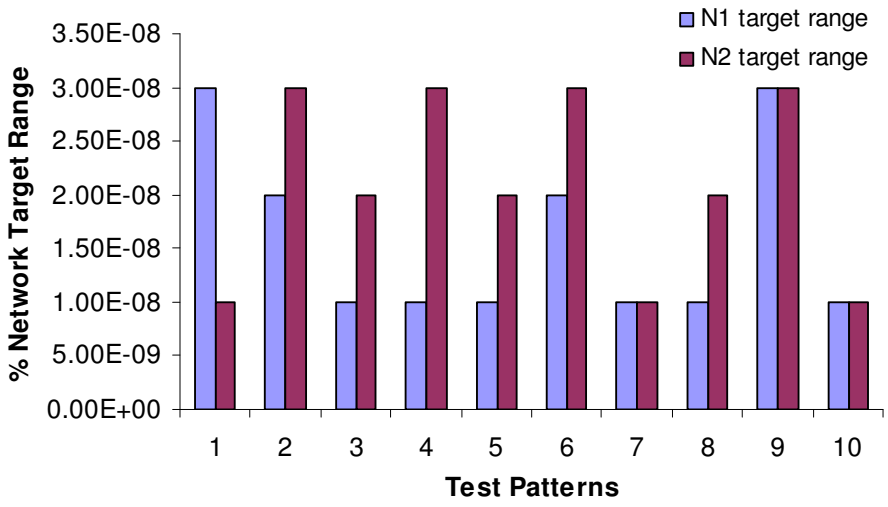

Figure A.9.3 Expected output range for N1 and N2 from network

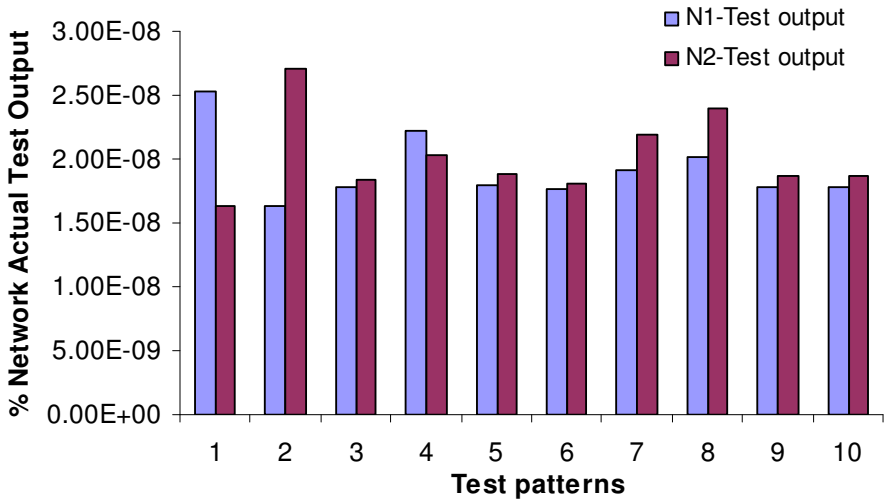

Figure A.9.4 Actual network output for N1 and N2

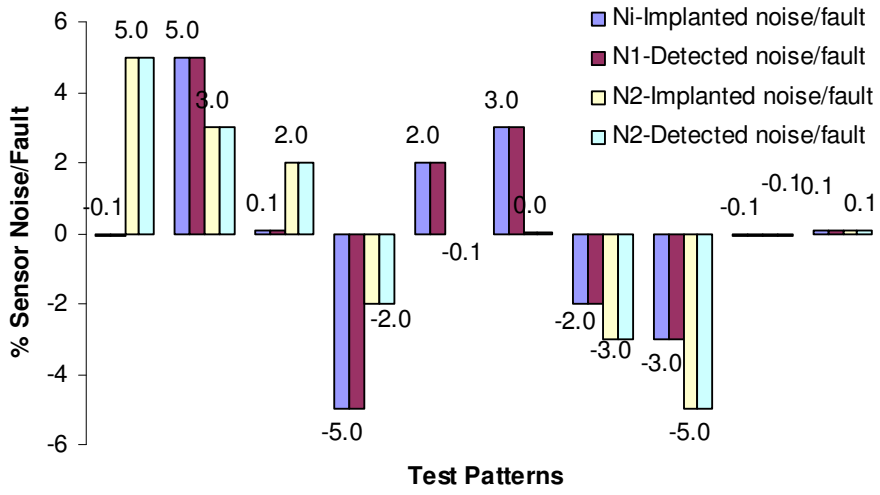

Figure A.9.5 Comparison of implanted and detected dual sensor fault on N1 and N2

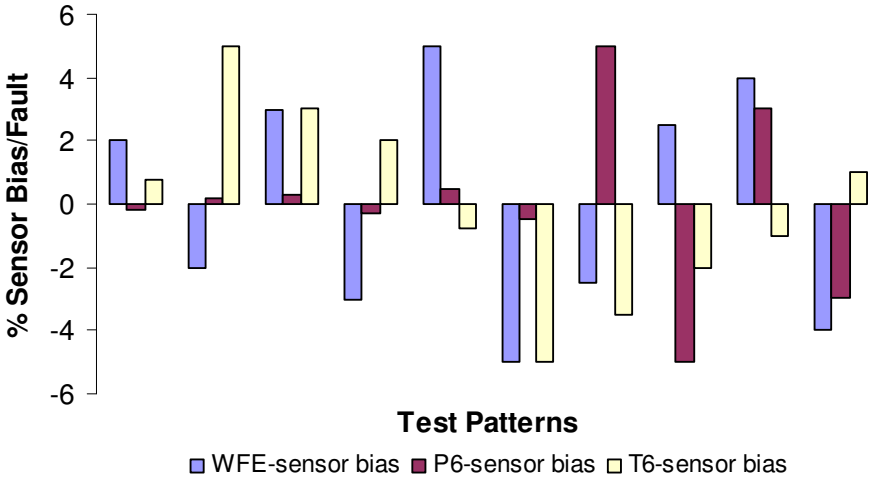

Figure A.9.6 Random fault implanted on fuel flow sensor (WFE), HPT outlet pressure (P6) and HPT outlet temperature (T6) indicating a triple sensor fault

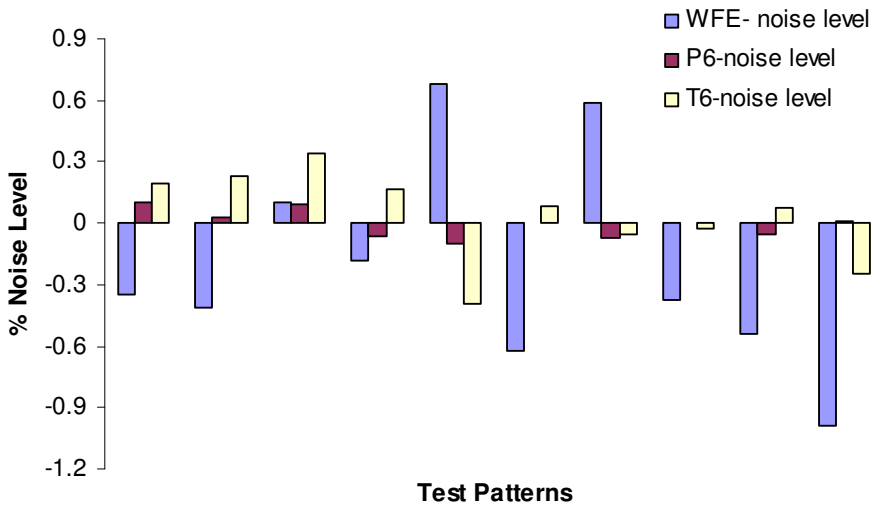

Figure A.9.7 Random noise levels applied to WFE, P6 and T6

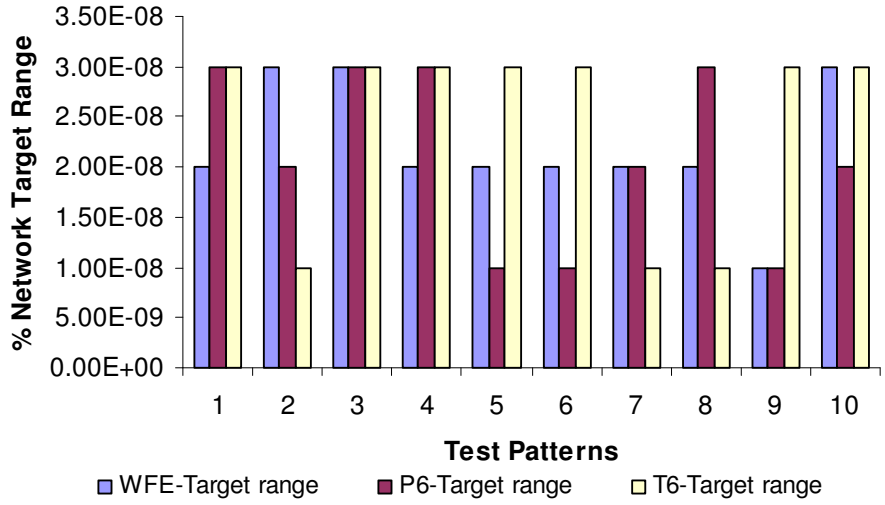

Figure A.9.8 Expected output range for WFE, P6 and T6 from network

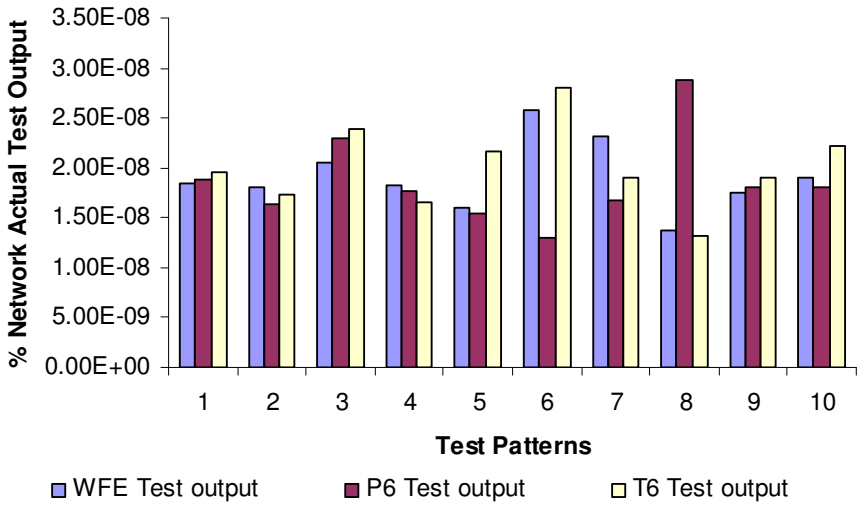

Figure A.9.9 Actual network output for WFE, P6 and T6

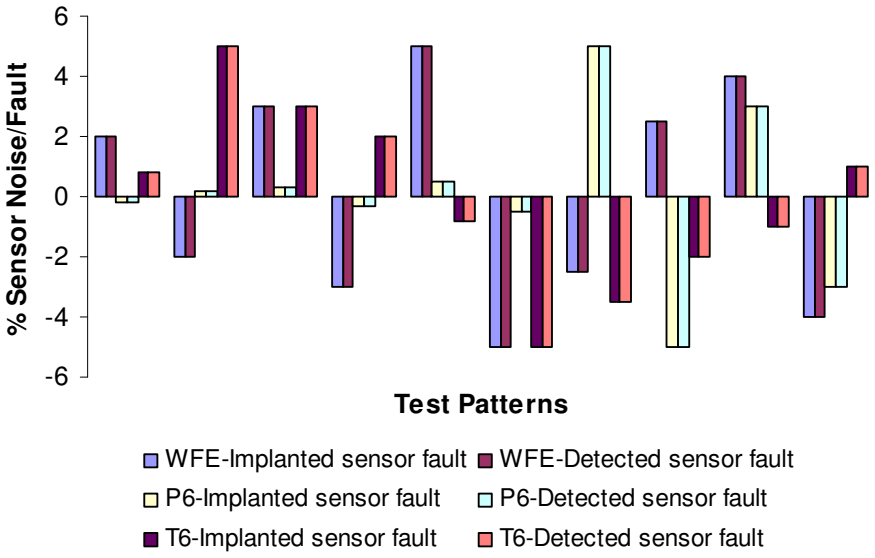

Figure A.9.10 Comparison of implanted and detected dual sensor fault on WFE, P6 and T6